

**Charakterisierung der Expression und Regulation
arzneistoffmetabolisierender Enzyme in Darm und Leber**

Inauguraldissertation

zur

Erlangung des akademischen Grades eines

Doktors der Naturwissenschaften

(Dr. rer. nat.)

der

Mathematisch-Naturwissenschaftlichen Fakultät

der

Universität Greifswald

vorgelegt von

Christoph Wenzel

Greifswald, 31.07.2023

Dekan:

Prof. Dr. Gerald Kerth

1. Gutachter:

Prof. Dr. Christoph Ritter

2. Gutachter:

Prof. Dr. Stefan Oswald

3. Gutachter:

Prof. Dr. Björn Burckhardt

Tag des Promotionskolloquiums:

11.01.2024

Inhaltsverzeichnis

1	Einleitung und Aufgabenstellung	1
2	Material und Methoden	9
2.1	Humane Gewebeprobe	9
2.2	Zellkultur	10
2.3	Genexpressionsanalyse	11
2.4	Herstellung der Gesamtgewebelysate	12
2.5	Isolation der nukleären Fraktion	13
2.6	Bestimmung des Gehaltes an Gesamtprotein mittels Bicinchoninsäure-Assay	13
2.7	<i>Filter-Aided-Sample-Preparation</i> (FASP)	14
2.8	<i>In-solution</i> -Verdau	15
2.9	<i>Targeted Proteomics</i>	15
2.10	Statistik	16
3	Ergebnisse und Diskussion	17
3.1	Entwicklung und Validierung einer <i>targeted proteomics</i> -Methode zur Quantifizierung arzneistoffmetabolisierender Enzyme (Publikation 1)	17
3.2	Anwendung der Methode auf gepaartes Leber- und Darmgewebe von gesunden Organspendern (Publikation 2).....	21
3.3	Anwendung der Methode auf eine Kohorte von Patienten mit Einschränkungen der Leberfunktion verschiedener Genese (Publikation 3)	23
3.4	Entwicklung, Validierung und Anwendung einer <i>targeted proteomics</i> Methode zur Quantifizierung nukleärer Rezeptoren (Publikation 4)	25
4	Zusammenfassung und Ausblick.....	28
5	Literaturverzeichnis	31
6	Publikationen	39
6.1	<i>Mass spectrometry-based targeted proteomics method for the quantification of clinically relevant drug metabolizing enzymes in human specimens</i>	39
6.2	<i>Comparative Intra-Subject Analysis of Gene Expression and Protein Abundance of Major and Minor Drug Metabolizing Enzymes in Healthy Human Jejunum and Liver</i>	53
6.3	<i>Gene Expression and Protein Abundance of Hepatic Drug Metabolizing Enzymes in Liver Pathology</i>	78
6.4	<i>Gene Expression and Protein Abundance of Nuclear Receptors in Human Intestine and Liver: A New Application for Mass Spectrometry-Based Targeted Proteomics</i>	98
7	Eigenständigkeitserklärung	113
8	Veröffentlichungen und andere wissenschaftliche Leistungen	114
8.1	Veröffentlichungen.....	114
8.2	Vorträge	115
8.3	Posterpräsentationen	115

1 Einleitung und Aufgabenstellung

Durch den Kontakt mit seiner Umwelt ist der Mensch unweigerlich einer Vielzahl an Fremdstoffen (Xenobiotika), natürlichen oder synthetischen Ursprungs, ausgesetzt. Darunter sind in erster Linie etwa 10 000 verschiedene Verbindungen, die mit der Nahrung in den Körper gelangen und von diesem nicht verwertet werden können. Der Großteil dieser Stoffe sind pflanzlichen Ursprungs und werden als Fraßgifte produziert. Pro Tag nimmt der Mensch mit der Nahrung etwa 1,5 g dieser aus Pflanzen stammenden Pestizide (Saponine, Flavonoide, phenolische Verbindungen) und Karzinogene (Pyrrolizidinalkaloide, Mono- und Diterpene) auf. In Lebewesen, die pflanzliche Nahrung aufnehmen, haben sich deshalb evolutionär Mechanismen in Form von Enzymen entwickelt, mit deren Hilfe diese Stoffe unschädlich gemacht und ausgeschieden werden können. Angesichts der enormen Vielfalt der mit der Nahrung aufgenommenen Fremdstoffe zeichnen sich diese Enzyme durch eine breite Substratspezifität aus. Daher sind diese Enzyme auch in der Lage, Arzneistoffe und andere chemisch-synthetische Verbindungen abzubauen [1]. Aufgrund der pharmakologischen Fragestellung der vorliegenden Arbeit, werden diese Enzyme im Folgenden als arzneistoffmetabolisierende Enzyme bezeichnet.

Der Abbau von Xenobiotika wird in Reaktionen der Phasen I und II unterteilt. Ziel aller dieser Reaktionen ist es, lipophile Moleküle so zu funktionalisieren beziehungsweise zu konjugieren, dass ihre Wasserlöslichkeit gegenüber der Ursprungsverbindung erhöht wird und eine beschleunigte renale oder biliäre Exkretion möglich wird. Reaktionen der Phase I sind Funktionalisierungsreaktionen, die polare funktionelle Gruppen in unpolare Moleküle einführen oder solche freilegen. Zu den katalysierten Reaktionen gehören Oxidation, Reduktion, Hydrolyse und Hydratisierung.

Die größte Rolle im oxidativen Phase-I-Metabolismus spielen die Cytochrom-P450-Enzyme. Dabei handelt es sich um Monooxygenasen, die Häm als prosthetische Gruppe enthalten und aus ca. 500 Aminosäuren bestehen. Bisher sind im menschlichen Genom 57 P450-Gene identifiziert worden [2]. Die Nomenklatur der Cytochrom-P450-Isoenzyme erfolgt durch Angabe der Familie als arabische Zahl und der Subfamilie als Buchstabe (beispielsweise wird als CYP3A4 das vierte Enzym der Subfamilie A aus der Familie 3 bezeichnet). Allen CYP-Enzymen ist gemeinsam, dass die Übertragung eines Sauerstoffatoms mit Hilfe eines Eisen(III)-Ions im aktiven Zentrum erfolgt. Weiterhin benötigen die katalysierten Reaktionen Nicotinamidadenindinukleotidphosphat in seiner reduzierten Form (NADPH), die Cytochrom-P450-Oxidoreduktase (POR) und Phospholipide. Die Aufklärung des Katalysemechanismus der Cytochrom-P450-Enzyme war Gegenstand zahlreicher Arbeiten, nach denen heute der Transfer von zwei Elektronen mit Hilfe des zentralen Eisen-Ions, welches während des

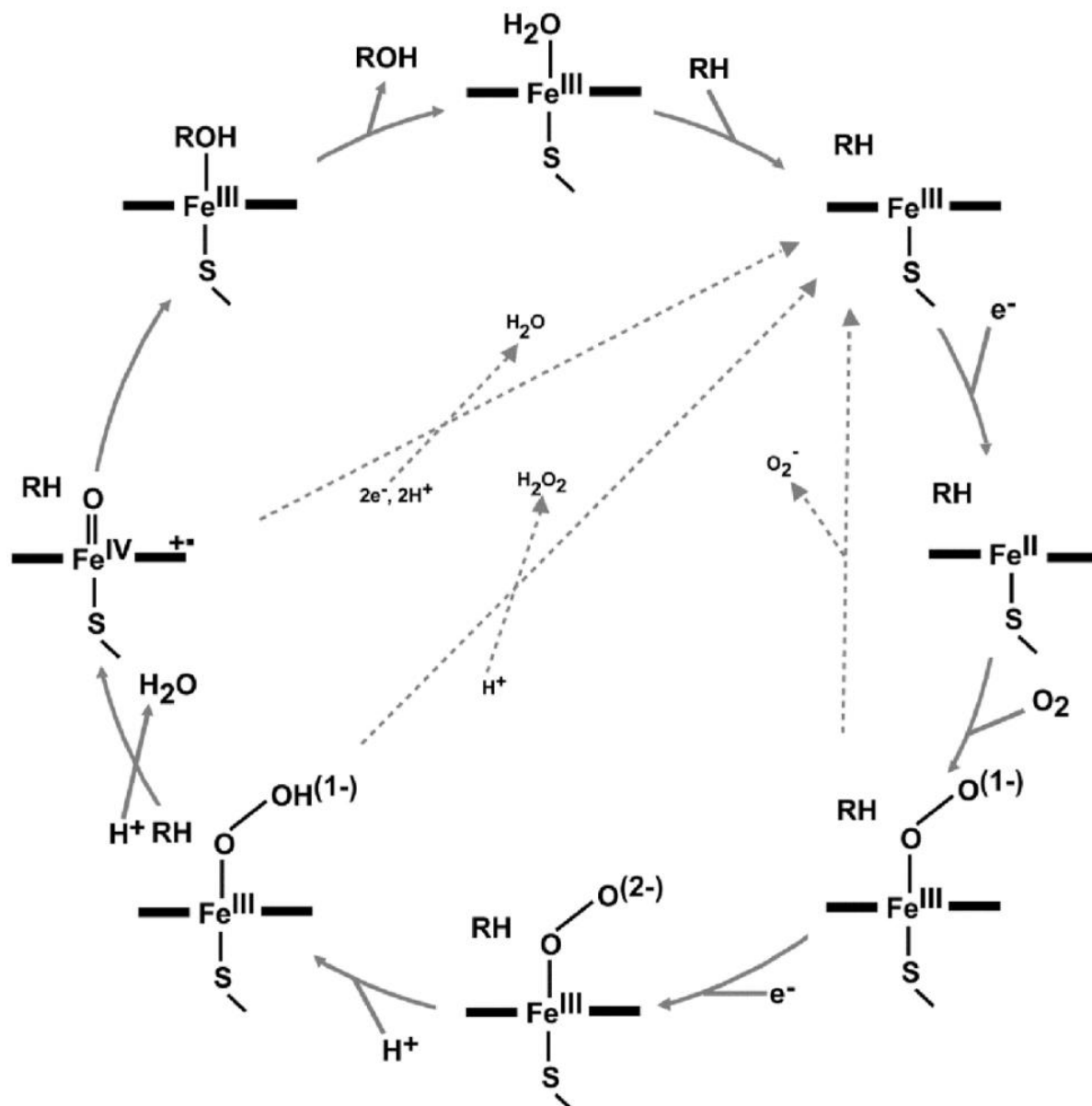


Abbildung 1: Katalysemechanismus von Cytochrom-P450-Enzymen. (Quelle: [3])

katalytischen Zyklus seine Oxidationszahl von III nach II ändert, als allgemein akzeptiert betrachtet werden kann (Abbildung 1) [2,4].

Ebenfalls zu den Enzymen des Phase-I-Metabolismus werden die Carboxylesterasen gezählt. In Säugetieren sind bis heute sechs Isoformen (CES1-6) gefunden worden, von denen CES1 und CES2 eine Bedeutung für den humanen Metabolismus von Xenobiotika besitzen [5,6]. Während die katalytische Triade aus Glutamat, Histidin und Serin bei allen Carboxylesterasen konserviert ist, unterscheiden sich die Isoformen hinsichtlich ihrer Substratspezifität: Während CES1 bevorzugt Carbonsäureester hydrolysiert, die aus einer kleinen Alkoholgruppe und einer großen Carbonsäuregruppe bestehen (z. B. Clopidogrel, Oseltamivir), werden solche Ester, die aus einer großen Alkoholgruppe und einer kleinen Säuregruppe bestehen (z. B. Dabigatran, Irinotecan), bevorzugt von CES2 hydrolysiert [7,8]. Der katalytische Mechanismus

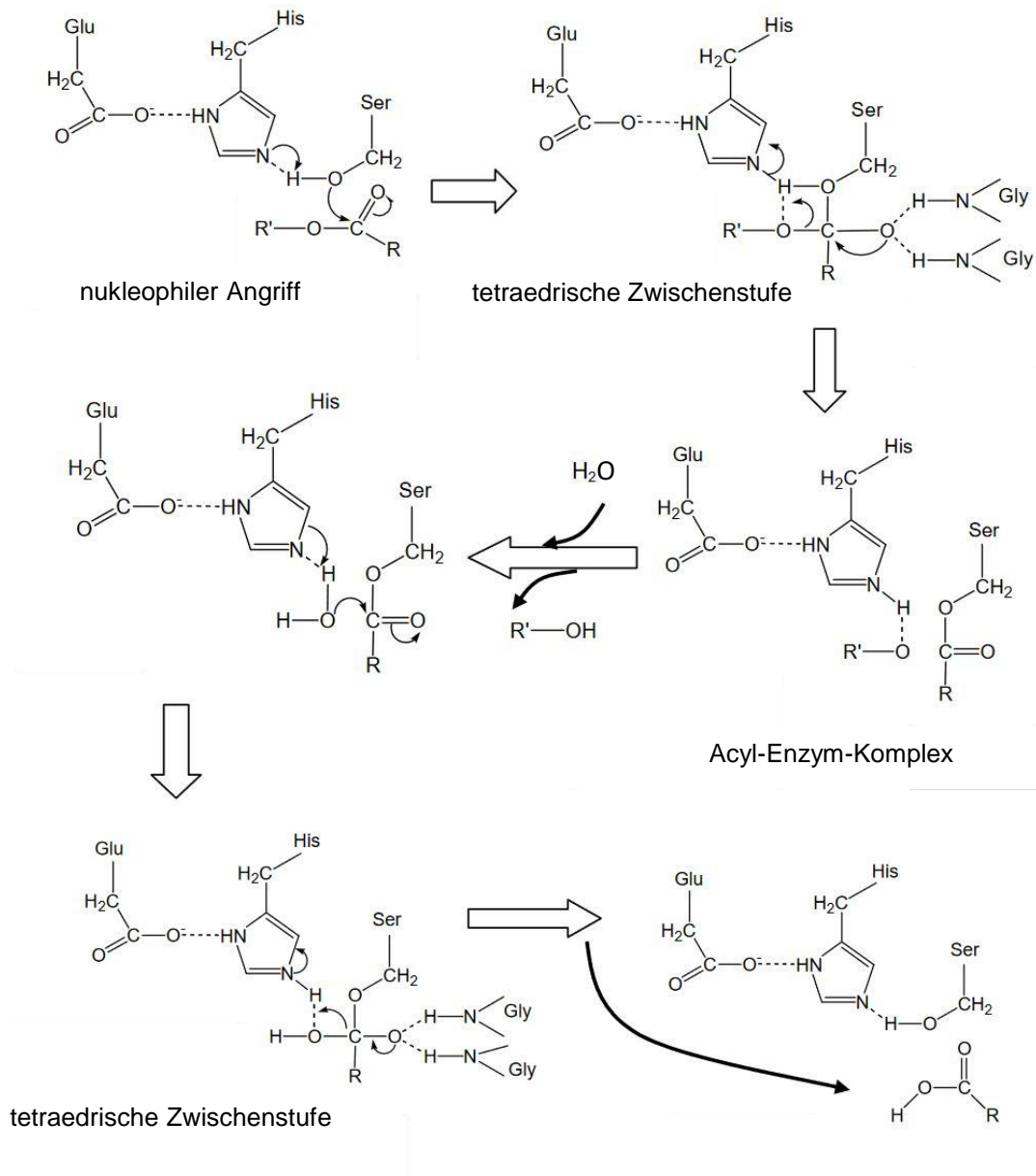


Abbildung 2: Postulierter Mechanismus der Esterhydrolyse durch Carboxylesterasen. Modifiziert nach [9]

über zwei tetraedrische Zwischenstufen ist gut verstanden und entspricht dem aller Esterasen mit derselben katalytischen Triade (Abbildung 2) [10].

Weitere Enzyme des Phase-I-Metabolismus, wie beispielsweise flavinhaltige Monooxygenasen (FMO), Alkohol- und Aldehyddehydrogenasen (ADH, ALDH) oder Aminoxydasen sind nicht Gegenstand dieser Arbeit und es wird an dieser Stelle auf die weiterführende Literatur verwiesen [11–13].

Reaktionen des Phase-II-Metabolismus sind Konjugationsreaktionen. Hierbei werden funktionelle Gruppen, die in Xenobiotika bereits vorhanden oder durch vorhergehenden Metabolismus der Phase-I eingeführt worden sind, an körpereigene Moleküle kovalent gebunden. Die wichtigste Reaktion ist in diesem Zusammenhang die Glucuronidierung, bei

der die Bindung an Glucuronsäure erfolgt, was die Polarität und damit die Hydrophilie der Moleküle deutlich erhöht und sie in der Regel bioinaktiviert.

Diese Reaktionen werden von den Uridin-5'-diphospho-glucuronosyltransferasen (UGTs) katalysiert. In der Superfamilie der menschlichen UGTs wurden bis heute 22 Proteine identifiziert. Die Nomenklatur der UGTs ist mit jener der Cytochrom-P450-Ezyme vergleichbar (s. o.). Die Konjugationsreaktion benötigt Uridin-5'-diphosphoglucuronsäure (UDPGA) als Kofaktor, die vom Körper aus Glucose-1-Phosphat synthetisiert wird. Der Mechanismus der katalysierten Reaktion ist mit einer nukleophilen Substitution (S_N2) am anomeren Kohlenstoffatom der Glucuronsäure vergleichbar. Dabei greift das Nucleophil (N- oder O-Atom, in seltenen Fällen S- oder acides C-Atom) am anomeren C-Atom der UDPGA an und verdrängt UDP unter Inversion (α -Anomer \rightarrow β -Anomer) aus dem Molekül (Abbildung 3) [14].

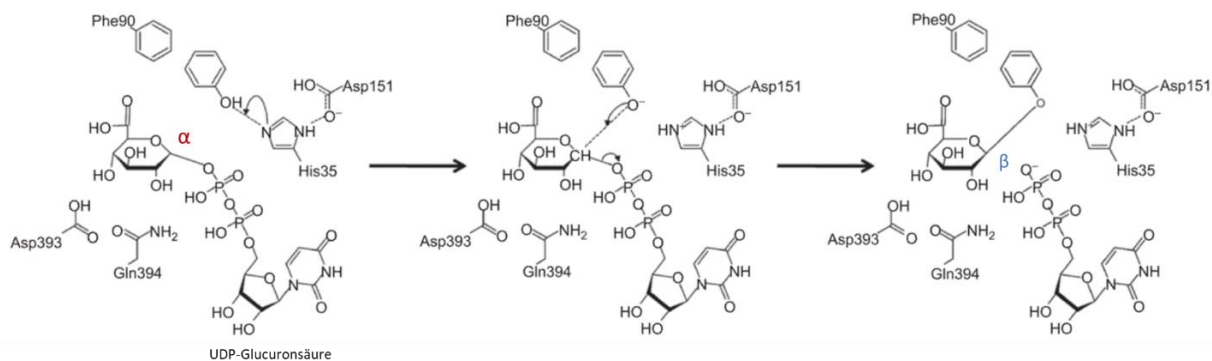


Abbildung 3: Postulierter Mechanismus der Konjugation eines Substrates (hier Phenol) zum Glucuronid durch UGTs. Beachte die Konfigurationsänderung am anomeren Kohlenstoffatom der Glucuronsäure. Modifiziert nach [15].

Andere Enzyme des Phase-II-Metabolismus wie Sulfotransferasen, N-Acetyltransferasen oder Glutathion-S-Transferasen finden in der vorliegenden Arbeit keine Berücksichtigung.

Das Blut aus dem venösen Kapillarsystem des Magen-Darm-Traktes -und mit ihm die dort aufgenommenen Stoffe- gelangt über die Pfortader direkt in die Leber als Organ des Fremdstoffmetabolismus, bevor es den systemischen Kreislauf erreicht. Dies ist aus evolutionärer Sicht sinnvoll, um den Körper vor den aufgenommenen Fremdstoffen zu schützen, stellt aber die orale Applikation von Arzneistoffen vor Herausforderungen. Die erwähnten Enzyme des Fremdstoffmetabolismus sind jedoch nicht nur in der Leber, sondern in bedeutender Menge auch im Darm lokalisiert [16]. Das Phänomen, dass nur ein Teil einer oral applizierten Dosis eines Arzneistoffes die systemische Zirkulation erreicht, wird *first-pass*-Effekt genannt und setzt sich demnach aus prähepatischer und hepatischer Metabolisierung zusammen.

Eine Reihe klinischer Studien bestätigte, dass der Darm in einem relevanten Maß zum Arzneistoffmetabolismus beiträgt. Paine *et al.* [17] konnten *in vivo* die Bildung von Hydroxymidazolam, dem nahezu ausschließlich durch CYP3A4 gebildeten Metaboliten des Midazolams, nach intraduodener Applikation von Midazolam während einer Lebertransplantation nachweisen. Die Applikation des Midazolams erfolgte in der Phase der Operation, in der die erkrankte Leber bereits entnommen, das Spenderorgan aber noch nicht eingesetzt war. Aus dem Erscheinen von Hydroxymidazolam im arteriellen Blut unter diesen Bedingungen kann geschlossen werden, dass der Darm einen relevanten Beitrag zum *first-pass*-Metabolismus durch CYP3A4 leistet. Der Anteil des intestinal metabolisierten Midazolams wurde in dieser Studie auf im Mittel 43% der applizierten Dosis berechnet.

Dies wird durch die Ergebnisse einer Studie von Skottheim *et al.* [18] unterstützt. Die Autoren konnten eine Verdoppelung der oralen Bioverfügbarkeit des CYP3A4- und CYP3A5-Substrats Atorvastatin in Patienten zeigen, deren Jejunum nach bariatrischer Operation durch einen *Bypass* umgangen wird. Das Fehlen des Jejunums, und damit auch seiner metabolischen Aktivität, zeigte sich hier in einer vergrößerten AUC des Atorvastatins nach dem Eingriff gegenüber dem vor dem Eingriff erhobenen Wert.

In einer klinischen Studie von Thummel *et al.* [19] wurde die hepatische Extraktionsrate von Midazolam auf 0,44 und die intestinale Extraktionsrate auf 0,43 bestimmt. Dies deckt sich mit den Ergebnissen einer späteren Studie von Tomalik-Scharte *et al.* [20]. Die Autoren geben die intestinale und hepatische Bioverfügbarkeit nach oraler und intravenöser Gabe von Midazolam mit 0,646 (intestinal) und 0,775 (hepatisch) an (Bioverfügbarkeit $F = 1 - \text{Extraktionsrate } E$). Diese Ergebnisse lassen auf eine etwa gleich hohe metabolische Aktivität von CYP3A4 in Leber und Darm schließen.

Aufgrund der bereits erwähnten Vielfalt der arzneistoffmetabolisierenden Enzyme, des großen personellen und finanziellen Aufwands, den klinische Studien verursachen und nicht zuletzt aufgrund von ethischen Bedenken ist diese Art von Studien für die Charakterisierung des *first-pass*-Metabolismus, besonders in frühen Phasen der Arzneimittelentwicklung, ungeeignet [21,22]. Unter den verschiedenen präklinischen Ansätzen haben in letzter Zeit die physiologiebasierten pharmakokinetischen (PBPK) Modelle an Bedeutung gewonnen [23,24]. In der Literatur finden sich zahlreiche Beispiele für erfolgreiche PBPK-Modellierungen von Plasmaspiegeln verschiedener Arzneistoffe, insbesondere auch unter Berücksichtigung des Einflusses von CYP-Enzymen [25–27]. Die Qualität dieser Modelle hängt wiederum von der Qualität der verwendeten Daten und Parameter ab. Ohtsuki *et al.* konnten zeigen, dass aus einer Expressionsanalyse der entsprechenden Gene keine Schlüsse hinsichtlich der metabolischen Aktivität des zugehörigen Enzyms gezogen werden können [28]. Zwar kann auch von der exprimierten Menge eines Enzymes auf Proteinebene nicht direkt auf seine

metabolische Aktivität geschlossen werden, aber die zuvor erwähnten Arbeiten zeigen, dass mit diesen Daten erfolgreiche Modellierungen möglich sind.

In der jüngeren Vergangenheit hat die Massenspektrometrie zur Identifizierung und Quantifizierung von Proteinen gegenüber den klassischen Techniken wie dem *Western-Blot* an Bedeutung gewonnen [29]. Als wichtigste Vorteile dieser Methode sind die hohe Empfindlichkeit, Reproduzierbarkeit und die große Spezifität, selbst bei Isoenzymen mit hoher Homologie, zu nennen. Außerdem ermöglicht die Massenspektrometrie die simultane Quantifizierung vieler unterschiedlicher Proteine in einem analytischen Lauf, was den Zeitaufwand gegenüber dem *Western-Blot* verringert und einen hohen Probendurchsatz ermöglicht. Zahlreiche Arbeiten haben seitdem mittels Massenspektrometrie arzneistoffmetabolisierende Enzyme in verschiedenen Geweben und Spezies charakterisiert [30–40]. Das Spektrum der untersuchten Enzyme unterscheidet sich jedoch stark zwischen den einzelnen Arbeiten und einige (beispielsweise CYP4F2, CYP4F12) sind noch nicht ausführlich untersucht worden. Die erwähnten Arbeiten beschränken sich entweder nur auf Darm- oder Lebergewebe oder es wurden Gewebeproben von verschiedenen Individuen untersucht. Eine Analyse von gepaarten Proben einer Kohorte, also Darm- und Lebergewebe von demselben Individuum, ermöglicht dagegen eine Bestimmung sowohl der intra- als auch der interindividuellen Variabilität des Gehaltes von arzneistoffmetabolisierenden Enzymen in den genannten Geweben.

Um belastbare Ergebnisse zu erhalten, sind umfassend charakterisierte analytische Prozesse und eine Validierung der verwendeten Messmethode nötig. Zur Interpretation der erhaltenen Ergebnisse ist zudem die Kenntnis der validierten Parameter (Linearität, Präzision und Richtigkeit, Reproduzierbarkeit und Stabilitätsparameter) von Vorteil. Die bisher zur massenspektrometrischen Quantifizierung von arzneistoffmetabolisierenden Enzymen publizierten Methoden erfüllen diese Anforderungen jedoch nur teilweise [31–33,37,38,41–45].

Eine Veränderung des Gehaltes an arzneistoffmetabolisierenden Enzymen in der Leber wurde bisher für einige Krankheitsbilder, darunter alkoholinduzierte Zirrhose [38], Hepatitis C [38,46], maligne Tumore der Leber [47] und Lebermetastasen [48] gezeigt. Eine Studie, die den Gehalt an arzneistoffmetabolisierenden Enzymen bei Erkrankungen, die mit einer Herabsetzung der Leberfunktion einhergehen, unabhängig von der zugrundeliegenden Erkrankung beschreibt, lag bisher noch nicht vor.

In allen bisher vorliegenden Studien ist die hohe interindividuelle Variabilität der Expression von arzneistoffmetabolisierenden Enzymen auffällig. Als am besten untersuchte Ursache für diese Variabilität gelten genetische Polymorphismen [49]. Das Wissen über die Regulation der Expression von arzneistoffmetabolisierenden Enzymen ist dagegen bisher begrenzt. Es werden Umwelteinflüsse auf transkriptionelle und epigenetische Mechanismen [50–52],

posttranslationale Modifikationen [53], sowie der Einfluss pathologischer, insbesondere entzündlicher Zustände [54,55], diskutiert.

Als gesichert gilt eine Regulation durch nukleäre Rezeptoren, die als zelluläre Transkriptionsfaktoren anzusehen sind [56,57]. Die Bindung eines Liganden durch einen solchen nukleären Rezeptor führt zu dessen Dimerisierung. Diese Dimere binden an rezeptorspezifische DNA-Bindedomänen und steigern durch die Rekrutierung von Koaktivatoren die Transkriptionsrate entsprechender Genabschnitte. Als Liganden können körpereigene und körperfremde Moleküle, wie auch Arzneistoffe, wirken. Über diesen Mechanismus verläuft die Induktion von arzneistoffmetabolisierenden Enzymen durch Rifampicin, Johanniskrautextrakt [58] und Carbamazepin [59]. Die Aktivierung eines nukleären Rezeptors führt zur Induktion eines charakteristischen Musters an Proteinen. Als klinisch besonders relevant gelten in diesem Zusammenhang der Aryl-Hydrocarbon-Rezeptor (AhR), der konstitutive Andostran-Rezeptor (CAR), der Farnesoid-X-Rezeptor (FXR), der Glucocorticoid-Rezeptor (GR), der *Hepatocyte Nuclear Factor 4 α* (HNF4 α), der Pregnan-X-Rezeptor (PXR) und der *Small Heterodimer Partner* (SHP) [60]. Eine Regulation über PXR ist für CYP3A4, CYP2C9 und UGT1A1 belegt, während die Regulation von CYP2B6 und CYP2C19 durch CAR erfolgt [60]. Aus der Literatur ist auf Genebene bekannt, dass die verschiedenen nukleären Rezeptoren in verschiedenen Geweben unterschiedlich stark exprimiert werden [61]. Dies legt den Schluss nahe, dass arzneistoffmetabolisierende Enzyme, deren Expression von den jeweiligen nukleären Rezeptoren abhängig ist, in verschiedenen Geweben unterschiedlich stark induzierbar sind. Auf Proteinebene wurden jedoch noch keine Daten zur Expression von nukleären Rezeptoren in den für den *first-pass*-Metabolismus wichtigen Organen, Darm und Leber, erhoben.

Vom beschriebenen Wissenstand ausgehend ergab sich für die vorliegende Dissertation die Aufgabe einer Erweiterung der Charakterisierung von Leber und Jejunum hinsichtlich ihrer Ausstattung mit arzneistoffmetabolisierenden Enzymen in physiologischem und pathologisch verändertem Zustand. Diese Aufgabe wurde in den folgenden Teilprojekten bearbeitet:

1. Erweiterung des Spektrums der quantifizierbaren arzneistoffmetabolisierenden Enzyme durch Entwicklung und Validierung einer LC/MS-MS basierten *targeted-proteomics*-Methode für die Enzyme CES1, CES2, CYP1A1, CYP1A2, CYP2A6, CYP2B6, CYP2C8, CYP2C9, CYP2C18, CYP2C19, CYP2D6, CYP2E1, CYP2J2, CYP3A4, CYP3A5, CYP3A7, CYP4F2, CYP4F12, CYP4A11, UGT1A1, UGT1A3, UGT2B7, UGT2B15 und UGT2B17. (Publikation 1)
2. Anwendung der Methode auf Gewebe von Leber und Jejunum einer Kohorte von elf gesunden Organspendern. Außerdem Charakterisierung der Gewebe hinsichtlich der

Expression der zugehörigen Gene und Untersuchung auf mögliche Korrelationen.
(Publikation 2)

3. Anwendung der Methode auf Lebergewebe von Patienten mit eingeschränkter Leberfunktion, stratifiziert nach Child-Pugh-Score, sowie hinsichtlich des zugrundeliegenden Krankheitsbildes. (Publikation 3)
4. Entwicklung und Validierung einer LC-MS/MS basierten *targeted proteomics*-Methode zur Quantifizierung von AhR, CAR, FXR, GR, HNF4 α , PXR und SHP in humanem Darm- und Lebergewebe. Darauf aufbauend die Bestimmung des Gehaltes der genannten Rezeptoren in den Geweben. (Publikation 4)

2 Material und Methoden

2.1 Humane Gewebeproben

Publikation 1

Es wurden kommerziell erhältliche humane intestinale (HIM) und Lebermikrosomen (HLM) verwendet. Diese stellen ein Gemisch aus Mikrosomen von verschiedenen Individuen (HLM: n=25; HIM: n=8) dar und wurden von der Firma BD Biosciences (Woburn, USA) erworben.

Publikation 2

Das Leber- und Darmgewebe (Jejunum) wurde von verstorbenen Organspendern im Rahmen einer Kooperation mit der Pommerschen Medizinischen Universität Stettin gewonnen. Die untersuchte Kohorte bestand aus drei Frauen und acht Männern im Alter von 19 bis 60 Jahren. Die Spender verstarben an intrakraniellen Blutungen, Multiorganversagen oder schweren Kopfverletzungen und litten nach Kenntnis der behandelnden Ärzte nicht unter chronischen Krankheiten oder nahmen regelmäßig Arzneimittel ein. Das entnommene Gewebe wurde zudem histologisch untersucht um sicherzugehen, dass nur Gewebe verwendet wurde, das nicht entzündet oder nekrotisch war. Alle Spender wurden unmittelbar vor der Gewebeentnahme mit kurzwirksamen Arzneimitteln der Notfall- und Intensivmedizin, darunter Dopamin, Dobutamin, Epinephrin, Lidocain, Nitroprussidnatrium, Vasopressin, Cephalosporinen, Gentamicin, Vancomycin, Clindamycin, Insulin und Mannitol behandelt. Von keinem dieser Arzneistoffe ist eine Induktion von Enzymen des Fremdstoffmetabolismus zu erwarten. Die Proben wurden innerhalb von 30-45 Minuten nach Stillstand des Blutkreislaufs gewonnen. Sofort nach Entnahme des Darmgewebes wurde die Mucosa vom darunterliegenden Gewebe getrennt und für die Proteinquantifizierung in flüssigem Stickstoff schockgefroren. Für die Genexpressionsanalyse wurden die Gewebeproben in RNAlater (Thermo Fisher Scientific, Waltham, USA) eingelegt. Das Lebergewebe wurde ebenfalls entsprechend behandelt. Alle Proben wurden bis zur Analyse bei -80°C gelagert. Die Studie wurde in Einklang mit den Regelungen des Organspenderechts der Republik Polen durchgeführt. Ein positives Votum der Ethikkommission der Pommerschen Medizinischen Universität Stettin lag vor.

Publikation 3

Das Lebergewebe der Kontrollgruppe wurde von Patienten mit Kolonkarzinomen, die in die Leber metastasiert hatten, gewonnen. Dabei wurde eine Entfernung von mindestens 5 cm zum Tumorgewebe eingehalten. Die Kontrollgruppe umfasste elf Männer und neun Frauen im Alter

zwischen 53 und 73 Jahren. Gemäß histologischer Untersuchung war das Gewebe ohne Anzeichen einer Entzündung oder Nekrose. Das Gewebe der Untersuchungsgruppe wurde von Patienten gewonnen, bei denen aufgrund der jeweiligen Erkrankung eine Lebertransplantation nötig war. Diese Erkrankungen umfassten in der Studie Hepatitis C (HCV), primär biliäre Cholangitis (PBC), primär sklerosierende Cholangitis (PSC), Autoimmunhepatitis (AIH) und alkoholtoxische Leberschäden (ALD). Das Gewebe wurde dabei während der Transplantation direkt aus dem entnommenen Organ gewonnen. Der Grad der Funktionseinschränkung wurde anhand des Child-Pugh-Scores [62] ermittelt. Keiner der Patienten wurde mit Arzneimitteln behandelt, die die Expression von CYP- oder UGT-Enzymen beeinflussen. Dies gilt auch für die während der Operation zur Allgemeinanästhesie verwendeten Arzneimittel (Propofol, Sevofluran, Rocuronium, Fentanyl und Metamizol). Für die Proteinbestimmung wurde das Gewebe direkt nach der Entnahme in flüssigem Stickstoff eingefroren, beziehungsweise für die Genexpressionsanalyse direkt in RNAlater (Thermo Fisher Scientific, Waltham, USA) eingelegt und dann bei -80°C bis zur Analyse gelagert. Das Studienprotokoll wurde von der Ethikkommission der Pommerschen Medizinischen Universität Stettin genehmigt. Eine schriftliche Einwilligungserklärung nach einem Aufklärungsgespräch liegt von allen beteiligten Patienten vor.

Publikation 4

Darmgewebe aus Jejunum, Ileum und Colon, sowie Lebergewebe wurden von jeweils acht Patienten während Operationen aufgrund unterschiedlicher Indikationen entnommen und makroskopisch auf Anzeichen einer Entzündung oder Nekrose untersucht. Die Gewebeproben wurden sofort in flüssigem Stickstoff schockgefroren und in gefrorenem Zustand im Edelstahlmörser zerkleinert. Das Gewebepulver wurde bis zur weiteren Aufarbeitung bei -80°C gelagert. Die Studie wurde von der Ethikkommission der Universitätsmedizin Greifswald zustimmend bewertet (BB 122/12).

2.2 Zellkultur

Publikation 4

MDCKII-Zellen wurden von der *European Collection of Cell Cultures* (Salisbury, Vereinigtes Königreich) erworben und in *Dubelco's Modified Eagle Medium*, das mit 10% fetalem Kälberserum (FCS), 4 mM Glutamin, $100 \frac{I.E.}{mL}$ Penicillin und $100 \frac{\mu g}{mL}$ Streptomycin versetzt wurde, bei 37°C, einer Luftfeuchtigkeit von 95% und 5% CO₂ kultiviert. Die codierenden Sequenzen von CAR und PXR wurden, bereits in einen retroviralen Expressionsvektor kloniert, anwendungsfertig bei Eurofins (Ebersberg, Deutschland) erworben. Die Infektion der

MDCKII-Zellen wurde nach Anleitung des Herstellers durchgeführt. Die Selektion der Zellen erfolgte mit Neomycin ($500 \frac{\mu\text{g}}{\text{mL}}$).

2.3 Genexpressionsanalyse

Publikation 2

Die gesamte RNA wurde aus 40-50 mg der Gewebeproben mittels des *miVana* miRNA Isolation Kit (Thermo Fisher Scientific, Waltham, USA) gemäß der Anleitung des Herstellers isoliert. Danach wurden etwa 300 ng der Gesamt-RNA in einem Reaktionsvolumen von 40 μL in cDNA umgeschrieben. Dazu wurde das VILO cDNA Synthesis Kit (Thermo Fisher Scientific, Waltham, USA) gemäß Anleitung verwendet. Die mRNA-Expression wurde schließlich mit individuell angefertigten TaqMan *low density array* (TLDA)-Karten, basierend auf der quantitativen Echtzeit-Polymerase-Kettenreaktion (*quantitative real-time polymerase chain reaction, rt-PCR*) bestimmt. Dabei wurden die Expression der folgenden Gene gemessen: *CES1* (Hs00275607_m1), *CES2* (Hs01077945_m1), *CYP1A1* (Hs01054796_g1), *CYP1A2* (Hs00167927_m1), *CYP2A6* (Hs00868409_s1), *CYP2B6* (Hs03044631_m1), *CYP2C8* (Hs04183483_g1), *CYP2C9* (Hs02383631_s1), *CYP2C18* (Hs02383413_s1), *CYP2C19* (Hs00426380_m1), *CYP2D6* (Hs00164385_m1), *CYP2E1* (Hs00559367_m1), *CYP2J2* (Hs00356035_m1), *CYP3A4* (Hs00604506_m1), *CYP3A5* (Hs01070905_m1), *CYP3A7* (Hs02511627_s1), *CYP4A11* (Hs00167961_m1), *CYP4F2* (Hs00426608_m1), *CYP4F12* (Hs02515808_s1), *UGT1A1* (Hs02511055_s1), *UGT1A3* (Hs04194492_g1), *UGT2B7* (Hs00426592_m1), *UGT2B15* (Hs00870076_s1) und *UGT2B17* (Hs00854486_sH). Für den quantitativen Vergleich der Expressionen der einzelnen Gene wurden die entsprechenden $2^{-\Delta Ct}$ -Werte berechnet. Zur Normalisierung wurde die jeweilige Expression von *GAPDH* (Hs02786624_g1) als *housekeeping*-Gen verwendet und die Grenzwerte der Fluoreszenzsignale (*Ct*) wurden individuell festgelegt. Die Messung erfolgte in einem ViiA 7 Real Time PCR System (Life Technologies, Carlsbad, USA) und die Auswertung mit der dazugehörigen ViiA 7 Software.

Publikation 3

Aus 25 mg jeder Gewebeprobe wurde die gesamte RNA mit dem Direct-zol RNA MiniPrep Kit (Zymo Research, Irvine, USA) isoliert. Menge und Reinheit der erhaltenen Präparation wurden mittels UV-Spektroskopie bestimmt (DS-11 FX Spektrophotometer, Denovix, Wilmington, USA). 500 ng der erhaltenen RNA wurden in einem Reaktionsvolumen von 20 μL mit dem SuperScript VILO cDNA Synthesis Kit (Thermo Fisher Scientific, Waltham, USA) gemäß der Anleitung des Herstellers in cDNA umgeschrieben. Die Bestimmung der Genexpression erfolgte in Duplikaten nach Zugabe des TaqMan Fast Advanced Master Mix durch validierte,

kommerziell erhältliche TaqMan-assays. Folgende Gene wurden dabei untersucht: *CYP1A1* (Hs00153120_m1), *CYP1A2* (Hs00167927_m1), *CYP2B6* (Hs03044631_m1), *CYP2C8* (Hs02383390_s1), *CYP2C9* (Hs02383631_s1), *CYP2C19* (Hs00426380_m1), *CYP2D6* (Hs00164385_m1), *CYP2E1* (Hs0055-9367_m1), *CYP3A4* (Hs00604506_m1), *CYP3A5* (Hs01070905_m1), *UGT1A1* (Hs02511055_s1), *UGT1A3* (Hs04194492_g1), *UGT2B7* (Hs00426592_m1) und *UGT2B15* (Hs00870076_s1). Zum Vergleich der einzelnen Expressionen wurden die $2^{-\Delta Ct}$ -Werte berechnet. Zur Normalisierung wurde der geometrische Mittelwert aus den folgenden *housekeeping*-Genen herangezogen [63]: *GAPDH* (Hs99999905_m1), *HMBS* (Hs00609297_m1), *PPIA* (Hs04194521_s1), *RPLP0* (Hs99999902_m1), *RPS9* (Hs02339424_g). Die Grenzwerte der Fluoreszenzsignale (*Ct*) wurden individuell festgelegt. Messung und Auswertung erfolgten mit dem ViiA 7 Real Time PCR System (Life Technologies, Carlsbad, USA).

Publikation 4

Mit dem NucleoSpin miRNA Kit (Macherey-Nagel, Düren, Deutschland) wurde die gesamte RNA aus ca. 30 mg Gewebepulver gemäß der Anleitung des Herstellers extrahiert. Menge und Reinheit der erhaltenen RNA wurden mit dem NanoDrop ND-1000 (NanoDrop Technologies, Wilmington, USA) spektrophotometrisch untersucht. Außerdem wurden die RIN (*RNA integrity number*)-Werte mit dem Agilent 2100 Bioanalyzer (Agilent Technologies, Waldbronn, Deutschland) bestimmt (Werte zwischen 6,6 und 9,0). 2 µg der RNA wurden mit dem High-Capacity cDNA Reverse Transcription Kit (Applied Biosystems, Darmstadt, Deutschland) gemäß der Anleitung des Herstellers in cDNA umgeschrieben. Die quantitative *real-time* PCR wurde mit TaqMan *Gene Expression Assays* (Applied Biosystems) im 7900HT Sequence Detection System (Applied Biosystems, Waltham, USA) durchgeführt. Dabei wurden folgende Gene untersucht *AhR* (Hs00169233_m1), *NR1I3* [CAR] (Hs00901571_m1), *NR1H4* [FXR] (Hs01026590_m1), *NR3C1* [GR] (Hs00353740_m1), *HNF4A* (Hs00230853_m1), *NR1I2* [PXR] (Hs01114267_m1) und *NR0B2* [SHP] (Hs00222677_m1). Als Referenzgene wurden *18S rRNA* (Hs99999901_s1), *GAPDH* (Hs02758991_g1) und *PGK1* (Hs00943178_g1) verwendet. Jede Probe wurde in zwei technischen Replikaten vermessen und es wurde der Mittelwert der *Ct*-Werte gebildet. Die Normierung auf die Referenzgene erfolgte durch Berechnung der $2^{-\Delta Ct}$ -Werte.

2.4 Herstellung der Gesamtgewebelysate

Publikation 2 und 3

Das tiefgefrorene Gewebe wurde in einem eigens konstruierten Mörser aus Edelstahl, der zuvor mit flüssigem Stickstoff gekühlt wurde, zu Pulver zerkleinert. Auf 40 mg dieses Pulvers

wurden 1 mL kalte Lysislösung (0,2% Natriumdodecylsulfat, 5 mM Ethylendiamintetraacetat), die zuvor mit $5 \frac{\mu\text{L}}{\text{mL}}$ Protease-Inhibitor-Cocktail III (Merck, Darmstadt) versetzt wurden, gegeben. Nach intensivem Mischen wurde die Gewebesuspension in einem *Dounce Tissue Grinder* aus Glas (Wheaton, Millville, USA) weiter homogenisiert. Die Lyse erfolgt danach für 30 Minuten bei 4°C und leichtem Schütteln (40 rpm).

2.5 Isolation der nukleären Fraktion

Publikation 4

Etwa 300 mg des Gewebepulvers wurden mit 1 mL kalter Lysislösung (0,2% Natriumdodecylsulfat, 5 mM Ethylendiamintetraacetat), die zuvor mit $5 \frac{\mu\text{L}}{\text{mL}}$ Protease-Inhibitor-Cocktail III (Merck, Darmstadt) versetzt wurden, behandelt. Nach intensivem Mischen wurde die Gewebesuspension in einem *Dounce Tissue Grinder* aus Glas (Wheaton, Millville, USA) weiter homogenisiert. Die weitere Lyse erfolgte danach für 30 Minuten bei 4°C und leichtem Schütteln (40 rpm). Danach wurde das Homogenat für 5 Minuten bei 600 g und 4°C zentrifugiert. Der Überstand, in dem sich die zytosolische Fraktion befand, wurde verworfen. Das Pellet, das nun die nukleäre Fraktion und die membrangebundenen Proteine enthielt, wurde in 300 μL Puffer ($0,25 \frac{\text{mol}}{\text{L}}$ Sucrose, 1 mM Ethylendiamintetraacetat, $5 \frac{\mu\text{L}}{\text{mL}}$ Protease-Inhibitor-Cocktail III in Wasser bei pH=7,4) gelöst und bei -80°C bis zur Analyse gelagert.

2.6 Bestimmung des Gehaltes an Gesamtprotein mittels Bicinchoninsäure-Assay

Publikation 1,2,3 und 4

Dieser Assay basiert auf der Bildung eines blau-violetten Farbstoffkomplexes aus Bicinchoninsäure (BCA) und einwertigen Kupferionen im Verhältnis 2:1. Bei alkalischem pH-Wert werden zweiwertige Kupferionen von Peptidbindungen zu einwertigen Ionen reduziert, die dann für die Bildung des farbigen Komplexes zur Verfügung stehen [64]. Der Komplex zeigt ein Absorptionsmaximum bei 562 nm, was eine photometrische Quantifizierung in Mikrotiterplatten ermöglicht. Anhand von Kalibrationslösungen mit definiertem Proteingehalt kann so der Proteingehalt einer Testlösung berechnet werden. Für die folgenden Messungen wurde das *Pierce BCA Protein Assay Kit* (Thermo Fisher Scientific, Waltham, USA) verwendet, das die anwendungsfertigen Lösungen von Kupfersulfat und BCA, sowie bovines Serumalbumin (BSA) als Standard enthält. Um im linearen Bereich der Absorption messen zu können, mussten die Gesamtgewebelysate zunächst mit PBS verdünnt werden (7 μL Gesamtgewebelysat in 213 μL PBS). Da der Assay verhältnismäßig störanfällig gegenüber

anderen Substanzen ist, wurden die Kalibrationslösungen mit einer Matrixlösung hergestellt, die aus PBS und Lysislösung (s. o.) in diesem Verhältnis bestand. Aus dem BSA-Standard wurden durch Verdünnung mit Matrixlösung sieben Kalibrationslösungen im Bereich von $10 \frac{\mu\text{g}}{\text{mL}}$ bis $1000 \frac{\mu\text{g}}{\text{mL}}$ hergestellt. In den Vertiefungen einer Mikrotiterplatte wurden dann 100 μL Kalibrations- bzw. Probelösung mit 100 μL BCA-Mischung versetzt. Nach Inkubation für 30 Minuten bei 37°C erfolgte die Messung bei 562 nm im Plattenphotometer (Synergy HT, Biotek, Winooski, USA).

2.7 Filter-Aided-Sample-Preparation (FASP)

Publikation 2 und 3

Während der FASP-Prozedur erfolgen alle Schritte der Probenvorbereitung wie Reduktion der Disulfidbrücken, Alkylierung der Cysteinreste, Verdau durch Trypsin und Entsalzung auf einer Zellulosemembran. Die Reagenzien werden in gelöster Form nacheinander auf die Membran gegeben, wodurch eine Aufarbeitung ohne Gewebeverlust ermöglicht wird. Nach Abschluss des tryptischen Verdau werden die entstandenen Peptide mittels Zentrifugation bei 14000 g für 15 Minuten bei 4°C durch die Membran gedrückt. Da diese Technik in der Literatur bereits ausführlich beschrieben wurde [65–67], erfolgt im Folgenden nur eine kurze Beschreibung der wichtigsten Schritte.

Das Volumen an Gesamtgewebelysat, das eine Menge von 200 μg Gesamtprotein enthält, wurde mit UT-Puffer (8 M Harnstoff, 2 M Thioharnstoff) auf 200 μL aufgefüllt und auf die aktivierte Zellulosemembran der Filtereinheit (Vivacon 500, 10000 MWCO Hydrosart, Sartorius, Göttingen) gegeben. Darauf folgte ein Waschschrift mit Harnstoffpuffer (8 M Harnstoff, 10 mM TRIS; pH=8,5). Die anschließende Spaltung der Disulfidbrücken erfolgte mit 100 μL einer 8 mM Dithiothreitol-Lösung (DTT) durch Inkubation bei 56°C für 15 Minuten. Nach zwei Waschschriften mit jeweils 100 μL Harnstoffpuffer wurden die Cysteinreste durch Zugabe von 100 μL einer 50 nM Iodacetamid-Lösung (IAA) durch Inkubation bei 37°C unter Lichtausschluss alkyliert. Die Inaktivierung des IAA erfolgte nach einem weiteren Waschschrift dann erneut wie beschrieben mit DTT. Nach Auswaschen des DTT mit Harnstoffpuffer wurde drei Mal mit 100 μL einer 65 mM Ammoniumhydrogencarbonat-Lösung (AHC) gewaschen. Danach wurde die Trypsinlösung, die 2 μg *Sequencing Grade Modified Trypsin* (Promega, Madison, USA) und 0,01% ProteaseMax (Promega, Madison, USA) in 20 mM AHC enthielt, auf die Filtereinheit gegeben. Der Verdau erfolgte anschließend bei 37°C in einer feuchten Kammer für 16 Stunden. Die Elution der entstandenen Peptide geschah durch Zentrifugation und Spülen mit 40 μL AHC. Die fertigen Proben wurden dann mit 10%iger Ameisensäure auf eine Endkonzentration von 0,2% angesäuert und bei -80°C bis zur Messung gelagert. Diese

Ansäuerung dient einerseits der Beendigung des Verdau und andererseits der Spaltung des zugesetzten Detergens (ProteaseMax).

2.8 *In-solution-Verdau*

Publikation 1 und 4

Anhand des Ergebnisses der BCA-Messung wurde der Gehalt an Gesamtprotein der jeweiligen Probe mit 50 mM AHC-Lösung auf eine Konzentration von $2 \frac{mg}{mL}$ eingestellt. 100 μ L der Probe (entspricht 200 μ g Gesamtprotein) wurden mit weiteren 40 μ L AHC, 10 μ L DTT (200 mM) und 10 μ L ProteaseMax-Lösung (1%), die gemäß der Anleitung des Herstellers zubereitet wurde, versetzt. Die Spaltung der Disulfidbrücken erfolgte anschließend durch Inkubation für 30 Minuten bei 60°C im Heizblock. Danach wurden die Proben auf Eis kurz abgekühlt, bevor 10 μ L IAA (400 mM) zugegeben wurden. Die Alkylierung der Cysteinreste geschah durch Inkubation bei 37°C für 15 Minuten. Zum Verdau wurden 10 μ L der anwendungsfertigen Trypsinlösung (s. o.) hinzugegeben, was einem Verhältnis von 2,5 μ g pro 100 μ g Gesamtprotein (1:40) entspricht. Danach erfolgte eine Inkubation für 16 Stunden bei 37°C. Der Verdau wurde durch Zugabe von 20 μ L 10%iger Ameisensäure gestoppt und die Ansätze wurden für 15 Minuten bei 16000 g und 4°C zentrifugiert. Der klare Überstand wurde entnommen und bei -80°C bis zur Messung gelagert.

2.9 *Targeted Proteomics*

Publikation 1,2 und 3

Die Bestimmung des absoluten Enzymgehaltes erfolgte mittels der eigens dafür entwickelten LC-MS/MS *targeted proteomics*-Methode, die Gegenstand dieser Arbeit ist. Für die einzelnen Enzyme wurden je nach Enzym, ein oder zwei proteospezifische Surrogatpeptide verwendet. Zur Quantifizierung wurde der Wert des Peptides angegeben, das den höheren Enzymgehalt ergibt, da davon auszugehen ist, dass der Verdau für dieses Peptid vollständiger abgelaufen ist (*Quantifier*). Das zweite Peptid diente in diesem Fall dann zum sicheren Nachweis des Vorhandenseins des jeweiligen Enzyms (*Qualifier*). Je Peptid wurden drei Massenübergänge aufgenommen und eine Quantifizierung erfolgte, wenn mindestens zwei Massenübergänge detektiert werden konnten. Es wurde der Mittelwert aus allen aufgenommenen und auswertbaren Massenübergängen je Peptid gebildet.

Publikation 4

Die Entwicklung und Validierung einer LC-MS/MS-basierten *targeted proteomics*-Methode zur Quantifizierung ausgewählter nukleärer Rezeptoren ist Teil dieser Arbeit. Für die einzelnen

nukleären Rezeptoren wurde jeweils ein Surrogatpeptid verwendet und der Proteingehalt auf Basis dieses Peptides berechnet und angegeben. Dazu wurden pro Peptid drei Massenübergänge aufgenommen und eine Quantifizierung erfolgte, wenn mindestens zwei Massenübergänge detektiert werden konnten. Es wurde der Mittelwert aus allen aufgenommenen und auswertbaren Massenübergängen je Peptid gebildet.

2.10 Statistik

Zur Untersuchung möglicher Zusammenhänge zwischen mRNA-Expression und Proteingehalt, sowie der Proteingehalte zwischen den Geweben wurde der Rangkorrelationskoeffizient nach *Spearman* berechnet. Dabei wurden Werte von $p \leq 0,05$ als signifikant angesehen. Zur Berechnung der Korrelationen und für die Erstellung der Grafiken wurde die Software Prism 8 (Version 8.0.2, GraphPad Software, Boston, USA) genutzt. Die Berechnung der statistischen Parameter wie Mittelwert, Standardabweichung und Variationskoeffizient erfolgte in Microsoft Excel 2019 (Microsoft Corporation, Redmond, USA).

3 Ergebnisse und Diskussion

3.1 Entwicklung und Validierung einer *targeted proteomics*-Methode zur Quantifizierung arzneistoffmetabolisierender Enzyme (Publikation 1)

Auf der Massenspektrometrie basierende Methoden haben sich zur Methode der Wahl für die quantitative Bestimmung von arzneistoffmetabolisierenden Enzymen entwickelt, wie zahlreiche Publikationen zeigen [30–33,36–40,42–45,68–75]. In der vorliegenden Publikation wurde dazu ein *targeted proteomics*-Ansatz verwendet und das analytische Spektrum der bereits publizierten Methoden erweitert. Die Spezifität bestimmter Proteasen -in diesem Fall Trypsin, das Proteine spezifisch nach den Aminosäuren Arginin und Lysin schneidet- ermöglicht es, die beim Verdau entstehenden Peptide vorherzusagen. Ein Peptid, dessen Aminosäuresequenz spezifisch für das zu untersuchende Enzym ist (Proteospezifität) kann so zur Quantifizierung des gesamten Enzyms herangezogen werden (Surrogatpeptid). Die entsprechenden Peptide wurden zuvor durch *in silico*-Methoden ausgewählt. Dabei wurden von den, durch den Verdau mit Trypsin entstehenden Peptiden solche ausgeschlossen, die

- Cystein, Methionin oder Tryptophan enthalten (Gefahr der Oxidation).
- die die Aminosäuren Arginin und/oder Lysin direkt hintereinander enthalten (Gefahr einer unvollständigen Hydrolyse, sog. *missed cleavage* durch Trypsin).
- im zugehörigen Gen mit einer Häufigkeit $\geq 1\%$ einen nicht-synonymen Einzelnukleotidpolymorphismus aufweisen.
- Stellen enthalten, die nachgewiesenermaßen Orte von posttranslationalen Modifikationen wie Phosphorylierung oder Glykosylierung sind.

Die genannten Veränderungen führen zu einer Änderung der Masse des entsprechenden Peptides, wodurch sie der *targeted proteomics*-Methode nicht mehr zugänglich sind, was wiederum zu einer Unterschätzung des Gehaltes des entsprechenden Enzyms führen würde. Außerdem wurden nur solche Peptide ausgewählt, deren Massen im Messbereich des Massenspektrometers liegen (0-1250 Da). Da die Elektrosprayionisation (ESI) in der Ionenquelle des Massenspektrometers zu doppelt oder dreifach geladenen Molekülonen führt, können Peptide bis zu einer Masse von 3000 Da quantifiziert werden. Alle infrage kommenden Peptide wurden einer Suche mit dem *Basic Local Alignment Search Tool (BLAST)* gegen die Proteindatenbank unterzogen, um ihre Proteospezifität zu überprüfen.

Für 14 Enzyme (CYP1A1, CYP1A2, CYP2B6, CYP2C8, CYP2C9, CYP2C19, CYP2D6, CYP2E1, CYP3A4, CYP3A5, UGT1A1, UGT2B7, UGT2B15 und UGT2B17) wurden zwei Surrogatpeptide identifiziert und validiert, während für zehn Enzyme (CES1, CES2, CYP2A6,

CYP2C18, CYP2J2, CYP3A7, CYP4F2, CYP4F12, CYP4A11 und UGT1A3) ein Surrogatpeptid verwendet wurde. Von diesen 24 untersuchten Peptiden stimmen 22 Peptide mit der Literatur überein [28,30,37,38,43,45,68–85] und zwei Peptide (DIDITPIANAFGR für CYP2C18 und NSQSYIQAISDLNNLVFSR für CYP4A11) wurden erstmalig verwendet.

Für jedes dieser Peptide wurden die optimalen massenspektrometrischen Parameter (Kollisionsenergie, Declusteringpotential, Einganspotential und Kollisionszellenausgangspotential) durch direkte Infusion in das Massenspektrometer manuell bestimmt. Da diese stark geräteabhängig sind, kam es hier zu Abweichungen gegenüber den bereits publizierten Methoden. Insgesamt wurden die Parameter für 228 Massenübergänge erhoben. Die *scheduled multiple reaction monitoring (MRM)*-Funktion des verwendeten Massenspektrometers QTRAP 5500 (Sciex, Darmstadt) ermöglicht die Aufnahme einer großen Anzahl von Massenübergängen mit einer, für eine robuste Quantifizierung ausreichenden Anzahl an Datenpunkten pro chromatographischem Peak. Dabei werden die Peptide nur zu ihrer erwarteten Retentionszeit gemessen. Die Zahl der gleichzeitig gemessenen Massenübergänge wird reduziert und Verweilzeit (*dwell-time*) sowie Zykluszeit werden optimiert, was die Effizienz der massenspektrometrischen Analyse erhöht. Aufgrund der großen Anzahl an Peptiden und der Komplexität der Matrices, für die die Methode entwickelt wurde (Darm- und Lebergewebe), wurde ein verhältnismäßig langer Gradient von 65 Minuten gewählt (Tabelle 1).

Tabelle 1: Fließmittelzusammensetzung während der Gradientenelution proteospezifischer Peptide. Fließmittel A: Acetonitril mit 0,1% Ameisensäure; Fließmittel B: Wasser mit 0,1% Ameisensäure

Zeit in Minuten	Flussrate in $\frac{\mu L}{min}$	Anteil A in %	Anteil B in %
2	200	2	98
3	200	2	98
40	200	25	75
53	200	50	50
53,1	200	60	40
56	200	60	40
56,1	200	2	98
65	200	2	98

Da es sich bei den untersuchten Enzymen um endogene Analyten handelte, stand keine entsprechende Leermatrix zur Validierung zur Verfügung. Als Leermatrix wurde daher eine Lösung von bovinen Serumalbumin ($c=2 \frac{mg}{mL}$), die zuvor mit Trypsin verdaut wurde, verwendet. Gegenüber dem Gewebe weist BSA zwar eine deutlich geringere Komplexität auf, dies ist

jedoch vertretbar, da der lange Gradient (Tabelle 1) eine effiziente Trennung der Analyten von der Matrix gewährleistet. Zudem kann bei dem gewählten experimentellen Ansatz davon ausgegangen werden, dass sich die Ionensuppression der Matrix gleichermaßen auf die Analyten und die zugehörigen isotopenmarkierten internen Standards auswirkt. Abbildung 4 zeigt ein beispielhaftes Chromatogramm aller Analyten.

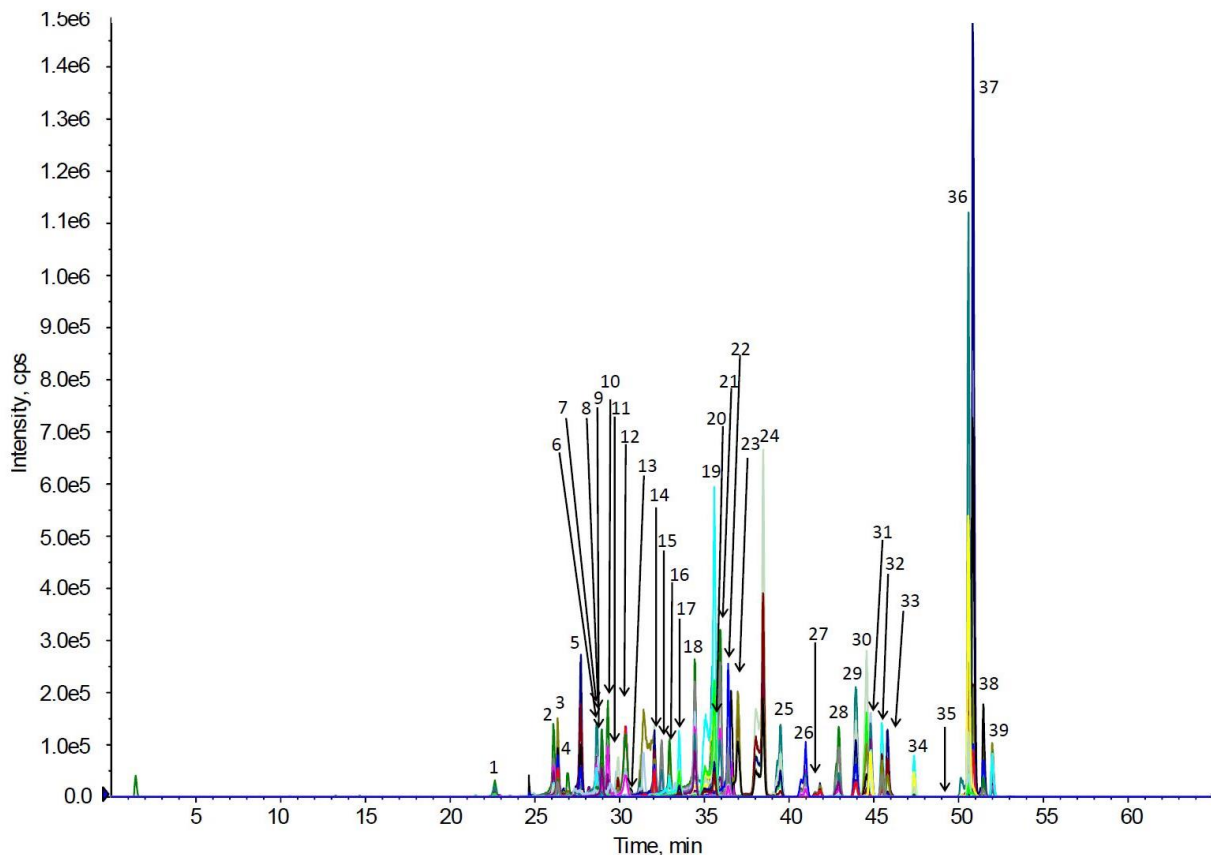


Abbildung 4: Chromatogramm einer Qualitätskontrollprobe, die alle 39 verwendeten Surrogatpeptide in einer Konzentration von $25 \frac{\text{nmol}}{\text{L}}$ in der Validierungsmatrix enthält.

Da keine expliziten Richtlinien zur Validierung von proteomischen Analysemethoden vorliegen, wurden aus den Richtlinien zur Validierung von bioanalytischen Methoden der europäischen und US-Amerikanischen Zulassungsbehörden (EMA und FDA) jene Parameter ausgewählt, die in diesem Zusammenhang sinnvoll erschienen. Die Bestimmungsgrenze betrug für alle Peptide $0,1 \frac{\text{nmol}}{\text{L}}$, mit Ausnahme von GYGVIFANGNR (CYP2B6) und VQEEIDHVLGR (CYP2C8) für die die Bestimmungsgrenze $0,25 \frac{\text{nmol}}{\text{L}}$ betrug, sowie von SVINDPIYK (UGT2B17) mit einer Bestimmungsgrenze von $0,5 \frac{\text{nmol}}{\text{L}}$. Über den gesamten Messbereich von $0,1 \frac{\text{nmol}}{\text{L}}$ bis $25 \frac{\text{nmol}}{\text{L}}$ bestand ein linearer Zusammenhang zwischen dem analytischen Signal und der Nominalkonzentration an zugegebenem Peptid. Bei sechs unabhängigen Messungen lagen die Korrelationskoeffizienten einer gewichteten Regression ($\frac{1}{x}$) zwischen 0,9793 und 1,0. Präzision und Richtigkeit der Methode lagen im

Akzeptanzbereich von $\pm 15\%$ beziehungsweise $\pm 30\%$ an der Bestimmungsgrenze. Hinsichtlich dieser Parameter ist die entwickelte Methode vergleichbar mit den bereits publizierten Methoden. Allerdings sind nur in wenigen Publikationen Angaben zur Validierung und den entsprechenden Parametern des analytischen Prozesses zu finden [42,43,45,72]. Weiterhin wurde die Stabilität der Surrogatpeptide während kritischer Schritte der Probenvorbereitung und Messung untersucht. Dies sind im Einzelnen der Verdau (16 Stunden bei 37°C), die Standzeit im gekühlten Probengeber (24 Stunden bei 4°C) und die Zwischenlagerung der Proben während der Vorbereitung bei Raumtemperatur (2 Stunden). Alle Peptide zeigten eine hinreichende Stabilität über die genannten Zeiträume (zwischen 82,6% und 118,3% des Nominalwertes).

Eine Bestimmung der Richtigkeit auf Proteinebene war nicht möglich, da die Enzyme als Analyten nicht in definierter Konzentration im Sinne eines Referenzstandards erhältlich sind. Auf dem Markt sind zwar rekombinant produzierte Mikrosomenpräparationen von nahezu allen arzneistoffmetabolisierenden Enzymen für Metabolismusversuche mit einer Konzentrationsangabe erhältlich, jedoch beruht diese Quantifizierung laut Angabe der Hersteller auf einer spektroskopischen Bestimmung des Eisenatoms der prosthetischen Häm-Gruppe (s. o.), da nur diejenigen Enzymmoleküle, die Häm enthalten, metabolisch aktiv sind. Die Präparationen enthalten jedoch auch einen wechselnden Anteil an metabolisch inaktiven Enzymmolekülen, die kein Häm enthalten. Diese werden von der massenspektrometrischen *targeted proteomics*-Methode miterfasst, weshalb die gemessenen Enzymgehalte deutlich über den Angaben der Hersteller lagen. Folglich war mit diesen rekombinant produzierten Enzymen keine Bestimmung der Richtigkeit der Methode möglich. Durch Aufarbeitung mehrerer Aliquote einer Mischung dieser rekombinant hergestellten Enzyme konnte aber die Präzision des gesamten analytischen Prozesses vom Enzym in der Probe bis zum Endergebnis bestimmt werden. Nach sechs voneinander unabhängigen Aufarbeitungen lagen die Variationskoeffizienten für die einzelnen Enzyme zwischen 5,24% und 15,51%. Diese Präzision ist für einen mehrstufigen und derart langen analytischen Prozess bemerkenswert hoch. Eine derartige Charakterisierung des gesamten Prozesses hinsichtlich seiner Präzision auf Proteinebene wurde bisher noch nicht publiziert. Außerdem konnte so gezeigt werden, dass alle Enzyme mit der Methode bestimmt werden können und dass die gewählten Peptide durch den Verdau mit Trypsin entstehen.

Zur Prüfung des analytischen Ansatzes wurde die Methode dann abschließend auf kommerziell erhältliche humane Leber- und Darmmikrosomen angewendet. Mit Ausnahme von CYP1A1 wurden alle arzneistoffmetabolisierenden Enzyme der Methode in Lebermikrosomen nachgewiesen, was die praktische Anwendbarkeit der Methode unterstreicht. Die so bestimmten Enzymmengen stehen in guter Übereinstimmung mit den Werten aus der Literatur [30,32,33,35,37,38,40,42,86–89].

3.2 Anwendung der Methode auf gepaartes Leber- und Darmgewebe von gesunden Organspendern (Publikation 2)

Die neu entwickelte und validierte Methode wurde auf eine Kohorte von elf gesunden Organspendern (8 Männer, 3 Frauen, Alter zwischen 19 und 60 Jahren) angewendet. Von diesen Organspendern lag jeweils eine Gewebeprobe aus dem Jejunum und aus der Leber vor, die wie zuvor beschrieben aufgearbeitet und vermessen wurden (Proteinquantifizierung mittels *targeted proteomics* und Genexpressionsanalyse).

Mit Ausnahme von CYP1A2 konnten alle 24 arzneistoffmetabolisierenden Enzyme auf Genebene nachgewiesen werden. Auf Proteinebene konnten in der Leber alle untersuchten Enzyme nachgewiesen werden. Einzig CYP4A11 war weder in der Leber noch im Jejunum nachweisbar. Bei CES2, CYP2C18, CYP3A4 und UGT2B17 war der Enzymgehalt im Jejunum höher oder vergleichbar gegenüber dem Gehalt in der Leber. Der hohe Gehalt an CYP3A4 in Darmgewebe wurde in dieser Studie erneut bestätigt und unterstreicht noch einmal die große Wichtigkeit des intestinalen CYP3A4-Metabolismus, dessen Effekte in zahlreichen Studien demonstriert wurden [17,90,91]. Der Gehalt von CYP4F2 als zweithäufigstes Enzym im Jejunum steht im Einklang mit den Ergebnissen anderer Studien [36,39]. Die Relevanz dieses Enzymes für den *first-pass*-Effekt bleibt dagegen fraglich, worauf später noch eingegangen wird. Die vergleichsweise hohen Gehalte von CYP2C9 (10%) und CYP2C19 (6%) im Darm sind ebenfalls aus der Literatur bekannt. [31,34–36,39]. Die beträchtliche Menge an CYP2C18 (6%) hingegen wurde in dieser Studie erstmalig beschrieben. Aufgrund der großen Überschneidungen der Substrate von CYP2C18 und CYP2C9 und/oder CYP2C19 ist die klinische Bedeutung von CYP2C18 allein aber nicht abschätzbar. Trotz geringer mRNA-Expression konnten CYP1A1, CYP2A6, CYP2B6, CYP2C8, CYP2E1, CYP3A7, CYP4A11 und UGT2B15 im Jejunum auf Proteinebene nicht nachgewiesen werden.

Bei den anderen Enzymen hingegen war der Gehalt in der Leber größer. Neben den bereits häufig untersuchten Enzymen wurden CYP2A6 und CYP4F2 in der Leber mit jeweils 7-8% nachgewiesen, was auf einen relevanten Beitrag dieser Enzyme zum *first-pass*-Metabolismus schließen lässt. Substrate von CYP2A6 sind unter anderem Valproinsäure, Dapagliflozin, Efavirenz und Tegafur. Fingolimod und Pafuramidin werden bevorzugt von CYP4F2 verstoffwechselt. Ein Blick auf die Pharmakokinetik dieser Arzneistoffe spricht jedoch gegen einen relevanten Beitrag dieser Enzyme zum *first-pass*-Metabolismus und zeigt eher, dass diese gut und mit hoher oraler Bioverfügbarkeit absorbiert werden. So führt eine Hemmung von CYP4F2 durch Ketoconazol zu einer vergleichsweise geringen, 1,7-fachen Vergrößerung der AUC von Fingolimod und eine Induktion durch Carbamazepin reduziert die AUC nur um etwa 40% [92].

Jejunum und Leber wiesen jeweils ein charakteristisches Muster hinsichtlich ihrer Enzymgehalte auf. Während CYP2E1 (30%), CYP2C9 (24%) und CYP3A4/CYP1A2/CYP2C8/CYP2A6 (jeweils etwa 7-8%) in der Leber die größten Anteile aufwiesen, sind dies im Jejunum CYP3A4 (56%), CYP4F2 (15%) und CYP2C9 (10%). Dies wurde auch bei den Phase-II-Enzymen beobachtet, bei denen in der Leber UGT2B7 (52%), UGT1A1 (28%) und UGT2B15 (15%) den größten Anteil ausmachten und im Jejunum UGT2B17 (47%), UGT1A1 (30%) und UGT2B7 (23%). Diese Rangordnung der Enzyme deckt sich mit den Befunden früherer Studien aus der eigenen und anderer Arbeitsgruppen. Bei den absoluten Enzymgehalten sind jedoch Unterschiede, besonders im Vergleich mit den Ergebnissen anderer Arbeitsgruppen sichtbar. Diese Unterschiede sind aus der Literatur bekannt und auf unterschiedliche Techniken bei der Probenvorbereitung, verschiedene Surrogatpeptide und unterschiedliche massenspektrometrische Ansätze zurückzuführen [93,94].

Von den untersuchten Phase-II-Enzymen wiesen UGT2B7, UGT1A1 und UGT2B15 die höchsten Enzymgehalte in der Leber auf, während dies im Jejunum für UGT2B17, UGT1A1 und UGT2B7 der Fall war. Dieses Muster ist aus anderen Studien bekannt, in denen allerdings ungepaarte Darm- und Leberproben untersucht wurden. Bemerkenswert ist hier die große Überschneidung der Expression von UGT1A1 und UGT2B7 in Jejunum und Leber, die eine Erklärung für die ausgeprägte Glucuronidierung von beispielsweise Morphin, Ezetimib und Mycophenolat sein könnte [95,96]. Im Jejunum war UGT2B17 das Phase-II-Enzym mit dem höchsten Gehalt, was auch in einer weiteren Studie berichtet wurde [97]. Über klinisch relevante pharmakokinetische Effekte, die auf der Expression von UGT2B17 basieren, ist bisher nur wenig bekannt. UGT2B17 zeigt jedoch einen hohen Grad an Polymorphie, was zu großen Unterschieden in der Expression führt [98], die auch in dieser Studie sichtbar sind. So beträgt der Variationskoeffizient des UGT2B17-Gehaltes in der Leber 162,2% und im Jejunum 96,7%. Eine aktuelle Studie gibt einen Hinweis darauf, dass der intestinale Metabolismus durch polymorphes UGT2B17 die Pharmakokinetik von oral appliziertem Diclofenac beeinflussen könnte [99].

Bei den Carboxylesterasen zeigten sich ebenfalls deutliche Unterschiede zwischen Jejunum und Leber. Die CES1 wird in der Leber deutlich stärker exprimiert als im Jejunum, was sowohl auf Gen- als auch auf Proteinebene sichtbar ist. Für die CES2 verhält es sich genau andersherum: Diese wird im Jejunum höher exprimiert, wie Genexpressionsanalyse und *targeted proteomics* übereinstimmend zeigen. Dies lässt auf einen Beitrag der CES2 zum intestinalen *first-pass*-Metabolismus schließen. In der Literatur gibt es Hinweise auf eine Beteiligung der CES2 an der späten Diarrhoe als dosislimitierender Nebenwirkung von Irinotecan, das durch Carboxylesterasen zu SN-38 aktiviert wird, welches eine höhere zytotoxische Wirkung aufweist und den aktiven Metaboliten darstellt. Durch eine Hemmung

der CES2 mit Loperamid oder Telmisartan konnte diese Nebenwirkung abgemildert werden [100,101]. Der hohe Gehalt an CES1 in der Leber ist bereits beschrieben worden und wird für den *first-pass*-Metabolismus von Clopidogrel, Oseltamivir und Methylphenidat verantwortlich gemacht [32,38,102].

Bemerkenswert ist weiterhin die hohe interindividuelle Variabilität in beiden untersuchten Organen, sowohl auf Protein- als auch auf Genebene, wobei im Darmgewebe eine deutlich höhere Variabilität beobachtet werden konnte. Der Variationskoeffizient beträgt im Mittel aller untersuchten Enzyme $89,3 \pm 67,8\%$ in der Leber und $106,6 \pm 70,3\%$ im Jejunum bei der Proteinquantifizierung. Auf Ebene der Genexpression ist diese Variabilität mit $84,5 \pm 43,8\%$ in der Leber gegenüber $117,3 \pm 65,7\%$ im Jejunum noch ausgeprägter. Ursächlich könnte hier der direkte Kontakt des Darms mit Umwelteinflüssen wie der Nahrung sein. Auch die individuell unterschiedliche Mikrobiota beeinflusst die Expression und Regulation zahlreicher Gene, sodass ein Einfluss auf arzneistoffmetabolisierende Enzyme wahrscheinlich ist.

Signifikante Korrelationen zwischen Genexpression und Proteingehalt wurden im Jejunum nur in zwei von 15 möglichen Fällen gefunden, in der Leber hingegen in 13 von 23 möglichen Fällen. Dieses Ergebnis steht im Einklang mit anderen Studien, die ebenfalls deutlich aussagekräftigere Korrelationen in der Leber berichtet haben [28,35]. Dies unterstreicht noch einmal, dass sich aus der Genexpression nicht direkt auf die Proteinmenge schließen lässt, was wiederum einen Hinweis auf etwaige regulatorische Mechanismen gibt.

Nur für CYP3A4 und UGT1A3 wurden signifikante Korrelationen zwischen den Enzymgehalten in Jejunum und Leber festgestellt. Dies demonstriert, dass innerhalb eines Individuums die Kenntnis der Ausstattung des Darms hinsichtlich arzneistoffmetabolisierender Enzyme keine Aussagen über diese Enzyme in der Leber zulässt. Vielmehr zeigt dies, dass es sich bei den beiden Organen um unterschiedliche stoffwechselaktive Kompartimente handelt, die sich gegenseitig ergänzen und so gemeinsam einen effizienten Fremdstoffmetabolismus gewährleisten.

3.3 Anwendung der Methode auf eine Kohorte von Patienten mit Einschränkungen der Leberfunktion verschiedener Genese (Publikation 3)

Aus der Literatur ist bekannt, dass einige Wirkstoffe bei der Anwendung in Patienten mit fortgeschrittener Leberschädigung eine veränderte Pharmakokinetik gegenüber gesunden Patienten aufweisen [103–105]. Daher ist davon auszugehen, dass mit dem Fortschreiten der Leberschädigung auch die metabolische Aktivität des Organs abnimmt. Ziel dieser Arbeit war es, diese Veränderungen auf der Ebene der arzneistoffmetabolisierenden Enzyme zu untersuchen. Dazu wurden die Patienten einmal hinsichtlich des Grades der Leberschädigung,

ausgedrückt durch den Child-Pugh-Score [62], stratifiziert und einmal hinsichtlich der der Leberschädigung zugrundeliegenden Erkrankung. Es wurden sowohl die mRNA-Expression als auch der Enzymgehalt der Gewebeproben untersucht.

Zunächst wurde eine deutliche Verminderung des Gesamtgehaltes an Enzymen festgestellt. In Child-Pugh-Klasse C betrug der Enzymgehalt nur noch 52%, verglichen mit der gesunden Kontrollgruppe. Hinsichtlich des Child-Pugh-Scores wurden Veränderungen auf Gen- und Proteinebene sowohl bei CYP- als auch bei UGT-Enzymen beobachtet. Eine verschlechterte Leberfunktion war mit einem verminderten Gehalt von CYP1A2, CYP2C8, CYP2C9, CYP2E1, CYP3A4 und UGT2B7 assoziiert. Dagegen blieben die Gehalte von CYP1A1, CYP2B6, CYP2C19, CYP2D6, UGT1A1, UGT1A3 und UGT2B15 unverändert.

Bei einer Betrachtung der zugrundeliegenden Krankheiten ergibt sich ein differenziertes Bild. Bei allen Erkrankungen wurden bei CYP2C9, CYP2C19, UGT1A1, UGT1A3 und UGT2B15 keine Veränderungen gegenüber den Kontrollproben gefunden, während die anderen untersuchten Enzyme herunterreguliert waren. Die prozentuale Verteilung der Enzyme war bei allen Erkrankungen ebenfalls deutlich verändert.

Bei den cholestatischen Krankheitsbildern fällt besonders eine Verminderung des Enzymgehaltes von CYP1A1 auf. Dieses wurde hier nur zu 0,03% in PBC und 0,04% in PSC gegenüber den Kontrollen gefunden. In PBC wurde eine Herunterregulation von CYP2B6 (44%), CYP2C8 (28%), CYP2E1 (39%) und CYP3A4 (47%) beobachtet. Beim Krankheitsbild HCV war Verminderung von CYP2E1 (52%) und UGT2B7 (49%) besonders auffällig. Die ALD war durch eine breite Reduktion des Gehaltes von Enzymen, nämlich CYP1A2 (33%), CYP2C8 (32%), CYP2D6 (14%), CYP2E1 (34%), CYP3A4 (27%) und UGT2B7 (47%), gekennzeichnet. Dagegen wurden für AIH keine signifikanten Veränderungen festgestellt. Die größten Veränderungen wurden bei ALD und PSC gefunden, bei denen sechs und fünf der 13 untersuchten Enzyme signifikant herunterreguliert waren. Als empfindlichstes Enzym wurde CYP2E1 identifiziert, das als einziges schon in der Child-Pugh-Klasse A eine signifikante Reduktion zeigte.

Aus der Literatur ist bereits bekannt, dass eine Beeinträchtigung der Leberfunktion pharmakokinetische Auswirkungen hat, die wiederum die Sicherheit und Effizienz einer Arzneitherapie beeinflussen können. Aufgrund des großen Aufwandes und der ethischen Bedenken, die mit klinischen Studien verbunden sind, ist die Datenlage zu pharmakokinetischen Auswirkungen von herabgesetzter Leberfunktion limitiert. Die Daten aus dieser Studie stellen eine Annäherung auf Gen- und Proteinebene dar und können helfen, das Ausmaß der verbleibenden metabolischen Aktivität abzuschätzen. Im Gegensatz zu früheren Studien, die eine Charakterisierung klinisch relevanter Stoffwechsellzyme in Abhängigkeit zu vorliegenden Lebererkrankungen vornahmen [38,39,48,106,107], wurden in dieser Studie

erstmalig quantitative Daten zu arzneistoffmetabolisierenden Enzymen, über ein breites Spektrum von Lebererkrankungen hinweg und in Abhängigkeit des Child-Pugh-Scores, publiziert. Diese Daten können von großem Nutzen für die Erstellung von PBPK-Modellen zur Abschätzung der pharmakokinetischen Auswirkungen der untersuchten Leberfunktionseinschränkungen sein.

3.4 Entwicklung, Validierung und Anwendung einer *targeted proteomics* Methode zur Quantifizierung nukleärer Rezeptoren (Publikation 4)

Nach den bereits genannten Kriterien für Surrogatpeptide wurden geeignete Peptide zunächst *in-silico* ausgewählt und in hochreiner Form isotoopenmarkiert und unmarkiert erworben. Dabei wurde für jeden nukleären Rezeptor ein Surrogatpeptid bestellt, das gleichzeitig als *Qualifier* und *Quantifier* dient. Die massenspektrometrischen Parameter wurden für jedes Peptid manuell optimiert, sodass eine LC-MS/MS-Methode für 14 Peptide (sieben unmarkierte Peptide und sieben isotoopenmarkierte Peptide) erstellt wurde. Um eine effiziente Abtrennung der Matrix zu erreichen und damit die Empfindlichkeit der Methode zu erhöhen, wurde eine verhältnismäßig lange Gradientenelution über 60 Minuten gewählt (vgl. Tabelle 1).

Zur Validierung der Methode wurde erneut eine Vereinfachung der Matrix durch den Einsatz von mit Trypsin verdautem humanem Serumalbumin (HSA) vorgenommen. Auch diese Matrix zeigte keine Interferenzen mit den Peptiden, was die Selektivität der Methode beweist. Eine lineare Korrelation zwischen analytischem Signal und Peptidkonzentration war über den gesamten Messbereich, der auf 0,1 bis 50 $\frac{nmol}{L}$ festgelegt wurde, gegeben. Auch an der Bestimmungsgrenze war das Signal-Rausch-Verhältnis mindestens 5:1 gegenüber der Leermatrix. Die Korrelationskoeffizienten der Kalibrationsgeraden lagen im Bereich von 0.9976 bis 0.9999 nach sechs Bestimmungen. Die Präzision der Methode am selben Tag (*within day*) lag zwischen 0,8% und 7,6%, während sie an verschiedenen Tagen (*between day*) zwischen 2,7% und 9,3% betrug. Die Werte für die Richtigkeit betrugen -2,5% bis 6,5% an verschiedenen Tagen und -3,5% bis 13,2% am selben Tag. Damit entspricht die Methode den Anforderungen international gültiger Richtlinien, die eine Abweichung von maximal 15% zulassen. Dies gilt ebenso für die Stabilität der Peptide. Diese lag für die Lagerung der Proben im Probengeber (24 Stunden bei 4°C) zwischen 93,6% und 104,6% und die Auftau-Einfrier-Stabilität zwischen 85,8% und 106,6% der Nominalwerte. Das Ausmaß des Matrixeffektes wurde auf 82,8% bis 113,8% bestimmt. Dieser Wert bezieht sich zwar auf die vereinfachte Matrix HSA, jedoch unterliegen in einer Realprobe der Analyt und der interne Standard gleichermaßen dem Effekt der jeweiligen Matrix, sodass der Einfluss auf das Messergebnis kompensiert wird.

Da PXR und CAR eine besonders wichtige Rolle bei der Regulation der Expression von arzneistoffmetabolisierenden Enzymen spielen, wurden stabil transfizierte Zelllinien generiert, die die jeweiligen nukleären Rezeptoren überexprimierten und als Positivkontrolle der Methode dienten. Nach der beschriebenen Aufarbeitung wurden beide Rezeptoren in der jeweiligen Zelllinie nachgewiesen, was die grundsätzliche Anwendbarkeit der Methode auf biologische Proben zeigt.

In der Genexpressionsanalyse wurde eine signifikant höhere Expression von PXR, HNF4 α und SHP im Jejunum, verglichen mit der Leber, nachgewiesen. Für CAR und FXR ergab sich ein umgekehrtes Bild, denn diese wurden in der Leber signifikant stärker exprimiert. Es wird vermutet, dass PXR eine größere Rolle bei der Regulation im Darm spielt und CAR an der Regulation in der Leber beteiligt ist [56,57,60]. Diese Vermutung wird durch die höhere Genexpression von PXR im Jejunum und von CAR in der Leber in dieser Arbeit unterstützt. Auf Proteinebene waren in den genannten Geweben nur AhR und HNF4 α überhaupt messbar. Für die anderen nukleären Rezeptoren konnten keine Messsignale identifiziert werden. Diese beiden nukleären Rezeptoren waren jedoch auch diejenigen, die auf Genebene die höchste Expression zeigten, sodass davon ausgegangen werden kann, dass die niedrigere Transkription der anderen Rezeptoren auch zu niedrigeren Proteingehalten führt. Für beide Rezeptoren wurde zudem ein signifikant höherer Proteingehalt in der Leber gegenüber dem Jejunum gefunden. Dies zeigte sich jedoch nicht in der Genexpressionsanalyse, bei der im Jejunum höhere Werte gemessen wurden. Hier zeigt sich erneut, dass Genexpression und Proteingehalt nicht notwendigerweise korrelieren. Der sehr geringe Proteingehalt hängt möglicherweise damit zusammen, dass die nukleären Rezeptoren schon von äußerst geringen Ligandkonzentrationen aktiviert werden und die Transkriptionsaktivität um ein Vielfaches steigern können.

Wie bereits erwähnt, spielt der Darm eine wichtige Rolle im *first-pass*-Metabolismus, sodass hier eine genauere Betrachtung einzelner Darmabschnitte sinnvoll ist. Auf Genebene wurde PXR in allen untersuchten Darmabschnitten (Jejunum, Ileum, Colon) stärker exprimiert als CAR. Diese Ergebnisse bestätigen frühere Untersuchungen [61,108]. Wie auch in der Leber, konnten in allen Darmabschnitten nur HNF4 α und AhR nachgewiesen werden, wobei für HNF4 α deutlich höhere Proteingehalte gefunden wurden.

Von den genannten nukleären Rezeptoren sind besonders PXR und CAR von großer klinischer Relevanz, da sie an der Regulation wichtiger arzneistoffmetabolisierender Enzyme beteiligt sind [56–58]. Diese Arbeit stellt die erste Publikation einer LC-MS/MS basierten *targeted proteomics*-Methode zur Quantifizierung von sieben nukleären Rezeptoren, die an der Regulation von arzneistoffmetabolisierenden Enzymen beteiligt sind, dar. Die Methode erfüllt zudem wichtige Kriterien der derzeit gültigen Richtlinien für bioanalytische Methoden.

Aufgrund der sehr geringen Proteingehalte der Gewebe konnten nur HNF4 α und AhR in Gewebeproben quantifiziert werden, während die Messung für CAR und PXR in überexprimierenden Zellen gelang. Die erhobenen Daten zur Genexpression und zu den Proteingehalten können einen Beitrag zum Verständnis der Regulation von arzneistoffmetabolisierenden Enzymen in den untersuchten Geweben leisten und helfen, Arzneimittelwechselwirkungen besser abzuschätzen.

4 Zusammenfassung und Ausblick

Die orale Einnahme stellt für Patienten die einfachste und unkomplizierteste Möglichkeit dar, ein Arzneimittel zu applizieren und ist das angestrebte Ziel der Arzneimittelentwicklung. Dem entgegen stehen jedoch die evolutionär entstandenen Möglichkeiten des Körpers, aufgenommene Fremdstoffe zu inaktivieren und zu eliminieren. Ein Zusammenspiel aus anatomischen Gegebenheiten und den Enzymen des Fremdstoffmetabolismus sorgt dafür, dass ein Teil der oral applizierten Dosis bereits verstoffwechselt wird, bevor er über das arterielle System an den Wirkort gelangen kann (*first-pass-Effekt*). Als Ort dieses Metabolismus wurde, neben der Leber, auch der Darm identifiziert. Um das Ausmaß des *first-pass-Effektes* abschätzen zu können, werden Daten über den Gehalt der arzneistoffmetabolisierenden Enzyme in diesen Organen benötigt. Als Methode der Wahl bietet sich dazu die LC-MS/MS an, da mit ihr verschiedene Enzyme in einem analytischen Lauf bestimmt werden können und sie sich durch eine hohe Empfindlichkeit, Reproduzierbarkeit und Spezifität auszeichnet.

Mit der vorliegenden Arbeit wurde das analytische Spektrum der bisher publizierten Methoden zur Bestimmung von CYP- und UGT-Enzymen erweitert. Mit der neuen Methode können nun zwei Carboxylesterasen, 17 CYP-Enzyme und fünf UGT-Enzyme quantifiziert werden. Weiterhin wurde die Methode anhand von Richtlinien für bioanalytische Methoden umfassend validiert. Durch die Verwendung von rekombinant hergestellten arzneistoffmetabolisierenden Enzymen konnte der gesamte analytische Prozess, von der Probe bis zum Endergebnis, erstmalig umfassend charakterisiert werden. Dabei zeigte sich eine, für einen derart komplexen Prozess bemerkenswerte Präzision von maximal 15,5% Variation nach sechsmaliger Durchführung.

Die entwickelte Methode wurde dann auf gepaarte Proben aus Leber und Jejunum von elf gesunden Organspendern angewendet. Im Jejunum wurden CES1, CES2, CYP2C9, CYP2C18, CYP2C19, CYP2D6, CYP2J2, CYP3A4, CYP3A5, CYP4F2, CYP4F12, UGT1A1, UGT1A3, UGT2B7 und UGT2B17 gefunden. In der Leber konnten alle untersuchten Enzyme (CES1, CES2, CYP1A1, CYP1A2, CYP2A6, CYP2B6, CYP2C8, CYP2C9, CYP2C18, CYP2C19, CYP2D6, CYP2E1, CYP2J2, CYP3A4, CYP3A5, CYP3A7, CYP4F2, CYP4F12, UGT1A1, UGT1A3, UGT2B7, UGT2B15 und UGT2B17), bis auf CYP4A11 nachgewiesen werden. Für einige Enzyme (CES2, CYP2C18, CYP2C19, CYP2J2, CYP3A4, CYP4F2, CYP4F12) wurden im Jejunum Enzymgehalte gemessen, die mit denen in der Leber vergleichbar sind, was noch einmal unterstreicht, dass der Darm auch als klinisch relevanter Ort des Arzneistoffmetabolismus betrachtet werden muss. Auffällig war hier zudem die deutlich höhere Variabilität in den Darmproben, verglichen mit den Leberproben, die ihre Ursache in Umwelteinflüssen oder dem Mikrobiom des Darms haben könnten. Außerdem wurde die

Expression der zugehörigen Gene mittels quantitativer *real-time* PCR untersucht. Hier bestand nur in einigen Fällen eine signifikante Korrelation zwischen Genexpression und Proteingehalt, was für zwischengeschaltete regulatorische Mechanismen spricht.

Weiterhin wurden mit dieser Methode Leberproben einer Kohorte von Patienten mit Krankheitsbildern, die mit einer Einschränkung der Leberfunktion einhergehen, untersucht. Dazu wurden die Patienten nach der verbleibenden Leberfunktion (Child-Pugh-Score) und nach der zugrundeliegenden Erkrankung eingeteilt. Es zeigt sich eine generelle Abnahme des Gehaltes an arzneistoffmetabolisierenden Enzymen mit fortschreitender Verschlechterung der Leberfunktion, wobei sich CYP2E1 als besonders anfällig erwiesen hat und bereits in Child-Pugh-Klasse A signifikant erniedrigt war. Bei den verschiedenen Erkrankungen zeigt sich ein uneinheitliches Bild, die prozentuale Verteilung der Enzyme ist jedoch bei allen Erkrankungen gegenüber den gesunden Kontrollproben verändert.

Über die Regulation der Expression von arzneistoffmetabolisierenden Enzymen ist bisher noch wenig bekannt. Es gibt aber Hinweise aus der Literatur, dass bestimmte nukleäre Rezeptoren an der Regulation der Enzyme beteiligt sein können. Deshalb wurde eine LC-MS/MS-basierte *targeted-proteomics*-Methode zur Quantifizierung von nukleären Rezeptoren in Darm- und Lebergewebe entwickelt und validiert. Im Gewebe konnten nur AhR und HNF4 α nachgewiesen werden, da die Empfindlichkeit des verwendeten experimentellen Ansatzes vermutlich nicht ausreichend ist. Dabei war HNF4 α in Darmgewebe deutlich höher exprimiert als AhR. Außerdem wurde die Expression der nukleären Rezeptoren auf Genebene durch quantitative *real-time* PCR untersucht. Dabei wurde eine höhere Expression von CAR in der Leber gefunden, während PXR in Darm stärker exprimiert wird. Dies entspricht den Erkenntnissen aus der Literatur, nach denen CAR einen regulatorischen Effekt auf arzneistoffmetabolisierende Enzyme in der Leber hat, während dies für PXR in Darm zutrifft. Diese Arbeit kann einen Beitrag zum weitergehenden Verständnis der Regulation von arzneistoffmetabolisierenden Enzymen durch nukleäre Rezeptoren beitragen.

Bei allen diesen Arbeiten gilt es zu beachten, dass das Vorhandensein eines Proteins nicht zwangsläufig mit seiner Aktivität gleichzusetzen ist. Jedoch zeigen zahlreiche Beispiele aus der Literatur, dass sich mit den Daten aus *Proteomics*-Studien PBPK-Modelle aufstellen lassen, die die in klinischen Studien erhobenen Daten mit beeindruckender Genauigkeit reproduzieren können [25–27,109–113]. Die Gewinnung von Probenmaterial stellt jedoch die Wissenschaftler auf diesem Gebiet vor große Herausforderungen. Als vielversprechend hat sich vor diesem Hintergrund die so genannte flüssige Biopsie (*liquid biopsy*) erwiesen. Dieser Ansatz beruht darauf, dass alle Organe extrazelluläre Vesikel (*small extracellular vesicles*; sEVs) in das Blut abgeben. Mittels immunchemischer Methoden ist es gelungen, diese Vesikel nach den Organen ihrer Herkunft spezifisch aus dem Blut anzureichern. Der Inhalt dieser

Vesikel ist repräsentativ für das Organ ihrer Herkunft, sodass arzneistoffmetabolisierende Enzyme in leberspezifischen Vesikeln quantifiziert werden konnten [114]. Zusammen mit dem technischen Fortschritt auf dem Gebiet der Massenspektrometrie, der diese Geräte immer empfindlicher werden lässt, stellt dies einen vielversprechenden Ansatz dar. Der große Vorteil liegt in der einfachen Gewinnung von Blutproben, wodurch die Untersuchung großer Kohorten ermöglicht wird. Ob damit wirklich das „goldene Zeitalter der translationalen Pharmakokinetik“ angebrochen ist, wie einige Autoren behaupten [115], wird die Zukunft zeigen.

5 Literaturverzeichnis

- 1 Eichelbaum M, Schwab M. Wirkungen des Organismus auf Pharmaka: allgemeine Pharmakokinetik. In: *Allgemeine und spezielle Pharmakologie und Toxikologie*. (Hrsg. Aktories K, Förstermann U, Hofmann FB, Starke K), 10. Aufl. Elsevier, Urban & Fischer, 2013: 36–61.
- 2 Guengerich FP. Cytochrome p450 and chemical toxicology. *Chemical research in toxicology* 2008; **21**(1): 70–83.
- 3 Mak PJ, Denisov IG. Spectroscopic studies of the cytochrome P450 reaction mechanisms. *Biochimica et biophysica acta. Proteins and proteomics* 2018; **1866**(1): 178–204.
- 4 Denisov IG, Makris TM, Sligar SG, Schlichting I. Structure and chemistry of cytochrome P450. *Chemical reviews* 2005; **105**(6): 2253–77.
- 5 Laizure SC, Herring V, Hu Z, Witbrodt K, Parker RB. The role of human carboxylesterases in drug metabolism: have we overlooked their importance? *Pharmacotherapy* 2013; **33**(2): 210–22.
- 6 Di L. The Impact of Carboxylesterases in Drug Metabolism and Pharmacokinetics. *Current drug metabolism* 2019; **20**(2): 91–102.
- 7 Yan B. Carboxylesterases. In: *Encyclopedia of Drug Metabolism and Interactions*. (ed. Lyubimov AV). John Wiley & Sons, Inc, 2011.
- 8 Zou L-W, Jin Q, Wang D-D *et al.* Carboxylesterase Inhibitors: An Update. *Current medicinal chemistry* 2018; **25**(14): 1627–49.
- 9 Satoh T, Hosokawa M. Carboxylesterases: Structure, Function and Polymorphism. *Biomolecules and Therapeutics* 2009; **17**(4): 335–47.
- 10 Satoh T, Hosokawa M. Structure, function and regulation of carboxylesterases. *Chemico-biological interactions* 2006; **162**(3): 195–211.
- 11 Rendic S, Guengerich FP. Contributions of human enzymes in carcinogen metabolism. *Chemical research in toxicology* 2012; **25**(7): 1316–83.
- 12 Meyer UA. Overview of enzymes of drug metabolism. *Journal of pharmacokinetics and biopharmaceutics* 1996; **24**(5): 449–59.
- 13 Benedetti MS, Whomsley R, Poggesi I *et al.* Drug metabolism and pharmacokinetics. *Drug metabolism reviews* 2009; **41**(3): 344–90.
- 14 Yin H, Bennett G, Jones JP. Mechanistic studies of uridine diphosphate glucuronosyltransferase. *Chemico-biological interactions* 1994; **90**(1): 47–58.
- 15 Radomska-Pandya A, Bratton SM, Redinbo MR, Miley MJ. The crystal structure of human UDP-glucuronosyltransferase 2B7 C-terminal end is the first mammalian UGT target to be revealed: the significance for human UGTs from both the 1A and 2B families. *Drug metabolism reviews* 2010; **42**(1): 133–44.
- 16 Kaminsky LS, Zhang Q-Y. The small intestine as a xenobiotic-metabolizing organ. *Drug metabolism and disposition: the biological fate of chemicals* 2003; **31**(12): 1520–5.
- 17 Paine MF, Shen DD, Kunze KL *et al.* First-pass metabolism of midazolam by the human intestine. *Clinical pharmacology and therapeutics* 1996; **60**(1): 14–24.
- 18 Skottheim IB, Jakobsen GS, Stormark K *et al.* Significant increase in systemic exposure of atorvastatin after biliopancreatic diversion with duodenal switch. *Clinical pharmacology and therapeutics* 2010; **87**(6): 699–705.

- 19 Thummel KE, O'Shea D, Paine MF *et al.* Oral first-pass elimination of midazolam involves both gastrointestinal and hepatic CYP3A-mediated metabolism. *Clinical pharmacology and therapeutics* 1996; **59**(5): 491–502.
- 20 Tomalik-Scharte D, Jetter A, Kinzig-Schippers M *et al.* Effect of propiverine on cytochrome P450 enzymes: a cocktail interaction study in healthy volunteers. *Drug metabolism and disposition: the biological fate of chemicals* 2005; **33**(12): 1859–66.
- 21 Peters SA, Jones CR, Ungell A-L, Hatley OJD. Predicting Drug Extraction in the Human Gut Wall: Assessing Contributions from Drug Metabolizing Enzymes and Transporter Proteins using Preclinical Models. *Clinical pharmacokinetics* 2016; **55**(6): 673–96.
- 22 Lin JH, Chiba M, Baillie TA. Is the role of the small intestine in first-pass metabolism overemphasized? *Pharmacological reviews* 1999; **51**(2): 135–58.
- 23 Alqahtani S, Bukhari I, Albassam A, Alenazi M. An update on the potential role of intestinal first-pass metabolism for the prediction of drug-drug interactions: the role of PBPK modeling. *Expert opinion on drug metabolism & toxicology* 2018; **14**(6): 625–34.
- 24 Lin W, Chen Y, Unadkat JD, Zhang X, Di Wu, Heimbach T. Applications, Challenges, and Outlook for PBPK Modeling and Simulation: A Regulatory, Industrial and Academic Perspective. *Pharmaceutical research* 2022; **39**(8): 1701–31.
- 25 Bansal S, Ladumor MK, Paine MF, Unadkat JD. A physiologically-based pharmacokinetic model for cannabidiol in healthy adults, hepatically-impaired adults, and children. *Drug Metab Dispos* 2023.
- 26 Bansal S, Maharao N, Paine MF, Unadkat JD. Predicting the Potential for Cannabinoids to Precipitate Pharmacokinetic Drug Interactions via Reversible Inhibition or Inactivation of Major Cytochromes P450. *Drug Metab Dispos* 2020; **48**(10): 1008–17.
- 27 Ladumor MK, Storelli F, Liang X *et al.* Predicting changes in the pharmacokinetics of CYP3A-metabolized drugs in hepatic impairment and insights into factors driving these changes. *CPT: pharmacometrics & systems pharmacology* 2023; **12**(2): 261–73.
- 28 Ohtsuki S, Schaefer O, Kawakami H *et al.* Simultaneous absolute protein quantification of transporters, cytochromes P450, and UDP-glucuronosyltransferases as a novel approach for the characterization of individual human liver: comparison with mRNA levels and activities. *Drug metabolism and disposition: the biological fate of chemicals* 2012; **40**(1): 83–92.
- 29 Oswald S, Gröer C, Drozdik M, Siegmund W. Mass spectrometry-based targeted proteomics as a tool to elucidate the expression and function of intestinal drug transporters. *The AAPS journal* 2013; **15**(4): 1128–40.
- 30 Achour B, Russell MR, Barber J, Rostami-Hodjegan A. Simultaneous quantification of the abundance of several cytochrome P450 and uridine 5'-diphospho-glucuronosyltransferase enzymes in human liver microsomes using multiplexed targeted proteomics. *Drug metabolism and disposition: the biological fate of chemicals* 2014; **42**(4): 500–10.
- 31 Al-Majdoub ZM, Couto N, Achour B *et al.* Quantification of Proteins Involved in Intestinal Epithelial Handling of Xenobiotics. *Clinical pharmacology and therapeutics* 2020.
- 32 Basit A, Neradugomma NK, Wolford C *et al.* Characterization of Differential Tissue Abundance of Major Non-CYP Enzymes in Human. *Molecular pharmaceutics* 2020; **17**(11): 4114–24.
- 33 Couto N, Al-Majdoub ZM, Achour B, Wright PC, Rostami-Hodjegan A, Barber J. Quantification of Proteins Involved in Drug Metabolism and Disposition in the Human Liver Using Label-Free Global Proteomics. *Molecular pharmaceutics* 2019; **16**(2): 632–47.

- 34 Couto N, Al-Majdoub ZM, Gibson S *et al.* Quantitative Proteomics of Clinically Relevant Drug-Metabolizing Enzymes and Drug Transporters and Their Intercorrelations in the Human Small Intestine. *Drug Metab Dispos* 2020; **48**(4): 245–54.
- 35 Drozdik M, Busch D, Lapczuk J *et al.* Protein Abundance of Clinically Relevant Drug-Metabolizing Enzymes in the Human Liver and Intestine: A Comparative Analysis in Paired Tissue Specimens. *Clinical pharmacology and therapeutics* 2018; **104**(3): 515–24.
- 36 Grangeon A, Clermont V, Barama A, Gaudette F, Turgeon J, Michaud V. Determination of CYP450 Expression Levels in the Human Small Intestine by Mass Spectrometry-Based Targeted Proteomics. *IJMS* 2021; **22**(23).
- 37 Harbourt DE, Fallon JK, Ito S *et al.* Quantification of human uridine-diphosphate glucuronosyl transferase 1A isoforms in liver, intestine, and kidney using nanobore liquid chromatography-tandem mass spectrometry. *Analytical chemistry* 2012; **84**(1): 98–105.
- 38 Prasad B, Bhatt DK, Johnson K *et al.* Abundance of Phase 1 and 2 Drug-Metabolizing Enzymes in Alcoholic and Hepatitis C Cirrhotic Livers: A Quantitative Targeted Proteomics Study. *Drug metabolism and disposition: the biological fate of chemicals* 2018; **46**(7): 943–52.
- 39 Wegler C, Wiśniewski JR, Robertsen I *et al.* Drug Disposition Protein Quantification in Matched Human Jejunum and Liver From Donors With Obesity. *Clinical pharmacology and therapeutics* 2022; **111**(5): 1142–54.
- 40 Zhang H, Wolford C, Basit A *et al.* Regional Proteomic Quantification of Clinically Relevant Non-Cytochrome P450 Enzymes along the Human Small Intestine. *Drug Metab Dispos* 2020; **48**(7): 528–36.
- 41 Ölander M, Wiśniewski JR, Artursson P. Cell-type-resolved proteomic analysis of the human liver. *Liver international official journal of the International Association for the Study of the Liver* 2020; **40**(7): 1770–80.
- 42 Grangeon A, Clermont V, Barama A, Gaudette F, Turgeon J, Michaud V. Development and validation of an absolute protein assay for the simultaneous quantification of fourteen CYP450s in human microsomes by HPLC-MS/MS-based targeted proteomics. *Journal of pharmaceutical and biomedical analysis* 2019; **173**: 96–107.
- 43 Gröer C, Busch D, Patrzyk M *et al.* Absolute protein quantification of clinically relevant cytochrome P450 enzymes and UDP-glucuronosyltransferases by mass spectrometry-based targeted proteomics. *Journal of pharmaceutical and biomedical analysis* 2014; **100**: 393–401.
- 44 Sato Y, Nagata M, Tetsuka K *et al.* Optimized methods for targeted peptide-based quantification of human uridine 5'-diphosphate-glucuronosyltransferases in biological specimens using liquid chromatography-tandem mass spectrometry. *Drug metabolism and disposition: the biological fate of chemicals* 2014; **42**(5): 885–9.
- 45 Fallon JK, Neubert H, Hyland R, Goosen TC, Smith PC. Targeted quantitative proteomics for the analysis of 14 UGT1As and -2Bs in human liver using NanoUPLC-MS/MS with selected reaction monitoring. *Journal of proteome research* 2013; **12**(10): 4402–13.
- 46 Drozdik M, Lapczuk-Romanska J, Wenzel C *et al.* Protein Abundance of Drug Metabolizing Enzymes in Human Hepatitis C Livers. *IJMS* 2023; **24**(5): 4543.
- 47 Vasilogianni A-M, El-Khateeb E, Al-Majdoub ZM *et al.* Proteomic quantification of perturbation to pharmacokinetic target proteins in liver disease. *Journal of proteomics* 2022; **263**: 104601.
- 48 Vasilogianni A-M, Al-Majdoub ZM, Achour B, Peters SA, Rostami-Hodjegan A, Barber J. Proteomics of colorectal cancer liver metastasis: A quantitative focus on drug elimination

- and pharmacodynamics effects. *British journal of clinical pharmacology* 2022; **88**(4): 1811–23.
- 49 Zanger UM, Schwab M. Cytochrome P450 enzymes in drug metabolism: regulation of gene expression, enzyme activities, and impact of genetic variation. *Pharmacology & therapeutics* 2013; **138**(1): 103–41.
 - 50 Peng L, Zhong X. Epigenetic regulation of drug metabolism and transport. *Acta pharmaceutica Sinica. B* 2015; **5**(2): 106–12.
 - 51 Hirota T, Tanaka T, Takesue H, Ieiri I. Epigenetic regulation of drug transporter expression in human tissues. *Expert opinion on drug metabolism & toxicology* 2017; **13**(1): 19–30.
 - 52 Zanger UM, Klein K, Thomas M *et al.* Genetics, epigenetics, and regulation of drug-metabolizing cytochrome p450 enzymes. *Clinical pharmacology and therapeutics* 2014; **95**(3): 258–61.
 - 53 Czuba LC, Hillgren KM, Swaan PW. Post-translational modifications of transporters. *Pharmacology & therapeutics* 2018; **192**: 88–99.
 - 54 Evers R, Piquette-Miller M, Polli JW *et al.* Disease-Associated Changes in Drug Transporters May Impact the Pharmacokinetics and/or Toxicity of Drugs: A White Paper From the International Transporter Consortium. *Clinical pharmacology and therapeutics* 2018; **104**(5): 900–15.
 - 55 Dunvald A-CD, Järvinen E, Mortensen C, Stage TB. Clinical and Molecular Perspectives on Inflammation-Mediated Regulation of Drug Metabolism and Transport. *Clinical pharmacology and therapeutics* 2022; **112**(2): 277–90.
 - 56 Brouwer KLR, Evers R, Hayden E *et al.* Regulation of Drug Transport Proteins-From Mechanisms to Clinical Impact: A White Paper on Behalf of the International Transporter Consortium. *Clinical pharmacology and therapeutics* 2022; **112**(3): 461–84.
 - 57 Staudinger JL, Woody S, Sun M, Cui W. Nuclear-receptor-mediated regulation of drug- and bile-acid-transporter proteins in gut and liver. *Drug metabolism reviews* 2013; **45**(1): 48–59.
 - 58 Willson TM, Kliewer SA. PXR, CAR and drug metabolism. *Nature reviews. Drug discovery* 2002; **1**(4): 259–66.
 - 59 Oscarson M, Zanger UM, Rifki OF, Klein K, Eichelbaum M, Meyer UA. Transcriptional profiling of genes induced in the livers of patients treated with carbamazepine. *Clinical pharmacology and therapeutics* 2006; **80**(5): 440–56.
 - 60 Urquhart BL, Tirona RG, Kim RB. Nuclear receptors and the regulation of drug-metabolizing enzymes and drug transporters: implications for interindividual variability in response to drugs. *Journal of clinical pharmacology* 2007; **47**(5): 566–78.
 - 61 Nishimura M, Naito S, Yokoi T. Tissue-specific mRNA expression profiles of human nuclear receptor subfamilies. *Drug metabolism and pharmacokinetics* 2004; **19**(2): 135–49.
 - 62 Pugh RN, Murray-Lyon IM, Dawson JL, Pietroni MC, Williams R. Transection of the oesophagus for bleeding oesophageal varices. *The British journal of surgery* 1973; **60**(8): 646–9.
 - 63 Vandesompele J, Preter K de, Pattyn F *et al.* Accurate normalization of real-time quantitative RT-PCR data by geometric averaging of multiple internal control genes. *Genome biology* 2002; **3**(7): RESEARCH0034.
 - 64 Smith PK, Krohn RI, Hermanson GT *et al.* Measurement of protein using bicinchoninic acid. *Analytical biochemistry* 1985; **150**(1): 76–85.

- 65 Wiśniewski JR. Filter-Aided Sample Preparation: The Versatile and Efficient Method for Proteomic Analysis. *Methods in enzymology* 2017; **585**: 15–27.
- 66 Wiśniewski JR. Filter-Aided Sample Preparation for Proteome Analysis. *Methods in molecular biology (Clifton, N.J.)* 2018; **1841**: 3–10.
- 67 Wiśniewski JR. Filter Aided Sample Preparation - A tutorial. *Analytica chimica acta* 2019; **1090**: 23–30.
- 68 Fallon JK, Neubert H, Goosen TC, Smith PC. Targeted precise quantification of 12 human recombinant uridine-diphosphate glucuronosyl transferase 1A and 2B isoforms using nano-ultra-high-performance liquid chromatography/tandem mass spectrometry with selected reaction monitoring. *Drug metabolism and disposition: the biological fate of chemicals* 2013; **41**(12): 2076–80.
- 69 Sato Y, Nagata M, Kawamura A, Miyashita A, Usui T. Protein quantification of UDP-glucuronosyltransferases 1A1 and 2B7 in human liver microsomes by LC-MS/MS and correlation with glucuronidation activities. *Xenobiotica; the fate of foreign compounds in biological systems* 2012; **42**(9): 823–9.
- 70 Langenfeld E, Zanger UM, Jung K, Meyer HE, Marcus K. Mass spectrometry-based absolute quantification of microsomal cytochrome P450 2D6 in human liver. *Proteomics* 2009; **9**(9): 2313–23.
- 71 Seibert C, Davidson BR, Fuller BJ, Patterson LH, Griffiths WJ, Wang Y. Multiple-approaches to the identification and quantification of cytochromes P450 in human liver tissue by mass spectrometry. *Journal of proteome research* 2009; **8**(4): 1672–81.
- 72 Sakamoto A, Matsumaru T, Ishiguro N *et al.* Reliability and robustness of simultaneous absolute quantification of drug transporters, cytochrome P450 enzymes, and Udp-glucuronosyltransferases in human liver tissue by multiplexed MRM/selected reaction monitoring mode tandem mass spectrometry with nano-liquid chromatography. *Journal of pharmaceutical sciences* 2011; **100**(9): 4037–43.
- 73 Kawakami H, Ohtsuki S, Kamiie J, Suzuki T, Abe T, Terasaki T. Simultaneous absolute quantification of 11 cytochrome P450 isoforms in human liver microsomes by liquid chromatography tandem mass spectrometry with in silico target peptide selection. *Journal of pharmaceutical sciences* 2011; **100**(1): 341–52.
- 74 Wang MZ, Wu JQ, Dennison JB *et al.* A gel-free MS-based quantitative proteomic approach accurately measures cytochrome P450 protein concentrations in human liver microsomes. *Proteomics* 2008; **8**(20): 4186–96.
- 75 Williamson BL, Purkayastha S, Hunter CL *et al.* Quantitative protein determination for CYP induction via LC-MS/MS. *Proteomics* 2011; **11**(1): 33–41.
- 76 Lang D, Radtke M, Bairlein M. Highly Variable Expression of CYP1A1 in Human Liver and Impact on Pharmacokinetics of Riociguat and Granisetron in Humans. *Chemical research in toxicology* 2019; **32**(6): 1115–22.
- 77 Dai Z-R, Feng L, Jin Q *et al.* A practical strategy to design and develop an isoform-specific fluorescent probe for a target enzyme: CYP1A1 as a case study. *Chemical science* 2017; **8**(4): 2795–803.
- 78 Savaryn JP, Liu N, Sun J, Ma J, Stresser DM, Jenkins G. Enrichment-free High-throughput Liquid Chromatography-Multiple-Reaction Monitoring Quantification of Cytochrome P450 Proteins in Plated Human Hepatocytes Direct from 96-Well Plates Enables Routine Protein Induction Measurements. *Drug metabolism and disposition: the biological fate of chemicals* 2020; **48**(7): 594–602.
- 79 Tanner J-A, Prasad B, Claw KG *et al.* Predictors of Variation in CYP2A6 mRNA, Protein, and Enzyme Activity in a Human Liver Bank: Influence of Genetic and Nongenetic

- Factors. *The Journal of pharmacology and experimental therapeutics* 2017; **360**(1): 129–39.
- 80 Li J, Zhou L, Wang H *et al.* A new sample preparation method for the absolute quantitation of a target proteome using (18)O labeling combined with multiple reaction monitoring mass spectrometry. *The Analyst* 2015; **140**(4): 1281–90.
 - 81 Shirasaka Y, Chaudhry AS, McDonald M *et al.* Interindividual variability of CYP2C19-catalyzed drug metabolism due to differences in gene diplotypes and cytochrome P450 oxidoreductase content. *The pharmacogenomics journal* 2016; **16**(4): 375–87.
 - 82 Evangelista EA, Aliwarga T, Sotoodehnia N *et al.* CYP2J2 Modulates Diverse Transcriptional Programs in Adult Human Cardiomyocytes. *Scientific reports* 2020; **10**(1): 5329.
 - 83 Russell MR, Achour B, Mckenzie EA *et al.* Alternative fusion protein strategies to express recalcitrant QconCAT proteins for quantitative proteomics of human drug metabolizing enzymes and transporters. *Journal of proteome research* 2013; **12**(12): 5934–42.
 - 84 Schaefer O, Ohtsuki S, Kawakami H *et al.* Absolute quantification and differential expression of drug transporters, cytochrome P450 enzymes, and UDP-glucuronosyltransferases in cultured primary human hepatocytes. *Drug metabolism and disposition: the biological fate of chemicals* 2012; **40**(1): 93–103.
 - 85 Yu A-M, Qu J, Felmlee MA, Cao J, Jiang X-L. Quantitation of human cytochrome P450 2D6 protein with immunoblot and mass spectrometry analysis. *Drug metabolism and disposition: the biological fate of chemicals* 2009; **37**(1): 170–7.
 - 86 Paine MF, Hart HL, Ludington SS, Haining RL, Rettie AE, Zeldin DC. The human intestinal cytochrome P450 "pie". *Drug metabolism and disposition: the biological fate of chemicals* 2006; **34**(5): 880–6.
 - 87 Akazawa T, Uchida Y, Miyauchi E, Tachikawa M, Ohtsuki S, Terasaki T. High Expression of UGT1A1/1A6 in Monkey Small Intestine: Comparison of Protein Expression Levels of Cytochromes P450, UDP-Glucuronosyltransferases, and Transporters in Small Intestine of Cynomolgus Monkey and Human. *Molecular pharmaceuticals* 2018; **15**(1): 127–40.
 - 88 Zhang QY, Dunbar D, Ostrowska A, Zeisloft S, Yang J, Kaminsky LS. Characterization of human small intestinal cytochromes P-450. *Drug metabolism and disposition: the biological fate of chemicals* 1999; **27**(7): 804–9.
 - 89 Al-Majdoub ZM, Achour B, Couto N *et al.* Mass spectrometry-based abundance atlas of ABC transporters in human liver, gut, kidney, brain and skin. *FEBS letters* 2020.
 - 90 Gorski JC, Vannaprasaht S, Hamman MA *et al.* The effect of age, sex, and rifampin administration on intestinal and hepatic cytochrome P450 3A activity. *Clinical pharmacology and therapeutics* 2003; **74**(3): 275–87.
 - 91 Kolars JC, Awni WM, Merion RM, Watkins PB. First-pass metabolism of cyclosporin by the gut. *Lancet (London, England)* 1991; **338**(8781): 1488–90.
 - 92 Novartis Pharma. Fachinformation Gilenya® Hartkapseln. unter <https://www.fachinfo.de/pdf/012954>. abgerufen am 26.06.2023.
 - 93 Wegler C, Gaugaz FZ, Andersson TB *et al.* Variability in Mass Spectrometry-based Quantification of Clinically Relevant Drug Transporters and Drug Metabolizing Enzymes. *Molecular pharmaceuticals* 2017; **14**(9): 3142–51.
 - 94 Prasad B, Achour B, Artursson P *et al.* Toward a Consensus on Applying Quantitative Liquid Chromatography-Tandem Mass Spectrometry Proteomics in Translational Pharmacology Research: A White Paper. *Clinical pharmacology and therapeutics* 2019; **106**(3): 525–43.

- 95 Oswald S, Haenisch S, Fricke C *et al.* Intestinal expression of P-glycoprotein (ABCB1), multidrug resistance associated protein 2 (ABCC2), and uridine diphosphate-glucuronosyltransferase 1A1 predicts the disposition and modulates the effects of the cholesterol absorption inhibitor ezetimibe in humans. *Clinical pharmacology and therapeutics* 2006; **79**(3): 206–17.
- 96 Lloret-Linares C, Miyauchi E, Luo H *et al.* Oral Morphine Pharmacokinetic in Obesity: The Role of P-Glycoprotein, MRP2, MRP3, UGT2B7, and CYP3A4 Jejunal Contents and Obesity-Associated Biomarkers. *Molecular pharmaceutics* 2016; **13**(3): 766–73.
- 97 Zhang H, Basit A, Busch D *et al.* Quantitative characterization of UDP-glucuronosyltransferase 2B17 in human liver and intestine and its role in testosterone first-pass metabolism. *Biochemical pharmacology* 2018; **156**: 32–42.
- 98 Bhatt DK, Basit A, Zhang H *et al.* Hepatic Abundance and Activity of Androgen- and Drug-Metabolizing Enzyme UGT2B17 Are Associated with Genotype, Age, and Sex. *Drug Metab Dispos* 2018; **46**(6): 888–96.
- 99 Ahire D, Heyward S, Prasad B. Intestinal Metabolism of Diclofenac by Polymorphic UGT2B17 Correlates with its Highly Variable Pharmacokinetics and Safety across Populations. *Clinical pharmacology and therapeutics* 2023.
- 100 Wang X, Shi J, Zhu H-J. Functional Study of Carboxylesterase 1 Protein Isoforms. *Proteomics* 2019; **19**(4): e1800288.
- 101 Tang L, Li X, Wan L, Xiao Y, Zeng X, Ding H. Herbal Medicines for Irinotecan-Induced Diarrhea. *Frontiers in pharmacology* 2019; **10**: 182.
- 102 Boberg M, Vrana M, Mehrotra A *et al.* Age-Dependent Absolute Abundance of Hepatic Carboxylesterases (CES1 and CES2) by LC-MS/MS Proteomics: Application to PBPK Modeling of Osetamivir In Vivo Pharmacokinetics in Infants. *Drug Metab Dispos* 2017; **45**(2): 216–23.
- 103 Adedoyin A, Arns PA, Richards WO, Wilkinson GR, Branch RA. Selective effect of liver disease on the activities of specific metabolizing enzymes: investigation of cytochromes P450 2C19 and 2D6. *Clinical pharmacology and therapeutics* 1998; **64**(1): 8–17.
- 104 Frye RF, Zgheib NK, Matzke GR *et al.* Liver disease selectively modulates cytochrome P450-mediated metabolism. *Clinical pharmacology and therapeutics* 2006; **80**(3): 235–45.
- 105 Pentikäinen PJ, Välisalmi L, Himberg JJ, Crevoisier C. Pharmacokinetics of midazolam following intravenous and oral administration in patients with chronic liver disease and in healthy subjects. *Journal of clinical pharmacology* 1989; **29**(3): 272–7.
- 106 El-Khateeb E, Achour B, Al-Majdoub ZM, Barber J, Rostami-Hodjegan A. Non-uniformity of Changes in Drug-Metabolizing Enzymes and Transporters in Liver Cirrhosis: Implications for Drug Dosage Adjustment. *Molecular pharmaceutics* 2021; **18**(9): 3563–77.
- 107 El-Khateeb E, Al-Majdoub ZM, Rostami-Hodjegan A, Barber J, Achour B. Proteomic Quantification of Changes in Abundance of Drug-Metabolizing Enzymes and Drug Transporters in Human Liver Cirrhosis: Different Methods, Similar Outcomes. *Drug Metab Dispos* 2021; **49**(8): 610–8.
- 108 Fritz A, Busch D, Lapczuk J, Ostrowski M, Drozdik M, Oswald S. Expression of clinically relevant drug-metabolizing enzymes along the human intestine and their correlation to drug transporters and nuclear receptors: An intra-subject analysis. *Basic & clinical pharmacology & toxicology* 2019; **124**(3): 245–55.
- 109 Ke AB, Nallani SC, Zhao P, Rostami-Hodjegan A, Unadkat JD. Expansion of a PBPK model to predict disposition in pregnant women of drugs cleared via multiple CYP

- enzymes, including CYP2B6, CYP2C9 and CYP2C19. *British journal of clinical pharmacology* 2014; **77**(3): 554–70.
- 110 Kumar V, Yin J, Billington S *et al.* The Importance of Incorporating OCT2 Plasma Membrane Expression and Membrane Potential in IVIVE of Metformin Renal Secretory Clearance. *Drug Metab Dispos* 2018; **46**(10): 1441–5.
- 111 Vildhede A, Mateus A, Khan EK *et al.* Mechanistic Modeling of Pitavastatin Disposition in Sandwich-Cultured Human Hepatocytes: A Proteomics-Informed Bottom-Up Approach. *Drug Metab Dispos* 2016; **44**(4): 505–16.
- 112 Ishida K, Ullah M, Tóth B, Juhasz V, Unadkat JD. Successful Prediction of In Vivo Hepatobiliary Clearances and Hepatic Concentrations of Rosuvastatin Using Sandwich-Cultured Rat Hepatocytes, Transporter-Expressing Cell Lines, and Quantitative Proteomics. *Drug Metab Dispos* 2018; **46**(1): 66–74.
- 113 Bosgra S, van de Steeg E, Vlaming ML *et al.* Predicting carrier-mediated hepatic disposition of rosuvastatin in man by scaling from individual transfected cell-lines in vitro using absolute transporter protein quantification and PBPK modeling. *European journal of pharmaceutical sciences official journal of the European Federation for Pharmaceutical Sciences* 2014; **65**: 156–66.
- 114 Rodrigues AD, van Dyk M, Sorich MJ *et al.* Exploring the Use of Serum-Derived Small Extracellular Vesicles as Liquid Biopsy to Study the Induction of Hepatic Cytochromes P450 and Organic Anion Transporting Polypeptides. *Clinical pharmacology and therapeutics* 2021; **110**(1): 248–58.
- 115 Rodrigues D, Rowland A. From Endogenous Compounds as Biomarkers to Plasma-Derived Nanovesicles as Liquid Biopsy; Has the Golden Age of Translational Pharmacokinetics-Absorption, Distribution, Metabolism, Excretion-Drug-Drug Interaction Science Finally Arrived? *Clinical pharmacology and therapeutics* 2019; **105**(6): 1407–20.

6 Publikationen

6.1 *Mass spectrometry-based targeted proteomics method for the quantification of clinically relevant drug metabolizing enzymes in human specimens*

Wenzel C, Drozdik M, Oswald S

Journal of chromatography B, Analytical technologies in the biomedical and life sciences
2021;1180:122891. doi: 10.1016/j.jchromb.2021.122891.

Projektdesign: S. O.

Projektdurchführung: C. W.

Datenanalyse: C.W., S.O.

Erstellung des Manuskriptes: C. W., M. D., S. O.



Mass spectrometry-based targeted proteomics method for the quantification of clinically relevant drug metabolizing enzymes in human specimens

Christoph Wenzel^a, Marek Drozdziak^b, Stefan Oswald^{c,*}

^a Department of Pharmacology, Center of Drug Absorption and Transport, University Medicine Greifswald, Greifswald, Germany

^b Department of Experimental and Clinical Pharmacology, Pomeranian Medical University, Szczecin, Poland

^c Institute of Pharmacology and Toxicology, Rostock University Medical Center, Rostock, Germany

ARTICLE INFO

Keywords:

LC-MS/MS
Protein quantification
Drug metabolizing enzymes
CYP
UGT
Carboxylesterase

ABSTRACT

Biotransformation by phase I and II metabolizing enzymes represents the major determinant for the oral bioavailability of many drugs. To estimate the pharmacokinetics, data on protein abundance of hepatic and extrahepatic tissues, such as the small intestine, are required. Targeted proteomics assays are nowadays state-of-the-art for absolute protein quantification and several methods for quantification of drug metabolizing enzymes have been published. However, some enzymes remain still uncovered by the analytical spectra of those methods. Therefore, we developed and validated a quantification assay for two carboxylesterases (CES-1, CES-2), 17 cytochrome P450 enzymes (CYP) (CYP1A1, CYP1A2, CYP2A6, CYP2B6, CYP2C8, CYP2C9, CYP2C18, CYP2C19, CYP2D6, CYP2E1, CYP2J2, CYP3A4, CYP3A5, CYP3A7, CYP4F2, CYP4F12, CYP4A11) and five UDP-glucuronosyltransferases (UGTs) (UGT1A1, UGT1A3, UGT2B7, UGT2B15, UGT2B17). Protein quantification was performed by analyzing proteospecific surrogate peptides after tryptic digestion with stable isotope-labelled standards. Chromatographic separation was performed on a Kinetex® 2.6 µm C18 100 Å core-shell column (100 × 2.1 mm) with a gradient elution using 0.1% formic acid and acetonitrile containing 0.1% formic acid with a flow rate of 200 µl/min. Three mass transitions were simultaneously monitored with a scheduled multiple reaction monitoring (sMRM) method for each analyte and standard. The method was partly validated according to current bioanalytical guidelines and met the criteria regarding linearity (0.1–25 nmol/L), within-day and between-day accuracy and precision as well as multiple stability criteria. Finally, the developed method was successfully applied to determine the abundance of the aforementioned enzymes in human intestinal and liver microsomes. Our work offers a new fit for purpose method for the absolute quantification of CES, CYPs and UGTs in various human tissues and can be used for the acquisition of data for physiologically based pharmacokinetic modelling.

1. Introduction

Bioavailability of orally administered drugs is mainly determined by first pass metabolism. In this regard, a substantial fraction of the administered dose is subjected to biotransformation by phase I (e.g. oxidation) and / or phase II (e.g. conjugation) drug metabolizing enzymes [1]. Thus, in many cases, only a minor fraction of the administered dose reaches the site of action after distribution via the arterial system. A main role in the biotransformation processes play cytochrome P450 (CYP) enzymes, carboxylesterases (CES) and UDP-glucuronosyltransferases (UGTs). Despite of their great impact on the

pharmacokinetics of many drugs, the abundance of those enzymes along the route of drug absorption remains partly unclear. In the past, the liver was assumed to be the only relevant organ for biotransformation [2] but there is convincing evidence that some drug metabolizing enzymes (DMEs) are highly abundant in the gut wall as well [3,4]. This leads to the conclusion, that alike the liver, the gut must be considered as relevant organ for drug metabolism. Recently, our group characterized the protein abundance of DMEs in different parts of the intestine as well as in the liver from the same individuals (organ donors), which verified in part substantial protein amounts in the intestinal tissue [5]. For this purpose, a mass-spectrometry-based targeted proteomics method for

* Corresponding author at: Institute of Pharmacology and Toxicology, Rostock University Medical Center, Schillingallee 70, D-18057 Rostock, Germany.
E-mail address: stefan.oswald@med.uni-rostock.de (S. Oswald).

<https://doi.org/10.1016/j.jchromb.2021.122891>

Received 26 January 2021; Received in revised form 6 July 2021; Accepted 30 July 2021

Available online 5 August 2021

1570-0232/© 2021 Elsevier B.V. All rights reserved.

Table 1
Comparison of our developed assay to other analytical methods in the field quantitation of DMEs by targeted and untargeted proteomics.

Reference	Investigated Enzymes	LLOQ	Run time	Validation parameters	Application
[20]	CYP2C9, CYP2C19, CYP2S1, CYP3A4, CYP4F2, CYP27A1, UGT1A1, UGT1A6, UGT1A10, UGT2A3, UGT2B7, UGT2B17, FMO1, FMO2GSTA2, GSTK11, GSTM2, GSTM4, GSTO1, GSTP1, SUL1A2, SUL1A3, SUL1B1, SUL1E1, SUL2A1, MGST2, MGST3,	n. d.	165 min	n. d.	human small intestine tissue
[21]	AO, CES-1, CES-2, UGT1A1, UGT1A3, UGT1A4, UGT1A6, UGT1A9, UGT1A10, UGT2B4, UGT2B7, UGT2B15, UGT2B17, SUL1A1, SUL1A3, SUL1B1, SUL1E1, SUL2A1	0.01–1.91 pmol/mg	27 min	n. d.	S9 subcellular fraction of human liver, kidney, heart and lung. HIM
[22]	CYP3A4, CYP2E1, CYP2A6, CYP2C9, CYP2C8, CYP2D6, CYP1A2, CYP2B6, CYP2C19, CYP2J2	n. d.	95 min	n. d.	different cell-types of human liver
[23]	CYP1A2, CYP2A6, CYP2A13, CYP2B6, CYP2C8, CYP2C9, CYP2C18, CYP2C19, CYP2D6, CYP2E1, CYP2J2, CYP3A4, CYP3A5, CYP3A7, CYP4F2, CYP4F11, CYP4F12, UGT1A1, UGT1A3, UGT1A4, UGT1A6, UGT1A9, UGT2B4, UGT2B7, UGT2B10, UGT2B15, UGT2B17	n. d.	100 min	n. d.	HLM
[19]	CYP1A1, CYP1A2, CYP1B1, CYP2B6, CYP2C8, CYP2C9, CYP2C19, CYP2D6, CYP2E1, CYP2J2, CYP3A4, CYP3A5, CYP3A7, CYP4F2	0.1 nmol/L	76 min	linearity, sensitivity, precision + accuracy, matrix-effect, concordance between peptides, stability	commercially available HIM and HLM, self-prepared HIM
[24]	CYP3A4, CYP2C9, CYP2D6, CYP2E1, CYP1A2, CYP2A6, CYP2C8, POR, UGT1A4, UGT1A6, UGT2B7, UGT2B15, CES1, CES2, ADH1A, ADH1B, ADH1C, ALDH1A1, CYP3A5, UGT2B6, UGT1A1, UGT2B17	n. d.	27 min	n. d.	human liver S9 fraction
[6]	CYP1A2, CYP3A4, CYP3A5, CYP2B6, CYP2C8, CYP2C9, CYP2C19, CYP2D6, CYP2E1, UGT1A1, UGT1A3, UGT2B7, UGT2B15	0.25–0.5 nmol/L	53 min	accuracy and precision, stability	commercially available HIM and HLM, self-prepared HIM
[25]	UGT1A1, UGT1A3, UGT1A4, UGT1A6, UGTUGT1A7, UGT1A8, UGT1A9, UGT1A10, UGT2B4, UGT2B7, UGT2B10, UGT2B15, UGT2B17	1 pmol/mg	54 min	n. d.	HLM, HIM, HKM
[26]	UGT1A1, UGT1A3, UGT1A4, UGT1A5, UGT1A6, UGT1A7, UGT1A8, UGT1A9, UGT1A10, UGT2B4, UGT2B7, UGT2B10, UGT2B15, UGT2B17	0.15–4 pmol/mg	35 min	selectivity, linearity, reproducibility, stability	HLM, liver S9 fraction
[27]	UGT1A1, UGT1A3, UGT1A4, UGT1A5, UGT1A6, UGT1A7, UGT1A8, UGT1A9, UGT1A10	0.5 pmol/mg	65 min	linearity, interday and intraday variability	HLM, HIM, HKM
this study	CES-1, CES-2, CYP1A1, CYP1A2, CYP2A6, CYP2B6, CYP2C8, CYP2C9, CYP2C18, CYP2C19, CYP2D6, CYP2E1, CYP2J2, CYP3A4, CYP3A5, CYP3A7, CYP4F2, CYP4F12, CYP4A11, UGT1A1, UGT1A3, UGT2B7, UGT2B15, UGT2B17	0.1–0.5 nmol/L (0.05–0.25 pmol/mg)	65 min	accuracy and precision, stability	HLM, HIM

HIM, human intestinal microsomes; HLM, human liver microsomes; HKM, human kidney microsomes; LLOQ, lower limit of quantitation; n. d.; not determined

absolute protein quantification in various tissues was developed by our group [6]. The analytical spectrum of this method covers enzymes being relevant for about 80% of the marketed drugs [7]. Consequently, there are still several under-investigated enzymes that have been not appropriately characterized yet. Among the substrates of these enzymes are many frequently used drugs with narrow therapeutic indices such as novel direct oral anticoagulants, antibiotics or cytostatics [8–14]. Data on the protein abundance of these enzymes may allow more precise estimations or even pharmacokinetic predictions of their respective substrates. Thereby, efficacy and safety of pharmacotherapy could be improved. Thus, there is a need for reliable methods for a highly selective and sensitive quantification of these proteins. Thus, it was the aim of this study to develop and validate an LC-MS/MS assay for the simultaneous and absolute quantification of 24 clinically relevant DMEs, i.e. CES-1, CES-2, CYP1A1, CYP1A2, CYP2A6, CYP2B6, CYP2C8, CYP2C9, CYP2C18, CYP2C19, CYP2D6, CYP2E1, CYP2J2, CYP3A4, CYP3A5, CYP3A7, CYP4F2, CYP4F12, CYP4A11, UGT1A1, UGT1A3, UGT2B7, UGT2B15 and UGT2B17. For this purpose, we used the technique of mass spectrometry-based targeted proteomics because this approach overcomes the limitations of formerly used immunological techniques (Western blotting or quantitative immunohistochemistry) such as poor reproducibility and accuracy as well as a narrow analytic range and a lack of specificity due to unspecific binding of the used antibodies [15,16]. In contrast, mass spectrometry-based proteomics also allows discrimination between isoenzymes that show high homology (e.g. CYP2C or UGT1A enzymes). Another advantage of this method constitutes the opportunity to quantify a large number of proteins

simultaneously in one analytical run. The analytical approach is based on the detection of proteospecific surrogate peptides, resulting from tryptic digestion, via mass spectrometry after separation by liquid chromatography. The use of corresponding stable-isotope labelled peptides as internal standards allows an absolute quantification of the peptides of interest [17,18]. To the best of our knowledge, no method for the simultaneous quantification of all drug metabolizing enzymes of interest has been so far reported. Our previously developed proteomic assay considered only 13 of the 24 enzymes, while the study by Grangeon et al. [19] covered 14 of the proteins of interest. Thus, our work presents a considerable extension of the so far published methods. By using a second surrogate peptide for the already studied enzymes, we expect improvement in precision of quantification. In order to expand the analytic spectrum of this innovative but costly technique, we decided to use initially one peptide for each of the minor DMEs. In addition, for most published targeted proteomics assays, no detailed data on method validation have been reported, which is important to ensure reliability of the generated method. Table 1 provides an overview about the so far published methods for absolute quantification of DMEs [6,19–27]. In some of the most recent studies, a label-free approach was used [20,22,23]. Label-free proteomics can be divided into methods using an external protein standard and those without standard free such as the total protein approach (TPA). Many of these studies are excellent application studies but they do not provide detailed information on method development and validation. Some published methods focus either on phase I or phase II DMEs. Because there is in many cases a close functional interplay of those enzymes, we decided to develop an assay

Table 2

Overview of tryptic proteospecific peptides and their respective ions and mass transitions used for enzyme quantification (*isotope-labeled amino acid). The labeling of Arg (R) and Lys (K) was done by introducing C-13 and N-15 as indicated by asterisks.

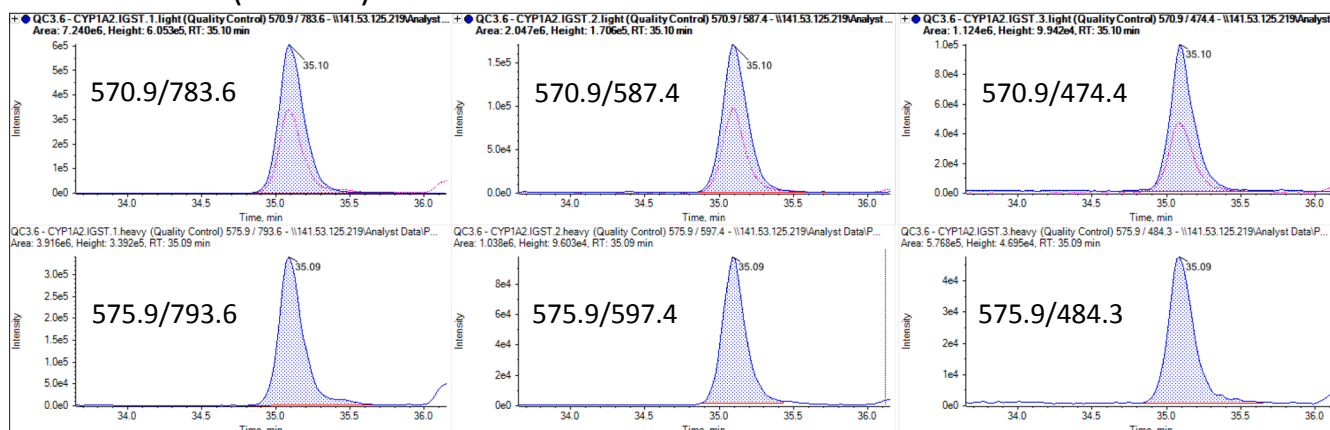
Protein	Peptide	Mass	Q1	Q3.1	CE	Q3.2	CE	Q3.3	CE
CES-1	AISESGVALTSVLVK	1473.9	737.2	830.6	30	759.5	31	986.5	31
	AISESGVALTSVLVK*	1481.9	741.2	838.6	30	767.5	31	994.5	31
CES-2	ADHGDELPPVFR	1402.7	468.7	665.4	19	421.2	24	568.5	23
	ADHGDELPPVFR*	1412.7	471.8	675.5	19	431.5	25	578.4	24
CYP1A1	IQEELDTVIGR	1272.7	637.3	660.5	30	345.6	30	1032.2	30
	IQEELDTVIGR*	1282.7	642.3	670.6	30	355.3	30	1042.4	30
	YLPNPSLNAFK	1263.7	632.8	776.5	31	294.2	45	987.5	24
CYP1A2	YLPNPSLNAFK*	1271.7	636.9	784.6	30	302.3	47	996.5	26
	IGSTPVLVLSR	1141.7	570.9	783.6	28	587.4	36	474.4	34
	IGSTPVLVLSR*	1151.7	575.9	793.6	28	597.4	36	484.4	34
CYP2A6	YLPNPALQR	1071.0	536.2	398.1	20	584.2	30	698.2	30
	YLPNPALQR*	1081.0	541.1	403.1	20	594.2	30	708.2	30
	GTGGANIDPTFFLSR	1552.8	777.1	867.6	41	982.5	35	522.4	38
CYP2B6	GTGGANIDPTFFLSR*	1562.8	782.1	877.6	44	992.5	36	532.7	37
	GYGVIFANGNR	1167.6	584.8	678.5	27	531.3	27	792.0	27
	GYGVIFANGNR*	1177.6	589.8	688.6	26	541.4	28	801.9	26
CYP2C8	TEAFIPFSLGK	1209.6	605.8	648.5	25	761.7	24	980.2	24
	TEAFIPFSLGK*	1217.0	609.8	656.5	25	769.8	25	988.5	23
	VQEEIDHIVGR	1294.6	647.7	581.2	42	1067.2	33	696.2	36
CYP2C9	VQEEIDHIVGR*	1304.0	652.7	591.2	42	1077.2	33	706.2	36
	GLGHSSNGK	945.5	473.7	605.4	20	775.7	20	405.3	30
	GLGHSSNGK*	953.6	477.0	613.6	20	783.8	20	413.4	30
CYP2C18	LPPGPTPLPVIGNILQIGIK	2037.2	680.1	671.2	24	317.2	23	955.6	27
	LPPGPTPLPVIGNILQIGIK*	2045.3	682.7	679.6	23	325.2	22	963.7	29
	GIFPLAER	902.5	451.6	585.2	20	366.6	17	732.3	17
CYP2C19	GIFPLAER*	912.0	456.2	594.2	20	371.2	17	741.3	17
	DIDITPIANAFGR	1402.7	702.3	845.6	27	946.7	28	1059.5	33
	DIDITPIANAFGR*	1412.7	707.2	855.8	29	956.4	28	1069.9	41
CYP2D6	GHFPLAER	926.5	464.2	585.5	25	732.5	22	488.4	29
	GHFPLAER*	936.0	469.2	595.5	24	742.8	23	498.1	32
	GTTLTSLTSLVLDHNK	1700.0	567.5	664.6	21	771.4	19	513.3	32
CYP2E1	GTTLTSLTSLVLDHNK*	1707.9	570.2	668.8	21	775.7	19	521.0	32
	DIEVQGFR	963.5	482.1	735.2	21	507.1	21	606.2	21
	DIEVQGFR*	973.0	487.1	745.2	21	517.1	21	616.2	21
CYP2J2	GTTLITNLSSVLK	1346.8	674.4	861.7	28	446.4	23	373.0	28
	GTTLITNLSSVLK*	1354.8	678.5	870.0	30	454.6	22	373.4	28
	FITLVPSNLPHEATR	1695.0	565.5	561.2	22	710.2	32	717.9	18
CYP3A4	FITLVPSNLPHEATR*	1705.0	568.8	566.1	22	720.2	32	722.8	18
	FGPVFTLYVGSQR	1470.8	735.6	923.4	37	709.3	37	1070.4	37
	FGPVFTLYVGSQR*	1480.8	740.7	933.3	37	719.3	37	1080.4	37
CYP3A5	EVTVDITLAGYHLPK	1643.9	548.4	608.2	19	785.4	27	714.4	27
	EVTVDITLAGYHLPK*	1651.9	551.1	612.3	19	793.3	27	722.6	27
	EVTNFLR	878.4	439.6	650.2	22	549.2	22	325.2	18
CYP3A7	EVTNFLR*	888.0	444.2	659.2	22	558.2	22	330.8	18
	LGIPGPTPLPFLGNILSYHK	2134.2	711.6	925.9	27	931.4	36	647.3	35
	LGIPGPTPLPFLGNILSYHK*	2142.2	714.2	929.9	27	939.5	36	655.3	35
CYP4F2	DTINFLSK	937.5	469.1	721.3	18	608.2	20	494.1	22
	DTINFLSK*	944.0	472.7	728.4	18	615.2	20	501.2	22
	LFPVAIR	815.5	407.8	555.4	18	359.3	27	458.4	26
CYP4F12	LFPVAIR*	825.5	412.8	565.5	18	369.3	27	468.5	26
	LGIPGPTPLPFLGNALSFR	1967.1	656.5	842.6	20	764.4	25	409.3	18
	LGIPGPTPLPFLGNALSFR*	1977.1	659.9	847.4	20	774.5	25	419.3	18
UGT1A1	SVINASAAIAPK	1141.7	571.0	478.3	22	728.5	27	657.4	23
	SVINASAAIAPK*	1149.7	574.9	482.4	22	736.5	27	665.4	23
	LVDHFTDAVIR	1285.7	429.3	288.2	19	458.4	21	387.4	19
UGT1A3	LVDHFTDAVIR*	1295.7	432.6	298.2	20	468.3	20	397.4	20
	NSQSYIQAISDLNLLVFSR	2169.1	724.2	508.4	32	409.4	24	849.7	31
	NSQSYIQAISDLNLLVFSR*	2179.1	727.8	419.5	23	518.7	30	859.3	30
UGT2B7	TYPVPFQR	1007.0	504.2	372.1	17	743.3	20	547.2	26
	TYPVPFQR*	1017.0	509.1	377.1	17	753.3	20	557.2	26
	DGAFYTLK	914.5	458.0	671.6	18	524.3	18	361.4	25
UGT2B15	DGAFYTLK*	922.5	461.8	679.5	18	532.3	18	369.4	25
	YLSIPTVFFLR	1355.7	678.3	879.3	29	1079.4	28	782.5	36
	YLSIPTVFFLR*	1366.0	683.1	889.3	29	1089.3	28	792.4	36
UGT2B17	ANVIASALAQIPQK	1423.8	712.6	684.6	28	797.7	30	955.8	30
	ANVIASALAQIPQK*	1431.8	716.4	692.6	28	805.5	30	963.7	30
	IEIYPTSLTK	1164.6	582.7	646.2	28	922.3	23	809.2	25
UGT2B15	IEIYPTSLTK*	1172.0	586.7	654.3	28	930.3	23	817.3	25
	SVINDPVYK	1034.5	517.6	848.4	20	735.2	23	506.1	30
	SVINDPVYK*	1042.0	521.6	856.3	20	743.3	23	514.2	30
UGT2B17	FSVGYTFEK	1077.5	539.3	744.4	24	930.6	26	687.4	24
	FSVGYTFEK*	1085.5	543.0	752.4	24	938.5	26	695.4	24
	SVINDPIYK	1048.6	525.3	310.3	38	862.8	21	749.9	24

(continued on next page)

Table 2 (continued)

Protein	Peptide	Mass	Q1	Q3.1	CE	Q3.2	CE	Q3.3	CE
	SVINDPIYK*	1056.6	529.3	318.2	37	871.5	23	758.7	23
	FSVGYTVEK	1029,5	515.7	795.6	21	696.7	24	883.8	24
	FSVGYTVEK*	1037,5	519.8	803.8	23	704.4	23	891.8	24

IGSTPVLVLSR (CYP1A2)



YLPNPALQR (CYP1A2)

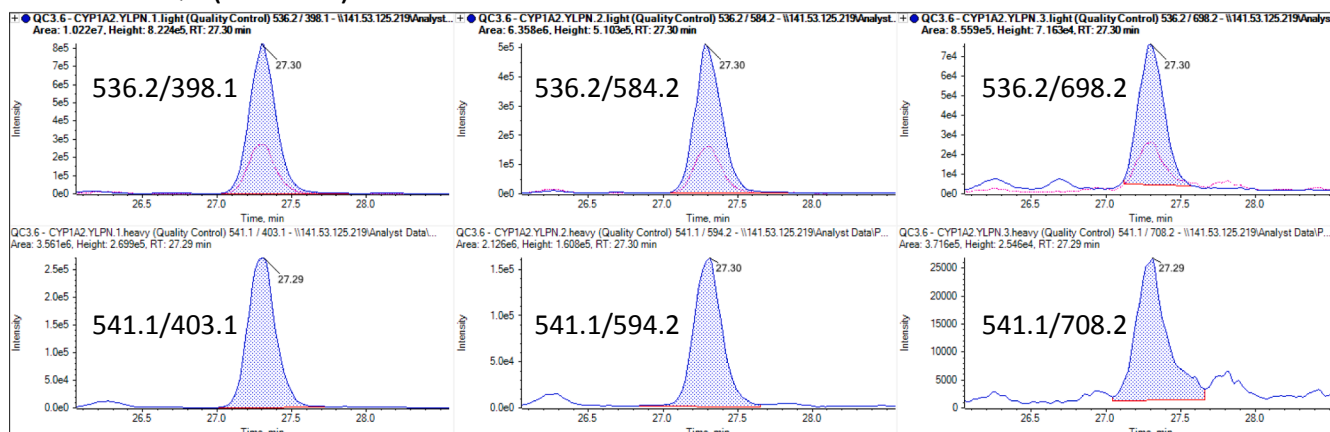


Fig. 1. Representative chromatograms of a quality control sample showing coelution of analyte (upper panel) and internal standard (lower panel) for both surrogate peptides used for quantification of CYP1A2.

which considers both of them simultaneously.

Finally, the developed assay was successfully applied to human intestinal microsomes (HIM) and human liver microsomes (HLM) and provided data on the protein abundance of major and so far underestimated DMEs. Therefore, the developed method is expected to extend our knowledge on the first pass metabolism of drugs and in turn to improve the precision of physiologically based pharmacokinetic modelling-based predictions of pharmacokinetics and drug-drug interactions.

2. Materials and methods

2.1. Materials/reagents

Ammonium bicarbonate, dithiothreitol (DTT) and LC-MS grade acetonitrile were purchased from Carl Roth (Karlsruhe, Germany). Iodoacetamide (IAA) was obtained from Sigma (Steinheim, Germany). The BCA kit to quantify the whole protein content was from Thermo Scientific (Schwerte, Germany). Sequencing Grade Modified Trypsin

and ProteaseMAXTM surfactant were purchased from Promega (Mannheim, Germany). LC-MS grade formic acid (FA) was obtained from J. T. Baker (Gliwice, Poland). Custom made peptide standards and the corresponding stable isotope-labelled internal standards were synthesized by New England Peptide (Boston, MA, USA), JPT Peptide Technologies (Berlin, Germany) or ThermoFisher Scientific (Schwerte, Germany). All peptides were of analytical grade (>95%) which was verified by exact quantification via amino acid analysis and certified by the respective manufacturers. Deionized water (conductance $\leq 0.055\mu\text{S}/\text{cm}$; pH 5.0–6.0) was generated with the system Astacus (Membrapure, Henningsdorf, Germany).

2.2. Identification of proteotypic peptides and optimal mass transitions

The prediction of surrogate peptides for mass spectrometry is described elsewhere [28]. Suitable proteospecific peptides for absolute quantification of the aforementioned metabolic enzymes were identified throughout a dual (*in-silico* and wet-lab) approach. At first, all theoretically appropriate tryptic peptides were predicted by the use of a web-

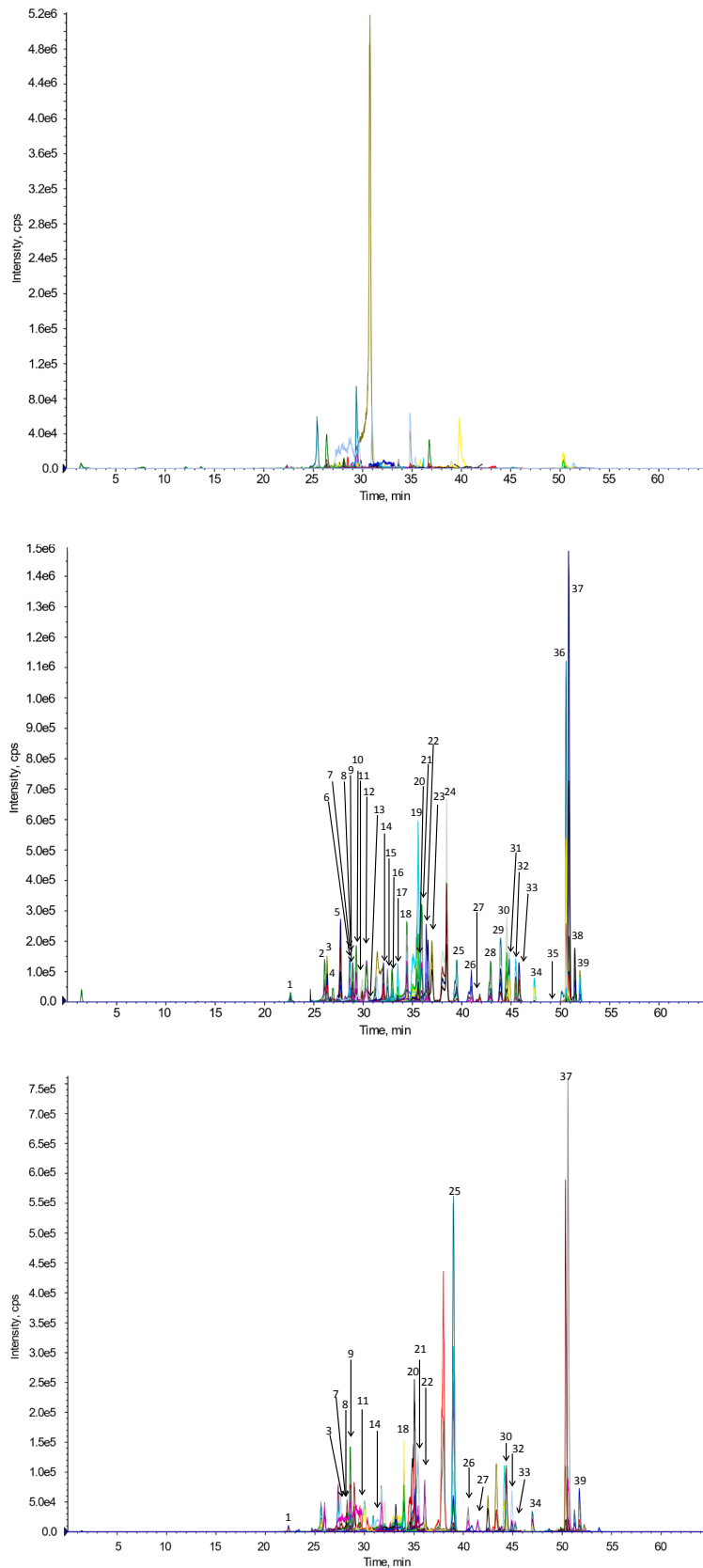


Fig. 2. Total ion chromatograms for the developed LC-MS/MS methods applied to measure proteotypic peptides and their stable isotope-labelled internal standards for CYP2C19.GHFP (1), CYP2C8.GLGI (2), UGT2B15.SVIN (3), CYP2C8.VQEE (4), CYP1A2.YLPN (5), UGT2B17.FSVG (6), CYP3A4.EVTN (7), CYP4F2.SVIN (8), UGT2B17.SVIN (9), CYP2D6.DIEV (10), UGT1A1.DGAF (11), UGT1A1.TYPV (12), CYP2B6.GYGV (13), CYP4F12.LVHD (14), CYP3A5.DTIN (15), CYP1A1.IQEE (16), UGT2B15.FSVG (17), UGT2B7.IEIV (18), CYP1A2.IGST (19), CYP3A5.LFPV (20), CYP2C9.GIFP (21), CYP2J2.EVTV (22), CYP1A1.YLPN (23), CYP2E1.FITL (24), CES-2.ADHG (25), CES-1.AISE (26), UGT2B7.ANVI (27), CYP2A6.GTGG (28), CYP2B6.TEAF (29), CYP2C18.DIDI (30), CYP2E1.FGPV (31), CYP2D6.GTTL (32), CYP2C19.GTTI (33), CYP2C9.GTTI (34), CYP4A11.NSQS (35), UGT1A3.YLSI (36), CYP3A4.LGIP (37), CYP3A7.LGIP (38) and CYP2C9.LPPG (39) in a blank matrix sample (top); in validation matrix spiked with in each case 25 nmol/L for all analytes and the internal standards (middle); and in a digested human intestinal microsomal sample (bottom).

Table 3

Within- and between-day accuracy and precision data for the determination of metabolic enzymes. Data were derived from in each case six calibration curves (between-day data) or six quality control sample sets (within-day data) and are presented as relative errors (accuracy) or coefficients of variation (precision) of nominal and respective mean concentrations.

Protein	Peptide	within-day data		between-day data		Range (nmol/L)
		Accuracy (%)	Precision (%)	Accuracy (%)	Precision (%)	
CES-1	AISESGVALTSVLVK	-2.4 to 5.0	2.3 - 3.9	-2.0 to 2.6	1.2-7.0	0.1-25
CES-2	ADHGDELFPVFR	-1.7 to 5.5	0.7 - 3.5	-4.4 to 11.2	1.7 - 16.1	0.1-25
CYP1A1	IQEELDTVIGR	0.2 - 5.6	2.2 - 6.4	-3.9 to 4.0	1.6 - 8.9	0.1-25
	YLPNPSLNFAFK	0.2 - 9.1	2.9 - 8.4	-2.9 to 4.2	1.7 - 10.3	0.1-25
CYP1A2	IGSTPVLVLSR	2.6 - 4.9	1.5 - 6.9	-2.4 to 4.4	1.3 - 10.2	0.1-25
	YLPNPALQR	-2.9 to 7.4	2.9 - 3.5	-3.2 to 3.4	1.1 - 6.9	0.1-25
CYP2A6	GTGGANIDPTFFLSR	-3.4 to 5.4	0.6 - 6.0	-4.1 to 4.2	2.3 - 14.6	0.1-25
CYP2B6	GYGVIFANGNR	0.7 - 8.0	1.9 - 7.7	-1.1 to 1.4	1.1 - 7.0	0.25-25
	TEAFIPFSLGK	1.2 - 6.2	2.0 - 4.1	-2.2 to 5.1	1.8 - 11.4	0.1-25
CYP2C8	VQEEIDHVIGR	-6.0 to 4.0	2.9 - 6.8	-2.2 to 4.2	3.6 - 12.7	0.25-25
	GLGISSNGK	1.1 - 6.7	1.4 - 5.5	-4.6 to 3.5	1.3 - 11.4	0.1-25
CYP2C9	LPPGPTPLPVIGNILQIGIK	0.7 - 5.6	1.7 - 3.4	-2.7 to 4.5	1.5 - 7.4	0.1-25
	GIFPLAER	-0.5 to 7.3	2.1 - 5.2	-3.9 to 4.2	1.7 - 11.3	0.1-25
CYP2C18	DIDITPIANAFGR	-2.4 to 2.5	2.1 - 7.1	-2.1 to 6.3	1.6-5.6	0.1-25
CYP2C19	GHPFLAER	6.6 to 7.4	5.5 - 6.6	-2.6 to 3.7	2.2 - 13.8	0.5-25
	GTTLTSLTSLVLDHDK	-6.4 to 4.0	2.6 - 4.4	-4.4 to 5.2	1.8 - 9.8	0.1-25
CYP2D6	DIEVQGFR	1.8 - 6.3	4.2 - 5.2	-4.4 to 2.0	1.1 - 5.8	0.1-25
	GTTLITNLSSVLK	-3.2 to 5.7	2.5 - 5.7	-3.9 to 4.0	1.8 - 9.7	0.1-25
CYP2E1	FITLVPSNLPHEATR	3.3 - 6.2	2.0 - 3.8	-3.3 to 3.7	1.0 - 6.7	0.1-25
	FGPVFTLYVGSQR	-7.1 to 10.1	2.1 - 3.0	-9.3 to 8.0	1.6 - 6.8	0.1-25
CYP2J2	EVTVDITLGYHLPK	-5.0 to 9.3	1.5 - 7.3	-3.2 to 2.6	7.5 - 8.5	0.1-25
CYP3A4	EVTNFLR	-1.1 to 8.0	2.5 - 5.2	-2.1 to 5.2	1.6 - 10.4	0.1-25
	LGIPGPTPLPFLGNILSYHK	-2.4 to 5.2	2.0 - 3.5	-3.2 to 7.1	1.1 - 5.5	0.1-25
CYP3A5	DTINFLSK	0.7 - 7.8	3.1 - 6.1	-3.4 to 3.1	1.3 - 6.4	0.1-25
	LFPVAIR	-0.4 to 4.4	2.3 - 4.3	-6.6 to 2.8	1.2 - 8.7	0.1-25
CYP3A7	LGIPGPTPLPFLGNALSFR	-2.9 to 6.5	1.3-2.4	5.1 to 5.7	1.8 - 7.0	0.1-25
CYP4F2	SVINASAAIAPK	-1.7 to 5.0	1.9 - 6.3	-2.6 to 5.3	1.7 - 13.5	0.25-25
CYP4F12	LVDHFTDAVIR	-5.6 to 1.8	2.9 - 5.5	-3.1 to 4.5	1.9 - 12.5	0.1-25
CYP4A11	NSQSYIQAISDLNNLVFSR	-4.2 to -1.8	3.5 - 4.6	-5.1 to 3.9	1.2 - 6.4	0.1-25
UGT1A1	TYPVPFQR	-3.6 to 7.0	1.8 - 4.4	2.1 to 5.6	0.7 - 10.7	0.1-25
	DGAFTLTK	-3.0 to 7.5	4.2 - 5.7	-3.0 to 6.0	2.0 - 11.7	0.1-25
UGT1A3	YLSIPTVFFLR	-3.9 to 1.5	1.5 - 4.8	-3.6 to 5.4	1.2 - 6.9	0.1-25
UGT2B7	ANVIASALAIQIPQK	1.3 - 7.4	3.6 - 4.3	-3.44 to 2.7	2.5 - 12.0	0.1-25
	IEIYPTSLTK	1.8 - 11.6	2.5 - 4.6	-3.3 to 7.3	1.7 - 7.0	0.1-25
UGT2B15	SVINDPVYK	3.3 - 9.7	2.0-6.0	-3.0 to 5.3	1.1 - 9.3	0.1-25
	FSVGYTFEK	3.1 - 8.6	2.2 - 6.9	-3.9 to 2.3	1.2 - 6.0	0.1-25
UGT2B17	FSVGYTVEK	-5.3 to 4.8	2.4 - 11.2	-3.7 to 3.1	3.3 - 14.7	0.1-25
	SVINDPIYK	-0.8 to 4.9	2.7 - 4.5	-2.8 to 10.1	0.3 - 5.8	0.5-25

based prediction tool (https://web.expasy.org/peptide_mass/) (requested in June 2019). The respective protein sequences were retrieved from the UniProtKB/Swiss-Prot database. According to the mass range of the MS and to ensure protein specificity, peptides with a sequence length of 7–20 amino acids were considered as suitable candidates. Peptides with one or more of the following features were excluded: (a) containing cysteine, methionine or tryptophan because of decreased stability by oxidation; (b) non-synonymous genetic polymorphisms with an allele frequency > 1%; (c) experimentally proven post-translational modifications; (d) repeated sequences of arginine and lysine which bear the risk of missed cleavages by trypsin. The chosen sequence candidates underwent a NCBI protein blast search to assure their protein specificity.

At the end of this process, the identified sequences were ordered as crude peptides (SpikeTides from JPT Peptide Technologies, Berlin, Germany) to characterize them in terms of mass spectrometric and chromatographic properties. Here, eligible mass transitions and parameters for optimal fragmentation were determined for each peptide by manual infusion to the mass spectrometer 5500 QTRAP (AB Sciex, Darmstadt, Germany). For each peptide, the retention time was determined, and three to four mass transitions with the highest intensity were selected. To proof the suitability of the chosen surrogate peptides for detection of the respective enzymes, they were applied to tryptic digests of human liver and intestinal samples. The best observable peptides were selected and ordered both, in unlabeled and isotope-labelled form with a high purity of > 95% (AQUA Peptides, ThermoFisher Scientific), suitable for absolute quantification.

2.3. Sample preparation and digestion procedure

Before the tryptic digestion of commercially available (BD Biosciences, Woburn, MA, USA) pooled human intestinal (4 males, 4 females; age 24–70) and liver (18 males, 7 females; age 21–64) microsomes, their whole protein content was determined via bicinchoninic acid assay and adjusted to a concentration of 2 mg/ml. Then, 100 µl of each sample were mixed with 10 µl DTT (200 mM), 10 µl ProteaseMAXTM surfactant trypsin enhancer prepared according to the manufacturer's instructions, 40 µl ammonium bicarbonate (50 mM, pH 7.8) and incubated at 60 °C for 30 min (denaturation). For alkylation, samples were cooled down, than 10 µl IAA (400 mM) were added, and incubated for 15 min at 37 °C in the dark. Afterwards, isotope-labelled internal standards were added, and the digestion was performed by adding trypsin (trypsin/protein ratio 1:40) and incubation at 37 °C. The digestion was stopped after 16 h by the addition of 20 µl FA (10% v/v). After centrifugation at 16.000 × g and 4 °C for 15 min, the clear supernatants were transferred into HPLC vials for LC-MS/MS analysis. All steps of sample preparation and digestion were performed in Protein LoBind-tubes (Eppendorf, Hamburg, Germany). The digestion of microsomes was performed in triplicates.

2.4. LC-MS/MS analysis

For the LC-MS/MS analysis, a 5500 QTRAP triple quadrupole mass spectrometer (AB Sciex) coupled to an Agilent 1260 Infinity Binary

Table 4

Results of stability testing for proteospecific peptides used as surrogates for metabolizing enzymes. Data are given as mean values in percent of the respective initial concentrations. All values were derived from in each case three quality control sample sets (0.25, 2.5 and 25 nmol/L).

Parameter		short-term (bench-top) stability (%)	post-preparative (rack) stability (%)	Digestion stability (%)
Protein	Peptide	2 h @ room temperature	24 h @ 5 °C (autosampler)	16 h @ 37 °C
CES-1	AISESGVALTSVLVK	88.8 – 104.1	96.6 – 110.8	87.9 – 104.4
CES-2	ADHGDELPPVFR	86.7 – 102.9	94.7 – 109.6	83.5 – 96.1
CYP1A1	IQEELDTVIGR	88.3 – 104.4	89.3 – 107.7	92.2 – 110.3
	YLPNPSLNAFK	87.0 – 98.1	93.2 – 108.4	86.5 – 102.1
CYP1A2	IGSTPVLVLSR	88.7 – 102.6	87.7 – 116.4	92.2 – 106.4
	YLPNPALQR	89.7 – 100.0	87.5 – 110.9	89.5 – 102.4
CYP2A6	GTGGANIDPTFFLSR	87.8 – 105.2	94.2 – 107.8	81.5 – 106.9
CYP2B6	GYGVIFANGNR	89.7–104.2	84.1 – 111.6	90.1 – 102.3
	TEAFIPFSLGK	83.0 – 100.0	93.3 – 114.1	96.8 – 109.4
CYP2C8	VQEEIDHVIGR	85.7 – 112.8	93.8 – 107.8	85.4 – 117.9
	GLGISSNGK	84.8 – 117.0	95.0 – 107.6	88.8 – 108.0
CYP2C9	LPPGPTPLPVIGNILQIGIK	82.6 – 101.0	94.8 – 105.9	83.0 – 102.0
	GIFPLAER	86.8 – 100.0	91.4 – 101.5	87.4 – 105.9
CYP2C18	DIDITPIANAFGR	85.9 – 101.0	99.7 – 105.7	92.7 – 103.1
CYP2C19	GHFPLAER	88.8–104.1	86.3 – 116.0	84.6 – 110.9
	GTTLTSLTSLVLDHNK	85.3 – 108.3	96.8 – 113.7	87.4 – 104.8
CYP2D6	DIEVQGFR	82.8 – 114.3	99.3 – 112.5	89.8 – 107.1
	GTTLITNLSSVLK	83.1 – 104.1	90.7 – 106.2	87.2 – 100.0
CYP2E1	FITLVPNLPHAEATR	85.9 – 98.5	89.2 – 105.7	90.9 – 102.9
	FGPVFTLYVGSQR	88.4 – 98.7	96.9 – 104.4	102.9 – 118.7
CYP2J2	EVTVDTTLAGYHLPK	90.4–110.6	86.0 – 108.3	94.0 – 103.7
CYP3A4	EVTNFLR	84.3 – 108.5	83.3 – 110.0	89.9–104.2
	LGIPGPTPLPFLGNILSYHK	84.0 – 98.7	90.2 – 109.2	81.6 – 97.4
CYP3A5	DTINFLSK	82.1 – 99.0	96.2 – 115.8	85.7 – 104.3
	LFPVAIR	86.1 – 108.9	92.0 – 112.5	88.7 – 113.3
CYP3A7	LGIPGPTPLPFLGNALSFR	80.8 – 94.4	94.7 – 105.1	80.5 – 93.4
CYP4F2	SVINASAAIAPK	85.5 – 101.4	96.3 – 108.7	88.6 – 100.3
CYP4F12	LVDHFTDAVIR	85.5 – 119.4	90.7 – 105.0	87.8 – 107.0
CYP4A11	NSQSYIAISDLNLLVFSR	89.1 – 104.7	84.3 – 108.2	84.6 – 118.1
UGT1A1	TYPVPFQR	82.9–105.0	97.4 – 109.7	89.4 – 101.3
	DGAFYTLK	84.0 – 104.7	87.0 – 107.3	97.0 – 116.8
UGT1A3	YLSIPTVFFLR	84.1 – 98.7	95.2 – 109.6	93.4 – 110.5
UGT2B7	ANVIASALAQIPQK	84.0 – 106.9	85.2 – 111.9	87.6 – 105.6
	IEIYPTSLTK	86.1 – 117.9	90.4 – 108.7	89.3 – 104.5
UGT2B15	SVINDPVYK	86.2 – 103.7	90.4 – 113.8	81.8 – 98.1
	FSVGYTFEK	88.7 – 101.1	92.4 – 107.5	80.0 – 99.4
UGT2B17	FSVGYTVEK	81.7 – 115.0	91.8 – 106.1	96.4 – 101.7
	SVINDPIYK	86.6–103.6	85.7 – 114.3	82.5 – 101.7

HPLC system (Agilent Technologies, Waldbronn, Germany) was used. The system was controlled by the Analyst 1.6.3 software (Sciex, Darmstadt, Germany). Chromatographic separation was performed on a Kinetex® 2.6 µm C18 100 Å core-shell column (100 × 2.1 mm, Phenomenex, Aschaffenburg, Germany) with gradient elution using acetonitrile containing 0.1% formic acid (solvent A) and water containing 0.1% formic acid (solvent B). Flow rate of mobile phase was set at 200 µl/min and injection volume was 20 µl. The gradient applied was as follows: 2% solvent A for 5 min, followed by a linear gradient of 2–25% solvent A over 35 min, than increase of solvent A to 50% within 13 min, switching to 60% for 3 min before coming back to 2% solvent A within 9 min. Column oven temperature was set to 50 °C while autosampler temperature was adjusted to 4 °C. The mass spectrometer was equipped with an electrospray ionization (ESI) Turbo V™ Ion Source interface operated in positive mode using the following conditions: source temperature, 500 °C; ion spray voltage, 5500 V; curtain gas, 50 psi; ion source gas 1, 50 psi; ion source gas 2, 50 psi and high collision activated gas (all nitrogen). Mass spectrometry parameters such as declustering potential and collision energy were manually optimized for each single peptide as mentioned above and are summarized in Table 2. Three to four mass transitions were monitored for each analyte and internal standard. All chromatograms were evaluated with the MultiQuant™ 3.0.2 software using the internal standard method and peak area ratios for calculation of absolute protein amounts (linear regression, 1/x weighting).

2.5. Preparation of calibration curves, method validation and sample measurements

Bovine serum albumin (BSA, 2 mg/ml), digested with trypsin, was used as a blank matrix for preparation of calibration curves and quality controls (QC). It was spiked with peptide standards to the following final concentrations: 0.1, 0.25, 0.5, 1.0, 2.5, 5.0, 10.0 and 25.0 nmol/L, which equals to 2–500 fmol on the column. Quality control samples were prepared resulting in the concentrations of 0.25, 2.5 and 25 nmol/L. Stable isotope-labelled standards were added to all samples reaching final concentration of 25 nmol/L. To confirm linearity, the peak area ratios of analyte over the internal standard peptide was plotted against the spiked concentration. Selectivity has been investigated by digesting and analyzing six different batches of BSA. The inter-day accuracy and precision was evaluated by preparing and measuring six calibration curves prepared and measured on six different days. To assess the intra-day accuracy and precision, six QC sample sets were prepared and measured on one day. To evaluate the reproducibility of the entire process including sample preparation, protein digestion and LC-MS/MS analysis, a mixture of 21 recombinant DMEs (Supersomes®, BD Biosciences, Woburn, MA, USA; Corning, NY, USA) was prepared by adding 25 to 50 µl of each recombinant enzyme (depending on the enzyme content given in the respective analytical certificates) to a final volume of 1 ml of digested BSA solution (2 mg/ml), which was aliquoted (N = 5) and subjected to digestion and analysis on one day (intra-day precision). This analysis was repeated on four days to assess inter-day precision of the entire process. Stability was studied throughout the whole process of

Table 5

Results of freeze–thaw stability for proteospecific peptides used as surrogates for metabolizing enzymes. Data are given as mean values in percent of the respective initial concentrations. All values were derived from in each case three quality control sample sets (0.25, 2.5 and 25 nmol/L) prepared in 2 mg/ml digested bovine serum albumin (BSA) solution.

Parameter	Peptide	freeze–thaw stability (%)		
		1st freeze–thaw cycle	2nd freeze–thaw cycle	3rd freeze–thaw cycle
CES-1	AISESGVALTSVLVK	88.9 – 102.9	87.5 – 109.2	87.9 – 107.8
CES-2	ADHGDELFPVFR	95.4 – 107.1	88.7 – 109.3	87.1 – 112.1
CYP1A1	IQEELDTVIGR	90.0 – 107.7	88.8 – 112.3	87.5 – 110.3
	YLPNPSLNAFK	86.8 – 104.7	86.7 – 112.8	90.6 – 112.8
CYP1A2	IGSTPVVLVLSR	95.5 – 116.8	90.3 – 110.4	95.3 – 104.8
	YLPNPALQR	90.4 – 105.9	88.5 – 99.3	82.7 – 102.2
CYP2A6	GTGGANIDPTFFLSR	94.2–115.2	85.1 – 105.8	83.2 – 98.7
CYP2B6	GYGVIFANGNR	83.5 – 112.5	90.0 – 111.5	92.6 – 117.6
	TEAFIFPSLGGK	89.0 – 105.0	85.3 – 105.2	86.2 – 107.4
CYP2C8	VQEEIDHVIGR	91.9 – 108.2	82.7 – 110.1	88.5 – 110.0
	GLGISSNGK	91.9 – 109.4	89.8 – 108.3	89.8 – 109.4
CYP2C9	LPPGPTPLPVIQIGIK	90.0 – 116.7	86.0 – 109.1	88.7 – 107.0
	GIFPLAER	84.2 – 111.1	89.3 – 105.7	85.5 – 106.7
CYP2C18	DIDITPIANAFGR	86.9 – 105.0	84.4 – 101.7	89.9 – 106.9
CYP2C19	GHFPLAER	87.0 – 106.4	83.3 – 101.7	86.9 – 104.2
	GTTLTSLTSLVLDNK	93.5 – 107.9	82.7 – 111.9	89.0 – 112.8
CYP2D6	DIEVQGFGR	96.4 – 113.6	89.8 – 113.6	87.6 – 113.6
	GTTLITNLSSVLK	92.1 – 104.1	87.5 – 102.4	87.1 – 101.0
CYP2E1	FITLVPSNLPHEATR	95.4 – 104.2	86.9 – 105.9	90.2 – 110.3
	FGPVFTLYVGSQR	88.9 – 102.9	87.5 – 113.0	84.0 – 108.0
CYP2J2	EVTVDITLAGYHLPK	93.6 – 108.8	89.5 – 118.4	83.2 – 103.2
CYP3A4	EVTNFLR	85.4 – 105.4	85.4 – 114.0	83.5 – 102.3
	LGIPGPTPLPFLGNILSYHK	93.4 – 103.3	86.8 – 103.3	89.7 – 101.4
CYP3A5	DTINFLSK	87.8 – 103.4	84.4 – 108.8	92.8 – 107.4
	LFPVAIR	87.9 – 119.4	89.5 – 116.4	91.9 – 117.9
CYP3A7	LGIPGPTPLPFLGNALSFR	95.6 – 107.1	84.0 – 107.4	90.7–117.1
CYP4F2	SVINASAAIAPK	96.8 – 116.3	88.6 – 110.6	87.4 – 110.6
CYP4F12	LVHDFDVAIR	83.0 – 108.9	92.0 – 113.6	88.5 – 109.0
CYP4A11	NSQSYQAIISDLNNLVFSR	92.5 – 105.0	90.1 – 108.3	90.7 – 105.5
UGT1A1	TYPVPFQR	92.7 – 106.3	93.7 – 114.7	90.1–103.7
	DGAFYTLK	83.6 – 103.9	80.8 – 107.0	83.6 – 114.0
UGT1A3	YLSIPTVFFLR	93.5 – 107.5	88.3 – 106.9	85.7 – 109.1
UGT2B7	ANVIASALAQIPQK	87.5 – 109.5	87.8–106.5	89.2 – 101.0
	IEIYPTSLTK	98.0 – 114.0	85.0 – 113.9	92.1 – 108.5
UGT2B15	SVINDPVYK	91.6 – 102.0	84.7 – 97.4	90.1 – 102.9
	FSVGYTFEK	93.8 – 111.6	88.7 – 110.9	92.4 – 114.5
UGT2B17	FSVGYTV EK	91.0 – 118.3	85.0 – 102.9	82.6 – 109.0
	SVINDPIYK	88.5 – 113.5	90.1 – 112.0	85.1 – 113.0

sample preparation and analysis by using in each case three QC sample sets. The immediately prepared and measured samples served as the reference to the samples subjected to different treatment, as specified below. To address bench-top stability, samples were stored 2 h at room temperature before further preparation. Rack stability was investigated by storing samples in the cooled autosampler for 24 h before measuring them. Samples underwent up to three freeze–thaw cycles (storage at $-80\text{ }^{\circ}\text{C}$) before being analyzed to study freeze–thaw stability of the peptides. In order to investigate the stability of the intact proteins, the aforementioned mixture of 21 recombinant DMEs (Supersomes[®], BD Biosciences) in digested BSA solution was aliquoted ($N = 5$) and subjected to three freeze–thaw cycles prior digestion and analysis. To assure peptide stability during the overnight tryptic digestion, prepared samples were stored for 16 h at $37\text{ }^{\circ}\text{C}$ before quantitative analysis.

Calibration curves and QC sample sets were freshly prepared and measured on each day of the analysis as described above. QC samples were measured during the entire analytical run and represented at least 10% of all analytical samples. An analytical run was accepted if at least 4 out of 6 of all measured QC samples were within a relative error range of $\pm 15\%$ ($\pm 20\%$ at the lower limit of detection) of the nominal values, which was in line with the respective FDA/EMA guidelines

3. Results and discussion

A LC-MS/MS-based method for the absolute quantification of clinically relevant human DMEs of phase I and II was developed and

validated in this study. Prior to the wet-lab experiments, an in-silico prediction of possible peptides for absolute quantification was conducted. To ensure reliable and reproducible results, only peptides without adverse features such as instability against oxidation (due to cysteine, methionine or tryptophan residues), genetic polymorphisms and post-translational modifications were chosen. Additionally, the protein specificity was confirmed for all used peptides by BLAST search. Finally, possible mass transitions for all peptides were predicted in-silico and confirmed by wet-lab experiments at the mass spectrometer.

For all proteospecific peptides, corresponding stable isotope-labelled internal standards were used. They showed a distinct mass difference of 8–10 Da, due to the introduction of C-13 and N-15 for labelling at the terminal amino acid. The mass spectrometer operated in the positive mode and the ionization was done by electrospray ionization. For maximal sensitivity, the respective m/z ratios of the parent ions showing the highest signal intensity were used as Q1 filter setting. For the majority of the peptides, doubly charged parent ions were observed to cause the highest signal intensity and therefore used as Q1 mass filter setting. However, for a significant number of peptides the triply charged parent ion showed the highest signal intensity. This was namely the case for ADHGDELFPVFR (CES-2), LPPGPTPLPVI-GNLIQIGIK (CYP2C9), GTTLTSLTSLVLDNK (CYP2C9), GTTLTSLTSLVLDNK (CYP2C19), FITLVPSNLPHEATR (CYP2E1), EVTVDITLAGYHLPK (CYP2J2), LGIPGPTPLPFLGNIL-SYHK (CYP3A4), LGIPGPTPLPFLGNALSFR (CYP3A7), LVHDFDVAIR (CYP4F12) and NSQSYQAIISDLNNLVFSR (CYP4A11). It is conspicuous that most of the aforementioned peptides

Table 6

Protein amounts of clinically relevant metabolizing enzymes as observed in pooled human liver microsomes from 25 donors and human intestinal microsomes from three individuals. Data are given in mean \pm SD.

protein	peptide	human liver	human intestinal
		microsomes	microsomes
		protein amount in pmol/mg	
CES-1	AISESGVALTSLVK	3537 \pm 476	6.35 \pm 0.47
CES-2	ADHGDELPFVFR	226 \pm 21.7	395 \pm 36.7
CYP1A1	IQEELDTVIGR	0.72 \pm 0.07	<LLOQ
	YLPNPSLNAFK	<LLOQ	<LLOQ
CYP1A2	IGSTPVLVLSR	140 \pm 8.58	<LLOQ
	YLPNPALQR	86.9 \pm 7.08	<LLOQ
CYP2A6	GTGGANIDPTFFLSR	295 \pm 31.2	<LLOQ
CYP2B6	GYGVIFANGNR	30.2 \pm 0.29	<LLOQ
	TEAFIPFSLGK	12.6 \pm 0.77	<LLOQ
CYP2C8	VQEEIDHVGIR	220 \pm 24.2	<LLOQ
	GLGISSNGK	119 \pm 12.5	<LLOQ
CYP2C9	LPPGPTPLPVIGNILQIGIK	218 \pm 20.5	9.04 \pm 0.68
	GIFPLAER	456 \pm 33.6	8.79 \pm 3.15
CYP2C18	DIDITPIANAFGR	4.42 \pm 1.81	1.48 \pm 1.56
CYP2C19	GHFPLAER	20.1 \pm 0.57	2.53 \pm 0.11
	GTTLTSLTSLVHNDK	44.2 \pm 1.86	8.83 \pm 0.68
CYP2D6	DIEVQGFGR	30.2 \pm 3.56	<LLOQ
	GTTLITNLSSVLK	153 \pm 15.0	3.72 \pm 0.80
CYP2E1	FITLVPSNLPHEATR	546 \pm 53.6	<LLOQ
	FGPVFTLYVGSQR	44.10 \pm 2.03	<LLOQ
CYP2J2	EVTVDITLAGYHLPK	4.98 \pm 0.68	1.10 \pm 0.07
CYP3A4	EVTNFLR	217 \pm 4.06	24.8 \pm 1.02
	LGIPGPTPLPFLGNLSYHK	26.9 \pm 2.47	1.29 \pm 0.11
CYP3A5	DTINFLSK	9.46 \pm 5.34	<LLOQ
	LFPVAIR	14.6 \pm 0.85	1.53 \pm 0.59
CYP3A7	LGIPGPTPLPFLGNLSFR	2.83 \pm 0.25	<LLOQ
CYP4F2	SVINASAAIAPK	138 \pm 8.98	19.9 \pm 1.09
CYP4F12	LVHDFDVAIR	6.34 \pm 0.60	5.82 \pm 1.47
CYP4A11	NSQSYIQAISDLNLLVFSR	1175 \pm 257	<LLOQ
UGT1A1	TYPVPFQR	43.8 \pm 3.30	<LLOQ
	DGAFTYTK	91.1 \pm 8.94	6.40 \pm 0.60
UGT1A3	YLSIPTVFLLR	4.47 \pm 0.15	<LLOQ
UGT2B7	ANVIASALAIQIPQK	1416 \pm 197	75.2 \pm 6.45
	IEIYPTSLTK	486 \pm 56.0	22.4 \pm 1.59
UGT2B15	SVINDPVYK	314 \pm 26.1	<LLOQ
	FSVGYTFEK	124 \pm 2.09	<LLOQ
UGT2B17	FSVGYTVEK	23.0 \pm 3.26	42.3 \pm 9.66
	SVINDPIYK	19.6 \pm 3.30	141 \pm 17.5

contain histidine residues, which are known to promote multiple charged states. For all selected peptides, a manual product ion scan was performed for all the identified parent ions in order to identify fragments showing the highest signal intensity. Three to four mass transitions per peptide were chosen, which are listed in Table 2. Optimal fragmentation conditions were identified by ramping the parameters collision energy, declustering potential, entrance potential and collision cell exit potential. The optimal parameters were used for the final analytical method. The chosen surrogate peptides and most of the respective mass transitions are in good agreement to the literature for CES-1, CES-2, CYP1A1, CYP1A2, CYP2A6, CYP2B6, CYP2C8, CYP2C9, CYP2C18, CYP2C19, CYP2D6, CYP2E1, CYP2J2, CYP3A4, CYP3A5, CYP3A7, CYP4F2, CYP4F12, CYP4A11, UGT1A1, UGT1A3, UGT2B7, UGT2B15 and UGT2B17 [6,24,26,27,29–48]. For CYP2C18 (DIDITPIANAFGR) and CYP4A11 (NSQSYIQAISDLNLLVFSR), we here report peptides, that have not been used so far for the absolute protein quantification. In some cases, peptides found in the literature do not match to our stated stability criteria. For a number of peptides, we found different MRM mass transitions than published. A reason for this could be that the optimal conditions highly depend on the used experimental setup, in particular on the available mass spectrometer. This shows again the importance of manually optimizing the analytical parameters to the individual experimental setup and not to rely on in-silico predictions alone. Furthermore, optimal parameters ensure an increased sensitivity. To address the risk of receiving misleading results due to different isoforms,

posttranslational modifications, truncated forms of the protein or interferences with other peptides, in most cases we used two surrogate peptides for each protein monitored by three mass transitions. In contrast, many quantitative proteomics studies, including our previous assay [6] are based on just one surrogate peptide. Due to the large number of analytes and the expected complexity of the matrix (liver and intestinal tissue), to which the method is supposed to be applied, a partially long gradient elution method of 60 min for chromatography was used. This leads to chromatographic separation of different peptides and matrix constituents. All included mass transitions for each peptide and its corresponding internal standard peptides showed co-elution (Fig. 1). Optimal mass spectrometric detection, which is crucial for reliable quantitative results [28], was achieved by the use of the scheduled MRM algorithm by the Analyst software [49]. The dwell time was dynamically adapted to a fixed cycle time of 1.0 s and altogether 264 mass/charge transitions (20–30 data points per peak width of 20–30 s) were monitored over the entire analytical run.

Only few [6,19,26,42] of the so far published methods in the literature for the absolute quantification of DMEs are validated according to the current bioanalytical guidelines. We decided to use the Bioanalytical Method Validation Guidance for Industry (FDA) because there are so far no clear guidelines dedicated to quantitative targeted proteomics analysis and this guidance considers relevant bioanalytical issues that are missing in rather chemically oriented guidelines (e.g. ICH). However, due to the fact that our method is not expected to be used in decision making processes (e.g. drug approval), we performed no full validation but included only the most relevant parameters for routine analysis, namely linearity, within- and between day accuracy and precision and stability of the analytes during different conditions.

Moreover, most of the published methods show a limited analytical spectrum concerning either phase I [19,30,32,38,46,47,50,51] or phase II [26,27,37,43] metabolizing enzymes. In case of human tissue, the analytes of interest are expected to be constitutionally abundant in any specimens, which leads to a non-availability of a classical blank matrix. To address this issue, we chose digested bovine serum albumin (2 mg/ml) as blank matrix for all validation steps to simulate a digested protein background. The used total protein concentration of BSA is the same as in our tryptic digestion experiments. Digested BSA is clearly a less complex matrix than human tissues but it is in our opinion a suitable approximation to complex protein-containing matrices. We are aware that this represents a considerable limitation because the complexity of the biological matrix may be underestimated. However, as we applied a long gradient elution (65 min) and used stable isotope-labelled internal standards, which are subjected to identical ion suppression as the analytes, we estimate only little impact of the matrix on the analytical outcome of the method. This approach was also used by other targeted proteomics assays [6,26].

Our unspiked matrix samples from six different batches of digested BSA did not show any analytical signals, whereas spiked matrix samples, as well as human intestinal and liver microsomes, showed analytical signals for all used peptides (Fig. 2). Thus, selectivity of the developed method can be concluded, and chromatographic and mass spectrometric interferences between analytes, internal standards and matrices can be ruled out.

For every analyte, a linear correlation between spiked concentration and analytical signal was observed over the entire validation range (0.10–25 nM; 1/x weighting). The correlation coefficients (r) were determined in a range between 0.9793 and 1.0 (in each case N = 6).

The lower limit of quantification was determined to 0.1 nmol/L for the large majority of the mentioned enzymes. For GYGVIFANGNR (CYP2B6) and VQEEIDHVLGR (CYP2C8) it was set to 0.25 nmol/L, while for SVINDPIYK (UGT2B17) to 0.5 nmol/L (Table 3). The sensitivity of the developed method is comparable to previously published methods [19,21,26,37–39,42,46,52] and can be seen as state-of-the-art in protein quantification via LC-MS/MS. However, some of the aforementioned methods lack information about their lower limit of

Table 7

Concentrations of surrogate peptides of recombinant drug metabolizing enzymes (supersomes) after tryptic digestion. Data are given in mean of six independent digests.

Protein	Peptide	Supersomes		
		protein concentration after digest (nmol/L)	standard deviation (nmol/L)	coefficient of variation (%)
CES-1	AISESGVALTSVLVK	372.73	30.73	8.24
CES-2	ADHGDELPEVFR	272.98	25.31	9.27
CYP1A1	IQEELDTVIGR	n. a.		
	YLPNPSLNAFK	n. a.		
CYP1A2	IGSTPVLVLSR	101.24	8.7	8.6
	YLPNPALQR	152.05	14.81	9.74
CYP2A6	GTGGANIDPTFFLSR	21.39	1.55	7.25
CYP2B6	GYGVIFANGNR	132.66	8.94	6.74
	TEAFIPFSLGK	115.32	7.44	6.45
CYP2C8	VQEEIDHVIGR	27.35	2.69	9.82
	GLGISSNGK	12.86	0.63	4.87
CYP2C9	LPPGPTPLPVIGNILQIGIK	77.21	4.04	5.24
	GIFPLAER	97.8	7.31	7.48
CYP2C18	DIDITPIANAFGR	97.12	6.5	6.7
CYP2C19	GHFPLAER	48.86	2.59	5.29
	GTTLTSLTSLVLDHDK	85.06	4.96	5.83
CYP2D6	DIEVQGFGR	136.7	20.68	15.13
	GTTLITLNLSSVLK	156.13	11.82	7.57
CYP2E1	FITLVPNSLPHEATR	46.36	3.41	7.35
	FGPVFTLYVGSQR	0.59	0.04	6.78
CYP2J2	EVTVDTTLAGYHLPK	77.67	4.11	5.29
CYP3A4	EVTNFLR	52.86	5.96	11.27
	LGIPGPTPLPFLGNILSYHK	0.11	0.01	9.1
CYP3A5	DTINFLSK	19.98	2.05	10.28
	LFPVAIR	20.92	2.39	11.42
CYP3A7	LGIPGPTPLPFLGNALSFR	0.21	0.03	14.3
CYP4F2	SVINASAAIAPK	108.36	6.35	5.86
CYP4F12	LVHDFDVAIVR	72.43	4.87	6.72
CYP4A11	NSQSYIQAISDLNLLVFSR	n. a.		
UGT1A1	TYPVPFQR	74.6	7.69	10.31
	DGAFTYTLK	84.18	8.25	9.81
UGT1A3	YLSIPTVFLR	n. a.		
UGT2B7	ANVIASALAQIPQK	228.5	21.2	9.28
	IEIYPTSLTK	30.91	2.75	8.91
UGT2B15	SVINDPVYK	43.69	4.29	9.83
	FSVGYTFEK	20.56	3.19	15.51
UGT2B17	FSVGYTVEK	22.99	2.4	10.44
	SVINDPIYK	35.9	2.8	7.79

n. a. not commercially available.

quantification or the respective analytical range, which counteracts direct comparisons.

In order to assess the stability of analytes as well as internal standards, we conducted several stability experiments. Bench-top stability was assessed upon storing at room temperature for 2 h, while rack stability was assessed by storing for 24 h in the cooled autosampler. Stability during the overnight digestion procedure was simulated by keeping the samples for 16 h at 37 °C. A sufficient stability was observed for all peptides at low, medium and high concentrations ($\pm 20\%$ of initial concentrations) (Table 4). QCs underwent up to three freeze–thaw cycles to investigate stability during handling of samples and internal standards. All peptides showed sufficient stability during this procedure (Table 5).

We have not investigated the digestion efficiency of the included proteins as we have comprehensively studied this aspect for 13 of our 24 proteins in a previous study [6]. Moreover, the digestion time profiles of nearly all additional of our included proteins have been already characterized [19,26].

Finally, recombinant DMEs were used to investigate the reproducibility of entire process including digestion and LC-MS/MS analysis. For this purpose, a mixture of 21 different supersomes, containing the respective enzymes, was prepared and digested as mentioned above. Coefficients of variation were found to be 15.5% or lower (Table 6). An additional analysis of the mixture of 21 different isoenzymes confirmed the between-day precision to be $< 15.5\%$, while coefficients of variation for the intra-day analysis were found to be $< 7.0\%$ (Supplemental

Table 2). In order to examine the stability of the intact proteins, the mentioned mixture of recombinant enzymes underwent three freeze–thaw cycles. All analytes showed sufficient stability over all cycles (Supplemental Table 3). Thus, the entire analytical process including sample preparation, tryptic digestion and LC-MS/MS analysis of the peptides were in the acceptable range as defined by the guidelines. Due to the fact, that commercially available recombinant enzyme supersomes and human liver / intestinal microsomes do not contain a fixed amount of protein, we were not able to analyze the accuracy of the method using biological samples.

3.1. Application of the method

The developed and validated method was successfully applied for the absolute quantification of clinically relevant drug-metabolizing enzymes in commercially available pooled human liver and intestinal microsomes (Table 7). The following proteins were detected in both types of specimens: CES-1, CES-2, CYP2C9, CYP2C18, CYP2C19, CYP2D6, CYP2J2, CYP3A4, CYP3A5, CYP4F2, CYP4F12, UGT1A1, UGT2B7 and UGT2B17. These findings are in line with previous studies [5,15,19,21,27,53,54] (Supplemental Table 1). However, comparisons of absolute protein amounts are challenging and should be interpreted with caution because the sample preparation has a major impact. This issue was already addressed by Wegler et al. 2017 [55]. Especially, the process of microsome preparation plays an important role and differences can arise between commercially and self-prepared microsomes

[56]. Although commercially available pooled microsomes are expected to be somewhat comparable, direct comparability is hampered when using different batches, i.e. different source of organ donors, because individual characteristics such as genetics, nutrition, smoking or diseases have considerable effects on the enzyme abundance [57].

As proteins with the highest abundances in human intestinal microsomes CES-2 > UGT2B17 > UGT2B7 > CYP3A4 and CYP2C9 were observed. To our knowledge, this is the first report on CYP4F12 abundance in the human intestine. The high abundance of CES-2 and UGT2B17 in human intestine corresponds with our [58] and others [21] findings.

With the exception of CYP1A1, all investigated proteins were found in human liver microsomes. CES-1 > UGT2B7 > CYP4A11 > CYP2E1 > CYP2C9 showed the highest abundances in human liver microsomes. The remarkable high abundance of CES-1, UGT2B7 as well as UGT2B15 are in line with results of Basit et al. [21]. CYP2C9, CYP2A6, CYP4F2 and CYP2E1 were also reported to be highly abundant in the human liver [5,19,38]. It has to be emphasized that discrepancies between studies may result from different sample preparation approaches or individual factors such as genetics. Prasad et al [57] recently emphasized this critical issue. Therefore, more data, especially inter-individual comparisons between liver and intestine, are needed for reliable predictions on pharmacokinetics or drug-drug interactions. Moreover, the selection of different surrogate peptides may have a substantial impact on the observed protein levels. In this study, the observed differences varied from 1.2-fold (UGT2B19) to 12-fold (CYP2E1) (Table 7). This issue was already described by Fallon et al. in 2013 [26], who found for several UGT enzymes comparable variability between different peptides (1.1– 8-fold). Differences in surrogate peptide amount are suspected to result from the digestion process resulting in different cleavage efficiency between the single surrogate peptides. Thus, the use of at least two surrogate peptide was recently recommended in a white paper for targeted proteomics in pharmacology [57]. Unfortunately, there is so far no consensus on appropriate surrogate peptides for certain drug metabolizing enzymes. Thus, our manuscript may provide appropriate candidates of surrogate peptides which could be used and which should be confirmed and extended by other groups working in the field.

4. Conclusions

We developed a robust and sensitive LC-MS/MS method for the simultaneous quantification of CES-1, CES-2, CYP1A1, CYP1A2, CYP2A6, CYP2B6, CYP2C8, CYP2C9, CYP2C18, CYP2C19, CYP2D6, CYP2E1, CYP2J2, CYP3A4, CYP3A5, CYP3A7, CYP4F2, CYP4F12, CYP4A11, UGT1A1, UGT1A3, UGT2B7, UGT2B15 and UGT2B17 by measuring proteospecific tryptic surrogate peptides. Crucial steps of the developed method were validated according to the current bioanalytical guidelines. Additionally, the variability of the entire targeted proteomic procedure including sample preparation, digestion and LC-MS/MS analysis was investigated and demonstrated high reproducibility. The method was successfully applied to determine the protein abundance of clinically relevant drug-metabolizing enzymes in pooled human intestinal and liver microsomes. It is clear that this first application is rather a proof-of-concept study than an extensive expression analysis. In order to provide sufficient data on protein abundance which can be used for PBPK modeling, this method should be applied to a larger cohort of human intestinal and liver samples.

CRedit authorship contribution statement

Christoph Wenzel: Writing of the manuscript, performed experiments, data analysis. Marek Drozdziak: Writing, editing and review of the manuscript. Stefan Oswald: Conceptualization of the study, writing of the manuscript, data analysis.

Declaration of Competing Interest

The authors declare that they have no known competing financial interests or personal relationships that could have appeared to influence the work reported in this paper.

Acknowledgements

The project was funded by the German federal ministry of economic affairs and energy (ZIM, project number: 16KN077223) and the program of the Polish Ministry of Science and Higher Education under the name “Regional Initiative of Excellence” in 2019-2022 project number 002 / RID / 2018/19. Moreover, the project was supported by institutional grants of the Department of Pharmacology, Greifswald and the Institute of Pharmacology and Toxicology, Rostock, Germany. C. W. thanks the Evangelisches Studienwerk Villigst e.V. for financial support of the Ph.D. studies.

Appendix A. Supplementary material

Supplementary data to this article can be found online at <https://doi.org/10.1016/j.jchromb.2021.122891>.

References

- [1] M.S. Benedetti, R. Whomsley, I. Poggesi, W. Cawello, F.-X. Mathy, M.-L. Delporte, P. Papeleu, J.-B. Watelet, Drug metabolism and pharmacokinetics, *Drug Metab. Rev.* 41 (2009) 344–390, <https://doi.org/10.1080/10837450902891295>.
- [2] J.H. Lin, M. Chiba, T.A. Baillie, Is the role of the small intestine in first-pass metabolism overemphasized? *Pharmacol. Rev.* 51 (1999) 135–158.
- [3] S.A. Peters, C.R. Jones, A.-L. Ungell, O.J.D. Hatley, Predicting drug extraction in the human gut wall: assessing contributions from drug metabolizing enzymes and transporter proteins using preclinical models, *Clin. Pharmacokinet.* 55 (2016) 673–696, <https://doi.org/10.1007/s40262-015-0351-6>.
- [4] M.B. Fisher, G. Labissiere, The role of the intestine in drug metabolism and pharmacokinetics: an industry perspective, *Curr. Drug Metab.* 8 (2007) 694–699, <https://doi.org/10.2174/138920007782109788>.
- [5] M. Drozdziak, D. Busch, J. Lapczuk, J. Müller, M. Ostrowski, M. Kurzawski, S. Oswald, Protein Abundance of Clinically Relevant Drug-Metabolizing Enzymes in the Human Liver and Intestine: A Comparative Analysis in Paired Tissue Specimens, *Clin. Pharmacol. Ther.* 104 (2018) 515–524, <https://doi.org/10.1002/cpt.967>.
- [6] C. Gröer, D. Busch, M. Patrzyk, K. Beyer, A. Busemann, C.D. Heidecke, M. Drozdziak, W. Siegmund, S. Oswald, Absolute protein quantification of clinically relevant cytochrome P450 enzymes and UDP-glucuronosyltransferases by mass spectrometry-based targeted proteomics, *J. Pharm. Biomed. Anal.* 100 (2014) 393–401.
- [7] U.M. Zanger, M. Schwab, Cytochrome P450 enzymes in drug metabolism: regulation of gene expression, enzyme activities, and impact of genetic variation, *Pharmacol. Ther.* 138 (2013) 103–141, <https://doi.org/10.1016/j.pharmthera.2012.12.007>.
- [8] C. Weinz, T. Schwarz, D. Kubitzka, W. Mueck, D. Lang, Metabolism and excretion of rivaroxaban, an oral, direct factor Xa inhibitor, in rats, dogs, and humans, *Drug Metab. Dispos.* 37 (2009) 1056–1064, <https://doi.org/10.1124/dmd.108.025569>.
- [9] D. Lang, C. Freudenberger, C. Weinz, In vitro metabolism of rivaroxaban, an oral, direct factor Xa inhibitor, in liver microsomes and hepatocytes of rats, dogs, and humans, *Drug Metab. Dispos.* 37 (2009) 1046–1055, <https://doi.org/10.1124/dmd.108.025551>.
- [10] P.C. Wong, D.J.P. Pinto, D. Zhang, Preclinical discovery of apixaban, a direct and orally bioavailable factor Xa inhibitor, *J. Thromb. Thrombolysis* 31 (2011) 478–492, <https://doi.org/10.1007/s11239-011-0551-3>.
- [11] N. Raghavan, C.E. Frost, Z. Yu, K. He, H. Zhang, W.G. Humphreys, D. Pinto, S. Chen, S. Bonacorsi, P.C. Wong, D. Zhang, Apixaban metabolism and pharmacokinetics after oral administration to humans, *Drug Metab. Dispos.* 37 (2009) 74–81, <https://doi.org/10.1124/dmd.108.023143>.
- [12] D. Zhang, K. He, N. Raghavan, L. Wang, J. Mitroka, B.D. Maxwell, R.M. Knabb, C. Frost, A. Schuster, F. Hao, Z. Gu, W.G. Humphreys, S.J. Grossman, Comparative metabolism of 14C-labeled apixaban in mice, rats, rabbits, dogs, and humans, *Drug Metab. Dispos.* 37 (2009) 1738–1748, <https://doi.org/10.1124/dmd.108.025981>.
- [13] S. Blech, T. Ebner, E. Ludwig-Schwelling, J. Stangier, W. Roth, The metabolism and disposition of the oral direct thrombin inhibitor, dabigatran, in humans, *Drug Metab. Dispos.* 36 (2008) 386–399, <https://doi.org/10.1124/dmd.107.019083>.
- [14] K.P. Cabral, Pharmacology of the new target-specific oral anticoagulants, *J. Thromb. Thrombolysis* 36 (2013) 133–140, <https://doi.org/10.1007/s11239-013-0929-5>.
- [15] M.F. Paine, H.L. Hart, S.S. Ludington, R.L. Haining, A.E. Rettie, D.C. Zeldin, The human intestinal cytochrome P450 “pie”, *Drug Metab. Dispos.* 34 (2006) 880–886, <https://doi.org/10.1124/dmd.105.008672>.

- [16] T. Shimada, H. Yamazaki, M. Mimura, Y. Inui, F.P. Guengerich, Interindividual variations in human liver cytochrome P-450 enzymes involved in the oxidation of drugs, carcinogens and toxic chemicals: studies with liver microsomes of 30 Japanese and 30 Caucasians, *J. Pharmacol. Exp. Ther.* 270 (1994) 414–423.
- [17] V. Brun, A. Dupuis, A. Adrait, M. Marcellin, D. Thomas, M. Court, F. Vandenesch, J. Garin, Isotope-labeled protein standards: toward absolute quantitative proteomics, *Mol. Cell. Proteomics* 6 (2007) 2139–2149, <https://doi.org/10.1074/mcp.M700163-MCP200>.
- [18] S.A. Gerber, J. Rush, O. Stemman, M.W. Kirschner, S.P. Gygi, Absolute quantification of proteins and phosphoproteins from cell lysates by tandem MS, *Proc. Natl. Acad. Sci. U. S. A.* 100 (2003) 6940–6945, <https://doi.org/10.1073/pnas.0832254100>.
- [19] A. Grangeon, V. Clermont, A. Barama, F. Gaudette, J. Turgeon, V. Michaud, Development and validation of an absolute protein assay for the simultaneous quantification of fourteen CYP450s in human microsomes by HPLC-MS/MS-based targeted proteomics, *J. Pharm. Biomed. Anal.* 173 (2019) 96–107, <https://doi.org/10.1016/j.jpba.2019.05.006>.
- [20] Z.M. Al-Majdoub, N. Couto, B. Achour, M.D. Harwood, G. Carlson, G. Warhurst, J. Barber, A. Rostami-Hodjegan, Quantification of proteins involved in intestinal epithelial handling of xenobiotics, *Clin. Pharmacol. Ther.* (2020), <https://doi.org/10.1002/cpt.2097>.
- [21] A. Basit, N.K. Neradugomma, C. Wolford, P.W. Fan, B. Murray, R.H. Takahashi, S. C. Khojasteh, B.J. Smith, S. Heyward, R.A. Totah, E.J. Kelly, B. Prasad, Characterization of differential tissue abundance of major non-cyp enzymes in human, *Mol. Pharm.* (2020), <https://doi.org/10.1021/acs.molpharmaceut.0c00559>.
- [22] M. Ölander, J.R. Wiśniewski, P. Artursson, Cell-type-resolved proteomic analysis of the human liver, *Liver Int.* 40 (2020) 1770–1780, <https://doi.org/10.1111/liv.14452>.
- [23] N. Couto, Z.M. Al-Majdoub, B. Achour, P.C. Wright, A. Rostami-Hodjegan, J. Barber, Quantification of Proteins Involved in Drug Metabolism and Disposition in the Human Liver Using Label-Free Global Proteomics, *Mol. Pharm.* 16 (2019) 632–647, <https://doi.org/10.1021/acs.molpharmaceut.8b00941>.
- [24] B. Prasad, D.K. Bhatt, K. Johnson, R. Chapa, X. Chu, L. Salphati, G. Xiao, C. Lee, C. E.C.A. Hop, A. Mathias, Y. Lai, M. Liao, W.G. Humphreys, S.C. Kumer, J. D. Unadkat, Abundance of Phase 1 and 2 Drug-Metabolizing Enzymes in Alcoholic and Hepatitis C Cirrhotic Livers: A Quantitative Targeted Proteomics Study, *Drug Metab. Dispos.* 46 (2018) 943–952, <https://doi.org/10.1124/dmd.118.080523>.
- [25] Y. Sato, M. Nagata, K. Tetsuka, K. Tamura, A. Miyashita, A. Kawamura, T. Usui, Optimized methods for targeted peptide-based quantification of human uridine 5'-diphosphate-glucuronosyltransferases in biological specimens using liquid chromatography-tandem mass spectrometry, *Drug Metab. Dispos.* 42 (2014) 885–889, <https://doi.org/10.1124/dmd.113.056291>.
- [26] J.K. Fallon, H. Neubert, R. Hyland, T.C. Goosen, P.C. Smith, Targeted quantitative proteomics for the analysis of 14 UGT1As and -2Bs in human liver using NanoUPLC-MS/MS with selected reaction monitoring, *J. Proteome Res.* 12 (2013) 4402–4413, <https://doi.org/10.1021/pr4004213>.
- [27] D.E. Harbourn, J.K. Fallon, S. Ito, T. Baba, J.K. Ritter, G.L. Glish, P.C. Smith, Quantification of human uridine-diphosphate glucuronosyl transferase 1A isoforms in liver, intestine, and kidney using nanobore liquid chromatography-tandem mass spectrometry, *Anal. Chem.* 84 (2012) 98–105, <https://doi.org/10.1021/ac201704a>.
- [28] D.K. Bhatt, B. Prasad, Critical Issues and Optimized Practices in Quantification of Protein Abundance Level to Determine Interindividual Variability in DMET Proteins by LC-MS/MS Proteomics, *Clin. Pharmacol. Ther.* 103 (2018) 619–630, <https://doi.org/10.1002/cpt.819>.
- [29] B. Achour, M.R. Russell, J. Barber, A. Rostami-Hodjegan, Simultaneous quantification of the abundance of several cytochrome P450 and uridine 5'-diphospho-glucuronosyltransferase enzymes in human liver microsomes using multiplexed targeted proteomics, *Drug Metab. Dispos.* 42 (2014) 500–510, <https://doi.org/10.1124/dmd.113.055632>.
- [30] D. Lang, M. Radtke, M. Bairlein, Highly Variable Expression of CYP1A1 in Human Liver and Impact on Pharmacokinetics of Riociguat and Granisetron in Humans, *Chem. Res. Toxicol.* 32 (2019) 1115–1122, <https://doi.org/10.1021/acs.chemrestox.8b00413>.
- [31] Z.-R. Dai, L. Feng, Q. Jin, H. Cheng, Y. Li, J. Ning, Y. Yu, G.-B. Ge, J.-N. Cui, L. Yang, A practical strategy to design and develop an isoform-specific fluorescent probe for a target enzyme: CYP1A1 as a case study, *Chem. Sci.* 8 (2017) 2795–2803, <https://doi.org/10.1039/C6SC03970G>.
- [32] J.P. Savaryn, N. Liu, J. Sun, J. Ma, D.M. Stresser, G. Jenkins, Enrichment-free High-throughput Liquid Chromatography-Multiple-Reaction Monitoring Quantification of Cytochrome P450 Proteins in Plated Human Hepatocytes Direct from 96-Well Plates Enables Routine Protein Induction Measurements, *Drug Metab. Dispos.* 48 (2020) 594–602, <https://doi.org/10.1124/dmd.120.090480>.
- [33] J.-A. Tanner, B. Prasad, K.G. Claw, P. Stapleton, A. Chaudhry, E.G. Schuetz, K. E. Thummel, R.F. Tyndale, Predictors of Variation in CYP2A6 mRNA, Protein, and Enzyme Activity in a Human Liver Bank: Influence of Genetic and Nongenetic Factors, *J. Pharmacol. Exp. Ther.* 360 (2017) 129–139, <https://doi.org/10.1124/jpet.116.237594>.
- [34] J. Li, L. Zhou, H. Wang, H. Yan, N. Li, R. Zhai, F. Jiao, F. Hao, Z. Jin, F. Tian, B. Peng, Y. Zhang, X. Qian, A new sample preparation method for the absolute quantification of a target proteome using (18O) labeling combined with multiple reaction monitoring mass spectrometry, *Analyst* 140 (2015) 1281–1290, <https://doi.org/10.1039/c4an02092h>.
- [35] Y. Shirasaka, A.S. Chaudhry, M. McDonald, B. Prasad, T. Wong, J.C. Calamia, A. Fohner, T.A. Thornton, N. Isoharranen, J.D. Unadkat, A.E. Rettie, E.G. Schuetz, K.E. Thummel, Interindividual variability of CYP2C19-catalyzed drug metabolism due to differences in gene diplotypes and cytochrome P450 oxidoreductase content, *Pharmacogenomics J.* 16 (2016) 375–387, <https://doi.org/10.1038/tpj.2015.58>.
- [36] E.A. Evangelista, T. Aliwarga, N. Sotoodehnia, P.N. Jensen, B. McKnight, R. N. Lemaitre, R.A. Totah, S.A. Gharib, CYP2J2 Modulates Diverse Transcriptional Programs in Adult Human Cardiomyocytes, *Sci. Rep.* 10 (2020) 5329, <https://doi.org/10.1038/s41598-020-62174-w>.
- [37] J.K. Fallon, H. Neubert, T.C. Goosen, P.C. Smith, Targeted precise quantification of 12 human recombinant uridine-diphosphate glucuronosyl transferase 1A and 2B isoforms using nano-ultra-high-performance liquid chromatography/tandem mass spectrometry with selected reaction monitoring, *Drug Metab. Dispos.* 41 (2013) 2076–2080, <https://doi.org/10.1124/dmd.113.053801>.
- [38] H. Kawakami, S. Ohtsuki, J. Kamiie, T. Suzuki, T. Abe, T. Terasaki, Simultaneous absolute quantification of 11 cytochrome P450 isoforms in human liver microsomes by liquid chromatography tandem mass spectrometry with in silico target peptide selection, *J. Pharm. Sci.* 100 (2011) 341–352, <https://doi.org/10.1002/jps.22255>.
- [39] E. Langenfeld, U.M. Zanger, K. Jung, H.E. Meyer, K. Marcus, Mass spectrometry-based absolute quantification of microsomal cytochrome P450 2D6 in human liver, *Proteomics* 9 (2009) 2313–2323, <https://doi.org/10.1002/pmic.200800680>.
- [40] S. Ohtsuki, O. Schaefer, H. Kawakami, T. Inoue, S. Liehner, A. Saito, N. Ishiguro, W. Kishimoto, E. Ludwig-Schwelling, T. Ebner, T. Terasaki, Simultaneous absolute protein quantification of transporters, cytochromes P450, and UDP-glucuronosyltransferases as a novel approach for the characterization of individual human liver: comparison with mRNA levels and activities, *Drug Metab. Dispos.* 40 (2012) 83–92, <https://doi.org/10.1124/dmd.111.042259>.
- [41] M.R. Russell, B. Achour, E.A. McKenzie, R. Lopez, M.D. Harwood, A. Rostami-Hodjegan, J. Barber, Alternative fusion protein strategies to express recalcitrant QconCAT proteins for quantitative proteomics of human drug metabolizing enzymes and transporters, *J. Proteome Res.* 12 (2013) 5934–5942, <https://doi.org/10.1021/pr400279u>.
- [42] A. Sakamoto, T. Matsumaru, N. Ishiguro, O. Schaefer, S. Ohtsuki, T. Inoue, H. Kawakami, T. Terasaki, Reliability and robustness of simultaneous absolute quantification of drug transporters, cytochrome P450 enzymes, and Udp-glucuronosyltransferases in human liver tissue by multiplexed MRM/selected reaction monitoring mode tandem mass spectrometry with nano-liquid chromatography, *J. Pharm. Sci.* 100 (2011) 4037–4043, <https://doi.org/10.1002/jps.22591>.
- [43] Y. Sato, M. Nagata, A. Kawamura, A. Miyashita, T. Usui, Protein quantification of UDP-glucuronosyltransferases 1A1 and 2B7 in human liver microsomes by LC-MS/MS and correlation with glucuronidation activities, *Xenobiotica* 42 (2012) 823–829, <https://doi.org/10.3109/00498254.2012.665950>.
- [44] O. Schaefer, S. Ohtsuki, H. Kawakami, T. Inoue, S. Liehner, A. Saito, A. Sakamoto, N. Ishiguro, T. Matsumaru, T. Terasaki, T. Ebner, Absolute quantification and differential expression of drug transporters, cytochrome P450 enzymes, and UDP-glucuronosyltransferases in cultured primary human hepatocytes, *Drug Metab. Dispos.* 40 (2012) 93–103, <https://doi.org/10.1124/dmd.111.042275>.
- [45] C. Seibert, B.R. Davidson, B.J. Fuller, L.H. Patterson, W.J. Griffiths, Y. Wang, Multiple-approaches to the identification and quantification of cytochromes P450 in human liver tissue by mass spectrometry, *J. Proteome Res.* 8 (2009) 1672–1681, <https://doi.org/10.1021/pr800795r>.
- [46] M.Z. Wang, J.Q. Wu, J.B. Dennison, A.S. Bridges, S.D. Hall, S. Kornbluth, R. R. Tidwell, P.C. Smith, R.D. Voyksner, M.F. Paine, J.E. Hall, A gel-free MS-based quantitative proteomic approach accurately measures cytochrome P450 protein concentrations in human liver microsomes, *Proteomics* 8 (2008) 4186–4196, <https://doi.org/10.1002/pmic.200800144>.
- [47] B.L. Williamson, S. Purkayastha, C.L. Hunter, L. Nuwaysir, J. Hill, L. Easterwood, J. Hill, Quantitative protein determination for CYP induction via LC-MS/MS, *Proteomics* 11 (2011) 33–41, <https://doi.org/10.1002/pmic.201000456>.
- [48] A.-M. Yu, J. Qu, M.A. Felmler, J. Cao, X.-L. Jiang, Quantitation of human cytochrome P450 2D6 protein with immunoblot and mass spectrometry analysis, *Drug Metab. Dispos.* 37 (2009) 170–177, <https://doi.org/10.1124/dmd.108.024166>.
- [49] J. Stahl-Zeng, V. Lange, R. Ossola, K. Eckhardt, W. Krek, R. Aebbersold, B. Domon, High Sensitivity Detection of Plasma Proteins by Multiple Reaction Monitoring of N-Glycosites, *Mol. Cell. Proteomics* 6 (2007) 1809–1817, <https://doi.org/10.1074/mcp.M700132-MCP200>.
- [50] F. Weiß, H.S. Hammer, K. Klein, H. Planatscher, U.M. Zanger, A. Norén, C. Wegler, P. Artursson, T.O. Joos, O. Poetz, Direct Quantification of Cytochromes P450 and Drug Transporters-A Rapid, Targeted Mass Spectrometry-Based Immunoassay

- Panel for Tissues and Cell Culture Lysates, *Drug Metab. Dispos.* 46 (2018) 387–396, <https://doi.org/10.1124/dmd.117.078626>.
- [51] F. Weiß, A. Schnabel, H. Planatscher, B.H.J. van den Berg, B. Serschnitzki, A. K. Nuessler, W.E. Thasler, T.S. Weiss, M. Reuss, D. Stoll, M.F. Templin, T.O. Joos, K. Marcus, O. Poetz, Indirect protein quantification of drug-transforming enzymes using peptide group-specific immunoaffinity enrichment and mass spectrometry, *Sci. Rep.* 5 (2015) 8759, <https://doi.org/10.1038/srep08759>.
- [52] H. Zhang, C. Wolford, A. Basit, A.P. Li, P.W. Fan, B.P. Murray, R.H. Takahashi, S. C. Khojasteh, B.J. Smith, K.E. Thummel, B. Prasad, Regional Proteomic Quantification of Clinically Relevant Non-Cytochrome P450 Enzymes along the Human Small Intestine, *Drug Metab Dispos* 48 (2020) 528–536, <https://doi.org/10.1124/dmd.120.090738>.
- [53] T. Akazawa, Y. Uchida, E. Miyauchi, M. Tachikawa, S. Ohtsuki, T. Terasaki, High Expression of UGT1A1/1A6 in Monkey Small Intestine: Comparison of Protein Expression Levels of Cytochromes P450, UDP-Glucuronosyltransferases, and Transporters in Small Intestine of Cynomolgus Monkey and Human, *Mol. Pharm.* 15 (2018) 127–140, <https://doi.org/10.1021/acs.molpharmaceut.7b00772>.
- [54] Q.Y. Zhang, D. Dunbar, A. Ostrowska, S. Zeisloft, J. Yang, L.S. Kaminsky, Characterization of human small intestinal cytochromes P-450, *Drug Metab. Dispos.* 27 (1999) 804–809.
- [55] C. Wegler, F.Z. Gaugaz, T.B. Andersson, J.R. Wiśniewski, D. Busch, C. Gröer, S. Oswald, A. Norén, F. Weiss, H.S. Hammer, T.O. Joos, O. Poetz, B. Achour, A. Rostami-Hodjegan, E. van de Steeg, H.M. Wortelboer, P. Artursson, Variability in Mass Spectrometry-based Quantification of Clinically Relevant Drug Transporters and Drug Metabolizing Enzymes, *Mol. Pharm.* 14 (2017) 3142–3151, <https://doi.org/10.1021/acs.molpharmaceut.7b00364>.
- [56] J.R. Wiśniewski, Dilemmas With Absolute Quantification of Pharmacologically Relevant Proteins Using Mass Spectrometry, *J. Pharm. Sci.* 110 (2021) 17–21, <https://doi.org/10.1016/j.xphs.2020.10.034>.
- [57] B. Prasad, B. Achour, P. Artursson, C.E.C.A. Hop, Y. Lai, P.C. Smith, J. Barber, J. R. Wisniewski, D. Spellman, Y. Uchida, M.A. Zientek, J.D. Unadkat, A. Rostami-Hodjegan, Toward a Consensus on Applying Quantitative Liquid Chromatography-Tandem Mass Spectrometry Proteomics in Translational Pharmacology Research: A White Paper, *Clin. Pharmacol. Ther.* 106 (2019) 525–543, <https://doi.org/10.1002/cpt.1537>.
- [58] H. Zhang, A. Basit, D. Busch, K. Yabut, D.K. Bhatt, M. Drozdziak, M. Ostrowski, A. Li, C. Collins, S. Oswald, B. Prasad, Quantitative characterization of UDP-glucuronosyltransferase 2B17 in human liver and intestine and its role in testosterone first-pass metabolism, *Biochem. Pharmacol.* 156 (2018) 32–42, <https://doi.org/10.1016/j.bcp.2018.08.003>.

6.2 Comparative Intra-Subject Analysis of Gene Expression and Protein Abundance of Major and Minor Drug Metabolizing Enzymes in Healthy Human Jejunum and Liver

Wenzel C, Lapczuk-Romanska J, Malinowski D, Ostrowski M, Drozdik M, Oswald S

Zur Begutachtung bei „Clinical Pharmacology & Therapeutics“ am 27.06.2023 eingereicht

Projektdesign: C. W., M. D., M. K., S. O.

Projektdurchführung: C. W., J. L.-R., M. K., M. O., M. D., S. O.

Datenanalyse: C. W., J. L.-R., M. K., M. D., S. O.

Erstellung des Manuskriptes: C. W., M. D., S. O.

**COMPARATIVE INTRA-SUBJECT ANALYSIS OF GENE EXPRESSION AND PROTEIN
ABUNDANCE OF MAJOR AND MINOR DRUG METABOLIZING ENZYMES IN HEALTHY
HUMAN JEJUNUM AND LIVER**

Christoph Wenzel¹, Joanna Lapczuk-Romanska², Damian Malinowski³, Marek Ostrowski⁴,
Marek Drozdziak², and Stefan Oswald⁵

¹Department of Pharmacology, University Medicine Greifswald, Greifswald, Germany;
²Department of Experimental and Clinical Pharmacology, Pomeranian Medical University,
Szczecin, Poland; ³Department of Pharmacokinetics and Therapeutic Drug Monitoring,
Pomeranian Medical University, Szczecin, Poland; ⁴Department of Surgery, Pomeranian
Medical University, Szczecin, Poland and ⁵Institute of Pharmacology and Toxicology,
Rostock University Medical Center, Rostock, Germany.

Corresponding Author

Prof. Dr. Stefan Oswald
Institute of Pharmacology and Toxicology
Rostock University Medical Center
Schillingallee 70
18057 Rostock
Germany
E-Mail: stefan.oswald@med.uni-rostock.de
Phone: +49-381-494-5894

Conflict of Interest Statement

The authors report no conflicts of interest

Funding Information

This project was supported by funding of the German Research Foundation (project number:
505943254)

Keywords

drug metabolism, CYP-enzymes, UGT-enzymes, CES-enzymes, first-pass effect, targeted
proteomics, human liver, human jejunum, absolute protein quantification

Abstract

First pass metabolism by phase I and phase II-enzymes in the intestine and liver is a major determinant of the oral bioavailability of many drugs. Several studies analyzed expressions of major drug-metabolizing enzymes (DMEs) such as CYP3A4 and UGT1A1 in the human gut and liver. However, there is still a lack of knowledge regarding other DMEs, i.e. “minor” DMEs, although several clinically relevant drugs are affected by those enzymes. Moreover, there is very limited intra-subject data on hepatic and intestinal expression levels of minor DMEs. To fill this gap of knowledge, we analyzed gene expression (qRT-PCR) and protein abundance (targeted proteomics) of 24 clinically relevant DMEs, i.e. carboxylesterases (CES), UDP-glucuronosyltransferases (UGT) and cytochrome P450 (CYP)-enzymes. We performed our analysis using jejunum and liver tissue specimens from the same 11 healthy organ donors (8 males, 3 females, aged 19-60 y). Protein amounts of all investigated DMEs, with the exception of CYP4A11, were detected in human liver samples. CES2, CYP2C18, CYP3A4 and UGT2B17 protein abundance was similar or even higher in the jejunum, and all other DMEs were found in higher amounts in the liver. Significant correlations between gene expression and protein levels were observed only for 2 of 15 jejunal, but 13 of 23 hepatic DMEs. Intestinal and hepatic protein amounts only significantly correlated for CYP3A4 and UGT1A3. Our results demonstrated a notable variability between the individuals, which was even higher in the intestine than in the liver. Our intra-subject analysis of DMEs in the jejunum and liver from healthy donors may be useful for PBPK-based modelling and prediction in order to improve efficacy and safety of oral drug therapy.

Introduction

The oral bioavailability of many drugs is significantly affected by phase I and II metabolizing enzymes as well as drug transporters expressed in the first pass route of drugs. In contrast to former concepts, which assumed the intestine to be a simple diffusion barrier and the liver as the sole site of drug metabolism, it is now well established that both, the intestine and liver are involved in drug metabolism.¹ In some cases, the intestinal processing by drug metabolizing enzymes (DMEs) contributes equally or even exceeds the hepatic metabolism, which was demonstrated for cytochrome P450 (CYP) 3A4 (e.g. simvastatin, nifedipine, midazolam) and UDP-glucuronosyltransferases (UGT) 1A1 (e.g. ezetimibe, irinotecan).²⁻⁵ Likewise, the extent of drug-drug interactions (DDIs) leading to an increase or decrease in the area under the curve (AUC) of a victim drug caused by inhibition and induction of DMEs is markedly higher in case of oral compared to intravenous administration.^{4,6,7} This emphasizes the importance of the involvement of intestinal epithelial metabolism in oral drug therapy.

Consequently, intestinal and hepatic expression levels of clinically relevant DMEs are required in order to estimate or even predict metabolism of orally administered drugs. Given the uncertain correlation of gene expression and protein amounts of DMEs, protein data would be preferable. In this regard, highly specific and sensitive mass spectrometric methods for quantitative protein analysis, such as the targeted proteomic approach, are today's methods of choice.^{8,9} In contrast to former antibody-based, semi-quantitative methods, such as Western blotting, this approach does not require antibodies, which are not always commercially available and suffer from uncertain specificity due to cross-reactivity with other proteins. Moreover, Western blotting is not suitable for multiplex analysis of several proteins and is characterized by a poor reproducibility, which challenges its application for accurate quantitative purposes.^{9,10}

In this context, several studies investigated the expression of DMEs in the human gut or liver using mass spectrometry methods including global and targeted proteomic approaches

(Supplemental Tables 1, 2). However, most of those studies predominately investigated “major” enzymes, such as CYP3A4, CYP2C9, CYP2D6 or UGT1A1 despite of important contribution of “minor” enzymes in the metabolism of several clinically relevant drugs, such as carboxylesterases (CES) 1/2 (e.g. oseltamivir, remdesivir, clopidogrel), CYP2A6 (e.g. selegiline, cyclophosphamide, dapagliflozin), CYP2C18 (e.g. warfarin, lansoprazole, diclofenac), CYP2J2 (e.g. terfenadine, ebastine, astemizole) or UGT2B17 (testosterone, estradiol).^{11–16}

Moreover, so far in only very few studies an intra-subject analysis of hepatic and intestinal DMEs have been performed, i.e. studies analyzing hepatic and intestinal tissues from the same individuals.^{12,17–19} Considering the observed variability in the inter-individual protein abundance of DMEs in the human intestine and liver (Supplement Tables 1, 2), direct matching of hepatic and intestinal data from different individuals may lead to inaccurate estimations.

Another considerable limitation of some of available studies is merging and analysis of tissue samples from patients suffering from different diseases (e.g. tumors, obesity)^{11,13,15,16,19}, which may affect the expression and function of investigated enzymes as previously described.^{20–22}

Thus, our study aimed to overcome some of the aforementioned limitations by analyzing gene expression and protein abundance of a panel of 24 major and minor DMEs in the jejunum und hepatic samples harvested from the same healthy organ donor.

Methods and Materials

Tissue samples

Liver and intestinal tissues were collected from deceased organ donors of Caucasian ethnicity from Poland (three females; eight males; 19-60 years). Donors died from intracranial hemorrhage, multiorgan injury or head injury and did not suffer from chronic

diseases, except one donor medicated with amiodarone due to atrial fibrillation. A histological examination verified the collected tissues as free from any signs of inflammation or necrosis. Before tissue dissection, all subjects received short-term emergency drugs including dopamine, dobutamine, epinephrine, lidocaine, sodium nitroprusside, vasopressin, cephalosporines, gentamycin, vancomycin, clindamycin, insulin, and mannitol. None of these drugs is known to cause significant regulation of drug metabolizing enzymes. Tissue specimens were taken from the liver and from upper and lower jejunum, not later than 30 minutes after blood flow arrest. Immediately after specimen collection, the mucosa was dissected from the underlying intestinal tissues and snap-frozen in liquid nitrogen for protein quantification. For RNA analysis, specimens were stored in RNeasy (Thermo Fisher Scientific, Waltham, USA). Liver specimens were treated analogously. All specimens were stored at -80°C until further processing. The study was performed in line with the Polish national legislation on organ transplantation and approved by the local Bioethics Committee of the Pomeranian Medical University.

Gene expression analysis

Total RNA was isolated from 40-50 mg of each tissue specimen by using mirVana miRNA Isolation Kit (Thermo Fisher Scientific, Waltham, USA) in accordance to the manufacturer's instructions. Subsequently, cDNA was prepared from 300 ng of total RNA in 40 µL reaction volume by SuperScript VILO cDNA Synthesis Kit (Thermo Fisher, Waltham, USA) following the manufacturer's protocol. mRNA expression in each sample was quantified with custom predesigned TaqMan low density array (TLDA) cards, based on real-time PCR (rt-PCR) technology. The following genes were quantified: CES1 (Hs00275607_m1), CES2 (Hs01077945_m1), CYP1A1 (Hs01054796_g1), CYP1A2 (Hs00167927_m1), CYP2A6 (Hs00868409_s1), CYP2B6 (Hs03044631_m1), CYP2C8 (Hs04183483_g1), CYP2C9 (Hs02383631_s1), CYP2C18 (Hs02383413_s1), CYP2C19 (Hs00426380_m1), CYP2D6 (Hs00164385_m1), CYP2E1 (Hs00559367_m1), CYP2J2 (Hs00356035_m1), CYP3A4 (Hs00604506_m1), CYP3A5 (Hs01070905_m1), CYP3A7 (Hs02511627_s1), CYP4A11 (Hs00167961_m1), CYP4F2 (Hs00426608_m1), CYP4F12 (Hs02515808_s1), UGT1A1

(Hs02511055_s1), UGT1A3 (Hs04194492_g1), UGT2B7 (Hs00426592_m1), UGT2B15 (Hs00870076_s1) and UGT2B17 (Hs00854486_sH). For quantitative comparisons, the $2^{-\Delta Ct}$ values were used with a manually set threshold and normalized to the control gene GAPDH (Hs02786624_g1). Analyses were performed in ViiA 7 Real Time PCR System (Life Technologies, Carlsbad, USA) and data were calculated using the ViiA 7 software.

Protein quantification by LC-MS/MS

Sample preparation for mass spectrometry-based protein quantification was described earlier in detail (Drozdik et al, 2018). In brief, frozen tissue was crushed in a stainless steel mortar. Approximately 40 mg frozen tissue powder was treated with lysis solution containing 0,1% sodium dodecyl sulfate (SDS), 5 mM ethylenediaminetetraacetic acid (EDTA) and 5 μ L/mL Protease Inhibitor Cocktail Set III (Merck, Darmstadt, Germany), for 40 min at 4°C on a shaker. Total protein content of the whole tissue lysates was determined by bicinchoninic assay (Thermo Fisher, Waltham, USA) and 200 μ g total protein of each sample underwent the filter aided sample preparation (FASP). The final trypsin to protein ratio was 1:100. In order to improve the tryptic digestion step, acetonitrile and ProteaseMax™ (Promega, Madison, Wisconsin) were added to reach final concentrations of 10% (v/v) and 0.1% (m/m).

Absolute protein quantification of phase I (CES1, CES2, CYP1A1, CYP1A2, CYP2A6, CYP2B6, CYP2C8, CYP2C9, CYP2C18, CYP2C19, CYP2D6, CYP2E1, CYP2J2, CYP3A4, CYP3A5, CYP3A7, CYP4A11, CYP4F2, CYP4F12) and phase II (UGT1A1, UGT1A3, UGT2B7, UGT2B15, UGT2B17) enzymes was performed by means of mass spectrometry-based targeted proteomics. Details of the procedure, peptides used, mass transitions, instrument parameters, chromatographic conditions and method validation data were published previously (Wenzel et al, 2021). During sample analysis, the accuracy of the method as monitored by measuring quality control samples (at least 10% of all analyzed samples), which was $\leq \pm 15\%$.

Statistical analysis

All mRNA and protein expression data are presented as arithmetic means. The final protein amounts were normalized to the digested tissue mass and are given as fmol protein per mg tissue. Correlation analysis was investigated with the Spearman rank test where $P \leq 0,05$ was considered as significantly different. For statistical calculations and drawing of figures, the Prism 8 software (GraphPad, San Diego, USA) was used.

Results

We included into our analysis the jejunum and hepatic tissue samples from 11 healthy organ donors (8 males, 3 females, age: 19-60 years). All 24 investigated DMEs could be detected on gene expression levels in the human jejunum and liver, with the exception of intestinal CYP1A2 (Ct values > 35). With the exception of non-detectable CYP4A11, the protein data could be observed for all investigated DMEs in human liver tissues, while the protein abundance of CES2, CYP2C18, CYP3A4 and UGT2B17 was similar or even higher in the jejunum. All other studied DMEs were found in higher amounts in the liver. Despite low mRNA expression levels, the jejunal protein could not be detected for CYP1A1, CYP2A6, CYP2B6, CYP2C8, CYP2E1, CYP3A7, CYP4A11 and UGT2B15 (Figure 1).

The contribution of all investigated CYP and UGT enzymes was markedly different in the human jejunum and liver (Figure 2). While CYP2E1 (30%), CYP2C9 (24%) and CYP3A4 / CYP1A2 / CYP2C8 / CYP2A6 (each 7-8%) were the most abundant CYP enzymes in the liver, CYP3A4 (56%), CYP4F2 (15%) and CYP2C9 (10%) were observed at the highest values in the jejunum. The most abundant hepatic UGTs were UGT2B7 (52%), UGT1A1 (28%) and UGT2B15 (15%), while UGT2B17 (47%), UGT1A1 (30%) and UGT2B7 (23%) were in the jejunum.

We observed a considerable variability in the gene expression and protein data in both jejunum and liver (Supplemental Tables 3, 4). Interestingly, in most cases, the variability was substantially higher for intestinal than for hepatic enzymes (17 of 23 genes and 10 of 15 proteins). For example, the mean coefficient of variation for all detectable enzymes on protein levels was $89.1 \pm 67.9\%$ in the liver samples, but $106.1 \pm 70.7\%$ in the jejunum

($p=0.09$). This variability in intestinal samples was even more pronounced on the mRNA level ($84.5 \pm 43.8\%$ vs. $107.9 \pm 48.3\%$, $p=0.02$).

The correlation analysis of gene expression and protein data revealed significant correlations only for 2 of 15 jejunal enzymes but for 13 of 23 hepatic DMEs (Table 1). Significant correlations between hepatic and jejunal protein amounts could only be found for CYP3A4 and UGT1A3 (Table 2).

Discussion

DMEs are of outstanding relevance for the pharmacokinetics and in turn the efficacy and safety of the majority of drugs on the market.²³ Thus, data on their expression and function is of great importance in order to predict human drug metabolism and disposition by using sophisticated *in vitro-in vivo* correlation approaches, such as physiologically based pharmacokinetic (PBPK) modeling and simulation.²⁴ During the recent years, several studies have been published, which characterized expression of clinically relevant DMEs in the human intestine and/or liver.^{11,13–16,19,25–28} In 2018, we already published data on the expression of 13 clinically highly important “major” enzymes, such as CYP3A4, CYP2C9, CYP2D6 and UGT1A1 in the human liver and intestine from the same organ donors.¹² In addition, several other groups published studies complemented previous gaps of knowledge in a comparable manner (Supplemental Table 1). Here, all groups took advantage of the recent advantages of mass spectrometry-based protein quantification, which enabled highly sensitive, specific and accurate protein quantification.^{8–10}

However, despite the great value of those data, there is a missing information about “minor” DMEs being beyond the scope of most previous investigations, but important for the metabolism of a significant number of drugs used in clinical practice.

In contrast to previous studies by us and others, our current analysis provides a comprehensive and complementary overview of gene expression and protein abundance of “major” and “minor” DMEs in the human jejunum and liver. In line with previous findings, we were able to verify that the enzymes with the highest gene expression and protein abundance levels in the liver are also considered to be the “major” enzymes in terms of their

relevance for general drug metabolism (e.g. CYP2C9, CYP2E1, CYP3A4, CYP2C8) (Supplemental Table 1). While DMEs quantitative rank orders reported are quite similar in the studies, the specific protein amounts may differ somewhat, most likely due to different sample preparation techniques, proteospecific peptides used and various mass spectrometry approaches with different quantitative algorithms (e.g. targeted vs. global proteomics).^{8,29} Likewise, different sample preparation techniques (e.g. microsomes vs. S9 fraction vs. whole tissue lysates) may add profound variability to the final proteomic data.²⁹ In addition, also individual factors such as genetics, environment and diseases of sample donors were shown to contribute to the inter-subject variability.²⁰⁻²³ In this regard, it is worth to mention that our analysis included only tissue samples from previously healthy organ donors, whereas several previous studies obtained samples from patients suffering from different diseases, which might affect DME expression.

In addition to the well-established “major” DMEs, we also observed considerably high protein amounts of the investigated “minor” cytochromes CYP2A6 and CYP4F2 (each 7-8% of all CYPs), which suggests their potential to determine the first pass effect of their respective substrates. However, although several frequently used clinical drugs are metabolized by CYP2A6 (e.g. valproic acid, dapagliflozin, efavirenz or tegafur) and CYP4F2 (e.g. fingolimod), there is no clinical evidence that these enzymes contribute to a substantial first pass metabolism; i.e. the drugs are well-absorbed with high oral bioavailability.

CYP4F2 was also reported to be involved in the biodegradation of vitamin E, leukotrienes and prostaglandins, which may explain its high expression levels in the liver.^{30,31} Interestingly, CYP4F2 expression and function was found to be impaired in nonalcoholic fatty liver disease (NAFLD) in vitro and in vivo, while genetic *CYP4F2* polymorphisms were reported to contribute to development of NAFLD in adults and children.^{32,33}

The other investigated “minor” enzymes CYP2C18, CYP2J2, CYP3A7 and CYP4F12 contribute in each case to only one percent (or less) of all hepatic CYPs. CYP1A1 could barely be detected in one of our eleven studied liver samples, whereas CYP4A11 was not detectable neither in the liver nor jejunum. The absence of CYP1A1 in the jejunum and liver

of most of our donors is in contrast to the study by Lang et al. 2019³⁴ but in line with a recent report of Wegler et al. and another recent analysis from our group.^{19,21,22} Thus, one may conclude that CYP1A substrates are predominantly metabolized by CYP1A2, which also shares nearly all substrates with CYP1A1 and shows a substantial hepatic protein amount (7%).³⁵ Moreover, one can anticipate that CYP1A metabolism takes exclusively place in the liver.

In the jejunum, the expression pattern of CYP enzymes was markedly different. Here, our analysis confirmed CYP3A4 as the dominant enzyme contributing to 56% of all intestinal CYPs being in agreement with experimental and clinical studies showing tremendous importance of intestinal CYP3A4, which equals in terms of function its hepatic expression.^{3,5-7,36,37}

Consequently, oral combination of CYP3A4 substrates and inhibitors or inducers results always in much more striking DDIs compared to the intravenous administration of the same victim and perpetrator drugs.^{4,6,7} Interestingly, CYP4F2 showed the second highest protein amount of all intestinal CYPs, which confirms previous findings.^{19,38} As already stated above, this does not translate to relevant pharmacokinetic consequences most likely due to high lipophilicity and limited drug metabolism of the respective substrates. In line with this assumption, inhibition of intestinal and hepatic CYP4F2 by simultaneously administered ketoconazole resulted in 1.7-fold increased AUC, while chronic pretreatment with carbamazepine decreased its serum exposure by about 40%, which is a comparatively minor pharmacokinetic effect for this potent CYP inhibitor (product information).

The comparatively high jejunal protein amounts of CYP2C9 (10%) and CYP2C19 (6%) have been also reported in previous studies.^{11,12,28,38} The finding of considerable amounts of CYP2C18 (6%) was so far not reported. However, it is not possible to estimate the isolated clinical role of CYP2C18 as its substrates are mostly also subjected to extensive biotransformation by CYP2C9 and/or CYP2C19 (e.g. omeprazole, warfarin or diclofenac).³⁹ Given the low protein abundance of CYP4F12, CYP2J2 and CYP2D6 (each 1-3%), only a negligible role in intestinal drug metabolism can be estimated.

Comparable differences in the expression pattern between human liver and jejunum samples could be also observed for UGTs and carboxylesterases. While the highest abundance was observed for UGT2B7, UGT1A1 and UGT2B15 in the liver, the most abundant enzymes in the jejunum were UGT2B17, UGT1A1 and UGT2B7. This expression pattern was also reported in several other inter-subject analyzes on both organs (Supplemental Table 1, 2). Interestingly, there is a considerable overlap in jejunal and hepatic expression of UGT1A1 and UGT2B7, which explains extensive first pass glucuronidation of some orally administered substrates (e.g. morphine, ezetimibe, mycophenolic acid).^{2,40} While inhibition of the respective UGT enzymes (e.g. by diclofenac) is not expected to cause clinically relevant interactions, up-regulation of UGTs by prototypic enzyme inducers such as rifampicin was shown to cause significantly changed pharmacokinetics and efficacy of respective substrates.^{2,41,42}

On the contrary, UGT2B17 was almost exclusively found in the jejunum, where it represents the most abundant UGT enzyme as already found in a previous collaboration study.⁴³ Several endogenous steroids, including testosterone and estradiol but also drugs such as asciminib, vorinostat and lorcaserin have been identified as substrates of UGT2B17. Despite its high intestinal expression, there is so far no clinical evidence that this may cause clinically relevant consequences (e.g. DDIs). However, *UGT2B17* is highly polymorphic resulting in different expression levels of the encoded protein⁴⁴, which can also be seen in the striking protein levels variability in the liver (CV, 162.6%) and jejunum (CV, 96.7%) as observed in our study. A very recent study has reported that the UGT2B17-mediated intestinal metabolism of diclofenac correlates with its highly variable pharmacokinetics and safety.⁴⁵ Moreover, this genetic variability was discussed to be associated with various types of cancer, i.e. genetic UGT2B17-deletion was identified as risk factor for head, neck and esophageal cancer, while it seems not to be associated with testosterone dependent tumors such as prostate cancer.^{46,47}

With respect to carboxylesterases, which were shown to be the most abundant of all investigated enzymes in the human intestine and liver, CES1 was significantly higher

expressed on gene and protein levels in the liver than in the jejunum, whereas it was the opposite for CES2. This finding was also reported by a previous study for pooled liver and intestinal S9 fractions from different donors.⁴⁸ The high expression of intestinal CES2 suggests its potential involvement in the first pass metabolism of drugs. Indeed, orally administered substrates such as dabigatran etexilate are characterized by extensive pre-systemic metabolism and low oral bioavailability.⁴⁹ Thus, inhibition of intestinal CES2 might reduce the hydrolysis of respective substrates, and thereby the systemic levels of the metabolite (e.g. dabigatran) and subsequently their efficacy and safety. However, respective DDIs have not yet been reported but involvement of hepatic CES2 may contribute to this as well. In this regard, irinotecan can cause severe diarrhea due to the CES2-mediated formation of 7-ethyl-10-hydroxycamptothecin (SN-38) in the small intestine, but co-administration of potent CES2 inhibitors such as loperamide or telimsartan may ameliorate this unwanted side effect in patients.^{50,51} The high hepatic abundance of CES1 is already well established and responsible for the extensive first pass metabolism of CES1 substrates such as clopidogrel, oseltamivir, methylphenidate and enalapril.^{13,48}

Our correlation analysis revealed that only 13% of the intestinal but 56% of the hepatic DMEs demonstrated significant correlations between gene expression and protein data. This discrepancy may be explained by the impact of regulatory miRNA, bile acids or food operating in the intestinal epithelia. In contrast to this, our previous study focusing on "major" enzymes and a more recent analysis reported by Grangeon et al. showed stronger correlations between DMEs intestinal gene and protein data.^{12,38} However, the limited number of samples used in our study, i.e. namely N=11 jejunal samples, compared to 36-54 samples from the entire small intestine in the aforementioned studies, could contribute to the observed discrepancies. It is obvious from the present and previous studies that respective correlations are much more robust in the liver.^{12,14} Hence, one may conclude that in the case of intestinal DMEs one should always prefer protein data over mRNA expression, additionally compromised by higher expression of mRNA degrading RNases and a more complex regulation by epigenetics and microbiome in the intestine compared to the liver.

Finally, only weak but significant correlations between the hepatic and jejunal DMEs protein amounts could be found for CYP3A4 and UGT1A3. This finding is in line with the known outstanding importance of CYP3A4 along the first pass absorption route of drugs.^{3,5-7} On the other side, this demonstrates that intestine and liver are individual metabolic compartments with only little overlap which work in a complementary manner combining phase I and II metabolism as well as drug transport to maintain an efficient detoxification machinery. As our protein quantification was done in an absolute manner and we analyzed whole tissue lysates without additional processing and potential sample loss, the total amount of the phase I and phase II enzymes for the human jejunum and liver can be estimated using previously reported scaling factors (liver mass: 1,500 g, mucosa mass for jejunum: 66 g) (Table 3).^{37,48} These data as derived from an intra-subject analysis is expected to be useful for implementation into PBPK models and may contribute to more precise predictions of drug metabolism, prevention of unwanted DDIs as well as accurate drug dosing.

Study Highlights

What is the current knowledge on the topic?

Despite the large number of studies dealing with drug-metabolizing enzymes (DMEs) in the intestine and liver, some enzymes are still not sufficiently investigated. This is especially true for studies that analyzed samples of liver and intestine from the same donor.

What question did this study address?

How much of these enzymes are expressed on both, protein and mRNA-level, in the jejunum and liver of the same individuals?

What does this study add to our knowledge?

The study provides data on the absolute protein amount of 24 clinically relevant major and minor DMES in hepatic and jejunal tissue from healthy organ donors. Additionally, respective

gene expression data are given. Thus, conclusions can be drawn on the relative and absolute expression of these enzymes in both organs. Correlation analysis of mRNA and protein data as well as of protein abundance in both tissues allow conclusion on the reliability of RNA data and potential interplay of intestinal and hepatic drug metabolism.

How might this change clinical pharmacology and translational science?

The data shown can be useful for predicting drug metabolism and disposition in healthy individuals using the PBPK-modeling approach. Thus, the efficacy and safety of drug therapy may be improved by predicting adequate drug dosing and avoiding unwanted drug-drug interactions.

Acknowledgements

C. W. thanks the Evangelisches Studienwerk Villigst e. V. for financial support through a doctoral scholarship.

Author Contributions

C.W., M.D. and S.O. wrote the article; C.W., M.D., M.K. and S.O. designed the research; C.W., J.L.-R., M.K., M.O., M.D. and S.O. performed the research; C.W., J.L.-R., M.K., M.D. and S.O. analyzed the data.

References

1. Jones, C. R., Hatley, O. J. D., Ungell, A.-L., Hilgendorf, C., Peters, S. A. & Rostami-Hodjegan, A. Gut Wall Metabolism. Application of Pre-Clinical Models for the Prediction of Human Drug Absorption and First-Pass Elimination. *The AAPS journal* **18**, 589–604 (2016).
2. Oswald, S. *et al.* Intestinal expression of P-glycoprotein (ABCB1), multidrug resistance associated protein 2 (ABCC2), and uridine diphosphate-glucuronosyltransferase 1A1 predicts the disposition and modulates the effects of the cholesterol absorption inhibitor ezetimibe in humans. *Clinical pharmacology and therapeutics* **79**, 206–217 (2006).
3. Kolars, J. C., Awni, W. M., Merion, R. M. & Watkins, P. B. First-pass metabolism of cyclosporin by the gut. *Lancet (London, England)* **338**, 1488–1490 (1991).
4. Holtbecker, N., Fromm, M. F., Kroemer, H. K., Ohnhaus, E. E. & Heidemann, H. The nifedipine-rifampin interaction. Evidence for induction of gut wall metabolism. *Drug metabolism and disposition: the biological fate of chemicals* **24**, 1121–1123 (1996).

5. Paine, M. F. *et al.* First-pass metabolism of midazolam by the human intestine. *Clinical pharmacology and therapeutics* **60**, 14–24 (1996).
6. Fromm, M. F., Busse, D., Kroemer, H. K. & Eichelbaum, M. Differential induction of prehepatic and hepatic metabolism of verapamil by rifampin. *Hepatology (Baltimore, Md.)* **24**, 796–801 (1996).
7. Gorski, J. C. *et al.* The effect of age, sex, and rifampin administration on intestinal and hepatic cytochrome P450 3A activity. *Clinical pharmacology and therapeutics* **74**, 275–287 (2003).
8. Prasad, B. *et al.* Toward a Consensus on Applying Quantitative Liquid Chromatography-Tandem Mass Spectrometry Proteomics in Translational Pharmacology Research: A White Paper. *Clinical pharmacology and therapeutics* **106**, 525–543 (2019).
9. Ahire, D., Kruger, L., Sharma, S., Mettu, V. S., Basit, A. & Prasad, B. Quantitative Proteomics in Translational Absorption, Distribution, Metabolism, and Excretion and Precision Medicine. *Pharmacological reviews* **74**, 769–796 (2022).
10. Oswald, S., Gröer, C., Drozdik, M. & Siegmund, W. Mass spectrometry-based targeted proteomics as a tool to elucidate the expression and function of intestinal drug transporters. *The AAPS journal* **15**, 1128–1140 (2013).
11. Couto, N. *et al.* Quantitative Proteomics of Clinically Relevant Drug-Metabolizing Enzymes and Drug Transporters and Their Intercorrelations in the Human Small Intestine. *Drug metabolism and disposition: the biological fate of chemicals* **48**, 245–254 (2020).
12. Drozdik, M. *et al.* Protein Abundance of Clinically Relevant Drug-Metabolizing Enzymes in the Human Liver and Intestine: A Comparative Analysis in Paired Tissue Specimens. *Clinical pharmacology and therapeutics* **104**, 515–524 (2018).
13. Prasad, B. *et al.* Abundance of Phase 1 and 2 Drug-Metabolizing Enzymes in Alcoholic and Hepatitis C Cirrhotic Livers: A Quantitative Targeted Proteomics Study. *Drug metabolism and disposition: the biological fate of chemicals* **46**, 943–952 (2018).
14. Ohtsuki, S. *et al.* Simultaneous absolute protein quantification of transporters, cytochromes P450, and UDP-glucuronosyltransferases as a novel approach for the characterization of individual human liver: comparison with mRNA levels and activities. *Drug metabolism and disposition: the biological fate of chemicals* **40**, 83–92 (2012).
15. Achour, B., Russell, M. R., Barber, J. & Rostami-Hodjegan, A. Simultaneous quantification of the abundance of several cytochrome P450 and uridine 5'-diphosphoglucuronosyltransferase enzymes in human liver microsomes using multiplexed targeted proteomics. *Drug metabolism and disposition: the biological fate of chemicals* **42**, 500–510 (2014).
16. Couto, N., Al-Majdoub, Z. M., Achour, B., Wright, P. C., Rostami-Hodjegan, A. & Barber, J. Quantification of Proteins Involved in Drug Metabolism and Disposition in the Human Liver Using Label-Free Global Proteomics. *Molecular pharmaceutics* **16**, 632–647 (2019).
17. Richter, O. von, Burk, O., Fromm, M. F., Thon, K. P., Eichelbaum, M. & Kivistö, K. T. Cytochrome P450 3A4 and P-glycoprotein expression in human small intestinal enterocytes and hepatocytes: a comparative analysis in paired tissue specimens. *Clinical pharmacology and therapeutics* **75**, 172–183 (2004).
18. Läpple, F. *et al.* Differential expression and function of CYP2C isoforms in human intestine and liver. *Pharmacogenetics* **13**, 565–575 (2003).
19. Wegler, C. *et al.* Drug Disposition Protein Quantification in Matched Human Jejunum and Liver From Donors With Obesity. *Clinical pharmacology and therapeutics* **111**, 1142–1154 (2022).

20. Dunvald, A.-C. D., Järvinen, E., Mortensen, C. & Stage, T. B. Clinical and Molecular Perspectives on Inflammation-Mediated Regulation of Drug Metabolism and Transport. *Clinical pharmacology and therapeutics* **112**, 277–290 (2022).
21. Drozdik, M. *et al.* Gene Expression and Protein Abundance of Hepatic Drug Metabolizing Enzymes in Liver Pathology. *Pharmaceutics* **13** (2021).
22. Drozdik, M. *et al.* Protein Abundance of Drug Metabolizing Enzymes in Human Hepatitis C Livers. *International journal of molecular sciences* **24** (2023).
23. Zanger, U. M. & Schwab, M. Cytochrome P450 enzymes in drug metabolism: regulation of gene expression, enzyme activities, and impact of genetic variation. *Pharmacology & therapeutics* **138**, 103–141 (2013).
24. Rostami-Hodjegan, A. & Tucker, G. T. Simulation and prediction of in vivo drug metabolism in human populations from in vitro data. *Nature reviews. Drug discovery* **6**, 140–148 (2007).
25. Harbourt, D. E. *et al.* Quantification of human uridine-diphosphate glucuronosyl transferase 1A isoforms in liver, intestine, and kidney using nanobore liquid chromatography-tandem mass spectrometry. *Analytical chemistry* **84**, 98–105 (2012).
26. Zhang, H.-F. *et al.* Physiological Content and Intrinsic Activities of 10 Cytochrome P450 Isoforms in Human Normal Liver Microsomes. *The Journal of pharmacology and experimental therapeutics* **358**, 83–93 (2016).
27. Miyauchi, E. *et al.* Quantitative Atlas of Cytochrome P450, UDP-Glucuronosyltransferase, and Transporter Proteins in Jejunum of Morbidly Obese Subjects. *Molecular pharmaceutics* **13**, 2631–2640 (2016).
28. Al-Majdoub, Z. M. *et al.* Quantification of Proteins Involved in Intestinal Epithelial Handling of Xenobiotics. *Clinical pharmacology and therapeutics* **109**, 1136–1146 (2021).
29. Wegler, C. *et al.* Variability in Mass Spectrometry-based Quantification of Clinically Relevant Drug Transporters and Drug Metabolizing Enzymes. *Molecular pharmaceutics* **14**, 3142–3151 (2017).
30. Sontag, T. J. & Parker, R. S. Cytochrome P450 omega-hydroxylase pathway of tocopherol catabolism. Novel mechanism of regulation of vitamin E status. *The Journal of biological chemistry* **277**, 25290–25296 (2002).
31. Jin, R., Koop, D. R., Raucy, J. L. & Lasker, J. M. Role of human CYP4F2 in hepatic catabolism of the proinflammatory agent leukotriene B4. *Archives of biochemistry and biophysics* **359**, 89–98 (1998).
32. Bartolini, D. *et al.* Nonalcoholic fatty liver disease impairs the cytochrome P-450-dependent metabolism of α -tocopherol (vitamin E). *The Journal of nutritional biochemistry* **47**, 120–131 (2017).
33. Athinarayanan, S. *et al.* Genetic polymorphism of cytochrome P450 4F2, vitamin E level and histological response in adults and children with nonalcoholic fatty liver disease who participated in PIVENS and TONIC clinical trials. *PLoS one* **9**, e95366 (2014).
34. Lang, D., Radtke, M. & Bairlein, M. Highly Variable Expression of CYP1A1 in Human Liver and Impact on Pharmacokinetics of Riociguat and Granisetron in Humans. *Chemical research in toxicology* **32**, 1115–1122 (2019).
35. Klomp, F., Wenzel, C., Drozdik, M. & Oswald, S. Drug-Drug Interactions Involving Intestinal and Hepatic CYP1A Enzymes. *Pharmaceutics* **12** (2020).
36. Tomalik-Scharte, D. *et al.* Effect of propiverine on cytochrome P450 enzymes: a cocktail interaction study in healthy volunteers. *Drug metabolism and disposition: the biological fate of chemicals* **33**, 1859–1866 (2005).

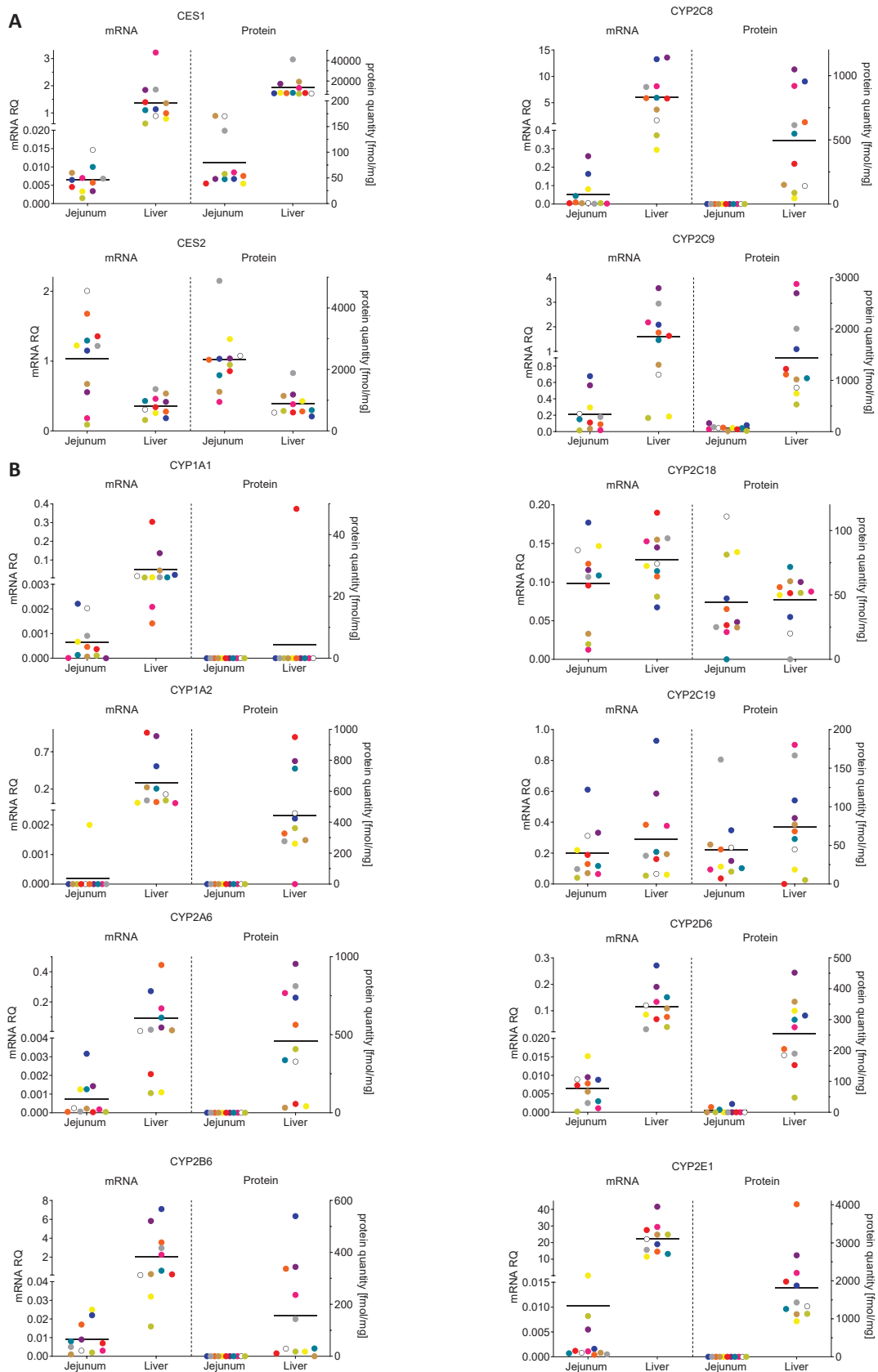
37. Paine, M. F., Hart, H. L., Ludington, S. S., Haining, R. L., Rettie, A. E. & Zeldin, D. C. The human intestinal cytochrome P450 "pie". *Drug metabolism and disposition: the biological fate of chemicals* **34**, 880–886 (2006).
38. Grangeon, A., Clermont, V., Barama, A., Gaudette, F., Turgeon, J. & Michaud, V. Determination of CYP450 Expression Levels in the Human Small Intestine by Mass Spectrometry-Based Targeted Proteomics. *International journal of molecular sciences* **22** (2021).
39. Zubiaur, P. & Gaedigk, A. CYP2C18: the orphan in the CYP2C family. *Pharmacogenomics* **23**, 913–916 (2022).
40. Lloret-Linares, C. *et al.* Oral Morphine Pharmacokinetic in Obesity: The Role of P-Glycoprotein, MRP2, MRP3, UGT2B7, and CYP3A4 Jejunal Contents and Obesity-Associated Biomarkers. *Molecular pharmaceutics* **13**, 766–773 (2016).
41. Uchaipichat, V., Rowland, A. & Miners, J. O. Inhibitory effects of non-steroidal anti-inflammatory drugs on human liver microsomal morphine glucuronidation: Implications for drug-drug interaction liability. *Drug metabolism and pharmacokinetics* **42**, 100442 (2022).
42. Fromm, M. F. *et al.* Loss of analgesic effect of morphine due to coadministration of rifampin. *Pain* **72**, 261–267 (1997).
43. Zhang, H. *et al.* Quantitative characterization of UDP-glucuronosyltransferase 2B17 in human liver and intestine and its role in testosterone first-pass metabolism. *Biochemical Pharmacology* **156**, 32–42 (2018).
44. Bhatt, D. K. *et al.* Hepatic Abundance and Activity of Androgen- and Drug-Metabolizing Enzyme UGT2B17 Are Associated with Genotype, Age, and Sex. *Drug metabolism and disposition: the biological fate of chemicals* **46**, 888–896 (2018).
45. Ahire, D., Heyward, S. & Prasad, B. Intestinal Metabolism of Diclofenac by Polymorphic UGT2B17 Correlates with its Highly Variable Pharmacokinetics and Safety across Populations. *Clinical pharmacology and therapeutics* (2023).
46. Urashima, M. *et al.* UGT2B17 deletion polymorphism is a risk factor for upper aero digestive-tract cancer in Japanese: a case-control study. *Epidemiology: Open Access* **5** (2015).
47. Gallagher, C. J., Kadlubar, F. F., Muscat, J. E., Ambrosone, C. B., Lang, N. P. & Lazarus, P. The UGT2B17 gene deletion polymorphism and risk of prostate cancer: A case-control study in Caucasians. *Cancer Detection and Prevention* **32**, 186–187 (2008).
48. Basit, A. *et al.* Characterization of Differential Tissue Abundance of Major Non-CYP Enzymes in Human. *Molecular pharmaceutics* **17**, 4114–4124 (2020).
49. Stangier, J. Clinical pharmacokinetics and pharmacodynamics of the oral direct thrombin inhibitor dabigatran etexilate. *Clinical pharmacokinetics* **47**, 285–295 (2008).
50. Wang, D., Zou, L., Jin, Q., Hou, J., Ge, G. & Yang, L. Human carboxylesterases: a comprehensive review. *Acta pharmaceutica Sinica. B* **8**, 699–712 (2018).
51. Tang, L., Li, X., Wan, L., Xiao, Y., Zeng, X. & Ding, H. Herbal Medicines for Irinotecan-Induced Diarrhea. *Frontiers in pharmacology* **10**, 182 (2019).

Figure legends

Figure 1: Measured gene expression (left side of each diagram) and protein abundance (right side of each diagram) of carboxylesterases (CES) (**A**), cytochromes P450 (CYP) (**B**) and uridine 5'-diphospho-glucuronosyltransferase 2B17 (UGT2B17) (**C**) in jejunal and hepatic tissues from eleven donors. Colors and letters indicate individuals.

Figure 2: Pie charts representing the abundance of drug-metabolizing cytochrome P450 (top) and uridine 5'-diphospho-glucuronosyltransferases (bottom) in hepatic (left) and jejunal (right) tissue. Abundance of each enzyme is shown as a percentage of the sum of all enzyme protein abundances.

Figure 1



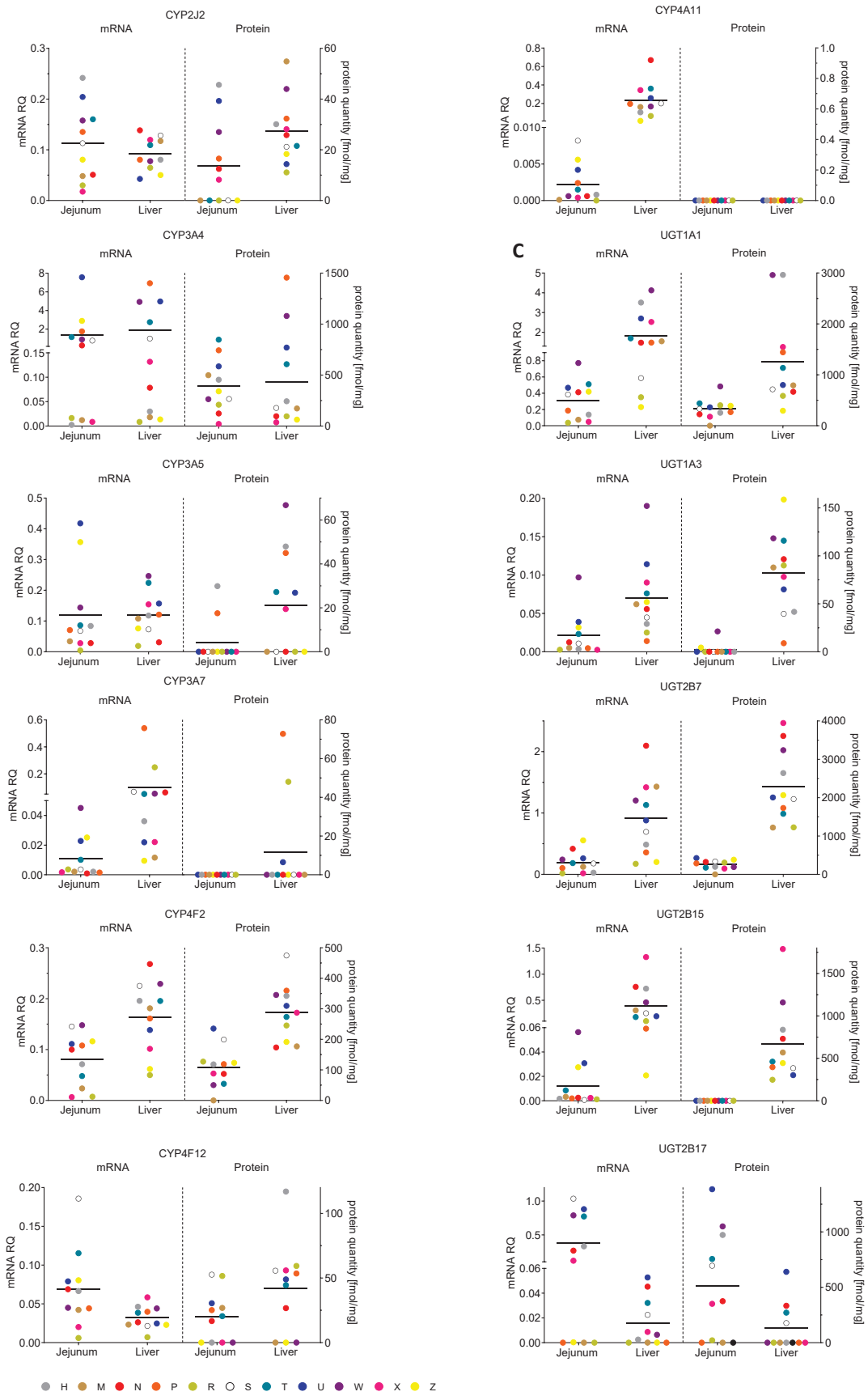
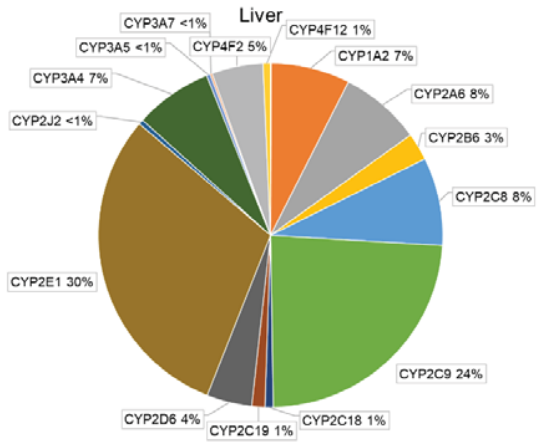
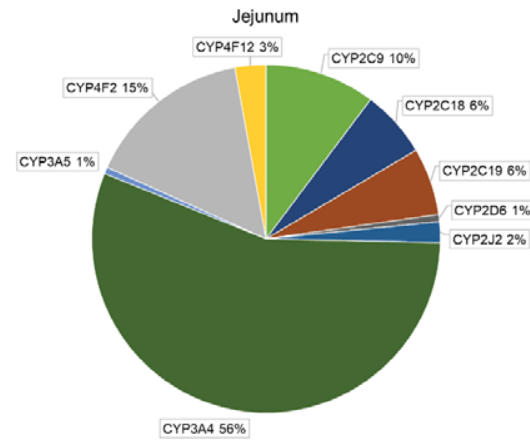


Figure 2

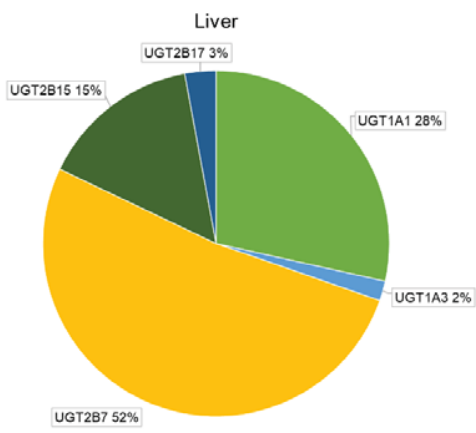
A



B



C



D

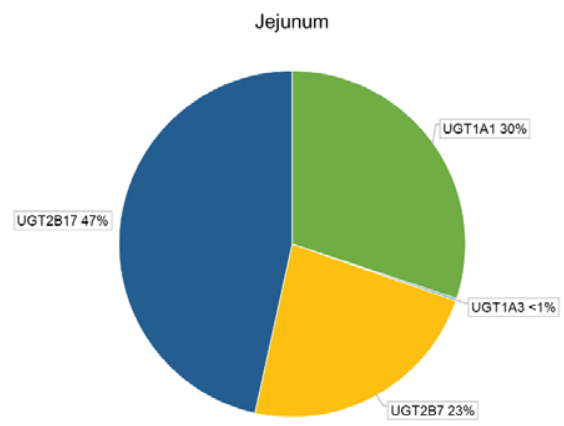


Table 1: Correlation (Spearman coefficient, r) between mRNA and protein level of carboxylesterases (CES), cytochrome P450 (CYP) enzymes and UDP-glucuronosyltransferases (UGT) in human jejunum and hepatic tissues from n=11 donors.

mRNA vs. Protein	Jejunum	Liver
CES 1	0.5364	0.7091*
CES 2	0.3000	0.6455*
CYP1A1	-	0.5000
CYP1A2	-	0.8182**
CYP2A6	-	0.5364
CYP2B6	-	0.8455**
CYP2C8	-	0.9727****
CYP2C9	0.7909*	0.9636****
CYP2C18	0.5818	-0.06364
CYP2C19	0.3091	0.6909*
CYP2D6	0.1098	0.6455*
CYP2E1	-	0.4091
CYP2J2	0.5911	0.3636
CYP3A4	0.4909	0.7909**
CYP3A5	0.08090	0.8009**
CYP3A7	-	0.4741
CYP4F2	0.2455	0.1909
CYP4F12	0.08374	0.1468
CYP4A11	-	-
UGT1A1	0.6000	0.8909***
UGT1A3	0.6068	0.5091
UGT2B7	0.5000	0.3364
UGT2B15	-	0.7545**
UGT2B17	0.8611**	0.8673***

*P≤0.05, **P≤0.01, ***P≤0.001, ****P≤0.0001

Table 2: Correlation (Spearman coefficient, r) between protein level of carboxylesterases (CES), cytochrome P450 (CYP) enzymes and UDP-glucuronosyltransferases (UGT) in human jejunum and hepatic tissues from n=11 donors.

Protein	Jejunum vs. Liver
CES1	0.4918
CES2	0.1273
CYP2C9	0.4727
CYP2C18	-0.5636
CYP2C19	0.5636
CYP2D6	0.1387
CYP2J2	0.2860
CYP3A4	0.6545*
CYP3A5	0.5515
CYP4F2	0.3455
CYP4F12	0.1972
UGT1A1	-0.07273
UGT1A3	0.6607*
UGT2B7	0.1000
UGT2B17	0.5207

*P≤0.05

Table 3: Estimated total protein amount (nmol) of the studied phase I and phase II enzymes in the whole human liver and jejunum.

mRNA vs. Protein	Jejunum	Liver
CES 1	5.3 ± 3.5	20162 ± 15152
CES 2	152.8 ± 67.5	1319 ± 610
CYP1A1	-	6.6 ± 22
CYP1A2	-	666 ± 418
CYP2A6	-	687 ± 498
CYP2B6	-	233 ± 275
CYP2C8	-	744 ± 557
CYP2C9	4.8 ± 2.9	2143 ± 1175
CYP2C18	2.9 ± 2.2	69 ± 31
CYP2C19	2.9 ± 2.8	111 ± 89
CYP2D6	0.3 ± 0.6	383 ± 168
CYP2E1	-	2722 ± 1356
CYP2J2	0.9 ± 1.1	41 ± 19
CYP3A4	26.1 ± 17.0	654 ± 719
CYP3A5	0.3 ± 0.7	32 ± 36
CYP3A7	-	17 ± 37
CYP4F2	7.2 ± 4.4	434 ± 137
CYP4F12	1.3 ± 1.3	63 ± 52
CYP4A11	-	-
UGT1A1	21.7 ± 12.7	1895 ± 1373
UGT1A3	0.2 ± 0.4	123 ± 63
UGT2B7	16.7 ± 8,1	3440 ± 1410
UGT2B15	-	998 ± 687
UGT2B17	33.6 ± 32,5	194 ± 315

6.3 Gene Expression and Protein Abundance of Hepatic Drug Metabolizing Enzymes in Liver Pathology

Drozdziak M, Lapczuk-Romanska J, Wenzel C, Szelag-Pieniek S, Post M, Skalski Ł, Kurzawski M, Oswald S

Pharmaceutics 2021;13(9). doi: 10.3390/pharmaceutics13091334.

Projektdesign: M. D., M. K., S. O.

Projektdurchführung: M. D., J. L.-R., C. W., M. P., Ł. S., S. S.-P., M. K., S. O.

Datenanalyse: M. D., J. L.-R., M. K., S. O.

Erstellung des Manuskriptes: M. D., S. O.

Article

Gene Expression and Protein Abundance of Hepatic Drug Metabolizing Enzymes in Liver Pathology

Marek Drozdziak ^{1,*}, Joanna Lapczuk-Romanska ¹, Christoph Wenzel ², Sylwia Szelag-Pieniek ¹, Mariola Post ³, Łukasz Skalski ¹, Mateusz Kurzawski ¹ and Stefan Oswald ⁴

¹ Department of Experimental and Clinical Pharmacology, Pomeranian Medical University, Powstancow Wlkp. 72 Str., 70-111 Szczecin, Poland; joanna.lapczuk@pum.edu.pl (J.L.-R.); sylwia.szelag@pum.edu.pl (S.S.-P.); lukasz.skalski@pum.edu.pl (Ł.S.); mkurz@pum.edu.pl (M.K.)

² Department of Pharmacology, Center of Drug Absorption and Transport, University Medicine Greifswald, 17489 Greifswald, Germany; Christoph.Wenzel@med.uni-greifswald.de

³ Department of General and Transplantation Surgery, County Hospital, 70-891 Szczecin, Poland; mariolapost@wp.pl

⁴ Institute of Pharmacology and Toxicology, Rostock University Medical Center, 18051 Rostock, Germany; stefan.oswald@med.uni-rostock.de

* Correspondence: drozdziak@pum.edu.pl

Abstract: Hepatic drug metabolizing enzymes (DMEs) markedly affect drug pharmacokinetics. Because liver diseases may alter enzymatic function and in turn drug handling and clinical efficacy, we investigated DMEs expression in dependence on liver pathology and liver failure state. In 5 liver pathologies (hepatitis C, alcoholic liver disease, autoimmune hepatitis, primary biliary cholangitis and primary sclerosing cholangitis) and for the first time stratified according to the Child–Pugh score, 10 CYPs (CYP1A1, CYP1A2, CYP2B6, CYP2C8, CYP2C9, CYP2C19, CYP2D6, CYP2E1, CYP3A4 and CYP3A5) and 4 UGTs (UGT1A1, UGT1A3, UGT2B7 and UGT2B) enzymes were quantified for protein abundance (LC-MS/MS) and gene expression (qRT-PCR). CYP2E1 was the most vulnerable enzyme, and its protein levels were significantly reduced just in Child–Pugh class A livers. The protein abundance of CYP1A1, CYP2B6, CYP2C19, CYP2D6 as well as UGT1A1, UGT1A3 and UGT2B15 was relatively stable in the course of progression of liver function deterioration. Alcoholic liver disease and primary biliary cholangitis were involved in the most prominent changes in the protein abundances, with downregulation of 6 (CYP1A2, CYP2C8, CYP2D6, CYP2E1, CYP3A4, UGT2B7) and 5 (CYP1A1, CYP2B6, CYP2C8, CYP2E1, CYP3A4) significantly downregulated enzymes, respectively. The results of the study demonstrate that DMEs protein abundance is affected both by the type of liver pathology as well as functional state of the organ.

Keywords: hepatic pathology; liver; drug metabolizing enzymes



Citation: Drozdziak, M.; Lapczuk-Romanska, J.; Wenzel, C.; Szelag-Pieniek, S.; Post, M.; Skalski, Ł.; Kurzawski, M.; Oswald, S. Gene Expression and Protein Abundance of Hepatic Drug Metabolizing Enzymes in Liver Pathology. *Pharmaceutics* **2021**, *13*, 1334. <https://doi.org/10.3390/pharmaceutics13091334>

Academic Editor: Dong Hyun Kim

Received: 13 July 2021

Accepted: 23 August 2021

Published: 25 August 2021

Publisher's Note: MDPI stays neutral with regard to jurisdictional claims in published maps and institutional affiliations.



Copyright: © 2021 by the authors. Licensee MDPI, Basel, Switzerland. This article is an open access article distributed under the terms and conditions of the Creative Commons Attribution (CC BY) license (<https://creativecommons.org/licenses/by/4.0/>).

1. Introduction

Drug metabolizing enzymes (DMEs) expressed in the liver play a very important role in drug biotransformation, and together with enzymes in the gastrointestinal tract, are major bioavailability determinants of orally administered pharmaceuticals and drug–drug interactions. The available pharmacokinetic information suggests deficient function of the enzymes in liver dysfunction states, e.g., increased bioavailability of orally administered caffeine (CYP1A2 substrate), S-mephenytoin (CYP2C19 substrate), debrisoquine (CYP2D6 substrate), chlorzoxazone (CYP2E1 substrate) and midazolam (CYP3A4 substrate) or not affected pharmacokinetics of debrisoquine [1–3]. However, other factors observed in cirrhotic patients may also contribute to the altered drug pharmacokinetics, e.g., reductions in portal and renal blood flow, glomerular filtration rate, serum albumin concentration or hematocrit value, altered membrane transporter expression in the liver and other tissues and the decrease in the remaining functional liver mass [4–6].

The available findings demonstrated that about 30% of patients with advanced liver failure suffered from adverse drug reactions and that almost 80% of those reactions were possibly preventable because inadequate dosages or contraindicated medicines were used [7]. Therefore, European Medicines Agency (EMA) and Food and Drug Administration (FDA) regulations recommend pharmacokinetic studies in patients with impaired hepatic function, when hepatic impairment is likely to significantly alter the pharmacokinetics (especially metabolism and biliary excretion) of the drug and/or its active metabolites (i.e., hepatic metabolism and/or excretion accounting for a substantial portion (>20 percent of the absorbed drug) of the elimination of a parent drug or active metabolite]. Dose adjustment may be required for such patients, taking into account the PK/PD relationship resulting in increased rates of side effects or drug-related toxicity [8,9]. However, ethical concerns virtually preclude methodologically rigorous pharmacokinetic or drug–drug interaction studies, especially for medicines of non-therapeutic value. This gap of knowledge may be to some extent compensated by proteomic studies, which provide quantitative data on hepatic DMEs in pathological states of the organ. The information about DMEs abundance in liver dysfunction states is of clinical relevance, as it enables stratification of potential risks derived from altered pharmacokinetics and pharmacodynamics of administered drugs and prediction of oral drug bioavailability and drug–drug interactions (DDI) using physiologically-based pharmacokinetic (PBPK) modeling and simulation.

The published information about protein abundance of DMEs in liver pathologies is very scarce. Several studies reported gene expression analysis. However, mRNA data may not be necessarily correlated to the encoded proteins [10,11]. The so far available protein-based data are limited to alcoholic liver disease and hepatitis C cirrhosis, as measured by liquid chromatography coupled with tandem mass spectrometry (LC-MS/MS) or in cholestatic cirrhosis (assayed by Western blot) [12–14]. Except for Guengerich et al., those reports did not stratify patients according to the functional state of the organ, i.e., the established Child–Pugh score [13]. Moreover, protein quantification by Western blotting regularly does not allow absolute protein quantification and is associated with several analytical issues such as unspecific binding of the antibodies, a narrow analytical range, which is limited to only a few proteins, a low samples throughput and a lack of reliable reproducibility [15].

In order to overcome the aforementioned limitations, a validated targeted proteomics method and quantitative RT-PCR were used to determine, respectively, protein abundance and mRNA levels of hepatic DMEs in a wide range of liver pathological states, i.e., hepatic virus C (HCV)-induced liver damage, alcoholic liver disease (ALD), autoimmune hepatitis (AIH) and cholestatic diseases, such as primary biliary cholangitis (PBC) and primary sclerosing cholangitis (PSC), in patients stratified according to the degree of hepatic insufficiency (based on the Child–Pugh score). The following enzymes were analyzed: CYPs (CYP1A1, CYP1A2, CYP2B6, CYP2C8, CYP2C9, CYP2C19, CYP2D6, CYP2E1, CYP3A4 and CYP3A5) and UGTs (UGT1A1, UGT1A3, UGT2B7 and UGT2B15) enzymes. The data from the study could be applied to develop more accurate PBPK-based prediction models for pathology states of the liver. The current study is complementary (includes the same set of the studied samples) to the previously published information about hepatic drug transporters in different forms of liver failure [5].

2. Materials and Methods

2.1. Liver Samples

The control samples were harvested from metastatic livers, from a site at least 5 cm distant of the tumor site. The tissues were collected from Caucasian patients, aged 63 ± 10 years, 11 males and 9 females, diagnosed with metastatic colon cancer. The collected tissues did not show any pathological signs as confirmed by histological examination. The hepatitis C (HCV), primary biliary cholangitis (PBC), primary sclerosing cholangitis (PSC), alcoholic liver disease (ALD) and autoimmune hepatitis (AIH) (diagnosed according to the standard clinical criteria) liver parenchymal tissue samples were dissected from

patients requiring liver transplantation. The liver tissue specimens were harvested during elective liver transplantation from the organ, immediately after excision. The stage of liver dysfunction was classified according to the Child–Pugh score. Characteristics of the subjects are presented in Table S1. The whole medication information is available for the control samples, i.e., one patient took bisoprolol, furosemide, and tamsulosin (hypertension, prostate hypertrophy), one was treated with bepridil (hypertension) and another one was medicated with amlodipine (hypertension). None of these drugs is known to be a potent regulator of CYP or UGT enzymes. The liver pathology samples were collected in the years 2007–2018, and treatment standards for the liver diseases were modified, and are also specific liver pathology and functional state dependent, therefore due to limited number of samples for a given liver pathology and functional state medication analysis is not reliable (which is a limitation of these samples). We were only able to select samples without co-existing co-morbidities. Tissue biopsies were taken from livers (control and pathological) under standard general anesthesia (propofol, sevoflurane, rocuronium, fentanyl, or dipyrone) not later than 15 min after blood flow arrest or directly after liver resection in metastatic controls. The liver samples were immediately snap frozen in liquid nitrogen for protein analysis or immersed in RNAlater (Applied Biosystems, Darmstadt, Germany) for RNA analysis, and then stored at $-80\text{ }^{\circ}\text{C}$. The study protocol was approved by Bioethics Committee of the Pomeranian Medical University (approval number BN-001/11/07). Informed consent was obtained from all subjects involved in the study.

2.2. mRNA Isolation and Quantitative Real-Time RT-PCR

Total RNA was isolated from 25 mg of each tissue sample using Direct-zol RNA MiniPrep kit (Zymo Research, Irvine, CA, USA). RNA concentration and purity was assessed using DS-11 FX spectrophotometer (Denovix, Wilmington, DE, USA). cDNA was prepared using SuperScript[®] VILO™ cDNA Synthesis Kit (Thermo Fisher Scientific, Waltham, MA, USA), with 500 ng of total RNA for 20 μL of reaction volume according to the manufacturer's procedure. The gene expression levels were examined in duplicate using TaqMan Fast Advanced Master Mix and pre-validated TaqMan assays: CYP1A1 (manufacturer's Assay ID: Hs00153120_m1), CYP1A2 (Hs00167927_m1), CYP2B6 (Hs03044631_m1), CYP2C8 (Hs02383390_s1), CYP2C9 (Hs02383631_s1), CYP2C19 (Hs00426380_m1), CYP2D6 (Hs00164385_m1), CYP2E1 (Hs0055-9367_m1), CYP3A4 (Hs00604506_m1), CYP3A5 (Hs01070905_m1), UGT1A1 (Hs02511055_s1), UGT1A3 (Hs04194492_g1), UGT2B7 (Hs00426592_m1), UGT2B15 (Hs00870076_s1) in ViiA 7 Real-Time PCR System (Life Technologies, Carlsbad, CA, USA). Threshold values for each gene were set manually and mean CT (cycles of threshold) values were recorded. Relative mRNA expression was calculated by the $2^{-\Delta\text{Ct}}$ method- normalized to the mean expression value obtained for the housekeeping genes: GAPDH (Hs99999905_m1), HMBS (Hs00609297_m1), PPIA (Hs04194521_s1), RPLP0 (Hs99999902_m1), RPS9 (Hs02339424_g)—presented in the figures and by $2^{-\Delta\Delta\text{Ct}}$ method- additionally normalized to the mean value for the control group—presented in the table (Supplementary Table S2).

2.3. Protein Quantification by LC–MC/MS

The tissues placed in liquid nitrogen were mechanically disrupted in a stainless steel mortar system. Approximately 40 mg tissue powder of each sample was lysed with 1 mL of 0.2% SDS and 5 mM EDTA containing 5 $\mu\text{L}/\text{mL}$ Protease Inhibitor Cocktail Set III (Merck, Darmstadt, Germany) for 30 min at $4\text{ }^{\circ}\text{C}$ on a platform shaker with 40 rpm (Polymax 1040, Heidolph, Schwabach, Germany). Total protein content of the whole tissue lysates was determined by bicinchoninic acid assay (Thermo Fisher Scientific, Waltham, MA, USA) and 100 μg of each sample was processed using filter aided sample preparation (FASP) based on the previously published protocol [16]. Protein abundances of nine CYP (CYP1A2, CYP2B6, CYP2C8, CYP2C9, CYP2C19, CYP2D6, CYP2E1, CYP3A4, CYP3A5) and four UGT (UGT1A1, UGT1A3, UGT2B7 and UGT2B15) enzymes were measured by mass spectrometry-based targeted proteomics using a validated LC–MS/MS method as

previously described [16,17]. The analytical variability during sample analysis was below 20% (accuracy). With the exception of UGT1A3, two proteospecific peptides were used for analysis. One peptide was used for quantification, whereas the other served as qualifier for the presence of the specific protein. For all peptides and their isotope-labeled internal standard peptides, three mass transitions were used, respectively. The calculated protein (per mg liver tissue) values represent the mean of at least 2–3 mass transitions/peptide.

2.4. Genotyping

Genomic DNA was extracted from tissue samples using Tissue DNA Purification Kit (EURx, Gdansk, Poland), subsequently standardized to a uniform concentration (20 ng/ μ L) and stored in -20°C . All samples were genotyped for common lack-of-function variants affecting protein concentrations (i.e., stop-codons, frameshifts and splicing defects, using ViiA7 Fast Real-Time PCR System and pre-validated TaqMan assays (Life Technologies, Carlsbad, CA, USA). Following variants were evaluated: CYP2C19*2 (rs4244285, Assay ID: C__25986767_70), CYP2D6*3 (rs35742686, C__32407232_50), CYP2D6*4: rs3892097, C__27102431_D0), and CYP3A5*3 (rs776746, C__26201809_30). Additionally, CYP2D6 gene deletion (CYP2D6*5) was evaluated using qPCR method with TaqMan probes for CYP2D6 (Hs00010001_cn) and the reference RPPH1 gene.

2.5. Statistical Analysis

All mRNA and protein level data: means \pm standard deviation, coefficient of variation %, median as well as minimum and maximum values are given in Tables S2 and S3 of Supplementary Information. The final protein amounts were normalized to the digested tissue amount. All samples were used for calculations, and those with undetectable protein concentration (LLOQ, lower or equal to 0.1 nmol/L) were replaced with zero. Differences between study groups were evaluated using the nonparametric Kruskal–Wallis test for multiple comparisons with post hoc Dunn’s test with Bonferroni correction, and correlations the Spearman rank (rs) test. *p* values of <0.05 were considered as significant. All statistical calculations were performed using Statistica 13.3 Software Package (TIBCO Software Inc., Palo Alto, CA, USA).

3. Results

3.1. Hepatic Drug Metabolizing Enzymes Abundance According to Liver Functional State (The Child–Pugh Score)

The Child–Pugh class was associated with changes in the transcriptional expression and protein levels of both, CYP and UGT enzymes. Worsening of liver function was associated with a significant decrease in protein abundance (compared to control samples) of CYP1A2 (to 45% in Child–Pugh score C), CYP2C8 (to 45% in Child–Pugh score C), CYP2C9 (to 57% in Child–Pugh score C), CYP2E1 (to 89% in Child–Pugh score C) and CYP3A4 (to 45% in Child–Pugh score C) as well as UGT2B7 (to 57% in Child–Pugh score C). The protein levels of CYP1A1, CYP2B6, CYP2C19 and CYP2D6 as well as that of UGT1A1, UGT1A3 and UGT2B15 remained stable. However, in some of the enzymes a downregulation trend was observed (Figures 1 and 2, Tables S2 and S3).

The percentage contributions of all investigated CYP proteins stratified according to the different Child–Pugh scores are given in Figure 3. Although the protein amounts and rank order of the enzymes were markedly affected by the liver functional states, CYP2C9 and CYP2E1 showed the highest abundances, while CYP2B6 was only found in traces (~ 1 –2%) in all liver pathologies (Figure 3, Table S3). Interestingly, CYP1A1 could be only detected in the control and the Child–Pugh score C livers at very low levels (1%).

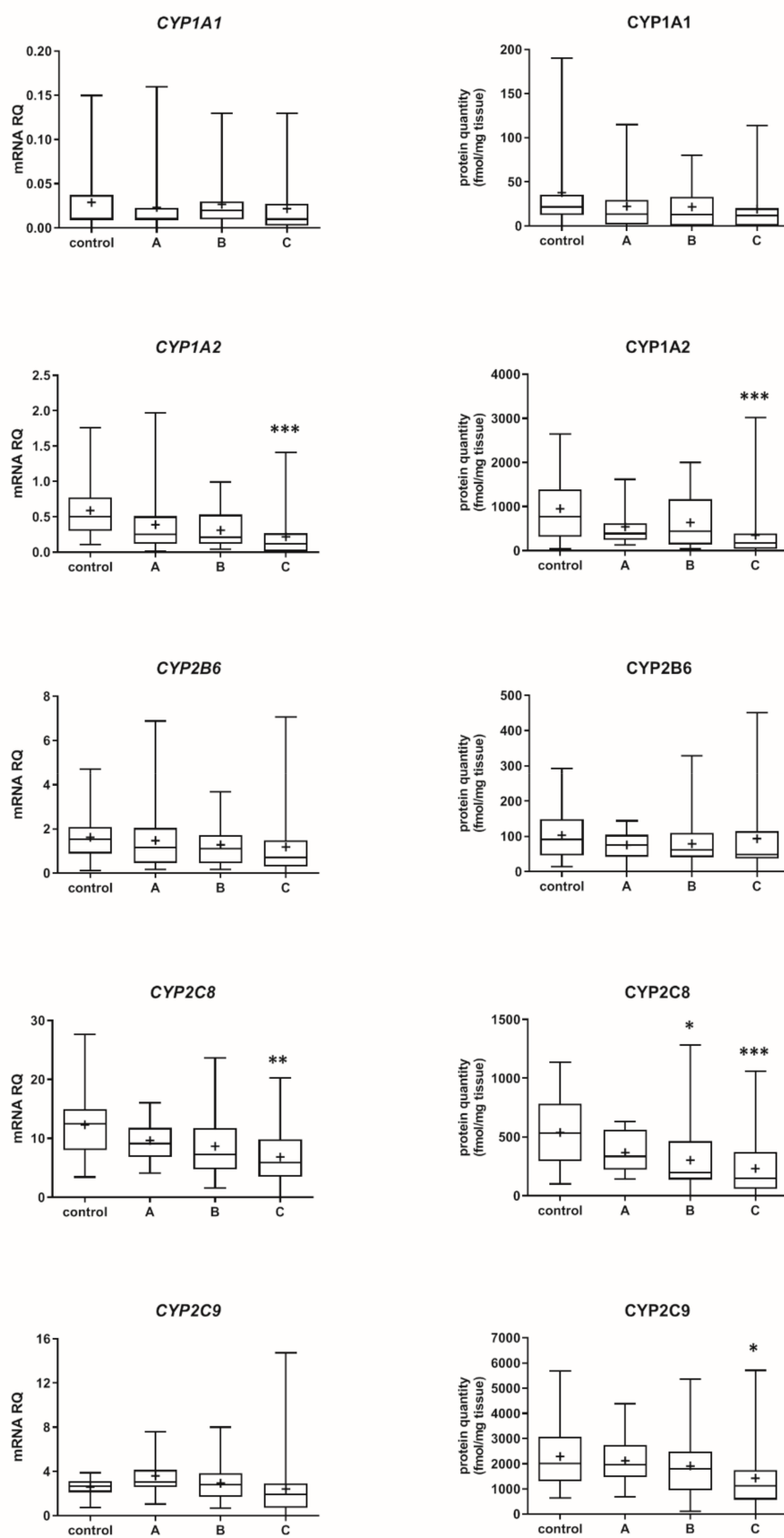


Figure 1. Cont.

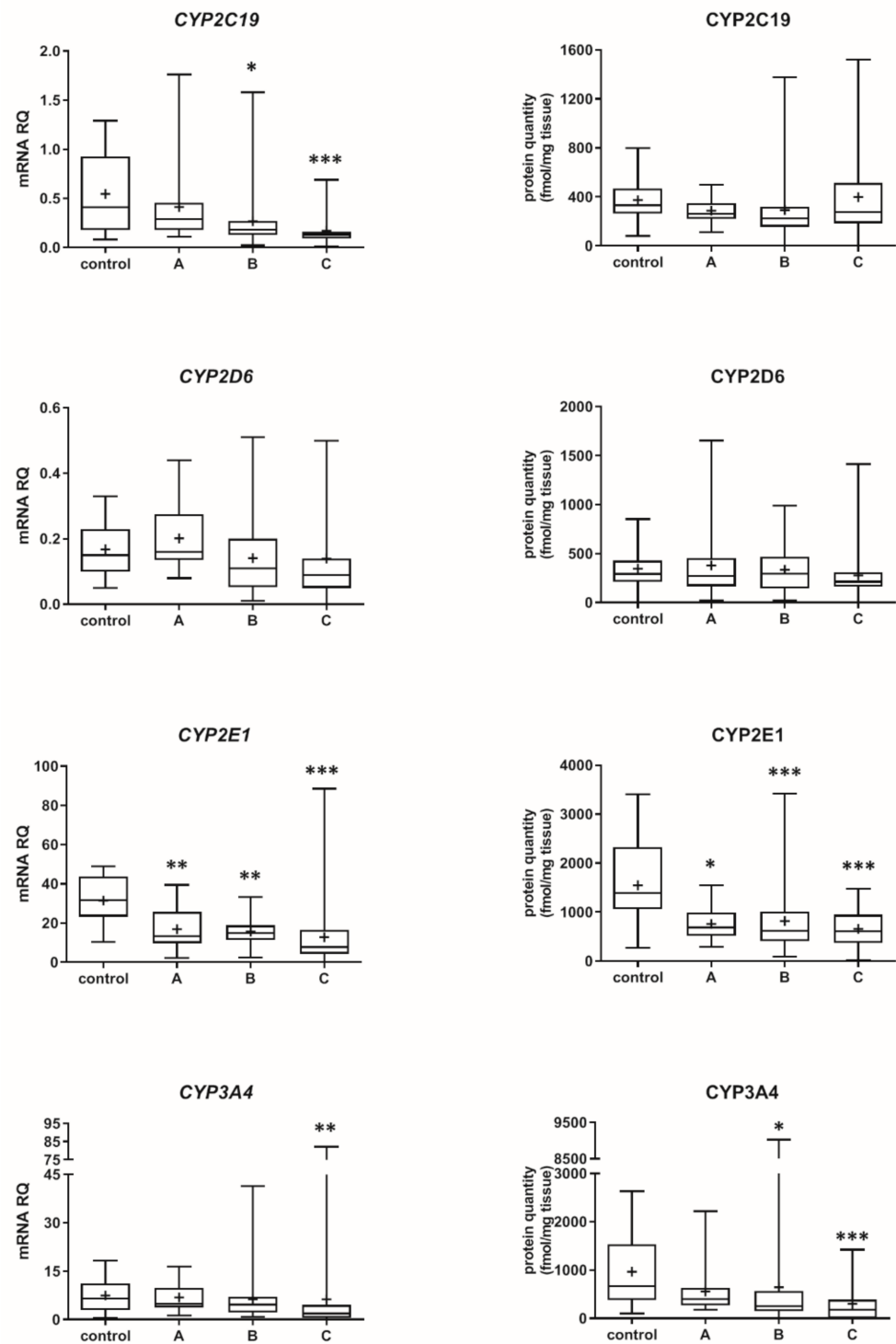


Figure 1. (also see page up) Gene expression (left) and protein abundance (right) of CYPs in hepatic tissues stratified according to the Child–Pugh score into stages: A ($n = 18$), B ($n = 31$) and C ($n = 28$). The data are represented as box-plots of the median (horizontal line), 75th (top of box), and 25th (bottom of box) quartiles, the smallest and largest values (whiskers) and mean (+) are shown. mRNA levels of the analyzed genes were expressed as relative amounts to the mean of five housekeeping genes (GAPDH, HMBS, PPIA, RPLP0, RPS9). Statistically significant differences: * $p < 0.05$, ** $p < 0.01$, *** $p < 0.001$ (Kruskal–Wallis test post hoc Dunn’s test with Bonferroni correction) in comparison to the controls.

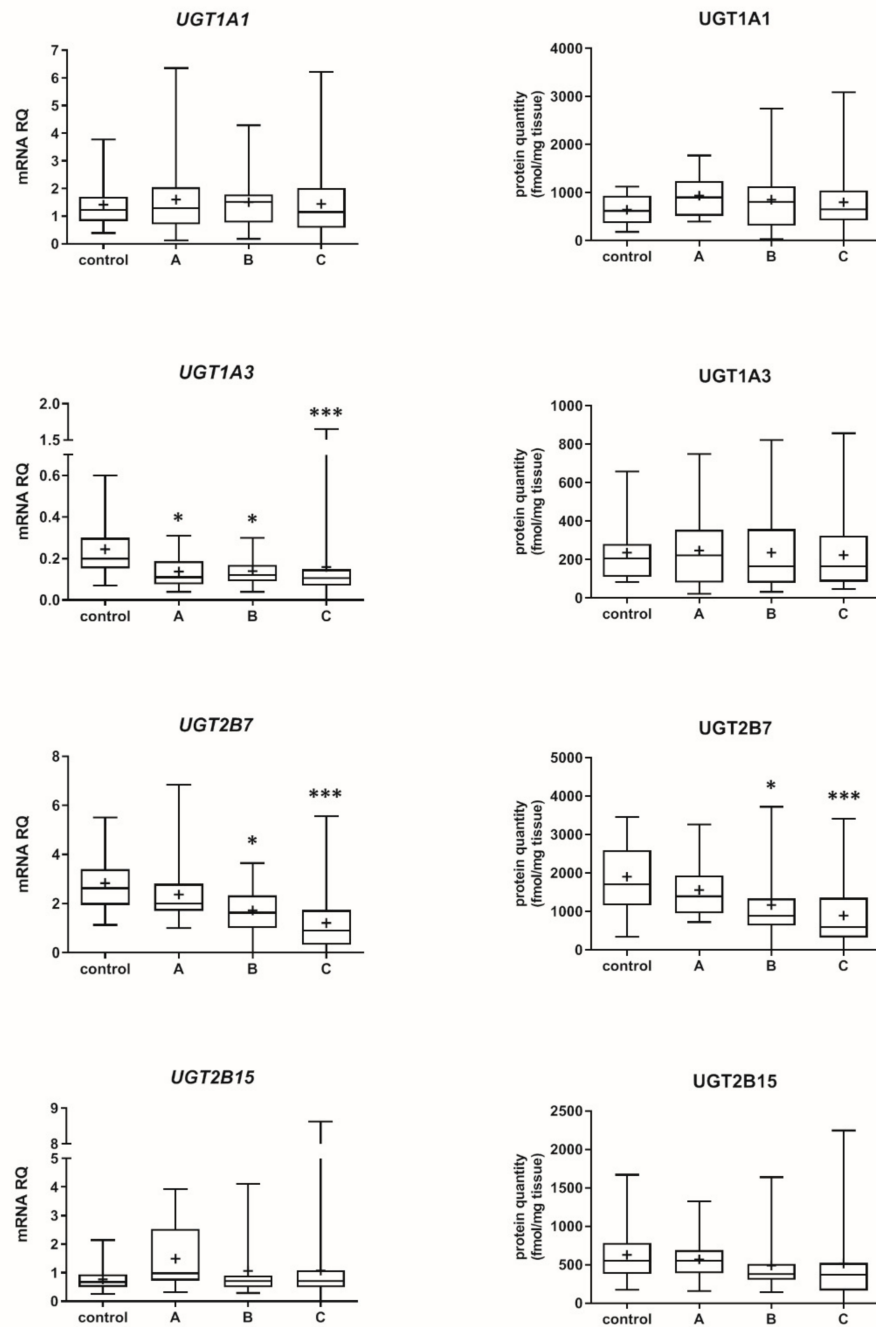


Figure 2. Gene expression (**left**) and protein abundance (**right**) of UGTs in hepatic tissues stratified according to the Child–Pugh score into stages: A ($n = 18$), B ($n = 31$) and C ($n = 28$). The data are represented as box-plots of the median (horizontal line), 75th (top of box), and 25th (bottom of box) quartiles, the smallest and largest values (whiskers) and mean (+) are shown. mRNA levels of the analyzed genes were expressed as relative amounts to the mean of five housekeeping genes (GAPDH, HMBS, PPIA, RPLP0, RPS9). Statistically significant differences: * $p < 0.05$, *** $p < 0.001$ (Kruskal–Wallis test post hoc Dunn’s test with Bonferroni correction) in comparison to the controls.

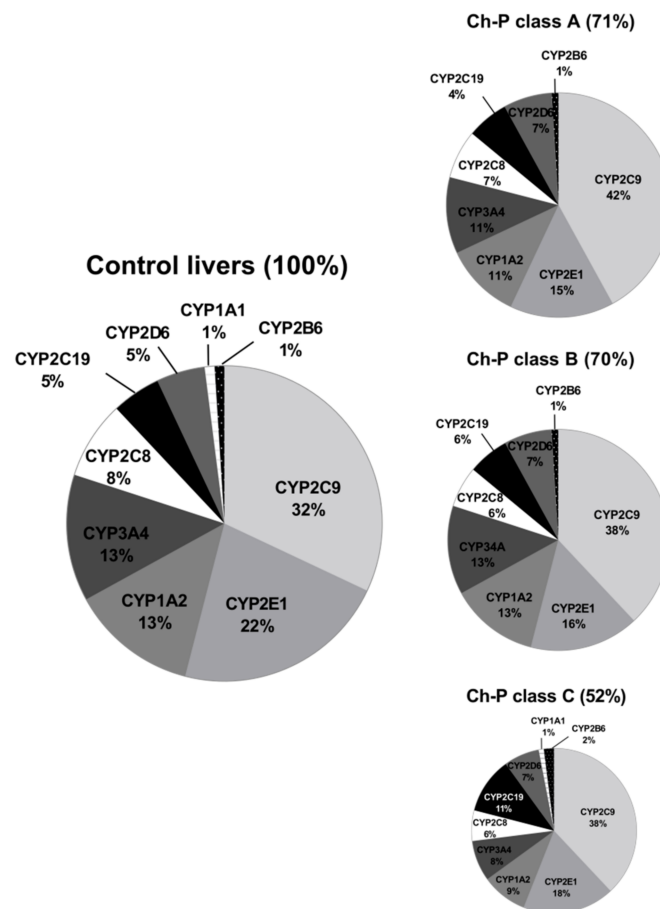


Figure 3. The pie chart of the individual enzyme proteins in livers stratified according to the Child–Pugh score (A, B, C class). The pie charts show the abundance of each enzymatic protein as a percentage of the sum of all enzyme proteins abundance. Percentages in brackets indicate a total enzyme protein abundance in comparison to the control livers (indicated as 100%).

Among the studied UGTs, the most abundant isoenzyme was UGT2B7, and the least one was UGT1A3, irrespectively of the stage of liver dysfunction (Table S3). Details on differences in the DMEs mRNA and protein abundance levels between the studied liver pathologies are presented in Table S4.

3.2. Hepatic Drug Metabolizing Enzymes in Different Forms of Liver Disease

Our data show that the type of liver damage may determine levels of DMEs in the organ (Figures 4 and 5, Tables S2 and S3). CYP2C9 and CYP2C19 remained stable in all liver pathological states, and in comparable levels to the controls. As for the UGTs, protein levels of UGT1A1, UGT1A3 and UGT2B15 were also not changed. All other investigated enzymes demonstrated a downregulation trend. CYP1A1 abundance was markedly reduced in cholestatic pathologies, i.e., PBC (to 0.03% of the controls) and PSC (to 0.04% of the controls). In PBC, apart from CYP1A1, a marked downregulation was observed for CYP2B6 (to 44% of mean value of the controls), CYP2C8 (to 28% of the controls), CYP2E1 (to 39% of the controls) and CYP3A4 (to 47% of the controls). HCV pathology entailed prominent decrease in CYP2E1 (to 52% of the controls) and UGT2B7 (to 49% of the controls) abundances. ALD was characterized with significant reduction of protein abundance of CYP1A2 (to 33% of the controls), CYP2C8 (to 32% of the controls), CYP2D6 (to 14% of the controls), CYP2E1 (to 35% of the controls), CYP3A4 (to 27% of the controls) and UGT2B7 (to 47% of the controls). In AIH no significant changes in the studied enzymes protein levels were determined.

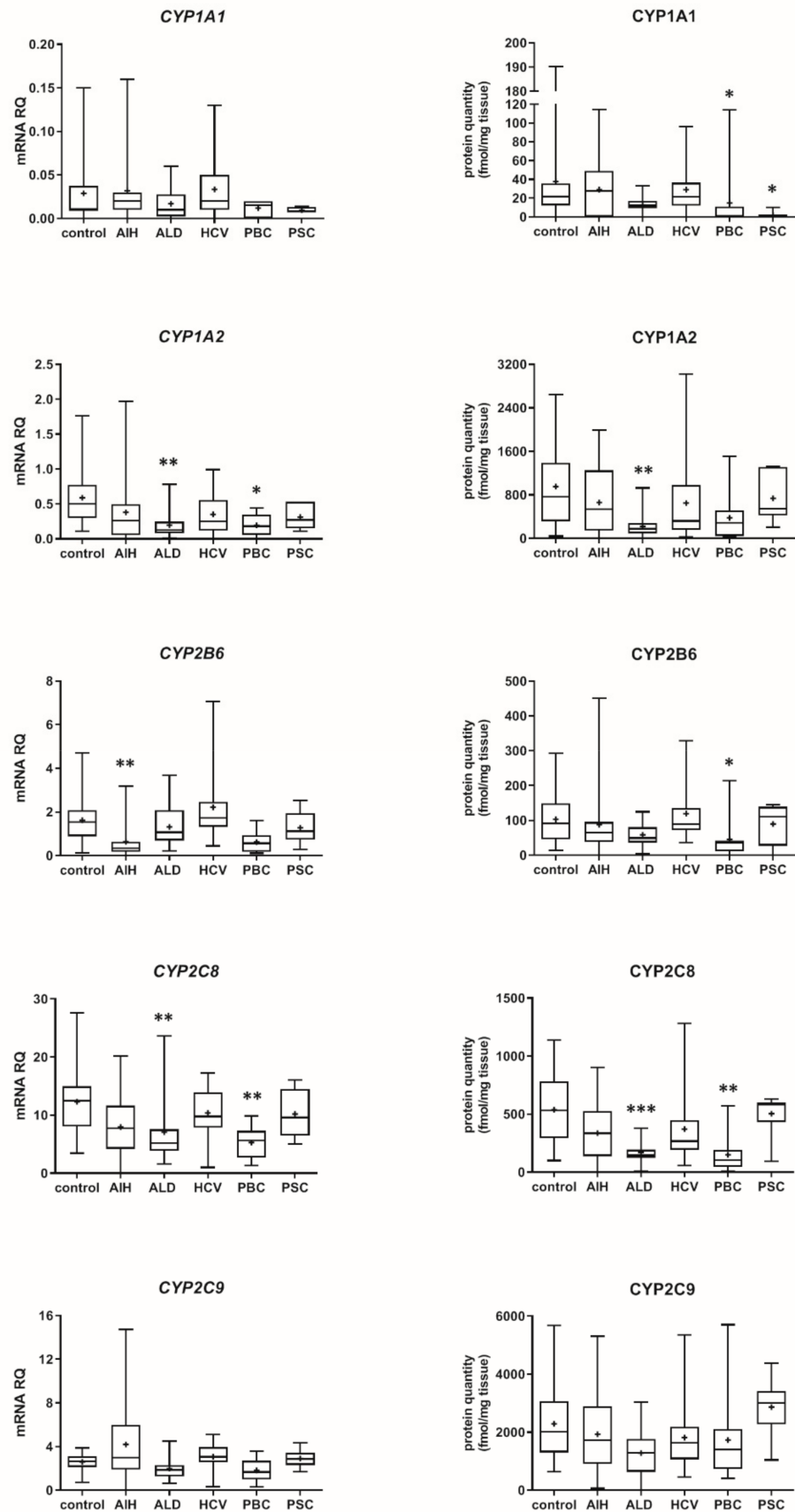


Figure 4. Cont.

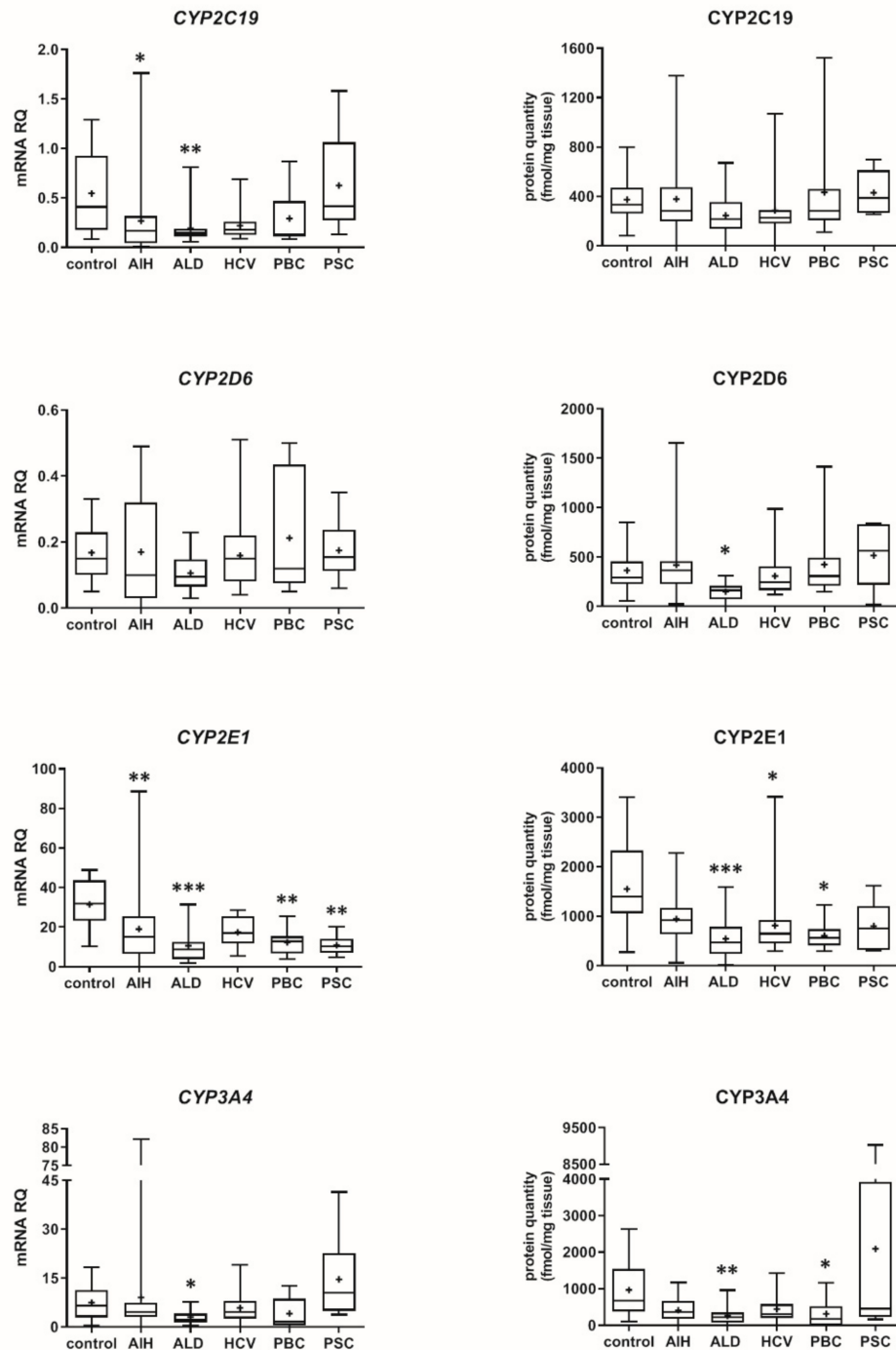


Figure 4. (also see page up) Gene expression (left) and protein abundance (right) of CYPs in hepatic tissues from hepatitis C (HCV, $n = 21$), primary biliary cholangitis (PBC, $n = 10$), primary sclerosing cholangitis (PSC, $n = 6$), alcoholic liver disease (ALD, $n = 20$) and autoimmune hepatitis (AIH, $n = 20$) patients and the controls ($n = 20$). The data are represented as box-plots of the median (horizontal line), 75th (top of box), and 25th (bottom of box) quartiles, the smallest and largest values (whiskers) and mean (+) are shown. mRNA levels of the analyzed genes were expressed as relative amounts to the mean of five housekeeping genes (*GAPDH*, *HMBS*, *PPIA*, *RPLP0*, *RPS9*). Statistically significant differences: * $p < 0.05$, ** $p < 0.01$, *** $p < 0.001$ (Kruskal–Wallis test post hoc Dunn’s test with Bonferroni correction) in comparison to the controls.

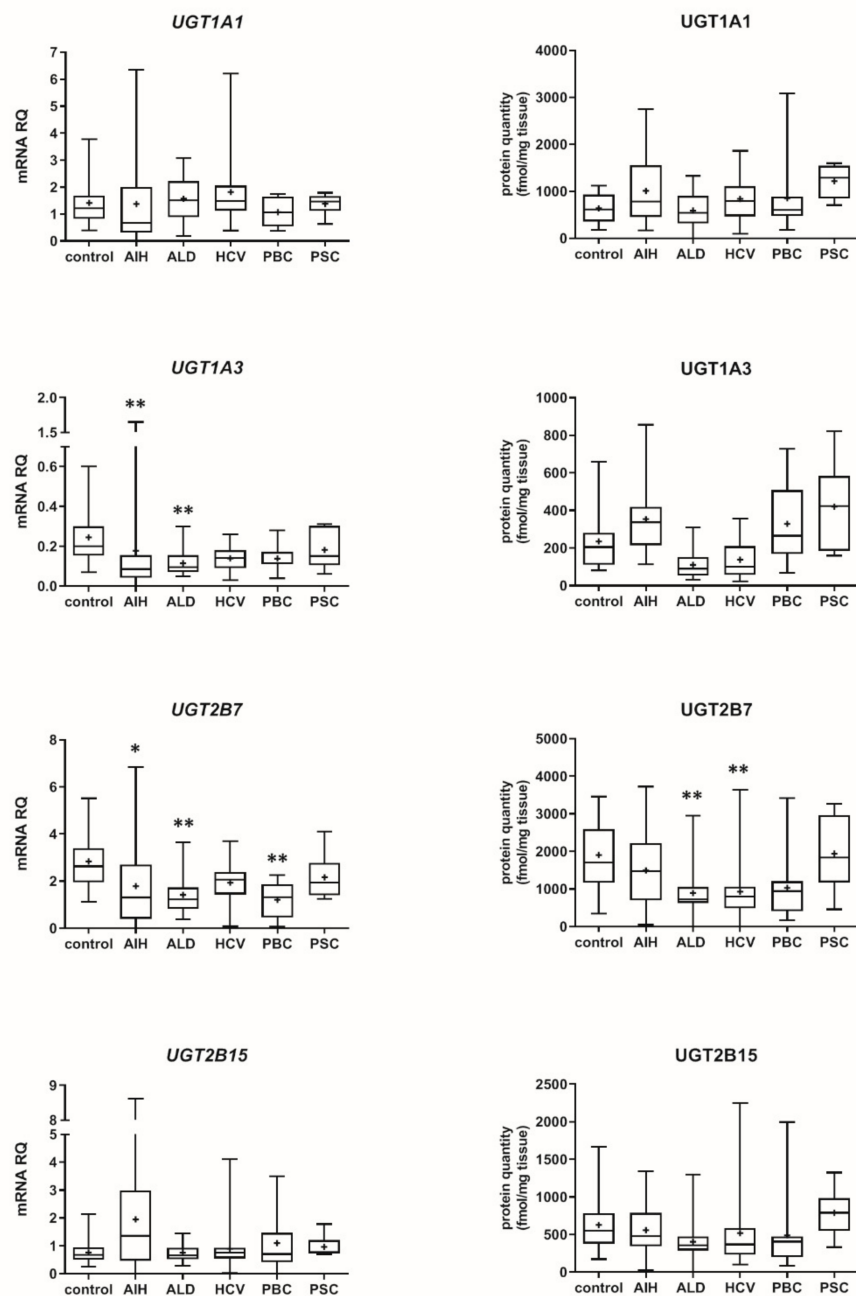


Figure 5. Gene expression (left) and protein abundance (right) of UGTs in hepatic tissues from hepatitis C (HCV, $n = 21$), primary biliary cholangitis (PBC, $n = 10$), primary sclerosing cholangitis (PSC, $n = 6$), alcoholic liver disease (ALD, $n = 20$) and autoimmune hepatitis (AIH, $n = 20$) patients and the controls ($n = 20$). The data are represented as box-plots of the median (horizontal line), 75th (top of box), and 25th (bottom of box) quartiles, the smallest and largest values (whiskers) and mean (+) are shown. mRNA levels of the analyzed genes were expressed as relative amounts to the mean of five housekeeping genes (GAPDH, HMBS, PPIA, RPLP0, RPS9). Statistically significant differences: * $p < 0.05$, ** $p < 0.01$ (Kruskal–Wallis test post hoc Dunn’s test with Bonferroni correction) in comparison to the controls.

The rank order of the studied CYPs was markedly affected by the studied liver pathologies. Figure 6 shows percentage contributions of all investigated CYP proteins stratified according to the different types of liver disease. In parallel to our analysis

stratified by the Child–Pugh score, CYP2C9 showed highest ((32–44%) and CYP2B6 (1–2%) the lowest protein amounts in all studied liver pathologies.

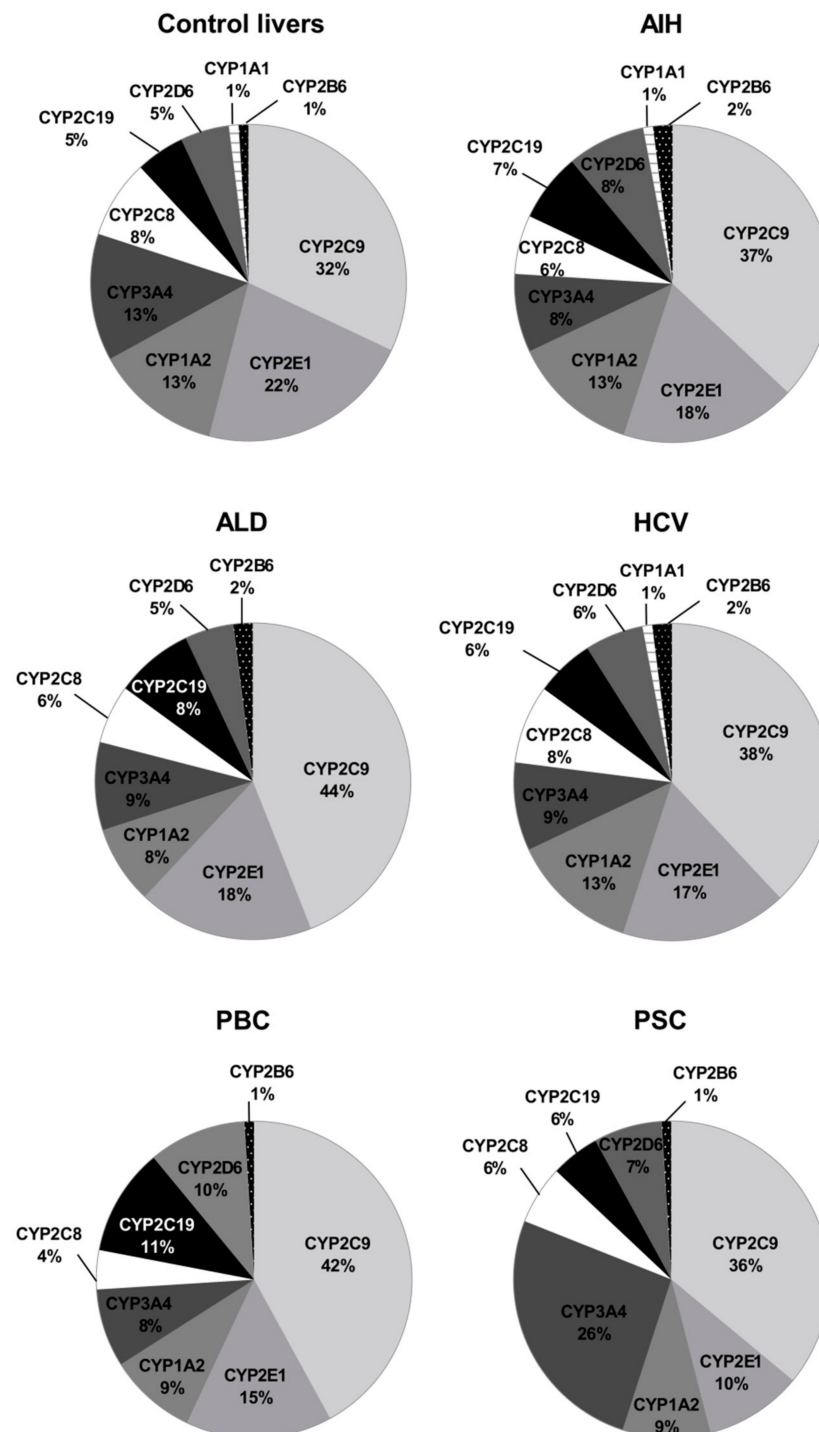


Figure 6. The pie chart of the individual enzyme proteins in livers tissues from hepatitis C (HCV), primary biliary cholangitis (PBC), primary sclerosing cholangitis (PSC), alcoholic liver disease (ALD) and autoimmune hepatitis (AIH) patients and the controls. The pie charts show the abundance of each enzymatic protein as a percentage of the sum of all enzyme proteins abundance.

In the control samples, for most of the studied DMEs, except for CYP2C19 and CYP2E1, significant, strong ($r_s > 0.6$) correlations between mRNA expression and protein abundance

(for CYP2D6 moderate) were observed. Liver pathologies affected the level of significant positive correlations. However, in AIH and to a lesser extent in PBC multiple positive correlations were still found (Table 1).

Table 1. Correlation (Spearman coefficient, *r*) between protein and mRNA levels of the P450s and UGTs in human livers stratified by the liver pathology.

Protein	mRNA vs. Protein Correlation Coefficient					
	Control <i>n</i> = 20 ^a	AIH <i>n</i> = 20 ^b	ALD <i>n</i> = 20	HCV <i>n</i> = 21 ^c	PBC <i>n</i> = 10 ^d	PSC <i>n</i> = 6
CYP1A1	0.664 ***	0.722 ***	0.443	0.736 ***	0.225	−0.393
CYP1A2	0.824 ***	0.857 ***	0.595 **	0.766 ***	0.867 **	1.000 **
CYP2B6	0.612 **	0.573 **	−0.036	0.394	0.900 ***	−0.257
CYP2C8	0.645 **	0.588 **	0.140	0.182	0.842 **	−0.086
CYP2C9	0.620 **	0.686 ***	0.498 *	0.347	0.867 **	0.829 *
CYP2C19	0.325	−0.038	−0.368	0.099	0.224	0.029
CYP2D6	0.586 **	0.614 **	0.105	0.470 *	0.600	0.086
CYP2E1	0.352	0.580 **	0.499 *	0.355	0.479	0.371
CYP3A4	0.889 ***	0.722 ***	0.714 ***	0.712 ***	0.890 ***	0.543
UGT1A1	0.675 **	0.684 ***	0.383	0.504 *	0.927 ***	0.143
UGT1A3	0.699 ***	0.453 *	−0.341	0.451 *	0.612	0.771
UGT2B15	0.800 ***	0.453 *	0.229	0.479 *	0.467	0.371
UGT2B7	0.725 ***	0.740 ***	0.505 *	0.264	0.782 **	0.829 *

* $p < 0.05$; ** $p < 0.01$; *** $p < 0.001$; ^a CYP2C19 *n* = 18, CYP2D6 *n* = 19; ^b CYP2D6 *n* = 19; ^c CYP2D6 *n* = 19; ^d CYP2D6 *n* = 9.

3.3. Genotyping

The genotyping studies of CYP2C19*, CYP2D6* and CYP3A5* resulted in the exclusion of the patient samples, who were genetically determined with the enzyme deficiency, i.e., for CYP2C19—2 controls, and for CYP2D6—1 control as well as AIH—1, HCV—1 and PBC—1 sample. In the case of CYP3A5, expresser status (*1/*3) was found in 12 subjects: 3 controls, 3 AIH, 1 ALD, 3 HCV, 1 PBC and 1 PSC. In all expressers, protein abundance exceeded 200 fmol/mg tissue, except for a PSC patient with the protein level of 46 fmol/mg tissue; in non-expressers CYP3A5 abundance ranged from 0 to 102.54 fmol/mg tissue (mean 26.21 fmol/mg tissue).

4. Discussion

It is known that impaired hepatic function may affect drug pharmacokinetics, and in turn efficacy and safety of drug therapy. However, due to ethical aspects and organizational issues, there is limited information about drug pharmacokinetics in liver diseases, especially in advanced stages. The published clinical pharmacokinetic studies suggest that liver failure can affect CYP1A2, CYP2C19, CYP2D6, CYP2E1 and CYP3A4 activities [1–3]. However, the estimation of precise contribution of the enzymes to overall altered drug kinetics in patients with deteriorated liver function is not possible due to a complex pathophysiology. Proteomic data on CYPs and UGTs offer a possibility to better characterize DMEs status in the liver, and to cover the gaps of quantitative information enabling construction of more adequate PBPK models of liver pathologies.

The present study provides for the first time precise quantitative data on the protein abundance of DMEs in the livers of patients with a wide spectrum of liver diseases stratified according to the Child–Pugh score. The study findings evidence that progression of liver dysfunction is associated with constant deterioration of most of the studied enzymes. However, protein abundances of CYP1A1, CYP2B6, CYP2C19 and CYP2D6 as well as UGT1A1, UGT1A3 and UGT2B15 did not differ significantly among the Child–Pugh class A, B and C livers. These observations are supported by the debrisoquine (CYP2D6 substrate) pharmacokinetic study, whose metabolism was found to be not affected by Child–Pugh class A and B liver disease [2]. However, the decrease in the apparent oral

clearance of S-mephenytoin (CYP2C19 substrate) along with a corresponding reduction in the urinary excretion of the metabolite 4'-hydroxymephenytoin (suggesting its decreased metabolism) is contrary to the findings from the present study [1,2]. The discrepancy between the studies could be related to the reduced hepatocyte volume in the liver, and thus the diminished total liver CYP2C19 metabolic capacity developing with liver failure progression [18], as well as to a genetic status of the subjects (the patients of Adedoyin et al. [2], were phenotyped and poor metabolizers were excluded from the study, but as stated above apart from quantitative changes of the enzymatic protein abundance many other factors can affect pharmacokinetics in liver failure patients; our study excluded poor metabolizers of CYP2C19 and CYP2D6). The immunoblot-based, semiquantitative determination of CYP2C in livers, which is a less reliable assay than LC-MS/MS method due to its methodological limitations, classified as the A and B (according to the Child–Pugh) class showed rather stable protein levels (with the exception of cholestatic livers in one study) [13,14].

There are no literature references for CYP1A1 and CYP2B6 abundances, and the present study for the first time provides information about stable protein levels of these enzymes in liver pathology states, as the same protein abundances for the controls and for the livers of the Child–Pugh class from A to C were observed.

The present study revealed significant downregulation of the protein abundance of CYP1A2, which is in agreement with semiquantitative, antibody-based observations of George et al. and Guengerich et al. [13,14]. The protein quantitative data are supported by clinical findings, which revealed an altered caffeine (CYP1A2 substrate) pharmacokinetics in liver diseases. Frye et al. observed a 69% significantly lower caffeine metabolic ratio in decompensated liver disease (Pugh score ≥ 6), and no pharmacokinetic effects of the compensated disease (Pugh score = 5) [1].

The progression of liver disease also entailed a decrease in protein abundance of CYP2E1, which significant reduction was observed even in the Child–Pugh class A patients (as the unique downregulated enzyme levels in the early stage of liver failure were seen). These quantitative data are in agreement with the immunoblot CYP2E1 protein determination in cholestatic livers and cirrhotic livers [13,14]. The observed reduction of CYP2E1 abundance may contribute to 40% lower chlorzoxazone (CYP2E1 substrate) metabolic ratio observed in patients with moderate-severe liver disease [1].

Contradictory to the present study findings, non-significantly altered levels of CYP3A abundance (measured by an immunoblot technique, without discrimination of CYP3A4 and CYP3A5 isoforms) were provided by George et al. (for cholestatic liver diseases) and Guengerich et al. [13,14]. However, CYP3A enzymes were significantly affected by the non-cholestatic form of liver diseases [14]. Likewise in the case of CYP2C19, these studies did not consider highly polymorphic nature of CYP3A5, which might result in inconsistent observations. However, the present study findings are in keeping with clinical observations on midazolam pharmacokinetics, which demonstrated significantly 38% higher oral bioavailability and 41% lower total clearance of the drug (and unchanged plasma protein binding and distribution) in patients with chronic liver disease [3]. In our study, we did not analyze CYP3A5, as only few cases of expressers were found upon genotyping. However, we found that CYP3A5 expressers in different liver pathologies demonstrated protein abundance exceeding 200 fmol/mg liver tissue (except for a PSC patient with the protein level of 46 fmol/mg). A common *CYP3A5*3* allele results in a cryptic splice site in intron 3, and an altered mRNA splicing and truncated non-functional protein in about 90% of Caucasian population, but the status of CYP3A5-expressor can affect drug pharmacokinetics (i.e., tacrolimus, midazolam, and possibly statins) in patients with the functional *CYP3A5*1* allele [19].

There is no information about the disease-related changes of UGT2B7 protein abundance, but the downregulation observed in our study is also supported by significantly lower mRNA expression level of UGT2B7 in human liver diseases, which is also consistent with our mRNA expression findings for the enzyme [20].

The present study provides also for the first-time proteomic characteristics of CYP2C8 and CYP2C9 in different stages of liver diseases. The levels of both enzymes were reduced stepwise down along the liver diseases severity.

The analysis of the liver samples according to the Child–Pugh class suggests that the most vulnerable enzyme was CYP2E1, which was downregulated in class A livers. The class B livers were characterized by a decrease in CYP2E1 and then CYP2C8, CYP3A4 as well as UGT2B7 abundances. In the Child–Pugh class C, the following enzymes were affected: CYP2E1, CYP2C8, CYP3A4 and CYP1A2, CYP2C9. These findings are only in part consistent with pharmacokinetic observations with substrates for CYP1A2, CYP2C9, CYP2D6 and CYP2E1. The reported pharmacokinetic study suggested that CYP2E1 was the most stable enzyme, whereas CYP2C19 (with CYP1A1 and CYP2D6 in the middle) was the most vulnerable in liver failure [1]. As stated above, lack of genetic information in the study of Frye et al. [1] could contribute to the reported discrepancies. The Child–Pugh scoring criteria are well-established and widely used to classify severity of liver dysfunction/cirrhosis, and the score parameters refer to hepatocyte function (albumin and bilirubin levels, prothrombin time), as well as to overall disease progression (encephalopathy and ascites; and these are more subjective) [21,22]. The Child–Pugh score is the most commonly used scale for assessing hepatic impairment in the case of drugs submitted for US FDA approval [23].

A pediatric population study on hepatic cytochrome P450 activity in livers, mainly with biliary atresia (explanted before transplantation), are mostly in keeping with the present study observations. A negative correlation of CYP1A2, CYP2C9, CYP2C19, CYP2D6, CYP2E1 and CYP3A4 activity with PELD score (pediatric end-stage liver disease score, range from 0 to 38) used to estimate relative disease severity and survival of patients awaiting liver transplantation was reported by de Bock et al. [24]. This study excluded poor metabolizers and gain-of-function subjects (CYP2C9, CYP2C19 and CYP2D6) after genotyping.

In the present study, an analysis of the specific type of liver disease and DMEs (both at mRNA and protein levels) was performed. Similar to other studies, some strong correlations between mRNA expression and protein levels could be found in normal livers [25]. However, liver pathological states affected the correlations, especially in PSC, ALD and HCV samples, which may suggest that the available mRNA data not reliably represent biological role of the enzymes. Only moderate correlations between cytochrome P450 mRNA expressions and corresponding cytochrome P450 activities were found for CYP2C19, CYP2D6 and CYP4A11 ($r_s = 0.44\text{--}0.56$) in the intestine [26]. However, strong correlations ($r_s > 0.6$) between hepatocyte protein levels and enzymatic activity were documented for CYP1A2, CYP2B6, CYP2D6 and CYP3A4 (of the studied relationships, a mild correlation was found for CYP2C9, $r_s = 0.42$) [27]. Direct comparison of mRNA and protein levels with enzymatic activity reported by Ohtsuki et al. revealed that except for CYP2B6, a better correlation of enzyme activity with protein abundance (CYP1A2, CYP2C8, CYP2C9, CYP2C19, CYP2D6, CYP2E1, CYP4A11, CYP3A4) than with mRNA expression [25]. Thus, studies based only on transcriptome analysis do not always reflect protein enzyme abundances. Therefore, it seems that quantitative proteomic information may better reflect functional state of the enzymes.

The study provides also information about DMEs abundance in different pathological states of the liver, i.e., viral—hepatitis C (HCV), toxic—alcoholic liver disease (ALD), immune/inflammatory—autoimmune hepatitis (AIH) and cholestatic—primary biliary cholangitis (PBC) and primary sclerosing cholangitis (PSC). Only one previous report has used a similar method to quantify hepatic drug metabolizing enzymes, but only in ALD and HCV-induced liver damage (without stratification to liver functional state) [12]. In ALD, the present study revealed stable protein levels of CYP1A1, CYP2B6, CYP2C9, CYP2C9, UGT1A1, UGT1A3 and UGT2B15 as well as downregulation of CYP1A2, CYP2C8, CYP2D6, CYP2E1, CYP3A4 and UGT2B7. These results corroborate observations of Prasad et al., who documented reduction in protein abundance of CYP1A2, CYP2C8, CYP2E1, CYP3A4 and UGT2B7 in ALD livers [12]. However, contrary to our findings, downregulations of

CYP2C9, CYP2D6, UGT2B15 protein levels were also observed. As for HCV pathology, the concordance was noted for CYP2D6 (in both studies not changed), CYP2E1 and UGT2B7 (in both studies downregulated), but reduction in CYP1A2, CYP2C9 and UGT2B15 was not reproduced. The observed discrepancies may be explained by different methodical procedures of sample preparation. While Prasad et al. isolated and analyzed the S9 fraction [12], the FASP procedure (eliminating any additional centrifugation steps that may cause loss of proteins) was used in the present study. In addition to other methodical differences (e.g., the use of different peptides), analysis of samples from different stages of liver disease might also contribute to the study results.

The present study demonstrates a significant decline of CYP1A2 and CYP2C9 abundances in the course of progression of liver disease, and similar trend is observed for UGT2B15). Liver samples analyzed by Prasad et al. were characterized as end-stage liver disease, and the authors assumed that they represented the Child–Pugh score C, as livers explanted during liver transplantation were analyzed [12]. However, transplantation protocols qualify even the Child–Pugh score A subjects to the procedure, depending on the patient clinical picture. The published clinical pharmacokinetic studies involved patients, who were characterized only as “having liver disease” (without etiology), and those published are in keeping with the merged LC-MS/MS proteomic studies results for the following enzymatic proteins in ALD: CYP1A2 (caffeine), CYP2E1 (chlorzoxazone) and CYP3A4 (midazolam) as well as in HCV: CYP2E1 (chlorzoxazone) and CYP2D6 (debrisoquine) [1–3].

The present study provides also for the first-time quantitative information about DMEs in cholestatic liver disease, i.e., primary biliary cholangitis (intrahepatic cholestasis) and primary sclerosing cholangitis (extrahepatic cholestasis). In both cholestatic pathologies, marked downregulation of CYP1A1 abundance was noted, and in the case of PBC, significantly lower levels of CYP2B6, CYP2C8, CYP2E1 and CYP3A4 were also noted. Reduced CYP2E1 levels were also observed in cholestatic livers examined by George et al. (using a semiquantitative blot method) [14].

The study also reports new findings on DMEs profile in autoimmune hepatitis, where only downregulation trend of the studied enzymes was documented (except for UGT1A1 and UGT1A3), but without reaching statistical significance ($p > 0.05$). So, AIH seems to be the liver pathological state with a relatively stable function of DMEs.

Small number of PBC and PSC samples belongs to the study limitations, which should be considered when interpreting data. However, information about gene expression and protein content in these cholestatic diseases has not been published yet (the prevalence of both diseases is very low), and these data can be considered as preliminary. Patients medication could also affect the present study results. The liver diseases medication standards were modified during the period of the liver samples harvesting, and treatment approaches are also liver pathology and functional state dependent. Therefore, due to a limited number of samples for a given liver pathology and functional state, medication analysis was not reliable. However, patients with co-morbidities were excluded. A liver harvesting of the samples could also pose some bias. This study, likewise other reports [12–14], includes livers from patients with the organ failure (including cirrhosis), involving progressing changes in a number of hepatocytes (reduction), and other components of liver structure, i.e., sinusoidal endothelial cells, Kupffer cells, and hepatic stellate cells, fibroblasts and transdifferentiated myofibroblasts and fibrous connective tissue (expansion) [28]. The functional liver mass in the Child–Pugh class A, B, and C was shown to be 69%, 55%, and 28%, respectively, as compared with the control samples [29]. To limit the tissue harvesting bias, efforts were made to dissect only the parenchymal/functional, hepatocyte rich liver tissue. The interpersonal variability in the studied enzyme protein abundance observed in the present study (from CYP2C9 5.5-fold to CYP1A1 33-fold in controls), which is consistent with data of Ohtsuki et al. [25], Achour et al. [27], Kawakami et al. [30], could also affect the data analysis outcome (to reduce impact of genetic factors poor metabolizers of CYP2C19 and CYP2D6 as well as CYP3A5 expressers were excluded from the analysis).

As already described in the Introduction, there are few studies available investigating impact of liver diseases on protein abundances of clinically relevant DMEs. The novelty of the study is represented by a variety of liver diseases evaluated, and in parallel the analysis of the samples according to the frequently used Child–Pugh score. The quantitative information about DMEs protein abundance can be implemented to PBPK models to calculate the clinical relevance in terms of the liver metabolic capacity. However, the application of the method itself (protein quantification) in diagnostics is not expected to be a clinical routine because the procedure is expensive, time-consuming and requires a certain level of methodical expertise.

5. Conclusions

In conclusion, it can be stated that the study provides the information about DMEs proteomic quantitative status in five liver pathologies of different etiology, i.e., hepatitis C, alcoholic liver disease, primary biliary cholangitis, primary sclerosing cholangitis and autoimmune hepatitis. ALD and PSC involved the most prominent changes in protein abundances of DMEs, with 6 and 5 significantly downregulated proteins (out of 13 studied), respectively. It seems that CYP2E1 is the most vulnerable enzyme, as it was the only one with markedly reduced protein levels in the Child–Pugh class A livers. The protein abundance of CYP1A1, CYP2B6, CYP2C19, CYP2D6 as well as UGT1A1, UGT1A3 and UGT2B15 was relatively stable in the course of progression of liver function deterioration. The results from the present study may be applied to optimize the existing in vitro in vivo extrapolation of drug metabolism in PBPK models. Moreover, information on disease-related changes in the hepatic protein abundance of DMEs may allow more precise predictions on drug pharmacokinetics and drug–drug interactions in patients suffering from different forms of liver disease and in turn appropriate dose-adjustments.

Supplementary Materials: The following are available online at <https://www.mdpi.com/article/10.3390/pharmaceutics13091334/s1>, Table S1: Characteristics of the subjects. Table S2: The mRNA (messenger RNA) expression (relative to the mean value of the control group) of the CYPs and UGTs in different liver pathologies (AIH, ALD, HCV, PBC, PSC) and disease stages (Child–Pugh class A, B and C) as well as in the controls. Table S3: Protein abundance (fmol/mg tissue) of the CYPs and UGTs in different liver pathologies (AIH, ALD, HCV, PBC, PSC) and disease stages (Child–Pugh class A, B and C) as well as in the controls. Table S4: Differences in the drug metabolizing enzymes protein abundance and mRNA levels between studied groups.

Author Contributions: M.D. and S.O. wrote the article; M.D., M.K. and S.O. designed the research; M.D., J.L.-R., C.W., M.P., Ł.S., S.S.-P., M.K. and S.O. performed the research; M.D., J.L.-R., M.K. and S.O. analyzed the data. All authors have read and agreed to the published version of the manuscript.

Funding: The study was funded a grant by the National Science Centre, Cracow, Poland UMO-2020/37/B/NZ7/01466.

Institutional Review Board Statement: The study has been approved by the by Bioethics Committee at the Pomeranian Medical University, approval number BN-001/11/07. The tissue samples were collected from participants who had provided informed consent. The study was conducted in accordance with the principles of the Declaration of Helsinki (2013).

Informed Consent Statement: Informed consent was obtained from all subjects involved in the study.

Data Availability Statement: Not applicable.

Conflicts of Interest: The authors declare no conflict of interest.

References

1. Frye, R.F.; Zgheib, N.K.; Matzke, G.R.; Chaves-Gnecco, D.; Rabinovitz, M.; Shaikh, O.S.; Branch, R.A. Liver disease selectively modulates cytochrome P450-mediated metabolism. *Clin. Pharmacol. Ther.* **2006**, *80*, 235–245. [[CrossRef](#)] [[PubMed](#)]
2. Adedoyin, A.; Arns, P.A.; Richards, W.O.; Wilkinson, G.R.; Branch, R.A. Selective effect of liver disease on the activities of specific metabolizing enzymes: Investigation of cytochromes P450 2C19 and 2D6. *Clin. Pharmacol. Ther.* **1998**, *64*, 8–17. [[CrossRef](#)]

3. Pentikäinen, P.J.; Välsalmi, L.; Himberg, J.L.; Crevoisier, C. Pharmacokinetics of midazolam following intravenous and oral administration in patients with chronic liver disease and in healthy subjects. *J. Clin. Pharmacol.* **1989**, *29*, 272–277. [[CrossRef](#)] [[PubMed](#)]
4. Edginton, A.N.; Willmann, S. Physiology-based simulations of a pathological condition: Prediction of pharmacokinetics in patients with liver cirrhosis. *Clin. Pharmacokinet.* **2008**, *47*, 743–752. [[CrossRef](#)]
5. Drozdziak, M.; Szelag-Pieniek, S.; Post, M.; Zeair, S.; Wrzesinski, M.; Kurzawski, M.; Prieto, J.; Oswald, S. Protein abundance of hepatic drug transporters in patients with different forms of liver damage. *Clin. Pharmacol. Ther.* **2020**, *107*, 1138–1148. [[CrossRef](#)] [[PubMed](#)]
6. Drozdziak, M.; Oswald, S.; Drozdziak, A. Extrahepatic drug transporters in liver failure: Focus on kidney and gastrointestinal tract. *Int. J. Mol. Sci.* **2020**, *21*, 5737. [[CrossRef](#)]
7. Franz, C.C.; Hildbrand, C.; Born, C.; Egger, S.; Rätz, B.; Krähenbühl, S. Dose adjustment in patients with liver cirrhosis: Impact on adverse drug reactions and hospitalizations. *Eur. J. Clin. Pharmacol.* **2013**, *69*, 1565–1573. [[CrossRef](#)] [[PubMed](#)]
8. European Medicines Agency 2005. Guideline on the Evaluation of the Pharmacokinetics of Medicinal Products in Patients with Impaired Hepatic Function. February 2005. Available online: https://www.ema.europa.eu/documents/scientific-guideline/guideline-evaluation-pharmacokinetics-medicinal-products-patients-impaired-hepatic-function_en.pdf (accessed on 14 March 2021).
9. FDA. Guidance for Industry Pharmacokinetics in Patients with Impaired Hepatic Function: Study, Design, Data Analysis, and Impact on Dosing and Labeling. 2003. Available online: <https://www.fda.gov/media/71311/download> (accessed on 14 March 2021).
10. Villeneuve, J.P.; Pichette, V. Cytochrome P450 and Liver Diseases. *Curr. Drug Metab.* **2004**, *5*, 273–282. [[CrossRef](#)] [[PubMed](#)]
11. Vogel, C.; Marcotte, E.M. Insights into the regulation of protein abundance from proteomic and transcriptomic analyses. *Nat. Rev. Genet.* **2012**, *13*, 227–232. [[CrossRef](#)] [[PubMed](#)]
12. Prasad, B.; Bhatt, D.K.; Johnson, K.; Chapa, R.; Chu, X.; Salphati, L.; Xiao, G.; Lee, C.; Hop, C.; Mathias, A.; et al. Abundance of phase 1 and 2 drug-metabolizing enzymes in alcoholic and hepatitis C cirrhotic livers: A quantitative targeted proteomics study. *Drug Metab. Dispos.* **2018**, *46*, 943–952. [[CrossRef](#)] [[PubMed](#)]
13. Guengerich, F.P.; Turvy, C.G. Comparison of levels of several human microsomal cytochrome P-450 enzymes and epoxide hydrolase in normal and disease states using immunochemical analysis of surgical liver samples. *J. Pharmacol. Exp. Ther.* **1991**, *256*, 1189–1194. [[PubMed](#)]
14. George, J.; Murray, M.; Byth, K.; Farrell, G.C. Differential alterations of cytochrome P450 proteins in livers from patients with severe chronic liver disease. *Hepatology* **1995**, *21*, 120–128. [[PubMed](#)]
15. Oswald, S.; Gröer, C.; Drozdziak, M.; Siegmund, W. Mass spectrometry-based targeted proteomics as a tool to elucidate the expression and function of intestinal drug transporters. *AAPS J.* **2013**, *15*, 1128–1140. [[CrossRef](#)] [[PubMed](#)]
16. Drozdziak, M.; Busch, D.; Lapczuk, J.; Müller, J.; Ostrowski, M.; Kurzawski, M.; Oswald, S. Protein abundance of clinically relevant drug-metabolizing enzymes in the human liver and intestine: A comparative analysis in paired tissue specimens. *Clin. Pharmacol. Ther.* **2018**, *104*, 515–524. [[CrossRef](#)] [[PubMed](#)]
17. Gröer, C.; Busch, D.; Patrzyk, M.; Beyer, K.; Busemann, A.; Heidecke, C.D.; Drozdziak, M.; Siegmund, W.; Oswald, S. Absolute protein quantification of clinically relevant cytochrome P450 enzymes and UDP-glucuronosyltransferases by mass spectrometry-based targeted proteomics. *J. Pharm. Biomed. Anal.* **2014**, *100*, 393–401. [[CrossRef](#)] [[PubMed](#)]
18. Johnson, T.; Boussery, K.; Rowland-Yeo, K.; Tucker, G.; Rostami-Hodjegan, A. A semi-mechanistic model to predict the effects of liver cirrhosis on drug clearance. *Clin. Pharmacokinet.* **2010**, *49*, 189–206. [[CrossRef](#)] [[PubMed](#)]
19. Lamba, J.; Hebert, J.M.; Schuetz, E.G.; Klein, T.E.; Altman, R.B. PharmGKB summary: Very important pharmacogene information for CYP3A5. *Pharm. Genom.* **2012**, *22*, 555–558. [[CrossRef](#)] [[PubMed](#)]
20. Congiu, M.; Mashford, M.L.; Slavin, J.L.; Desmond, P.V. UDP glucuronosyltransferase mRNA levels in human liver disease. *Drug Metab. Dispos.* **2002**, *30*, 129–134. [[CrossRef](#)]
21. Kamath, P.S.; Wiesner, R.H.; Malinchoc, M.; Kremers, W.; Therneau, T.M.; Kosberg, C.L.; D’Amico, G.; Dickson, E.R.; Kim, W.R. A model to predict survival in patients with end-stage liver disease. *Hepatology* **2001**, *33*, 464–470. [[CrossRef](#)]
22. Peng, Y.; Qi, X.; Guo, X. Child-Pugh versus MELD score for the assessment of prognosis in liver cirrhosis: A systematic review and meta-analysis of observational studies. *Medicine* **2016**, *95*, e2877. [[CrossRef](#)]
23. Talal, A.H.; Venuto, C.S.; Younis, I. Assessment of Hepatic Impairment and Implications for pharmacokinetics of Substance Use Treatment. *Clin. Pharmacol. Drug Dev.* **2017**, *6*, 206–212. [[CrossRef](#)] [[PubMed](#)]
24. De Bock, L.; Boussery, K.; van Winckel, M.; de Paepe, P.; Rogiers, X.; Stephenne, X.; Sokal, E.; van Boclaer, J. In vitro cytochrome p450 activity decreases in children with high pediatric end-stage liver disease scores. *Drug Metab. Dispos.* **2013**, *41*, 390–397. [[CrossRef](#)] [[PubMed](#)]
25. Ohtsuki, S.; Schaefer, O.; Kawakami, H.; Inoue, T.; Liehner, S.; Saito, A.; Ishiguro, N.; Kishimoto, W.; Ludwig-Schwelling, E.; Ebner, T.; et al. Simultaneous absolute protein quantification of transporters, cytochromes P450, and UDP-glucuronosyltransferases as a novel approach for the characterization of individual human liver: Comparison with mRNA levels and activities. *Drug Metab. Dispos.* **2012**, *40*, 83–92. [[CrossRef](#)] [[PubMed](#)]

26. Clermont, V.; Grangeon, A.; Barama, A.; Turgeon, J.; Lallier, M.; Malaise, J.; Michaud, V. Activity and mRNA expression levels of selected cytochromes P450 in various sections of the human small intestine. *Br. J. Clin. Pharmacol.* **2019**, *85*, 1367–1377. [[CrossRef](#)] [[PubMed](#)]
27. Achour, B.; Russell, M.R.; Barber, J.; Rostami-Hodjegan, A. Simultaneous quantification of the abundance of several cytochrome P450 and uridine 5-diphospho-glucuronosyltransferase enzymes in human liver microsomes using multiplexed targeted proteomics. *Drug Metab. Dispos.* **2014**, *42*, 500–510. [[CrossRef](#)]
28. Weiskirchen, R.; Weiskirchen, S.; Tacke, F. Recent advances in understanding liver fibrosis: Bridging basic science and individualized treatment concepts. *F1000Research* **2018**, *7*, 921. [[CrossRef](#)] [[PubMed](#)]
29. Virgolini, I.; Müller, C.; Angelberger, P.; Höbart, J.; Bergmann, H.; Sinzinger, H. Functional liver imaging with ⁹⁹Tcmgalactosyl-neoglycoalbumin (NGA) in alcoholic liver cirrhosis and liver fibrosis. *Nucl. Med. Commun.* **1991**, *12*, 507–517. [[CrossRef](#)]
30. Kawakami, H.; Ohtsuki, S.; Kamiie, J.; Suzuki, T.; Abe, T.; Terasaki, T. Simultaneous absolute quantification of 11 cytochrome P450 isoforms in human liver microsomes by liquid chromatography tandem mass spectrometry with in silico target peptide selection. *J. Pharm. Sci.* **2011**, *100*, 341–352. [[CrossRef](#)] [[PubMed](#)]

6.4 Gene Expression and Protein Abundance of Nuclear Receptors in Human Intestine and Liver: A New Application for Mass Spectrometry-Based Targeted Proteomics

Wenzel C, Gödtke L, Reichstein A, Keiser M, Busch D, Drozdik, M, Oswald S

Molecules (Basel, Switzerland) 2022;27(14):4629. Doi: 10.3390/molecules27144629.

Projektdesign: S. O., M. D.




Projektdurchführung: C. W., D. B., A. R., L. G.

Datenanalyse: C. W., D. B., A. R., L. G.

Erstellung des Manuskriptes: C. W., M. K., M. D., S. O.

Article

Gene Expression and Protein Abundance of Nuclear Receptors in Human Intestine and Liver: A New Application for Mass Spectrometry-Based Targeted Proteomics

Christoph Wenzel ¹, Lisa Gödtke ¹, Anne Reichstein ¹, Markus Keiser ¹, Diana Busch ¹, Marek Drozdziak ^{2,*}
and Stefan Oswald ^{3,*}

¹ Department of Pharmacology, Center of Drug Absorption and Transport, University Medicine Greifswald, 17475 Greifswald, Germany; christoph.wenzel@med.uni-greifswald.de (C.W.); lisa.godke@med.uni-greifswald.de (L.G.); anne.reichstein@med.uni-greifswald.de (A.R.); markus.keiser@web.de (M.K.); diana.busch@med.uni-greifswald.de (D.B.)

² Department of Experimental and Clinical Pharmacology, Pomeranian Medical University, 70-204 Szczecin, Poland

³ Institute of Pharmacology and Toxicology, Rostock University Medical Center, 18057 Rostock, Germany

* Correspondence: drozdziak@pum.edu.pl (M.D.); stefan.oswald@med.uni-rostock.de (S.O.)

Abstract: Background: Unwanted drug-drug interactions (DDIs), as caused by the upregulation of clinically relevant drug metabolizing enzymes and transporter proteins in intestine and liver, have the potential to threaten the therapeutic efficacy and safety of drugs. The molecular mechanism of this undesired but frequently occurring scenario of polypharmacy is based on the activation of nuclear receptors such as the pregnane X receptor (PXR) or the constitutive androstane receptor (CAR) by perpetrator agents such as rifampin, phenytoin or St. John's wort. However, the expression pattern of nuclear receptors in human intestine and liver remains uncertain, which makes it difficult to predict the extent of potential DDIs. Thus, it was the aim of this study to characterize the gene expression and protein abundance of clinically relevant nuclear receptors, i.e., the aryl hydrocarbon receptor (AhR), CAR, farnesoid X receptor (FXR), glucocorticoid receptor (GR), hepatocyte nuclear factor 4 alpha (HNF4 α), PXR and small heterodimer partner (SHP), in the aforementioned organs. Methods: Gene expression analysis was performed by quantitative real-time PCR of jejunal, ileal, colonic and liver samples from eight human subjects. In parallel, a targeted proteomic method was developed and validated in order to determine the respective protein amounts of nuclear receptors in human intestinal and liver samples. The LC-MS/MS method was validated according to the current bioanalytical guidelines and met the criteria regarding linearity (0.1–50 nmol/L), within-day and between-day accuracy and precision, as well as the stability criteria. Results: The developed method was successfully validated and applied to determine the abundance of nuclear receptors in human intestinal and liver samples. Gene expression and protein abundance data demonstrated marked differences in human intestine and liver. On the protein level, only AhR and HNF4 α could be detected in gut and liver, which corresponds to their highest gene expression. In transfected cell lines, PXR and CAR could be quantified. Conclusions: The substantially different expression pattern of nuclear receptors in human intestinal and liver tissue may explain the different extent of unwanted DDIs in the dependence on the administration route of drugs.

Keywords: nuclear receptors; intestine; liver; human; drug-drug interaction; enzymes; transporters



Citation: Wenzel, C.; Gödtke, L.; Reichstein, A.; Keiser, M.; Busch, D.; Drozdziak, M.; Oswald, S. Gene Expression and Protein Abundance of Nuclear Receptors in Human Intestine and Liver: A New Application for Mass Spectrometry-Based Targeted Proteomics. *Molecules* **2022**, *27*, 4629. <https://doi.org/10.3390/molecules27144629>

Academic Editor: Yanniss Dotsikas

Received: 28 June 2022

Accepted: 18 July 2022

Published: 20 July 2022

Publisher's Note: MDPI stays neutral with regard to jurisdictional claims in published maps and institutional affiliations.



Copyright: © 2022 by the authors. Licensee MDPI, Basel, Switzerland. This article is an open access article distributed under the terms and conditions of the Creative Commons Attribution (CC BY) license (<https://creativecommons.org/licenses/by/4.0/>).

1. Introduction

Human drug metabolism and transport are well accepted key determinants of the pharmacokinetics of many drugs and, in turn, of their efficacy and safety. There is a large body of evidence demonstrating a tremendous variability in gene expression and/or protein abundance of drug metabolizing enzymes (DMEs) and drug transporters in pharmacokinetically

and highly relevant tissues including the intestine, liver and kidney [1–3]. The background of the observed high inter-subject variability in the expression and function of DMEs and transporter proteins may include extensively studied genetic polymorphisms [3,4], but also less investigated aspects such as environmental impacts on transcriptional and epigenetic regulation [5–7], post-translational modifications [8] or disease-related changes [9,10]. In order to estimate or predict the impact of those individual factors on the expression and function of DMEs and drug transporters, a deeper understanding of the respective regulatory mechanisms in different organs is required.

In this regard, nuclear receptors represent, thus far, the best established mechanism of regulation [11,12]. These receptors act as transcription factors, i.e., binding of endogenous or exogenous molecules (e.g., drugs) to nuclear receptors, resulting in dimerization with another nuclear receptor (mostly RXR), and subsequent binding of the complex to specific DNA sequences (via receptor-specific DNA-binding domains), which finally initiates the process of gene transcription. As several nuclear receptors are involved in the regulation of DMEs and drug transporters, activation of these receptors results in markedly increased expression and function of the respective DMEs and drug transporters [13]. Thus, exposure to nuclear receptor ligands such as rifampicin, St. John's wort or carbamazepine, together with DMEs and transporter substrates, can result in unwanted drug–drug interactions (DDIs) due to diminished systemic or tissue drug exposure, which may threaten the intended therapeutic effect [14,15]. Associated to this, the nuclear receptors, pregnane X receptor (PXR) and constitutive androstane receptor (CAR), were especially reported to be of high clinical relevance [11,12]. The activation of different nuclear receptors is associated with a typical induction pattern; i.e., PXR is known to regulate, for example, cytochrome P450 (CYP) 3A4, CYP2C9, uridine diphosphate glucuronosyltransferase 1A1 (UGT1A1), P-glycoprotein (P-gp) and multidrug resistance-associated protein 2 (MRP2), whereas CAR controls the expression of CYP2B6, CYP2C19, breast cancer resistance protein (BCRP) and MRP4 [11,16]. There seems to be also a considerable regulatory overlap between PXR and CAR. However, our current knowledge is rather limited because the majority of the regulatory information was derived from various *in vitro* models [12].

A few studies demonstrating direct *in vivo* evidence for the regulation of human DMEs and drug transporters have been conducted in human intestinal tissue after oral administration of PXR ligands [17,18]. In these studies, nuclear receptor-mediated upregulation of intestinal drug transporters (e.g., P-gp, MRP2) or DMEs (e.g., CYP3A4, UGT1A1) resulted in markedly diminished plasma exposure of co-administered victim drugs. In addition to these rather experimental studies in healthy volunteers, this mechanism was also shown to cause dramatic interaction scenarios in clinical practice [14,19,20]. Until now, only very little was known about the expression pattern of nuclear receptors in different tissues, which makes it difficult to estimate an extent of potential DDIs in the dependence on the used administration route of perpetrator and victim drugs [21]. The same is true for the distinct tissue concentrations of ligands required for a pronounced activation of the nuclear receptors. The available expression data indicate substantial expression differences between tissues, which may translate to differences in induction potential of prototypical inducers in different organs, related to their binding affinity to different nuclear receptors and the respective expression profile of nuclear receptors [18,22]. However, available expression data are exclusively based on mRNA data, which may not necessarily correlate to the encoded proteins, i.e., the nuclear receptors [21]. Thus, it was the aim of this study to characterize the gene expression and protein abundance of clinically relevant nuclear receptors in human intestine and liver.

2. Results and Discussion

There is evidence from gene expression studies that there are tissue-specific nuclear receptor expression profiles, suggesting profound differences in the induction potential of nuclear receptor ligands in different organs [21–23]. In addition, several clinical DDI studies indicate that the extent of interaction, i.e., reduction of systemic drug exposure of

victim drugs, is markedly affected by the route of administration of the perpetrator drug (e.g., rifampicin). In this regard, the oral administration of nuclear receptor ligands and the victim drug (substrates of CYP3A4 and/or P-gp) caused strikingly lower plasma levels (i.e., higher degree of interaction) compared to the intravenous administration of the victim drug [18,24–28]. Finally, some nuclear receptor ligands such as efavirenz were shown to induce only hepatic, but not intestinal, DMEs and drug transporters [29,30]. Therefore, we investigated in this study the gene expression and protein abundance of the clinically relevant nuclear receptors CAR, FXR, GR, HNF4 α , PXR and SHP. A targeted proteomic method for absolute protein quantification was developed in order to provide reliable protein abundance data.

2.1. Assay Characteristics

The protein specificity of all predicted and finally used peptides was confirmed during method development by protein BLAST analysis. In order to develop a reliable quantification method, peptides with unfavorable features such as oxidative instability (due to cysteine, methionine, tryptophan or *N*-terminal glutamine), genetic polymorphisms and post-translational modifications were excluded. Finally, all used peptides and mass transitions applied for protein quantification were confirmed by wet-lab experiments.

For all peptides, stable isotope-labeled internal standards were used with a distinct mass difference of 8–10 Da (Table 1). All peptides were measured in the positive ionization mode using electrospray ionization, resulting, in each case, in doubly charged molecule ions. The observed *m/z* ratios of these ions were used as the Q1 filter setting. For all identified parent ions, manual product ion scans were performed to identify the three fragment ions with the highest intensity. After selecting the respective Q3 *m/z* ratios, the individual *m/z* transitions were manually optimized with respect to collision energy and declustering potential. The optimized mass spectrometer parameters are given in Table 1.

To the best of our knowledge, this is the first report on the LC-MS/MS-based quantification of nuclear receptors. Thus, our experimental details cannot be compared with other methods. As a potential limitation, our method used, in each case, only one proteospecific peptide for protein quantification (due to the high costs of quantitative peptides), which may bear the risk of obtaining misleading results due to different isoforms, incomplete protein digestion or truncated forms of the protein. However, the used peptides were also successfully identified by the Institute for Systems Biology (Seattle, WA, USA) as reported in their online repositories, i.e., the PeptideAtlas (<http://www.peptideatlas.org>, accessed on 20 June 2022) and the SRMATlas (<http://www.mrmatlas.org>, accessed on 20 June 2022).

To avoid chromatographic interferences of the individual peptides with each other and the complex biological matrix, the chromatography was performed using a 60-min gradient elution method. The peptides were chromatographically separated from each other and all included mass transitions for each peptide, where the internal standard peptides demonstrated co-elution (Figure 1). To assure optimal mass spectrometric detection and quantification, the dwell time was dynamically adapted to a fixed cycle time of 0.6 s using the scheduled MRM algorithm by the Analyst software that monitored altogether 30 *m/z* transitions (Table 1).

Table 1. Overview of used proteospecific peptides and mass spectrometry parameters for their detection in the positive multiple reaction monitoring mode (MRM). Dwell time was automatically optimized (scheduled MRM algorithm). CE, collision energy; DP, declustering potential; m/z , mass-to-charge ratio.

Analyte	Peptide	Mass Transitions (m/z)		CE [V]	DP [V]
		Q ₁	Q ₃		
AhR	NDFSGEVDFR	593.4	322.2	39	150
			809.5	27	150
			722.6	24	150
AhR *	NDFSGEVDF[R(13C6;15N4)]	598.2	332.2	39	150
			819.4	27	150
			732.4	24	150
CAR	AQQTPVQLSK	550.2	671.3	27	120
			900.5	23	120
			429.4	23	120
CAR *	AQQTPVQLS[K(13C6;15N2)]	554.1	679.4	27	120
			908.5	23	120
			429.1	23	120
FXR	LQEPLLDVLQK	648.5	371.3	27	190
			925.6	27	190
			388.4	39	190
FXR *	LQEPLLDVLQ[K(13C6;15N2)]	652.0	371.2	27	190
			933.6	27	190
			396.3	39	190
GR	LLEESIANLNR	635.9	787.4	31	170
			356.4	28	170
			485.2	26	170
GR *	LLEESIANLN[R(13C6;15N4)]	641.0	797.4	31	170
			356.2	28	170
			485.2	26	170
HNF4 α	DVLLLGNDYIVPR	743.6	554.4	25	180
			647.5	45	180
			876.4	36	180
HNF4 α *	DVLLLGNDYIVP[R(13C6;15N4)]	748.6	554.4	25	180
			657.3	45	180
			886.5	36	180
PXR	VVDQLQEQAIFLTK	816.2	361.2	33	170
			474.4	35	170
			1077.4	36	170
PXR *	VVDQLQEQAIFLTK[K(13C6;15N2)]	820.3	369.2	33	170
			482.4	35	170
			1085.4	36	170
SHP	VLLTASTLK	472.8	620.4	20	130
			326.1	17	130
			448.2	32	130
SHP *	VLLTASTL[K(13C6;15N2)]	476.7	628.3	20	130
			326.2	17	130
			456.2	32	130

(*) Stable isotope-labeled peptide.

2.2. Method Validation

Our method validation was mostly based on the current bioanalytical method validation guidelines from the FDA and EMA [31]. In this regard, we validated the method for specificity, linearity, within-day and between-day accuracy and precision, as well as for matrix effects and stability. As a classical blank matrix was not available (nuclear receptors are present in nearly all cells), digested HSA (2 mg/mL) was used as the blank matrix for

all validation procedures. Although this matrix is far off from being as complex as digested human tissue, it may mimic at least one digested protein of human origin and have the same total protein concentration (2 mg/mL) as used in our tryptic digested samples.

The developed method was found to be selective for the determination of all pro-teospecific peptides in digested has, as well as those in digested human intestinal and liver tissue, as concluded from the absence of analytical signals in different blank matrix samples and chromatographic or mass spectrometric interferences between the analytes, the internal standards and the biological matrix (Figure 1).

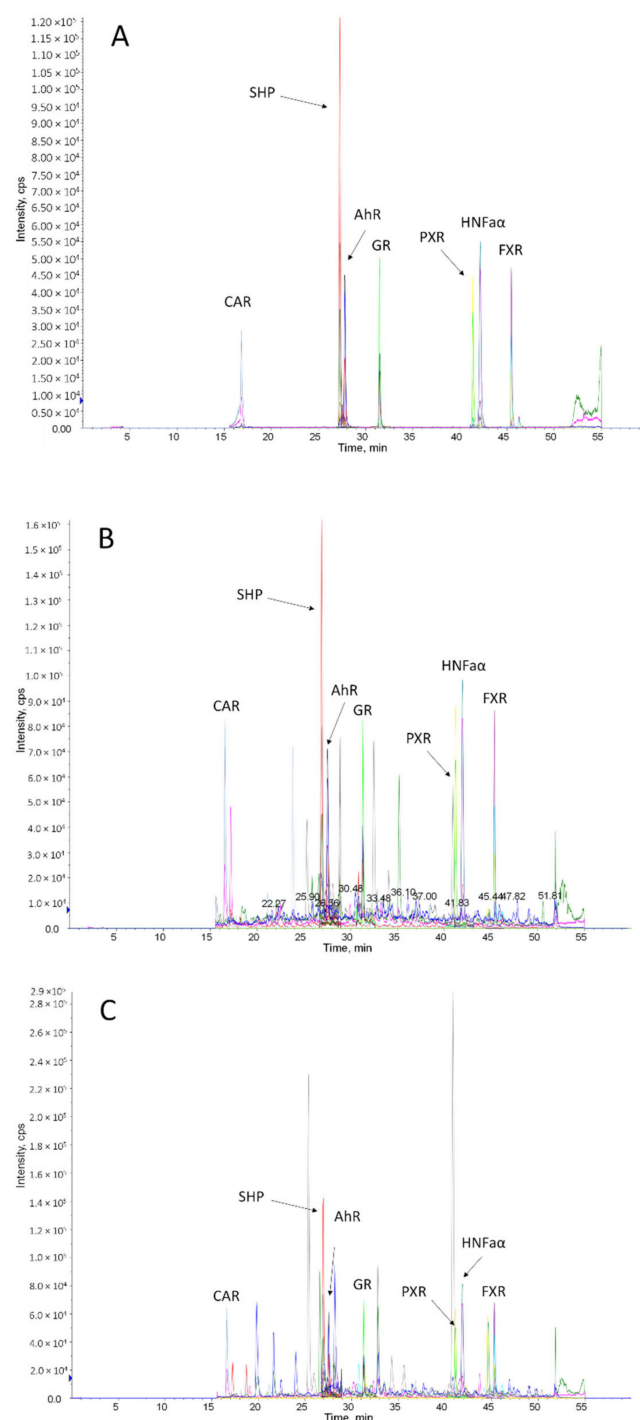


Figure 1. Total ion chromatogram of a digested HSA (validation matrix) sample (A), a human jejunum (B) and a human liver sample (C) spiked with internal standard peptides for all investigated nuclear receptors (each 5 nmol/L). Annotations indicate the respective nuclear receptor peptide.

For all peptides, a linear correlation between peptide concentration and the analytical signal over the entire analytical range (0.1–50 nmol/L) was observed. The resulting correlation coefficients (*r*) for all calibration curves and peptides ranged between 0.9976–0.9999 (in each case *N* = 6) (Table 2).

The lower limit of quantification (LLOQ) of our quantitative assays was 0.1 nmol/L (1.5 fmol on column) for all investigated nuclear receptors. Here, the analytical signal was at least >5 times above that of the respective blank matrix samples. The sensitivity of our method is comparable to other targeted LC-MS/MS methods for DMEs and drug transporters [32–36]. Within-day (intra-day) as well as between-day (inter-day) accuracy and precision in the validation matrix were within the range of $\pm 15\%$ of the nominal concentrations and <15% for the respective coefficients of variation (CV) of the mean values for all peptides (Table 2).

Table 2. Validation data of within-day and between-day accuracy and precision, as well as correlation coefficients, of the respective calibration curves for the simultaneous quantification of the nuclear receptor peptides. Validation range was 0.1–50 nmol/L and data were calculated from, in each case, six quality control samples sets (0.5, 5 and 50 nmol/L) measured on one day (within-day data) or on different days (between-day data). Accuracy is given as relative error of nominal concentrations and precision as coefficients of variation of mean concentrations. AhR, aryl hydrocarbon receptor; CAR, constitutive androstane receptor; FXR, farnesoid X receptor; GR, glucocorticoid receptor; HNF4 α , hepatocyte nuclear factor 4 α ; PXR, pregnane X receptor; SHP, small heterodimer partner.

	Accuracy [%]		Precision [%]		Correlation Coefficient <i>r</i>
	Within-Day	Between-Day	Within-Day	Between-Day	
AhR	−1.7–13.2	−1.2–0.3	2.3–4.5	3.2–9.3	0.9984–0.9999
CAR	0.5–12.0	−2.3–(−0.8)	4.4–7.6	2.7–7.6	0.9976–0.9999
FXR	−1.8–6.3	−3.0–2.3	0.9–3.5	3.3–5.4	0.9992–0.9999
GR	−0.2–11.5	−2.1–3.6	1.4–4.1	3.0–5.8	0.9992–0.9999
HNF4 α	−2.1–10.2	−2.3–3.2	0.8–3.7	3.8–7.3	0.9995–0.9998
PXR	−3.5–7.7	−2.1–6.5	2.1–6.8	4.3–5.5	0.9988–0.9999
SHP	−0.9–0.7	−2.5–1.2	0.9–5.9	3.7–5.9	0.9992–0.9998

All peptides demonstrated sufficient stability ($\pm 15\%$ of the initial concentrations at low, medium and high concentrations) during storage in the cooled autosampler rack for 24 h and during up to three freeze–thaw cycles (Table 3).

Table 3. Mean data for matrix effects and stability as assessed by analyzing, in each case, six quality control sample sets. AhR, aryl hydrocarbon receptor; CAR, constitutive androstane receptor; FXR, farnesoid X receptor; GR, glucocorticoid receptor; HNF4 α , hepatocyte nuclear factor 4 α ; PXR, pregnane X receptor; SHP, small heterodimer partner.

	Matrix Effect [%]	Rack Stability 24 h @ 4 °C [%]	Freeze–Thaw Stability [%]		
			1st Cycle	2nd Cycle	3rd Cycle
AhR	95.9–102.0	95.6–100.7	85.8–105.8	91.5–100.2	90.9–97.4
CAR	100.3–101.8	93.6–98.3	90.6–105.1	90.3–103.2	86.9–89.4
FXR	96.3–113.8	100.1–104.7	88.9–104.4	93.2–99.9	90.8–100.1
GR	91.2–101.5	97.1–102.9	90.8–106.6	92.9–102.1	95.1–99.5
HNF4 α	88.5–95.8	98.2–104.3	87.6–104.9	91.7–100.7	89.3–99.1
PXR	82.8–91.3	99.8–104.6	86.6–98.5	91.0–95.8	93.3–93.6
SHP	97.2–99.3	93.4–100.8	92.3–104.8	93.7–99.5	93.3–98.5

The classical investigation of matrix effects could not be achieved in our study due to the lack of availability of a blank, free-of-endogenous nuclear receptor matrix for human tissue lysates. However, our validation matrix was shown to have no impact on the accuracy of our quantitative method compared to the quality control samples without any matrix (Table 3). This is most likely due to our long gradient elution time combined with

high resolution chromatography and the use of stable isotope-labeled internal standard peptides which compensate for ion suppression or enhancement effects as caused by the biological matrix.

2.3. Application of the Method

The developed and validated method was applied to quantify the protein amounts of clinically relevant nuclear receptors in human tissue samples. Here, human liver, jejunum, ileum and colon samples from, in each case, eight donors have been analyzed (inter-subject comparison). In parallel, the respective mRNA expression was studied.

As shown in Figure 2, the expression pattern of nuclear receptors differed markedly within the liver and jejunum, which is the most relevant intestinal section for intestinal drug absorption.

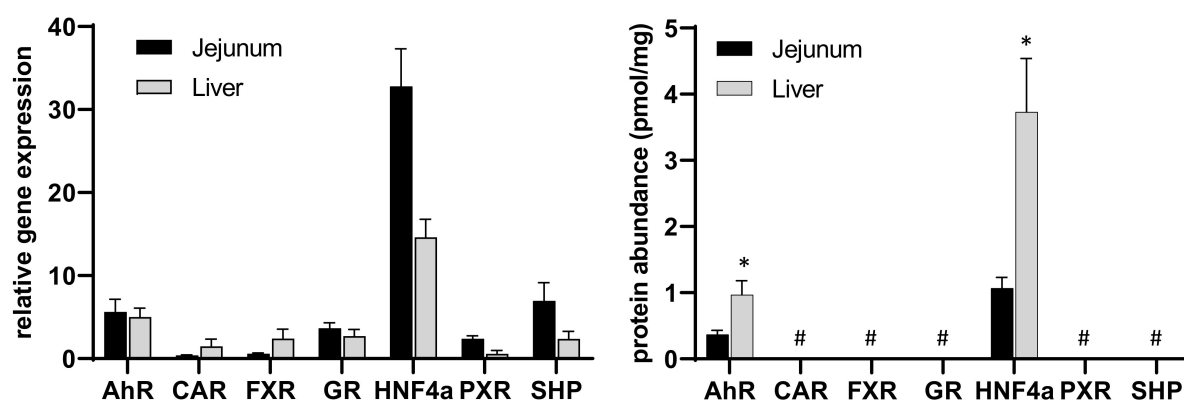


Figure 2. Data on gene expression (left) and protein abundance (right) of the investigated nuclear receptors in human jejunum and liver where, in each case, N = 8 different donors (inter-subject comparison). Data given as mean \pm SD. *: $p \leq 0.05$ compared to jejunum, #: < lower limit of quantification.

Associated to this, gene expression data demonstrated a significantly higher expression of PXR, HNF4 α and SHP in the jejunum than in the liver, whereas CAR and FXR were found to have a significantly higher expression in human livers (Figure 2, left panel). With the exception of AhR and HNF4 α , all other nuclear receptor abundances were below the lower limit of quantification (Figure 2, right panel). In contrast to the gene expression data, the protein abundance of HNF4 α and AhR were significantly higher in the liver than in the jejunum, which underlines the known fact that gene expression data do not necessarily correlate well with the encoded protein level. Interestingly, HNF4 α and AhR were also shown to be highly expressed on the mRNA level so that the lack of protein detection for the other investigated nuclear receptors fits to the lower transcriptional processing of the respective genes. The low or undetectable protein abundance may be explained by the mode of action of nuclear (hormone) receptors, which can be activated by very low ligand concentrations and act in a repetitive manner [11,15,16]. Thus, classical dose-response relationships may not apply for nuclear receptors.

The reason that we were able to quantify in a robust manner only two of our seven proteins of interest, in human intestine and liver, is most likely due to the limited sensitivity of the mass spectrometer. Although we used a high-sensitivity instrument (QTRAP 5500), this was not sensitive enough to quantify low-abundant nuclear hormone receptors in a complex biological matrix. In line with our observation, we are not aware of any study showing protein data of nuclear receptors independent from the analytical method (Western blotting, global or targeted proteomics) in human tissue. Another reason might be related to the chosen peptides, because different peptides may result in slightly different sensitivities to the method. However, due to economic reasons, we were not able to analyze multiple peptides for each nuclear receptor. In our selection process, we carefully chose the most promising peptides, which were also reported to be observable in proteomic databases (e.g., PeptideAtlas).

Based on our current knowledge, PXR seems to play an important role in the clinically relevant regulation of human intestinal drug transporters, whereas CAR and, to a lesser extent, PXR appear to be more relevant for DDIs in the liver [11,12,16]. Hence, the route of drug administration (i.e., oral vs. intravenous) can have a profound impact on the extent of DDIs for drugs undergoing significant NR-mediated regulation (e.g., CYP3A4 metabolism and/or P-gp efflux [18,24–28], 2020). This conclusion from clinical studies is confirmed by our expression data, at least on an mRNA level (i.e., intestinal PXR > hepatic PXR; intestinal PXR >> intestinal CAR) [21–23].

In line with this conclusion, and also as seen in the human intestine, PXR has a strikingly higher expression than CAR (Figure 3, left panel), which was also confirmed in a previous analysis [23]. The rank order of mRNA expression in the different intestinal fractions is HNF4 α > AhR > SHP > GR > PXR > FXR > CAR. Of the mentioned nuclear receptors, PXR and CAR especially (and partly FXR) are of great clinical importance as they regulate several highly important DMEs and drug transporters [11,12,15]. Comparable to the liver, only HNF4 α and AhR could be detected on a protein level in all intestinal sections (Figure 3, left panel) (HNF4 α > AhR).

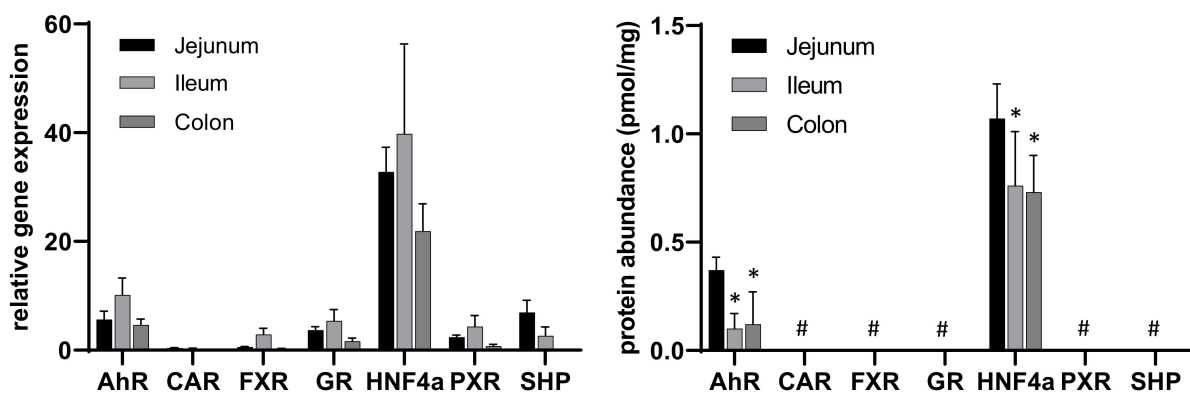


Figure 3. Data on gene expression (left) and protein abundance (right) of the investigated nuclear receptors along the human intestine (jejunum, ileum, colon) as measured, in each case, in N = 8 different donors (inter-subject comparison). Data given as mean \pm SD. *: $p \leq 0.05$ compared to jejunum, #: < lower limit of quantification.

Considering the outstanding role of PXR and CAR in the regulation of DMEs and drug transporters, we generated stably transfected MDCKII cells overexpressing PXR and CAR to, finally, check the functionality of our method in biological samples. Both proteins could be successfully identified in MDCKII-CAR and MDCKII-PXR cells, which confirms the feasibility of PXR and CAR detection using our method (Figure 4).

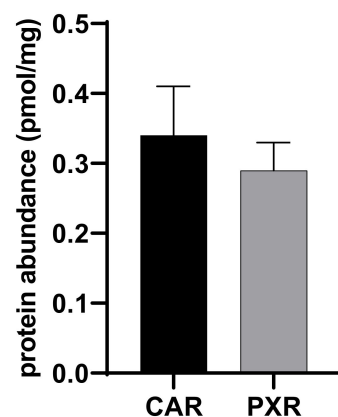


Figure 4. Protein abundance of CAR and PXR as measured in stably transfected MDCK-CAR and MDCKII-PXR cells. Data given as mean \pm SD.

3. Materials and Methods

3.1. Reagents and Consumables

LC-MS-grade acetonitrile (ACN) with 0.1% formic acid (FA) and LC-MS-grade water with 0.1% FA were purchased from Carl Roth (Karlsruhe, Germany). Deionized water (conductance: $\leq 0.055 \mu\text{S}/\text{cm}$, pH 5.0–6.0) was generated with the Astacus system (membrapure, Hennigsdorf, Germany). Ethylenediaminetetraacetic acid (EDTA), human serum albumin (HSA), iodoacetamide (IAA), phosphate-buffered saline (PBS) and formic acid (FA) were purchased from Sigma-Aldrich (Steinheim, Germany). Ammonium bicarbonate (ABC), dithiothreitol (DTT), sodium dodecyl sulfate (SDS), sucrose and Tris-(hydroxymethyl)-aminomethane hydrochloride (Tris-HCl) were obtained from Carl Roth (Karlsruhe, Germany). The BCA kit to measure unspecific protein concentrations was from Thermo Fisher Scientific (Schwerte, Germany). Protease inhibitor cocktail III was ordered from Merck (Darmstadt, Germany). Custom-made peptide standards and the corresponding stable isotope-labeled internal standards were synthesized by JPT Peptide Technologies (Berlin, Germany) or Thermo Fisher Scientific. All peptides were of analytical grade ($>95\%$), which was verified by exact quantification via amino acid analysis and certified by the respective manufacturers. Sequencing Grade Modified Trypsin and ProteaseMAXTM surfactant were purchased from Promega (Mannheim, Germany). Proteomic sample preparation was conducted in Protein LoBind Tubes (Eppendorf, Hamburg, Germany).

3.2. Intestinal Tissue

Intestinal tissue from the jejunum, ileum and colon, as well as liver tissue, was collected from, in each case, 8 different patients undergoing surgery for different medical reasons. Supplementary Table S1 gives an overview about the patient characteristics. All tissue samples were free of macroscopic signs of inflammation or necrosis as assessed by an experienced visceral surgeon. The collected samples were immediately snap frozen in liquid nitrogen and grinded in a stainless steel mortar to be finally stored at $-80 \text{ }^\circ\text{C}$ until further analysis. The study was approved by the local Ethics Committee of the University of Medicine, Greifswald.

3.3. Gene Expression Analysis

For isolation of total RNA, approximately 30 mg of each frozen tissue powder was used for extraction with the NucleoSpin[®] miRNA Kit (Macherey-Nagel, Düren, Germany). Quantity and purity of isolated RNA was determined by using a NanoDrop ND-1000 spectrophotometer (NanoDrop Technologies, Wilmington, DE, USA).

Quality and integrity of RNA samples was assured using the Agilent[®] 2100 Bioanalyzer[®] (Agilent Technologies, Waldbronn, Germany) and was stated as an RNA integrity number (RIN) ranging from 6.6 to 9.0 (Supplementary Table S1). cDNA was prepared from 2 μg of total RNA using the High-Capacity cDNA Reverse Transcription Kit (Applied Biosystems, Darmstadt, Germany) according to the manufacturer's instructions. The gene expression levels of AhR, NR1I3 (CAR), NR1H4 (FXR), NR3C1 (GR), HNF4A (HNF4 α), NR1I2 (PXR) and NR0B2 (SHP) were examined by quantitative real-time PCR analysis using TaqMan[®] Gene Expression Assays (Applied Biosystems) following the instructions of the manufacturer on MicroAmp[®] Optical 96-Well Reaction Plates. Table 4 provides an overview about the used predeveloped gene expression assays. Each sample was analyzed with a 7900HT Sequence Detection System (Applied Biosystems) simultaneously in two technical replicates; mean Ct (cycles of threshold) values were used for further analysis. Gene expression was calculated as the relative expression to the endogenous reference genes 18S rRNA, GAPDH (glyceraldehyde 3-phosphate dehydrogenase) and PGK1 (phosphoglycerate kinase 1) ($2^{-\Delta\text{Ct}}$ values).

Table 4. Overview of used gene expression assays and proteospecific peptides.

Protein (Alias)	Gene Name	TaqMan® Assay I.D.	Peptide
AhR (BHLHE76)	AhR	Hs00169233_m1	NDFSGEVDFR
CAR	NR1I3	Hs00901571_m1	AQQTPVQLSK
FXR (BAR)	NR1H4	Hs01026590_m1	LQEPLLDVQLK
GR (GCR)	NR3C1	Hs00353740_m1	LLEESIANLNR
HNF4α (HNF4, NR2A1)	HNF4A	Hs00230853_m1	DVLLLGNDYIVPR
PXR (BXR)	NR1I2	Hs01114267_m1	VVDQLQEQAIFLTK
SHP (SHP1)	NR0B2	Hs00222677_m1	VLLTASTLK
Reference gene(s)			
18S	18S	Hs99999901_s1	-
GAPDH	GAPDH	Hs02758991_g1	-
PGK1	PGK1	Hs00943178_g1	-

AhR, aryl hydrocarbon receptor; CAR, constitutive androstane receptor; FXR, farnesoid x receptor; GAPDH, glyceraldehyde 3-phosphate dehydrogenase; GR, glucocorticoid receptor; HNF4α, hepatocyte nuclear factor 4 alpha; LXR, liver x receptor; PGK1, phosphoglycerate kinase 1; PXR, pregnane x receptor; SHP, small heterodimer partner.

Isolation of the nuclear fraction: Approximately 300 mg of frozen tissue powder was placed in prechilled Douncers and homogenized with 1 mL of lysis buffer (0.2% SDS, 5 mmol/L EDTA) containing 5 µg/mL of protease inhibitor solution. Homogenates were placed in Protein LoBind tubes on a vertical shaker for 30 min at 40 rpm and 4 °C, and afterwards, centrifuged for 5 min at 600 × g and 4 °C. Subsequently, the supernatant (cytosolic fraction) was discarded and the resulting pellet containing membrane-bound proteins and the nuclear fraction was suspended in 300 µL of resuspension buffer (0.25 mol/L sucrose, 1 mmol/L EDTA in distilled water at pH 7.4) containing 5 µg/mL of protease inhibitor solution and stored at 80 °C until analysis.

3.4. Protein Quantification by LC-MS/MS Analysis

3.4.1. Identification of Proteotypic Peptides

Proteospecific peptides for CAR, FXR, GR, HNF4α, PXR and SHP were identified by using a combined approach of in silico predictions and experimental data as described elsewhere [37]. In brief, the respective protein sequences (database: UniProtKB/Swiss-Prot, <https://legacy.uniprot.org/uniprot/>, accessed on 20 June 2022) were subjected to an in silico trypsin digestion (https://web.expasy.org/peptide_mass/, accessed on 20 June 2022), allowing a sequence length of 7–20 amino acids and excluding any missed cleavages sites. Furthermore, peptides with the following features were excluded: 1. cysteine, methionine or tryptophan (prone to oxidation), 2. amino-terminal glutamine (to avoid in-source cyclization to pyroglutamate), 3. non-synonymous genetic polymorphisms (allele frequency >1%), 4. experimentally proven post-translational modifications (altered mass), and 5. repeated sequences of arginine and lysine (risk of missed cleavage by trypsin). Finally, the protein specificity of each observed peptide was assured by an NCBI protein BLAST search against the UniProtKB/Swiss-Prot database (<https://blast.ncbi.nlm.nih.gov/>, accessed on 20 June 2022).

The identified sequences were ordered as crude peptides (SpikeTides™, JPT Peptide Technologies, Berlin, Germany) to set up quantitative mass spectrometry methods and to identify the best peptides in terms of sensitivity and chromatographic properties. After identification of the best observable peptide for each protein, these peptides were ordered in unlabeled and stable isotope-labeled forms that were high-analytical-grade quality from Thermo Fisher Scientific. The appropriate mass transitions, collision energies and declustering potentials for each proteospecific peptide were identified and optimized by manual infusion to the tandem mass spectrometer QTRAP 5500 (Sciex, Darmstadt, Germany). For each peptide and the respective internal standard peptide, three mass transitions of highest intensity were selected (Table 4).

3.4.2. Sample Preparation and Digestion Procedure

The protein concentration of the isolated nuclear/membrane fraction from intestinal and hepatic tissue was determined with the BCA protein assay. The samples were adjusted to a protein concentration of 2 mg/mL with PBS. A total of 100 μ L of each sample was mixed with 10 μ L of DDT (200 mmol/L), 40 μ L of ABC (50 mmol/L, pH 7.8) and 10 μ L of ProteaseMax™ surfactant trypsin enhancer and incubated at 60 °C for 20 min (denaturation). After cooling down, 10 μ L of IAA (400 mmol/L) was added and the samples were incubated for 15 min at 37 °C in the dark (alkylation). For protein digestion, trypsin was added with a trypsin/protein ratio of 1:40 and samples were incubated at 37 °C for 16 h. The digestion was stopped by adding FA (20 μ L, 10% *v/v*). Finally, the samples were centrifuged for 10 min at 16,000 $\times g$ and 4 °C, stable isotope-labeled internal standards were added to the clear supernatant (final concentration: 5 nmol/L) and samples were transferred into HPLC vials prior to LC-MS/MS analysis. All sample preparation and digestion steps were performed by using Protein LoBind Tubes (Eppendorf) to avoid sample loss.

3.4.3. LC-MS/MS Analysis

LC-MS/MS analyses were conducted on a 5500 QTRAP triple quadrupole mass spectrometer (Sciex) coupled to an Agilent 1260 Infinity Binary HPLC system (Agilent Technologies, Waldbronn, Germany) controlled by the Analyst 1.6.3 software (Sciex). Chromatographic separation was performed on a Kinetex® 2.6 μ m C18 100 Å core-shell column (100 \times 2.1 mm, Phenomenex, Aschaffenburg, Germany) with gradient elution using acetonitrile containing 0.1% formic acid (solvent A) and water containing 0.1% formic acid (solvent B). The flow rate of the mobile phase was 200 μ L/min and injection volume was 15 μ L. The gradient applied was as follows: 2% solvent A for 5 min, followed by a linear gradient from 2–25% solvent A over 35 min, then increase solvent A to 50% within 13 min, switching to 60% for 3 min before coming back to 2% solvent A within 9 min. Column oven temperature was set to 50 °C, whereas the autosampler temperature was adjusted to 4 °C. The mass spectrometer was equipped with an electrospray ionization (ESI) Turbo V™ Ion Source interface operated in positive mode using the following gas parameters: source temperature, 500 °C; ion spray voltage, 5500 V; curtain gas, 50 psi; ion source gas 1, 50 psi; ion source gas 2, 50 psi and high collision activated gas (all nitrogen). Mass spectrometry parameters such as declustering potential and collision energy were manually optimized for each single peptide, as mentioned above, and are summarized in Table 2.

3.4.4. Preparation of Calibration Curves, Method Validation and Sample Measurements

For preparation of calibration curves and quality control (QC) samples, digested human serum albumin (HSA, 2 mg/mL) was used as the blank matrix and spiked with increasing amounts of each peptide to generate the following target concentrations: 0.1, 0.25, 0.5, 1.0, 2.5, 5, 10, 25 and 50 nmol/L (1.5–750 fmol on column) for calibration values and 0.5, 5 and 50 nmol/L for quality control (QC) samples. The stable isotope-labeled internal standard peptides were added to all samples (final concentration: 5 nmol/L).

Selectivity of the method was confirmed by analyzing six different batches of digested HSA; here, we compared the respective blank matrix samples with matrix containing either internal standard peptides, analytical peptides or both. Linearity was investigated by correlating the peak area ratios (analyte over the internal standard) with the spiked peptide concentrations and calculating calibration curves. Between-day (inter-day) accuracy and precision were evaluated by measuring six QC sample sets that were prepared and measured on different days. Within-day (intra-day) accuracy and precision were assessed by analyzing six QC sample sets prepared and measured on the same day. Accuracy was determined by calculating the relative error of the measured mean value compared to the nominal concentration, whereas precision represents the coefficient of variation of the measured values.

Stability was investigated by using, in each case, six QC sample sets. Post-preparative (rack) stability was assessed by measuring the samples immediately after preparation and

after storing them in the cooled autosampler (4 °C) for 24 h. Freeze-thaw stability was studied by measuring the samples before and after, for up to three freeze-thaw cycles (storage at −80 °C). Stability was assumed if the peptide content after the given storage condition was within the acceptable range of accuracy, i.e., ±15%. Matrix effects were investigated by comparing six quality control sample sets prepared in the blank matrix (HSA, 2 mg/mL), as well as in diluted stock solutions without any matrix.

On each day of analysis, calibration curves and QC sample sets were freshly prepared as mentioned above. QC samples represented at least 5–10% of all analytical samples and were measured during the entire analytical run. The criterion of acceptance for an analytical run was if at least 4 of 6 of all measured QC samples were within a relative error range of ±15% at the LLOQ of the nominal values, as suggested by the current FDA/EMA guidelines on bioanalytical method validation.

3.5. Generation of MDCKII-CAR and -PXR

MDCKII cells were purchased from the European Collection of Cell Cultures (Salisbury, United Kingdom) and were grown in Dulbecco's Modified Eagle Medium, supplemented with 10% fetal bovine serum, 4 mM/L glutamine, 100 units/ml penicillin, and 100 µg/ml streptomycin (PAA, Coelbe, Germany) at 37 °C, 95% humidity, and 5% CO₂.

The coding sequence of the full-length CAR (GenBank accession no. NM_001077482.3) and PXR (GenBank accession no. NM_003889.4) cloned into the retroviral expression vector pQCXIN (Takara Bio Europe/Clontech, Saint-Germain-en-Laye, France) were purchased from Eurofins, Ebersberg, Germany. MDCKII cells were infected according to the instructions of the manufacturer and selected by 500 µg/ml of neomycin.

3.6. Statistical Analysis

For each surrogate peptide and the respective internal standard, three mass transitions were monitored. All chromatograms were evaluated with the MultiQuant™ 3.0.2 software (Sciex) using the internal standard method and peak area ratios for calculation of absolute protein amounts (linear regression, 1/x weighting). Final peptide concentrations represent mean values of three transitions for each peptide. The resulting protein amount (pmol/mg) was calculated by normalizing the specific nuclear receptor concentration (nmol/L) to the individually observed protein concentration (BCA assay, mg/mL).

All mRNA and protein expression data are presented as mean ± standard deviation. Statistical analysis was performed using the GraphPad Prism 9 Software (GraphPad Software, Inc., San Diego, CA, USA). Statistical significance of differences in mRNA and protein expression between the different intestinal sections and between liver and jejunum were evaluated using the non-parametric Mann-Whitney U test. P-values less than 0.05 were considered as significant.

4. Conclusions

We developed an LC-MS/MS method for the simultaneous quantification of the nuclear receptors AhR, CAR, FXR, GR, HNF4α, PXR and SHP. The developed and validated method fulfilled the requirements of current bioanalytical guidelines with respect to specificity, accuracy, precision, stability and matrix effects. The quantitative assay was successfully applied to measure the protein abundance in human tissue samples. However, due to the very low protein amounts, only HNF4α and AhR could be detected in *in vivo* samples, whereas PXR and CAR could be quantified in transfected and overexpressing cell lines. Despite the challenges of detectability of nuclear receptors, the information about their tissue distribution can prove to be useful for the understanding and estimation of unwanted DDIs.

Supplementary Materials: The following supporting information can be downloaded at: <https://www.mdpi.com/article/10.3390/molecules27144629/s1>, Table S1: Overview of patient and sample characteristics.

Author Contributions: Conceptualization, S.O. and M.D.; methodology, C.W., D.B., A.R. and L.G.; validation, C.W., D.B., A.R. and L.G.; investigation, S.O.; data curation, C.W., D.B., A.R., L.G. and M.K.; writing—original draft preparation, S.O. and M.D.; writing—review and editing, C.W., M.K., M.D. and S.O.; visualization, S.O. All authors have read and agreed to the published version of the manuscript.

Funding: The research was supported by the grant 03IPT612A (InnoProfile-Transfer) of the German Federal Ministry for Education and Research. C.W. thanks the Evangelisches Studienwerk Villigst e. V. for financial support through a doctoral scholarship.

Institutional Review Board Statement: The use of human tissue was approved by the Ethics Committee of the University Medicine Greifswald, Germany (ethic votes BB122/12, BB 122/12a and BB 122/12b).

Informed Consent Statement: Not applicable.

Conflicts of Interest: The authors declare that they have no conflict of interest.

Sample Availability: Samples of the compounds are not available from the authors.

References

1. Giacomini, K.M.; Huang, S.-M.; Tweedie, D.J.; Benet, L.Z.; Brouwer, K.L.R.; Chu, X.; Dahlin, A.; Evers, R.; Fischer, V.; Hillgren, K.M.; et al. Membrane transporters in drug development. *Nat. Rev. Drug Discov.* **2010**, *9*, 215–236. [[CrossRef](#)] [[PubMed](#)]
2. Zamek-Gliszczyński, M.J.; Taub, M.E.; Chothe, P.P.; Chu, X.; Giacomini, K.M.; Kim, R.B.; Ray, A.S.; Stocker, S.L.; Unadkat, J.D.; Wittwer, M.B.; et al. Transporters in Drug Development: 2018 ITC Recommendations for Transporters of Emerging Clinical Importance. *Clin. Pharmacol. Ther.* **2018**, *104*, 890–899. [[CrossRef](#)] [[PubMed](#)]
3. Zanger, U.M.; Schwab, M. Cytochrome P450 enzymes in drug metabolism: Regulation of gene expression, enzyme activities, and impact of genetic variation. *Pharmacol. Ther.* **2013**, *138*, 103–141. [[CrossRef](#)] [[PubMed](#)]
4. Yee, S.W.; Brackman, D.J.; Ennis, E.A.; Sugiyama, Y.; Kamdem, L.K.; Blanchard, R.; Galetin, A.; Zhang, L.; Giacomini, K.M. Influence of Transporter Polymorphisms on Drug Disposition and Response: A Perspective from the International Transporter Consortium. *Clin. Pharmacol. Ther.* **2018**, *104*, 803–817. [[CrossRef](#)]
5. Hirota, T.; Tanaka, T.; Takesue, H.; Ieiri, I. Epigenetic regulation of drug transporter expression in human tissues. *Expert Opin. Drug Metab. Toxicol.* **2017**, *13*, 19–30. [[CrossRef](#)]
6. Peng, L.; Zhong, X. Epigenetic regulation of drug metabolism and transport. *Acta Pharm. Sin. B* **2015**, *5*, 106–112. [[CrossRef](#)]
7. Zanger, U.M.; Klein, K.; Thomas, M.; Rieger, J.K.; Tremmel, R.; Kandel, B.A.; Klein, M.; Magdy, T. Genetics, epigenetics, and regulation of drug-metabolizing cytochrome p450 enzymes. *Clin. Pharmacol. Ther.* **2014**, *95*, 258–261. [[CrossRef](#)]
8. Czuba, L.C.; Hillgren, K.M.; Swaan, P.W. Post-translational modifications of transporters. *Pharmacol. Ther.* **2018**, *192*, 88–99. [[CrossRef](#)]
9. Evers, R.; Piquette-Miller, M.; Polli, J.W.; Russel, F.G.M.; Sprowl, J.A.; Tohyama, K.; Ware, J.A.; de Wildt, S.N.; Xie, W.; Brouwer, K.L.R. Disease-Associated Changes in Drug Transporters May Impact the Pharmacokinetics and/or Toxicity of Drugs: A White Paper from the International Transporter Consortium. *Clin. Pharmacol. Ther.* **2018**, *104*, 900–915. [[CrossRef](#)]
10. Dunvald, A.-C.D.; Järvinen, E.; Mortensen, C.; Stage, T.B. Clinical and Molecular Perspectives on Inflammation-Mediated Regulation of Drug Metabolism and Transport. *Clin. Pharmacol. Ther.* **2021**, *112*, 277–290. [[CrossRef](#)]
11. Staudinger, J.L.; Woody, S.; Sun, M.; Cui, W. Nuclear-receptor-mediated regulation of drug- and bile-acid-transporter proteins in gut and liver. *Drug Metab. Rev.* **2013**, *45*, 48–59. [[CrossRef](#)]
12. Brouwer, K.L.R.; Evers, R.; Hayden, E.; Hu, S.; Li, C.Y.; Meyer Zu Schwabedissen, H.E.; Neuhoff, S.; Oswald, S.; Piquette-Miller, M.; Saran, C.; et al. Regulation of Drug Transport Proteins—From Mechanisms to Clinical Impact: A White Paper on Behalf of the International Transporter Consortium. *Clin. Pharmacol. Ther.* **2022**. [[CrossRef](#)] [[PubMed](#)]
13. Evans, R.M.; Mangelsdorf, D.J. Nuclear Receptors, RXR, and the Big Bang. *Cell* **2014**, *157*, 255–266. [[CrossRef](#)]
14. Gessner, A.; König, J.; Fromm, M.F. Clinical Aspects of Transporter-Mediated Drug-Drug Interactions. *Clin. Pharmacol. Ther.* **2019**, *105*, 1386–1394. [[CrossRef](#)] [[PubMed](#)]
15. Willson, T.M.; Kliewer, S.A. PXR, CAR and drug metabolism. *Nat. Rev. Drug Discov.* **2002**, *1*, 259–266. [[CrossRef](#)] [[PubMed](#)]
16. Urquhart, B.L.; Tirona, R.G.; Kim, R.B. Nuclear receptors and the regulation of drug-metabolizing enzymes and drug transporters: Implications for interindividual variability in response to drugs. *J. Clin. Pharmacol.* **2007**, *47*, 566–578. [[CrossRef](#)]
17. Rodrigues, A.D.; Lai, Y.; Shen, H.; Varma, M.V.S.; Rowland, A.; Oswald, S. Induction of Human Intestinal and Hepatic Organic Anion Transporting Polypeptides: Where Is the Evidence for Its Relevance in Drug-Drug Interactions? *Drug Metab. Dispos.* **2020**, *48*, 205–216. [[CrossRef](#)] [[PubMed](#)]
18. Rodrigues, A.D.; Rowland, A. Profiling of Drug-Metabolizing Enzymes and Transporters in Human Tissue Biopsy Samples: A Review of the Literature. *J. Pharmacol. Exp. Ther.* **2020**, *372*, 308–319. [[CrossRef](#)]

19. Barone, G.W.; Gurley, B.J.; Ketel, B.L.; Lightfoot, M.L.; Abul-Ezz, S.R. Drug interaction between St. John's wort and cyclosporine. *Ann. Pharmacother.* **2000**, *34*, 1013–1016. [[CrossRef](#)] [[PubMed](#)]
20. Ruschitzka, F.; Meier, P.J.; Turina, M.; Lüscher, T.F.; Noll, G. Acute heart transplant rejection due to Saint John's wort. *Lancet* **2000**, *355*, 548–549. [[CrossRef](#)]
21. Nishimura, M.; Naito, S.; Yokoi, T. Tissue-specific mRNA expression profiles of human nuclear receptor subfamilies. *Drug Metab. Pharmacokinet.* **2004**, *19*, 135–149. [[CrossRef](#)] [[PubMed](#)]
22. Brueck, S.; Bruckmueller, H.; Wegner, D.; Busch, D.; Martin, P.; Oswald, S.; Cascorbi, I.; Siegmund, W. Transcriptional and Post-Transcriptional Regulation of Duodenal P-Glycoprotein and MRP2 in Healthy Human Subjects after Chronic Treatment with Rifampin and Carbamazepine. *Mol. Pharm.* **2019**, *16*, 3823–3830. [[CrossRef](#)] [[PubMed](#)]
23. Fritz, A.; Busch, D.; Lapczuk, J.; Ostrowski, M.; Drozdziak, M.; Oswald, S. Expression of clinically relevant drug-metabolizing enzymes along the human intestine and their correlation to drug transporters and nuclear receptors: An intra-subject analysis. *Basic Clin. Pharmacol. Toxicol.* **2019**, *124*, 245–255. [[CrossRef](#)] [[PubMed](#)]
24. Greiner, B.; Eichelbaum, M.; Fritz, P.; Kreichgauer, H.P.; von Richter, O.; Zundler, J.; Kroemer, H.K. The role of intestinal P-glycoprotein in the interaction of digoxin and rifampin. *J. Clin. Investig.* **1999**, *104*, 147–153. [[CrossRef](#)] [[PubMed](#)]
25. Holtbecker, N.; Fromm, M.F.; Kroemer, H.K.; Ohnhaus, E.E.; Heidemann, H. The nifedipine-rifampin interaction. *Evid. Induction Gut Wall Metab. Drug Metab. Dispos.* **1996**, *24*, 1121–1123.
26. Westphal, K.; Weinbrenner, A.; Zschiesche, M.; Franke, G.; Knoke, M.; Oertel, R.; Fritz, P.; von Richter, O.; Warzok, R.; Hachenberg, T.; et al. Induction of P-glycoprotein by rifampin increases intestinal secretion of talinolol in human beings: A new type of drug/drug interaction. *Clin. Pharmacol. Ther.* **2000**, *68*, 345–355. [[CrossRef](#)]
27. Gorski, J. The effect of age, sex, and rifampin administration on intestinal and hepatic cytochrome P450 3A activity. *Clin. Pharmacol. Ther.* **2003**, *74*, 275–287. [[CrossRef](#)]
28. Fromm, M.F.; Busse, D.; Kroemer, H.K.; Eichelbaum, M. Differential induction of prehepatic and hepatic metabolism of verapamil by rifampin. *Hepatology* **1996**, *24*, 796–801. [[CrossRef](#)]
29. Oswald, S.; Meyer zu Schwabedissen, H.E.; Nassif, A.; Modess, C.; Desta, Z.; Ogburn, E.T.; Mostertz, J.; Keiser, M.; Jia, J.; Hubeny, A.; et al. Impact of efavirenz on intestinal metabolism and transport: Insights from an interaction study with ezetimibe in healthy volunteers. *Clin. Pharmacol. Ther.* **2012**, *91*, 506–513. [[CrossRef](#)]
30. Mouly, S.; Lown, K.S.; Kornhauser, D.; Joseph, J.L.; Fiske, W.D.; Benedek, I.H.; Watkins, P.B. Hepatic but not intestinal CYP3A4 displays dose-dependent induction by efavirenz in humans. *Clin. Pharmacol. Ther.* **2002**, *72*, 1–9. [[CrossRef](#)]
31. Kaza, M.; Karaźniewicz-Lada, M.; Kosicka, K.; Siemiątkowska, A.; Rudzki, P.J. Bioanalytical method validation: New FDA guidance vs. EMA Guideline. Better Or Worse? *J. Pharm. Biomed. Anal.* **2019**, *165*, 381–385. [[CrossRef](#)] [[PubMed](#)]
32. Gröer, C.; Brück, S.; Lai, Y.; Paulick, A.; Busemann, A.; Heidecke, C.D.; Siegmund, W.; Oswald, S. LC-MS/MS-based quantification of clinically relevant intestinal uptake and efflux transporter proteins. *J. Pharm. Biomed. Anal.* **2013**, *85*, 253–261. [[CrossRef](#)] [[PubMed](#)]
33. Fallon, J.K.; Neubert, H.; Hyland, R.; Goosen, T.C.; Smith, P.C. Targeted quantitative proteomics for the analysis of 14 UGT1As and -2Bs in human liver using NanoUPLC-MS/MS with selected reaction monitoring. *J. Proteome Res.* **2013**, *12*, 4402–4413. [[CrossRef](#)]
34. Gröer, C.; Busch, D.; Patrzyk, M.; Beyer, K.; Busemann, A.; Heidecke, C.D.; Drozdziak, M.; Siegmund, W.; Oswald, S. Absolute protein quantification of clinically relevant cytochrome P450 enzymes and UDP-glucuronosyltransferases by mass spectrometry-based targeted proteomics. *J. Pharm. Biomed. Anal.* **2014**, *100*, 393–401. [[CrossRef](#)]
35. Zhang, Y.; Li, N.; Brown, P.W.; Ozer, J.S.; Lai, Y. Liquid chromatography/tandem mass spectrometry based targeted proteomics quantification of P-glycoprotein in various biological samples. *Rapid Commun. Mass Spectrom.* **2011**, *25*, 1715–1724. [[CrossRef](#)] [[PubMed](#)]
36. Kawakami, H.; Ohtsuki, S.; Kamiie, J.; Suzuki, T.; Abe, T.; Terasaki, T. Simultaneous absolute quantification of 11 cytochrome P450 isoforms in human liver microsomes by liquid chromatography tandem mass spectrometry with in silico target peptide selection. *J. Pharm. Sci.* **2011**, *100*, 341–352. [[CrossRef](#)]
37. Oswald, S.; Gröer, C.; Drozdziak, M.; Siegmund, W. Mass spectrometry-based targeted proteomics as a tool to elucidate the expression and function of intestinal drug transporters. *AAPS J.* **2013**, *15*, 1128–1140. [[CrossRef](#)]

7 Eigenständigkeitserklärung

Hiermit erkläre ich, dass diese Arbeit bisher von mir weder an der Mathematisch-Naturwissenschaftlichen Fakultät der Universität Greifswald noch einer anderen wissenschaftlichen Einrichtung zum Zwecke der Promotion eingereicht wurde. Ferner erkläre ich, dass ich diese Arbeit selbstständig verfasst und keine anderen als die darin angegebenen Hilfsmittel und Hilfen benutzt und keine Textabschnitte eines Dritten ohne Kennzeichnung übernommen habe.

(Christoph Wenzel)

8 Veröffentlichungen und andere wissenschaftliche Leistungen

8.1 Veröffentlichungen

Meyer, M.J.; Tuerkova, A.; Römer, S.; Wenzel, C.; Seitz, T.; Gaedcke, J.; Oswald, S.; Brockmöller, J.; Zdrzil, B.; Tzvetkov, M.V. Differences in Metformin and Thiamine Uptake between Human and Mouse Organic Cation Transporter 1: Structural Determinants and Potential Consequences for Intrahepatic Concentrations. *Drug Metab Dispos*, **2020**, *48*, 1380–1392.

Klomp, F.; Wenzel, C.; Drozdik, M.; Oswald, S. Drug-Drug Interactions Involving Intestinal and Hepatic CYP1A Enzymes. *Pharmaceutics*, **2020**, *12*.

Wenzel, C.; Drozdik, M.; Oswald, S. Organic Cation Transporter 1 an Intestinal Uptake Transporter: Fact or Fiction? *Frontiers in pharmacology*, **2021**, *12*, 648388.

Wenzel, C.; Drozdik, M.; Oswald, S. Mass spectrometry-based targeted proteomics method for the quantification of clinically relevant drug metabolizing enzymes in human specimens. *Journal of chromatography. B, Analytical technologies in the biomedical and life sciences*, **2021**, *1180*, 122891.

Drozdik, M.; Lapczuk-Romanska, J.; Wenzel, C.; Szelağ-Pieniek, S.; Post, M.; Skalski, Ł.; Kurzawski, M.; Oswald, S. Gene Expression and Protein Abundance of Hepatic Drug Metabolizing Enzymes in Liver Pathology. *Pharmaceutics*, **2021**, *13*.

Deng, F.; Tuomi, S.-K.; Neuvonen, M.; Hirvensalo, P.; Kulju, S.; Wenzel, C.; Oswald, S.; Filppula, A.M.; Niemi, M. Comparative Hepatic and Intestinal Efflux Transport of Statins. *Drug Metab Dispos*, **2021**, *49*, 750–759.

Drozdik, M.; Lapczuk-Romanska, J.; Wenzel, C.; Skalski, Ł.; Szelağ-Pieniek, S.; Post, M.; Syczewska, M.; Kurzawski, M.; Oswald, S. Protein Abundance of Drug Transporters in Human Hepatitis C Livers. *IJMS*, **2022**, *23*, 7947.

Wenzel, C.; Gödtke, L.; Reichstein, A.; Keiser, M.; Busch, D.; Drozdik, M.; Oswald, S. Gene Expression and Protein Abundance of Nuclear Receptors in Human Intestine and Liver: A New Application for Mass Spectrometry-Based Targeted Proteomics. *Molecules (Basel, Switzerland)*, **2022**, *27*, 4629.

Kragl, A.; Schoon, J.; Tzvetkova, A.; Wenzel, C.; Blaschke, M.; Böcker, W.; Siggelkow, H.; Tzvetkov, M.V. Effects of HSD11B1 knockout and overexpression on local cortisol production and differentiation of mesenchymal stem cells. *Frontiers in bioengineering and biotechnology*, **2022**, *10*, 953034.

Drozdik, M.; Lapczuk-Romanska, J.; Wenzel, C.; Skalski, L.; Szelağ-Pieniek, S.; Post, M.; Parus, A.; Syczewska, M.; Kurzawski, M.; Oswald, S. Protein Abundance of Drug Metabolizing Enzymes in Human Hepatitis C Livers. *IJMS*, **2023**, *24*, 4543.

Kroll, M.-K.; Schloer, S.; Candan, P.; Korthals, N.; Wenzel, C.; Ihle, H.; Gilhaus, K.; Liedtke, K.R.; Schöfbänker, M.; Surmann, B.; Schröter, R.; Neugebauer, U.; Mall, G.; Oswald, S.; Ludwig, S.; Rescher, U.; Vollenbröcker, B.; Ciarimboli, G. Importance of ACE2 for SARS-CoV-2 Infection of Kidney Cells. *Biomolecules*, **2023**, *13*, 472.

8.2 Vorträge

Drozdik, M., Lapczuk-Romanska, J., Wenzel, C., Szelag-Pieniek, S., Post, M., Skalski, L., Kurzawski, M., Oswald, S.

Expression of hepatic drug-metabolizing enzymes is significantly affected by different forms of liver diseases and correlated with the liver functional state.

88. Jahrestagung der deutschen Gesellschaft für experimentelle und klinische Pharmakologie und Toxikologie; 7. - 10. März 2022; Bonn (Virtueller Kongress).

In: Abstracts of the 88th Annual Meeting of the German Society for Experimental and Clinical Pharmacology and Toxicology (DGPT). *Naunyn-Schmiedeberg's Arch Pharmacol*, **2022**, 395, S53.

8.3 Posterpräsentationen

Wenzel, C., Drozdik, M., Oswald, S.

Mass spectrometry-based targeted proteomics method for the quantification of clinically relevant drug metabolizing enzymes in human specimens.

87. Jahrestagung der deutschen Gesellschaft für experimentelle und klinische Pharmakologie und Toxikologie; 1. - 3. März 2021; Bonn (Virtueller Kongress).

In: Abstracts of the 87th Annual Meeting of the German Society for Experimental and Clinical Pharmacology and Toxicology (DGPT) with contribution of the Arbeitsgemeinschaft für Angewandte Humanpharmakologie e. V. (AGAH). *Naunyn-Schmiedeberg's Arch Pharmacol*, **2021**, 394, S52.

Wenzel, C., Lapczuk-Romanska, J., Ostrowski, M., Drozdik, M., Oswald, S.

Inter- and intra-subject analysis of gene expression and protein abundance of minor drug metabolizing enzymes in healthy human intestine and liver.

ISSX/MDO Meeting 2022; 11. – 14. September 2022; Seattle (USA).

Wenzel, C., Drozdik, M., Oswald, S.

“Minor” Drug Metabolizing Enzymes in Liver and Jejunum in Healthy Subjects – A Comparative Analysis in Paired Tissue Specimens.

DoktorandInnentagung der Deutschen Pharmazeutischen Gesellschaft; 1. – 3. März 2023; Bonn